LRH-1 as a target for the development of new breast cancer therapies

Fiona Kyle

Thesis submitted for the degree of Doctor of Philosophy

Supervisors: Prof. Simak Ali, Dr Laki Buluwela and Prof. Charles Coombes

Division of Cancer, Department of Surgery and Cancer, Imperial College London

September 2014

Abstract

Estrogen drives the growth and development of estrogen receptor alpha (ERα) positive breast cancer and ERα is the target for hormonal therapies that inhibit its activity. A substantial proportion of patients become resistant to these therapies, demonstrating a need for new therapies.

Gene expression microarray studies have been performed with a view to identifying potential novel therapeutic targets, biomarkers or forming the basis of identifying a molecular signature for endocrine resistance. These studies have identified candidate genes whose expression is altered in models of endocrine resistance. Investigation of the molecular pathways particularly highlights cell survival and regulation of apoptosis and indicates that these pathways play a key role in the development of resistance.

Microarray analysis also identified the liver receptor homolog 1 (LRH-1, NR5A2), a member of the nuclear receptor superfamily of transcription factors, as an estrogen regulated gene in MCF7 cells. Functional analysis showed that LRH-1 regulates breast cancer cell growth, acting in part by regulating ERα expression. Gene expression profiling of MCF-7 cells following RNAi for LRH-1 identified LRH-1 regulated genes. LRH-1 is known to regulate expression of CYP19A1 (aromatase), responsible for estrogen biosynthesis through the aromatisation of aromatase. Together, our findings identify LRH-1 as a potential therapeutic target for breast cancer treatment. Results of screening for small molecule inhibitors of LRH-1 will be presented, together with analysis of gene expression profiling for LRH-1 regulated genes.

Declaration of Originality

I, Fiona Kyle, declare that the work reported in this thesis is my own, or if not it is clearly stated and fully acknowledged. To the best of my knowledge and belief, this work contains no material previously published or written by another person or material which has to a substantial extent been accepted for the award of any dgree or diploma of Imperial College or any other institution of higher learning.

Copyright Declaration

The copyright of this thesis rests with the author and is made available under a Creative Commons Attribution Non-Commercial No Derivatives licence. Researchers are free to copy, distribute or transmit the thesis on the condition that they attribute it, that they do not use it for commercial purposes and that they do not alter, transform or build upon it. For any reuse or redistribution, researchers must make clear to others the licence terms of this work.

Acknowledgements

I firstly must thank my supervisors Simak Ali, Laki Buluwela and Charles Coombes. They have been endlessly patient and supportive both during my time in the laboratory and afterwards. I will always be grateful for having been given the opportunity to undertake my research with them. It has been a challenging and consequently rewarding experience during which I have learnt, and continue to learn an enormous amount that will be invaluable during my future career. I would also like to thank my fellow laboratory friends, especially Paul Thiruchelvam, Silvia Ottaviani, Hetal Dattani, Ciara Delaney (nee O'Hanlon Brown), Fui Chen Lai, Mani Periyasamy, Sean Delaney, Tony Dhillon and Anja Markert. During my early days in the lab I would like to thank Ross Thomas, Andy Photiou, Farah Al Beidh and Dean Heathcote for both guiding and teaching me as well as providing the entertainment. All my love and thanks goes to my gorgeous husband, Aron, and our two daughters, Leah and Ariel. Aron, thank you for putting up with my laterly singlemindedness. You are a constant inspiration to me, your ability to listen whilst I rant and rage and your love and care always supports me through everything I do. My beautiful girls, Leah and Ariel, it turns out you two have not been quite as helpful as you could have been, but I wouldn't have you any other way. I would like to thank my mother in law, Maria, and my father in law, Henry, who was always very enthusiastic and interested in the progress of this work and passed away earlier this year. Another big thank you must go to my siblings, Beckie, Tim and Andrew and their families who have all supported me in so many different ways during this time. A special thank you goes to my wonderful mum and dad. Thank you for always being there for me, knowing when to chivvy and when to listen. Thank you mum for trudging up and down on the packed train in the pouring rain to entertain and distract two busy little girls. Your energy for life is contagious. I am where I am because of you.

I would like to dedicate this work to my husband, Aron, my mum, Anne Kyle and my late father in law, Henry Rollin.

Table of Contents

Abstract……2

Declaration of Originality……3

Acknowledgements……4

Table of Contents……5

List of Figures……11

List of Tables……16

Abbreviations……17

1. Introduction……26

1.1 Endocrine Resistance……30

1.2 Mechanisms of Estrogen Receptor Function……31

1.2.1 ERα Structure……34

1.2.2 ERα Cofactors……36

1.2.3 ERα Ligands and Modulators……38

1.2.4 Mechanisms of Resistance to Endocrine Therapy……45

1.3 Liver Receptor Homolog 1 (LRH-1)……48

1.3.1 LRH-1 is a member of the Nuclear Receptor Superfamily of Transcription Factors……48

1.3.2 Crystallographic studies of the LRH-1 LBD…… 51

1.3.3 Expression and Function…… .54

1.3.3.1 Development/Role in Stem Cells……54

1.3.3.2 Metabolism……55

1.3.3.3 Proliferation……59

1.3.3.4 Steroidogenesis…… ….60

1.3.3.5 Immune response……61

1.3.4 LRH-1 is expressed in Breast Cancer and Breast Cancer Associated Stroma……62

1.3.4.1 LRH-1 regulation of Aromatase gene expression……63

1.3.4.2 LRH-1 is an ERα-regulated gene in breast cancer cells…68

1.3.5 LRH-1 Ligands……70

1.3.5.1 LRH-1 and SF-1 are Ftz-f1 subfamily members of the nuclear receptor superfamily that bind Phospholipids……70

1.3.5.2 Atrazine……72

1.3.5.3 Inverse agonists SF-1……73

1.3.5.4 Synthetic small molecule agonists of LRH-1 and SF1……74

1.3.6 LRH-1 Co-Factors……75

1.3.6.1 LRH-1 Co-Activators……75

1.3.6.2 LRH-1 Co-Repressors……76

1.3.7 Post-translational modifications of LRH-1……78

1.4 Aims……79

2 Materials and Methods……81

2.1 Materials……81

2.1.1 Chemicals and materials……81

2.1.2 Cell culture reagents……81

2.1.3 Cell Lines……82

2.1.4 Antibiotics……82
2.1.5 Sundries……83
2.1.6 Bacterial media and plates……83
2.1.7 General stock solutions……84
2.1.8 Antibodies……85
2.1.9 Real time RT-PCR Primers……86
2.1.10 Compounds……88
2.1.11 Coactivator Peptides……89
2.1.12 Equipment……89
2.2 Methods……90
2.2.1 Cell culture……90
2.2.2 Sulphorhodamine B (SRB) growth/toxicity assay……91
2.2.3 Total RNA preparation……92
2.2.4 cDNA by Reverse Transcription……92
2.2.5 Polymerase chain reaction (PCR) ……93
2.2.6 Real-time RT-PCR……93
2.2.7 Preparation of Protein lysates for Western Blotting……94
2.2.8 Western Blotting……94
2.2.9 Plasmid Preparation for Luciferase Reporter Assays……95
2.2.9.1 Bacterial Cell Transformation……95
2.2.9.2 Plasmid Preparation……96
2.2.10 Reporter Assays……96
2.2.11 siRNA Transfection……97
2.2.12 siRNA Oligonucleotides……98
2.2.13 Gene Expression Microarray Analysis……99

2.2.14 His tagged LRH-1 LBD Expression and Purification……99

2.2.14.1 Transformation into bacterial cells……99

2.2.14.2 Growth and Induction of Protein Expression……100

2.2.14.3 Purification……100

2.2.14.4 Dialysis…… 101

2.2.15 Cleavage and re-purification of His tagged LRH-1 LBD……102

2.2.16 Alpha Screen protocol……103

2.2.17 Fluorescence activated cell sorting (FACS) Analysis……104

3. Results……106

3.1 Gene Expression Profiling of MCF-7 and the MCF-7 derived, Estrogen-Independent MLET Cells …… 106

3.1.1 Principal component analysis (PCA) of gene expression microarray data……109

3.1.2 Estrogen regulated genes in MLET5 and MCF7 ……112

3.1.3 Estrogen independent activation of gene expression in MLET5……119

3.1.4 Functional group analysis of MLET5 differential gene expression……126

3.2 LRH-1 ……140

3.2.1 Microarray analysis of LRH-1 siRNA mediated gene knockdown……140

3.3 Approaches for the design and synthesis of small molecule antagonists of LRH-1……160

3.3.1 Space filling approaches for identifying compounds that are similar to phospholipids and synthetic LRH-1 agonists……..163

3.3.2 Scaffold Hopping (SHoP) Software for compound identification……..164

3.3.3 Nuclear Receptor Modulator Extension……..166

3.3.4 Coactivator binding Inhibitors (CBIs)……..173

3.4 Screening Assays for compounds with LRH-1 activity……..173

3.4.1 Cell-based LRH-1 regulated luciferase reporter gene assay for screening of selected compounds……..173

3.4.1.1 'Whitby' Compound Series……178

3.4.1.2 Compounds derived from "Cresset" screening……181

3.4.1.3 Design of LRH-1 inhibitors based on modeling of Nuclear Receptor antagonists in the LRH-1 LBD……196

3.4.1.4 Cresset Screen: Dax-1 peptide……202

3.4.1.5 α-helix mimetics……205

3.4.1.6 SHoP: 5L……207

3.4.2 Development of an in vitro screen for identification of compounds that bind the LRH-1 LBD, to block co-activator recruitment……209

3.4.2.1 Alpha Screen Optimisation…… 214

3.4.2.2 Confirmation of the utility of the LRH-1/Coactivator Alpha Screen assay using compound 5A Whitby agonist compound 5A…… 216

3.4.2.3 Sensitivity of the Alpha Screen to DMSO…….. 218

3.4.2.4 Alpha Screen Cascade……220

3.4.2.5 Subsequent Screening in the in vitro assay……232

4. Discussion……235

4.1 Models of Endocrine Resistance, MLET5 cells……235

4.1.1 Gene expression analysis in MCF7 derived models of endocrine-resistant breast cancer……235

4.1.2 Pro-survival pathways are upregulated in MLET5 cells……239

4.1.3 Future Directions……240

4.2 Evaluation of LRH-1 target gene expression in breast cancer cells……241

4.3 Development of Small Molecule Inhibitors of LRH-1……243

4.4 LRH1: Future direction……245

5. Conclusions……248

References……250

List of Figures

Figure 1.1 Global age standardised incidence and mortality rates for cancer in women……27
Figure 1.2 The mechanisms of action of anti-estrogens and Aromatase inhibitors in preventing or inhibiting ER activity……29
Figure 1.3 The repositioning of Helix 12 in the ER LBD by SERM Raloxifene……38
Figure 1.4 LRH-1 and the NR5A subfamily of nuclear receptor……48
Figure 1.5 Schematic representation of the LRH-1 LBD showing the four layers formed by the 12 helices……50
Figure 1.6 Coactivator binding to LRH-1 and RXR……51
Figure 1.7 The Role of LRH-1 in cholesterol metabolism……56
Figure 1.8 The Origins of Estrogen in Women……62
Figure 1.9 The CYP19 (Aromatase) gene……64
Figure 1.10 Regulation of aromatase gene expression in the breast……65
Figure 1.11 A schematic representation of the PLZF-ERα fusion protein……67
Figure 3.1 Principal Component Analysis (PCA) of Gene Expression Microarray Data Sets……108
Figure 3.2 33% of differentially regulated genes in MLET5 remain estrogen regulated……112
Figure 3.3 Validation of the expression of estrogen regulated genes……114
Figure 3.4A Differentially regulated genes in MLET5 versus MCF7……116
Figure 3.4B Estrogen Independent activation of genes in MLET5……117
Figure 3.5 Validation of the expression of the top four genes with the greatest up-regulation between MLET5 and MCF7……121
Figure 3.6A Validation of expression of genes involved in apoptosis in MCF7 and MLET5 cells……124
Figure 3.6B Validation of expression of genes involved in apoptosis in MCF7 and MLET5 cells……126

Figure 3.7 Altered protein expression of genes associated with apoptosis in MLET5 cells……..132
Figure 3.8 MLET5 cells are resistant to apoptosis……134
Figure 3.9 LRH-1 siRNA knockdown……..136
Figure 3.10 Gene expression profiling of LRH-1 knockdown in MCF-7 cells. ……138
Figure 3.11 Overlap of genes between LRH-1 SiRNA 2 and 3 with significant differential regulation of 1.5 fold or more……140
Figure 3.12 Pathway enrichment analysis for LRH-1-regulated genes……..141
Figure 3.13A List of probes included in Cluster 1, Response to estrogen, of the DAVID Pathway enrichment analysis for LRH-1-regulated genes… 142
Figure 3.13B Q-RT-PCR expression analysis of ER, SOCS2, BCL2, GATA3, CYP1A1 and CYP1B1. ……143
Figure 3.14 Estrogen regulation of differentially expressed genes in LRH-1 siRNA……145
Figure 3.15 Q-RT-PCR expression analysis of down regulated genes identified in the microarray analysis of siRNA LRH-1 versus NT SiRNA and shown to be estrogen regulated……..150
Figure 3.16 Q-RT-PCR expression analysis of over-expressed genes identified in the microarray analysis of siRNA LRH-1 versus NT siRNA and shown to be estrogen regulated……..151
Figure 3.17 Q-RT-PCR expression analysis of genes identified in the microarray analysis of siRNA LRH-1 versus NT siRNA……154
Figure 3.18 The LRH-1 LBD crystal structure. ……..157
Figure 3.19 Computer aided drug design……..160
Figure 3.20 Nuclear Receptor modulator extension……162
Figure 3.21A Raloxifene……163
Figure 3.21B Raloxifene Analogues……164
Figure 3.21C Raloxifene Analogues: Compounds from intermediate synthesis steps……165
Figure 3.22 Tamoxifen and analogues……166
Figure 3.23 Steroid based compounds……167

Figure 3.24 Cell based screening system for compounds targeting LRH-1……..170
Figure 3.25 Cell Based screening Strategy……172
Figure 3.26 Effects of Whitby 5A analogues on LRH-1 transcriptional activity…175
Figure 3.27 AB_WC Compound Screen (001-102)…… ……177
Figure 3.28 Determination of dose dependent activation of LRH-1 by AB_WC compounds……178
Figure 3.29 AB_WC 066 stimulates LRH-1 and ERα activity……179
Figure 3.30 AB_WC 088 stimulates LRH-1 and ERα activity……180
Figure 3.31 AB_WC 098 stimulates LRH-1 and ERα activity……181
Figure 3.32 Determination of dose dependent activation of compounds AB_WC057, 061 and 079……183
Figure 3.33 AB_WC 057 stimulates LRH-1 and ERα activity……184
Figure 3.34 AB_WC 107 shows no effect on LRH-1 and stimulates ERα activity at 10uM but does not show any effect on growth……185
Figure 3.35 AB_WC 111 stimulates LRH-1 and ERα activity but does not show any effect on growth……186
Figure 3.36 AB_WC 112 stimulates LRH-1 and ERα activity at 10μM and shows an effect on growth at 10μM……187
Figure 3.37 Determination of dose dependent activation/inhibition of LRH-1 by AB_WC compounds: Potential LRH-1 Antagonists……189
Figure 3.38 No abrogation of agonism with 5A by potential LRH-1 antagonists……190
Figure 3.39 Anti-estrogens and estrogen do not affect activity of LRH-1 in COS-1 cells……192
Figure 3.40 Effects of Raloxifene analogues on LRH-1 transcriptional activity……194
Figure 3.41 Effects of Tamoxifen analogues on LRH-1 transcriptional activity……195
Figure 3.42 Effects of steroid based analogues on LRH-1 transcriptional activity……196
Figure 3.43 Effects of Dax-1 mimetics on LRH-1 transcriptional activity……198

Figure 3.44 Effects of Dax-1 mimetic (AB_DC 12) analogues on LRH-1 transcriptional activity……199
Figure 3.45 Effects of α helix mimetics on LRH-1 transcriptional activity……..201
Figure 3.46 Effects of SHoP compounds on LRH-1 transcriptional activity……203
Figure 3.47 ALPHAScreen protein-peptide Interaction method……206
Figure 3.48 Generation and purification of His-tagged LRH-1 LBD……208
Figure 3.49 Optimisation and Validation: Co-Activator Peptides/ LRH-1 LBD……210
Figure 3.50 Optimisation and Validation: Increased binding with Whitby Compound 5A……212
Figure 3.51 DMSO is tolerated to 5%-10% in Alpha screen assay……213
Figure 3.52A Alpha Screen assay for determining effects of soluble compounds (10μM) on interaction of the LRH-1 LBD with the PGC1α coactivator peptide……216
Figure 3.52B Alpha Screen assay for determining effects of soluble compounds (10μM) on interaction of LRH-1 LBD with the PGC1α coactivator peptide……217
Figure 3.53 Alpha Screen assay for determining effects of soluble compounds (1μM) on interaction of LRH-1 LBD with PGC1α co-activator peptide……218
Figure 3.54 Alpha Screen assay for determining effects of poorly soluble compounds (10μM) on the interaction of the LRH-1 LBD with the PGC1α co-activator peptide……219
Figure 3.55 Alpha Screen assay for determining effects of poorly soluble compounds (1μM) on interaction of LRH-1 LBD with PGC1α co-activator peptide……220
Figure 3.56 Alpha Screen assay for determining non specific binding inhibition: effects of the 22 compounds previously shown to decrease the LRH-1/co-activator peptide interaction……222
Figure 3.57 Screening cascade for in vitro Alpha Screen……223

Figure 3.58 JR 430 has weak antagonism to LRH-1 and shows agonism of transcriptional activity……225
Figure 3.59 JR 449 shows weak/ no antagonism of LRH-1……226
Figure 3.60 Alpha Screen assay for determining the effects of compounds on interaction of the LRH-1 LBD with the PGC1α co-activator peptide……228
Figure 3.61 Alpha Screen assay for determining the effects of compounds on interaction of the LRH-1 LBD with the PGC1α co-activator peptide……229

List of Tables

Table 3.1A	Estrogen-responsive genes up-regulated in MLET5	110
Table 3.1B	Estrogen-responsive genes down-regulated in MLET5	111
Table 3.2	Functional group analysis of genes differentially regulated in MLET5, compared with MCF7cells, using DAVID	123
Table 3.3A	List of estrogen stimulated probes	146
Table 3.3B	List of estrogen repressed probes	147

List of Abbreviations

ABC	ATP Binding Cassette
ABI	Applied Biosystems
ABCA1	ATP-binding cassette transporter A1 (CERP)
ACOX2	Acyl-CoA oxidase 2
AD1	Activating domain 1
AD2	Activating domain 2
ADCY1	Adenylate cyclase 1
AIB1	Amplified in Breast Cancer-1 (SRC-3)
AF1	Activation Function 1
AF2	Activation Function 2
AHC	Adrenal Hypoplasia Congenital
AI	Aromatase Inhibitor
Annexin-V	FITC Annexin V-Fluorescein-Isothiocyanate
ANXA1	Annexin A1
AP1	Activator Protein 1
APL	Acute promyelocytic leukaemia
APS	Ammonium Persulphate
AR	Androgen Receptor
ASBT	Apical Sodium-dependent Bile acid Transporter
ATCC	American Type Culture Collection
ATP	Adenosine Triphosphate
BA	Bile Acid
BAD	BCL-2-associated Agonist of cell Death
BAK	BCL-2-Antagonist/Killer
BCAS1	Breast carcinoma amplified sequence 1
BCL-2	B-cell Lymphoma protein 2
BCL-6	B-cell Lymphoma protein 6
BH3	Bcl2 homology 3
bHLH-PAS	Basic helix-loop-helix-Per/ARNT/Sim

BID	BH3 interacting domain death agonist
BIK	BCL2-Interacting Killer
BIRC3	Baculoviral IAP repeat containing 3
bp	base pair
BSEP	Bile Salt Export Pump
C1P	Ceramide-1-Phosphate
CALB2	Calbindin 2
cAMP	Cyclic Adenosine Monophosphate
CARM-1	Coactivator-Associated Arginine Methyltransferase 1
CBI	Coactivator Binding Inhibitor
CBP	CREB Binding Protein
CCND1	Cyclin D1
CD36	Collagen type 1 receptor/Thrombospondin receptor
CDases	Ceramidases
CDK	Cyclin-Dependent Kinases
cDNA	complementary DNA
CEBPG	CCAAT/enhancer binding protein gamma
CEL	Carboxyl ester lipase
CETP	Cholesteryl-ester-transfer protein
ChIP	Chromatin Immunoprecipitation
ChIP-Seq	(ChIP)-Sequencing
ciz-1	CDKN1A Interacting Zinc finger protein 1
c-MYC	cellular Myelocytomatosis oncogene
CO_2	carbon dioxide
CORNR	Corepressor Nuclear Receptor
COS-1	CV-1 in Origin, carrying SV40-1
COX-2	Cyclo-Oxygenase-2
CRUK	Cancer Research UK
CYP1B1	Cytochrome p450 1B1
CYP1A1	Cytochrome p450 1A1
cSNP	coding Single Nucleotide Polymorphisms

c-SRC	v-src Sarcoma (Schmidt-Ruppin A-2) viral oncogene homolog
CRP	C reactive protein
Ct	Cycle threshold
CtBP	Carboxyl-terminal Binding Protein
CSTD	Cathepsin-D
CTE	C-Terminal Extension
CYP	Cytochrome P450
DAX-1	Dosage-sensitive sex reversal Adrenal hypoplasia critical region on chromosome X, gene 1
DBD	DNA Binding Domain
DFS	Disease Free Survival
DDW	Distilled De-ionised Water
DLPC	Dilauroyl phosphaditylcholine
DMEM	Dulbecco's Modified Eagle's Medium
DMBA	Dimethyl-Benzanthracene
DMSO	Dimethyl Sulfoxide
DNA	Deoxyribonucleic Acid
Dox	Doxycycline/doxytetracycline
DSS	Dextran-coated charcoal treated fetal calf Serum
DTT	Dithiothreitol (C4H12O2S2)
DUPC	Diundecanoyl phospatidylcholine
E2	17α-Estradiol
EDTA	Ethylenediaminetetraacetate
EGF	Epidermal Growth Factor
EGFR	Epidermal Growth Factor Receptors
ER	Estrogen Receptor
ERP-LUC	ERα-promoter-Luciferase
ERβ	Estrogen Receptor β
ERα	Estrogen Receptor α
ERE	Estrogen Response Element
ERK	Extracellularly-Regulated Kinase

ERK1/2	Extracellularly-Regulated Kinase-1 and -2
ERRα	Estrogen Related Receptor-α
FACS	Fluorescence-Activated Cell Sorting
FCS	Fetal Calf Serum
FRET	Fluoresence Resonance Energy Transfer
FOXP3	Forkhead box Protein P3
FSH	Follicle Stimulating Hormone
FSK	Forskolin
Ftz-F1	Fushi tarazu Factor-1
FXR	Farnesoid X Receptor
GAPDH	Glyceraldehyde 3-phosphate dehydrogenase
GATA	GATA binding protein
G418	Geneticin
GC	Granulosa Cells
GFRA1	GDNF family receptor alpha 1
GI	Gastrointestinal
GnRH	Gonadotrophin Releasing Hormone
GPCR	G-Protein Coupled Receptors
GPER	G-protein Coupled Estrogen Receptor
GR	Glucocorticoid Receptor
GRE	Glucocorticoid Receptor Element
GREB-1	Gene Regulated by Estrogen in Breast cancer
GRIP	Glucocorticoid Receptor Interacting Protein (SRC-2/TIF2)
GST	pull-down Glutathione S-Transferase pull-down
H12	Helix 12
HCC	Hepatocellular Carcinoma
HDAC	Histone Deacetylase
HDL	High density lipoprotein
HEO	Human Estrogen Receptor
HepG2	Human liver hepatocellular carcinoma cell line

HER2/neu	Human Epidermal growth factor Receptor 2, also known as ErbB-2/ ERBB2
HIS	Histidine
HRP	Horseradish peroxidase
Hsp90	Heat shock protein 90
ICI	ICI 182, 720 (Fulvestrant)
IGFBP3	Insulin-like growth factor-binding protein 3
IGF-1	Insulin-like Growth Factor-1
IGFL1	IGF-like family member 1
IGFR	Insulin-like Growth Factor Receptor
JNK	c-Jun N-terminal Kinase
kb	kilobase
kDa	kilodalton
LBD	Ligand Binding Domain
LCoR	Ligand-dependent Corepressor
LDL	Low density lipoprotein
LH	Luteinising Hormone
LRH-1	Liver Receptor Homolog-1
LUC	Luciferase
LXR	Liver X Receptor
µg	Microgram
MAPK	Mitogen Activated Protein Kinase
MBF	Multi-protein Bridging Factor
MCF-7-TO	MCF-7 Tetracycline-Off
MEK	Mitogen-activated protein kinase ERK-kinase
mg	milligram
miRNA	microRNA
ml	milliliter
MR	Mineralocorticoid Receptor
mRNA	messenger RNA
MRP	Multidrug Resistance Protein

mTOR	mammalian Target Of Rapamycin
MWCO	Molecular weight cut off
MYB	V-myb avian myeloblastosis oncogene homolog
MYC	Myelocytomatosis
MYCBP	c-MYC Binding Protein
NCoA	Nuclear Receptor Coactivator
NCoR1	Nuclear Receptor Corepressor 1
ng	nanogram
NF-κB	Nuclear Factor κB
NR	Nuclear Receptor
NR5A1	Nuclear Receptor subfamily 5, group A, member 1 (SF-1)
NR5A2	Nuclear Receptor subfamily 5, group A, member 2 (LRH-1/FTF/FTZ-F1)
NUPR1	Nuclear protein, transcriptional regulator 1(p8, com1)
OCT4	Octamer-binding transcription factor 4
OD	Optical Density
OHT	4-Hydroxy-Tamoxifen
OS	Overall Survival
PAS	Per/Amt/Sim
PAX-2	Paired Box-2
PCP4	Purkinje cell protein 4
PDGF	Platelet-Derived Growth Factor
PDX-1	Pancreatic and Duodenal Homeobox 1
PGE2	Prostaglandin E2
PBS	Phosphate Buffered Saline
PCR	Polymerase Chain Reaction
PE	Phospatidyl Ethanolamine
PG	Phospatidyl Glycerol
PGC-1α	Peroxisome proliferator-activated receptor Gamma Coactivator 1 Alpha
PGR	Progesterone receptor

PI3K	Phosphatidylinositol 3-kinase
PIAS	Protein Inhibitor of Activated STAT
PIP	Phosphatidylinositol 4-Phosphate
PKA	Protein Kinase A
PKC	Protein Kinase C
PLZF	Promyelocytic Leukaemia Zinc Finger
PMA	Phorbol-12-Myristate-13 Acetate
PMP22	Peripheral myelin protein 22
PolII	RNA polymerase II
PPAR	Peroxisome Proliferator Activated Receptor
PPT	Propyl Pyrazole Triol
PR	Progesterone Receptor
PRMT-2	Protein Arginine Methyltransferase 2
Prox-1	Prospero-related homeobox
pS2	Protein pS2
P/S/G	Penicillin/streptomycin/ L-glutamine solution
PTEN	Gadd45α and Phosphate and Tensin Homolog
qRT-PCR	quantitative Real Time Polymerase Chain Reaction
Rb	Retinoblastoma
RAMP3	Receptor Activity Modifying Protein 3
RAR	Retinoic Acid Receptor
RIP140	Receptor-Interacting Protein 140
RNA	Ribonucleic acid
RNAi	RNA interference
rpm	revolutions per minute
rRNA	ribosomal Ribonucleic Acid
RT	Reverse Transcriptase
RT-PCR	Reverse Transcription Polymerase Chain Reaction
RXR	Retinoid X Receptor
S1P	Sphingosine-1-Phosphate
SCNN1A	Sodium channel non voltage gated 1 alpha subunit

SDS	Sodium Dodecyl Sulphate
SEM	Standard Error of Mean
SERM	Selective Estrogen Receptor Modulator
SF-1	Steroidogenic Factor-1
SF-1-LUC	SF1 promoter-Luc
SHC	Src homology 2 domain containing transforming protein
SHP	Small Heterodimer Partner
siRNA	Small interfering RNA
SLC9A6	Solute Carrier Protein 9 subfamily A, member 6
SNP	Single Nucleotide Polymorphism
SPH	Sphingosine
SRB	Sulphordiamine B
SRC	Steroid Receptor Coactivator
SMRT	Silencing Mediator of Retinoic acid and Thyroid Hormone Receptor (NCoR2/TRAC2)
SNRIs	Selective Noradrenaline Re-uptake Inhibitor
SOCS2	Suppressor of cytokine signalling 2
SPHK	Spingosine Kinase
SP-1	Sp1 transcription factor
SSRIs	Selective Serotonin Re-uptake Inhibitors
StAR	Steroidogenic acute regulatory protein
STAT	Signal Transducer and Activator of Transcription
SUMO	Sumoylation
T3	Triiodothyronine
TACC1	Transforming, acidic coiled,coil containing protein 1
TBE	Tris-Borate-EDTA
TBP	TATA Binding Protein
TCA	Trichloroacetic Acid
TCGA	The Cancer Genome Atlas
TEMED	Tetramethylethylenediamine
TGF-β	Transforming Growth Factor-β

TIF-2	Transcriptional Intermediary Protein 2 (SRC-2/GRIP1)
TM4SF1	Transmembrane-4-L-six-family 1 (L6)
TNF-1	Tumour Necrosis Factor-1
TNFRSF21	Tumour necrosis factor receptor superfamily, member 21 (DR6)
TR	Thyroid Receptor
TRAM1	Translocation Associated Membrane Protein 1
TRAP220	Thyroid hormone Receptor-Associated Protein complex 220 kDa component
TTP	Time to progression
TTR	Time To recurrence
VDR	Vitamin D3 Receptor
VEGF	Vascular-Endothelial Growth Factor
XBP-1	X-box Binding Protein 1

1. Introduction

Breast cancer is the most common cancer diagnosed in women in the Western World. There were 130 age adjusted new cases per 100,000 people in UK in 2008, a prevalence of 297,769 on 31st December 2006 and a lifetime risk for developing breast cancer of 1 in 8, for women in the UK (Sasieni et al., 2011). Worldwide there were 1.38 million new cases and 458,400 deaths in 2008 (Figure 1.1) (Jemal et al., 2011).

The importance of estrogen on breast cancer development and progression have long been established. In the 1870s, Alfred Schinzinger noted that the permanent cessation of menstruation, the menopause, led to breast atrophy and proposed oopherectomy as a possible means to treat breast cancer (Ali and Coombes, 2002). In 1896, George Beatson published the successful use of oophorectomy to achieve tumour regression in a pre-menopausal woman with breast cancer (Beatson, 1896). Stanley Boyd reported on this case and forty others in the British Medical Journal (Boyd, 1900). The identification of the ovaries as the source of the hormone estrogen led to the proposal by Antoine Lacassagne of the concept of synthetic estrogen antagonists that could be used in the prevention of breast cancer (Lacassagne, 1936). However the actual discovery of synthetic antagonists and subsequently the estrogen receptor did not occur until the 1950/60s (MacGregor and Jordan, 1998) and has since led to a paradigm shift in individualizing the care of patients with breast cancer at a molecular level. The importance of estrogen in regulating breast cancer growth is now abundantly clear and drugs that inhibit estrogen biosynthesis, or those that bind competitively to estrogen receptors, have become very important agents in the treatment of breast cancer. Estrogenic actions are mediated by the estrogen receptors, ERα and ERß. The first important anti-estrogen was Tamoxifen, a selective estrogen receptor modulator (SERM), approved by the Food and Drug Administration (USA) in 1977 for use in management of metastatic breast cancer and subsequently in an adjuvant setting (Osborne, 1998).

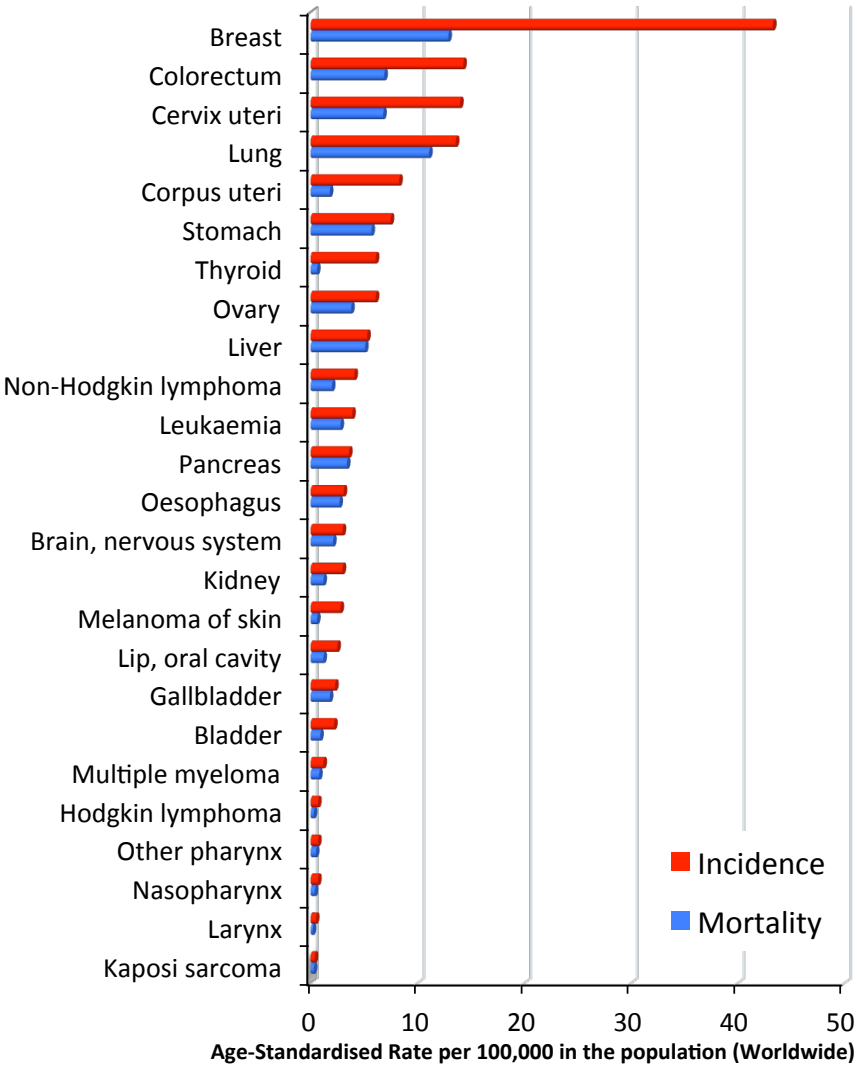


Figure 1.1 Global age standardised incidence and mortality rates for cancer in women. Data obtained from the International Agency for Research on Cancer GLOBOCAN 2012 (http://globocan.iarc.fr/Pages/fact_sheets_population.aspx)

The therapeutic use of anti-estrogens such as tamoxifen for five years has increased overall survival in the post-operative adjuvant setting (Lewis, 2007), with low toxicities compared to cytotoxic treatment, in ERα positive patients. The discovery of aromatase, the enzyme involved in the conversion pathway of androgens to estrogens (Figure 1.2), has now led to the development of aromatase inhibitors such as letrozole and anastrozole, which act via competitive inhibition of aromatase, and exemestane, which acts via an irreversible inactivation of aromatase (Johnston and Dowsett, 2003). Clinical trials with aromatase inhibitors show significant improvements in overall survival in both the adjuvant, neo-adjuvant and metastatic settings in post-menopausal ERα-positive patients (Cuzick, 2008) (Coombes et al., 2007; Ellis et al., 2001). Recent meta-analyses confirm that aromatase inhibitors significantly lower recurrence rates in initial adjuvant administration and significantly decrease mortality (0.7% and 1.6% for three and six years from treatment divergence, respectively) in a 'switch' setting following 2-3 years of tamoxifen (Dowsett et al., 2010; J. Ingle, 2008). This phasing of adjuvant endocrine therapies is increasingly becoming the standard of care in clinical practice.

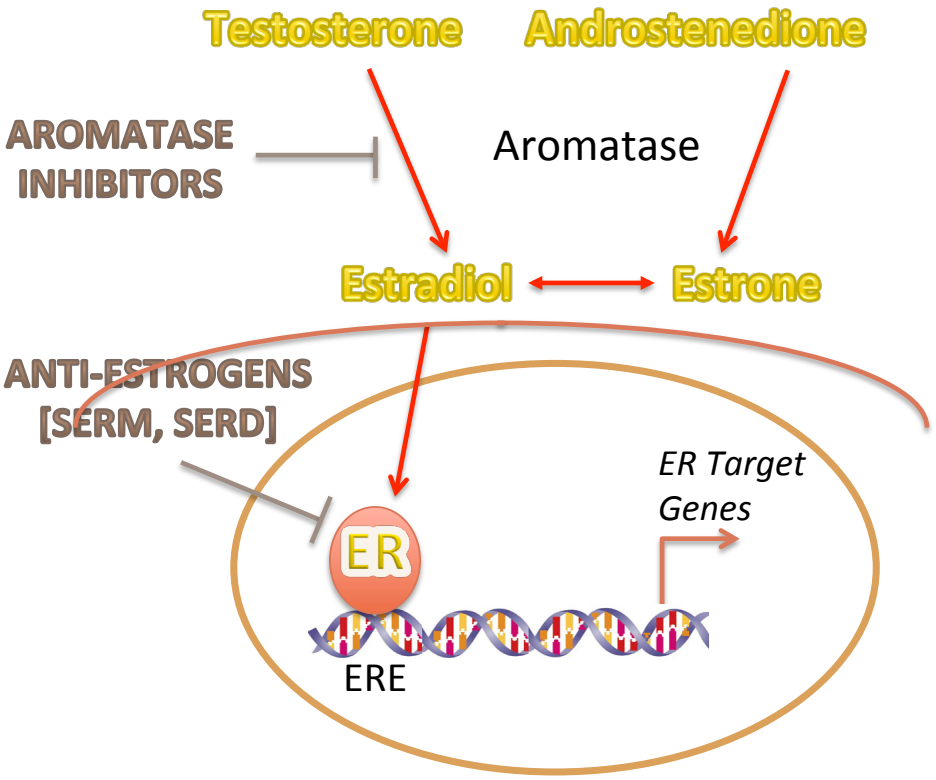


Figure 1.2 The mechanisms of action of anti-estrogens and Aromatase inhibitors in preventing or inhibiting ER activity.

Following the binding of estradiol to ER and receptor dimerisation, conformational changes occur leading to binding to estrogen response elements (ERE) of estrogen-regulated genes. Anti-estrogens act by competing with estrogen for binding to ER, to inhibit ER activity (selective ER modulators (SERMs), e.g. tamoxifen) or by promoting ER degradation (Selective ER downregulators (SERDs), e.g. fulvestrant). Aromatase inhibitors act by preventing the conversion of androgens to estrogens by inhibiting aromatase activity. Adapted from Johnston and Dowsett (2003).

1.1 Endocrine Resistance

Although it remains one of the greatest advances in cancer therapeutics, hormone therapy is not without problems. An important clinical issue is that of resistance, both *de novo* and acquired resistance to tamoxifen, as well as to aromatase inhibitors. Many patients presenting with localized disease progress on tamoxifen, or relapse following initial response. In the metastatic setting all patients treated with tamoxifen relapse (Ali and Coombes, 2002). Published data have shown that in the majority of cases ERα expression is maintained (Johnston et al., 1995) and approximately 20% of patients who relapse on tamoxifen will respond to second or third line endocrine treatments (Howell et al., 2002; Osborne et al., 2002), indicating that ERα continues to be important in the growth of endocrine resistant breast cancer. Despite this knowledge, definitive molecular causes of resistance are still uncertain; however it is these findings that have led to the idea of phasing endocrine treatments as a means of reducing the development of endocrine resistance (Coombes et al., 2007).

The increasing use of aromatase inhibitors as neoadjuvant treatment, phasing of adjuvant treatment (i.e. pre or post tamoxifen) and in the metastatic setting is leading to a different molecular scenario to tamoxifen resistance, as aromatase inhibitors act by decreasing systemic estrogen biosynthesis in contrast to acting directly on the estrogen receptor. We might assume that the clinical scenario of estrogen deprivation is a different model to that of tamoxifen resistance.

The incidence and mortality of breast cancer in some Western countries has decreased since 2000, but there has been an increase in many Asian and African countries and breast cancer remains the most commonly diagnosed cancer and the leading cause of cancer death, in women, worldwide (Jemal et al., 2011).

The efficacy and availability of hormonal therapies such as SERMs, faslodex and aromatase inhibitors, the convenience of administration and cost effectiveness means that we can expect use to continue to rise. This has provided the impetus for further efforts to determine the mechanisms underlying resistance to hormonal therapies.

1.2 Mechanisms of Estrogen Receptor Function

The clinical data outlined above shows that ERα continues to be important for tumour progression following the emergence of endocrine resistance (Howell et al., 2002; Johnston et al., 1995; Osborne et al., 2002). ERα is a member of the nuclear receptor superfamily. Nuclear receptors are ligand modulated gene regulatory proteins or small molecule activated transcription factors. Examples of nuclear receptors include ERα, the androgen receptor (AR), progesterone receptor (PgR), glucocorticoid receptors, retinoid receptors, vitamin D3 receptors and thyroid hormone receptors. Nuclear receptors regulate gene expression both directly by binding DNA, as well as through recruitment via interaction with other transcription factors (e.g. AP-1, SP-1) and in combination with transcriptional co-activators and co-repressors that remodel and modify chromatin (Gronemeyer et al., 2004). They are activated upon binding to small lipophilic molecules and in some cases it has been possible to identify synthetic activators or agonists, as well as inhibitors or antagonists, for example, the anti-estrogens tamoxifen and ICI 182,780, in the case of ERα (Jordan, 2003a, b; Osborne et al., 2004).

As stated previously, there are two ER genes in the human genome, ERα and ERß. Due to the more recent discovery of ERβ, together with uncertainty as to its significance in breast cancer, most of our knowledge about mechanisms of estrogen action arises from work carried out on ERα. The importance of ERα in breast cancer is clear, with 70-80% of tumours expressing ERα and the fact that patients with ERα-positive breast cancer respond to hormonal therapies. Thus, current immuno-histochemical determination of ERα status in breast tumours is used to make

treatment decisions, with patients with ERα-positive disease being offered endocrine therapy for at least 5 years.

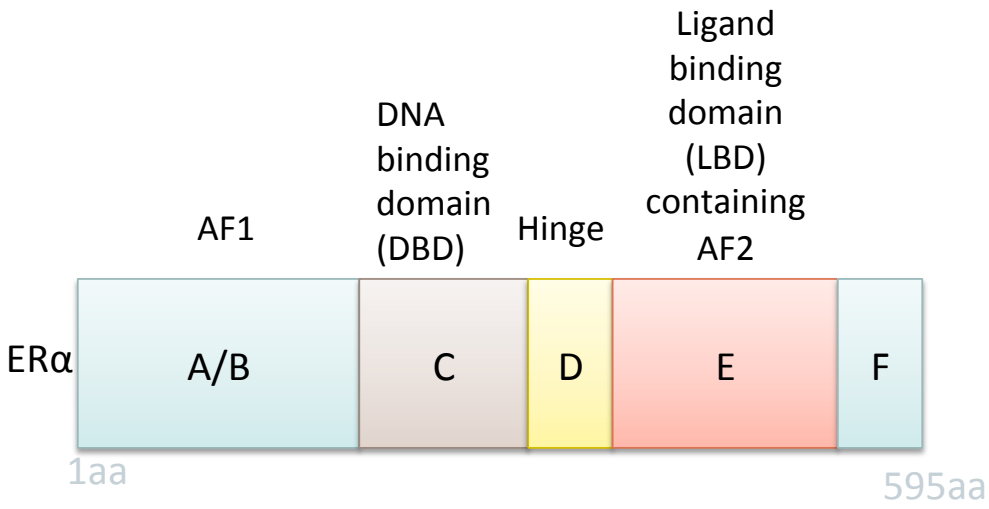


Figure 1.3 Schematic diagram depicting the ERα protein structure

1.2.1 ERα Structure

The human ERα gene codes for a 6.3 kb mRNA, which is translated to generate a 595 amino acid polypeptide. The ERα polypeptide can be functionally divided into six distinct regions, on the basis of homology, when comparing protein sequences for ERα, and other members of the nuclear receptor family, across different species. Following on from these analyses and functional characterization the most highly conserved domains in the ERα protein across different species are region C, encoding the DNA binding domain (DBD), comprised of two zinc finger motifs and responsible for specific binding to estrogen response elements in regulatory regions of estrogen-responsive genes, and the ligand binding domain (LBD, region E), which binds estrogen and anti-estrogens (Ali and Coombes, 2002). The LBD also encodes an intrinsic transcription activation function AF2, whose action requires ligand binding. N-terminal to the DBD is transcription activation function AF1, which can act in a ligand-independent manner, at least when separated from the ERα LBD (Ring and Dowsett, 2004). AF1 activity is regulated by growth factors and protein kinases causing phosphorylation at several sites, leading to stimulation of ERα activity, often in a ligand-independent manner. AF1 phosphorylation is mediated by ERK1/2 MAPK (at serines, 104, 106 and 118), by CDK7 (serine 118), by the MAPK-regulated p90RSK (at serine 167) and by AKT (also at serine 167) (Ali and Coombes, 2002). AF1 phosphorylation and consequent ERα activation by ERK1/2 and AKT provides a potential for crosstalk between ERα and cell surface receptors, such as EGFR and HER2, which have been implicated in resistance to endocrine therapies (Martin et al., 2005; Moy and Goss, 2006; Nicholson et al., 2007).

Estrogens regulate the growth of breast cancer cells by binding to the ERα LBD and promoting dissociation from heat shock proteins and leading to receptor dimerisation and localization in the nucleus. The ERα/estrogen complex binds to estrogen response elements (EREs) in the regulatory (promoter, enhancer) regions

of estrogen responsive genes, regulating expression and leading to the promotion of breast cancer cell growth. Gene regulation by ERα has been extensively studied. In common with other transcription factors, stimulation of gene expression by ERα requires the ordered association and dissociation of diverse enzyme activities that mediate chromatin remodeling and histone modification, resulting in the recruitment of RNA polymerase II and consequent transcription initiation (Metivier et al., 2006).

The crystal structure of the ERα and ERß LBD in complex with both estrogen and the synthetic selective antagonist raloxifene confirms that ligand binding to the LBD initiates conformational changes allowing the recruitment of co-activators or co-repressors. These cofactors act as scaffold proteins enabling interaction with the cellular transcription machinery resulting in the activation or repression of target genes (Brzozowski et al., 1997; Heery et al., 1997; Nagy et al., 1997; Shiau et al., 1998; Torchia et al., 1997).

The structure of ERα, as a ligand inducible nuclear transcription factor, is similar to that of other nuclear receptors, with a ligand binding domain (LBD) folded into a three layered anti-parallel α-helical sandwich (layer 1= H1, H2, H3, H4; layer 2= H5/6, H9, H10; layer 3= H7, H8, H11), forming a ligand binding cavity of 450Å, in combination with the secondary structural elements (2 stranded beta sheets, S1 and S2 and α-helix H12) (Brzozowski et al., 1997). ERα and ERß form homo-dimers in solution, mainly via H11 creating a stable backbone (Brzozowski et al., 1997; Klein-Hitpass et al., 1989; Ruff et al., 2000). The two receptors have also been shown to heterodimerise (McDonnell, 2004; Ogawa et al., 1998).

1.2.2 ERα Cofactors

At least 285 transcriptional cofactors (co-regulators) have been identified mainly through screens for genes that promote or repress nuclear receptor activities (Lonard et al., 2007). Transcriptional cofactors were initially noted to be of importance through their role in the interaction with DNA-binding transcription factors, creating a bridge to the general transcription machinery, to promote transcription initiation. Since then they have also been found to have enzymatic roles, to promote chromatin remodelling and modification, as well as including factors that have enzymatic roles in regulating transcriptional elongation, RNA splicing and mRNA transport.

The dysregulation of transcriptional co-factors in cancer is being increasingly recognized. A review on nuclear receptor co-factors (co-activators and co-repressors), using the Oncomine database in 2007, reported that 60% of transcriptional co-regulators are over-expressed in lung cancer, 38% in breast cancer and 43% in prostate cancer (Lonard et al., 2007).

An example of an ERα co-activator that is frequently amplified and/or over-expressed in breast cancer is AIB1 (Amplified in breast cancer 1) (Anzick et al 1997). Transgenic mice over-expressing AIB1 in the mammary gland develop malignant mammary tumours (Torres-Arzayus et al., 2004; Torres-Arzayus et al., 2010), directly implicating AIB1 in breast cancer initiation and progression.

The majority of identified nuclear receptor cofactors bind at the AF2 binding site. Other co-activators bind to the DBD, for example, Ciz1 binds to the DBD of ERα (den Hollander et al., 2006), PGC1-α that binds to the hinge region, as well as the AF2 (Tcherepanova et al., 2000) and p68 RNA helicase, which binds to the ERα AF1 (Endoh et al., 1999), have been described.

From various studies, three classes of co-activator peptides have been identified, based on the flanking sequences of the common, signature nuclear receptor LBD binding motif, LXXLL (NR binding box) where L is leucine and X any amino acid (Chang et al., 1999; Darimont et al., 1998; Heery et al., 1997; Nolte et al., 1998; Shiau et al., 1998). The steroid receptor co-activators (SRCs), which include AIB1 (SRC3) are an important group of co-activators with mostly class 1 or 2 LXXLL binding motifs. They share common functional domains including an N terminal basic helix-loop-helix-Per/ARNT/Sim (bHLH-PAS) domain (required for protein-protein interactions), a flanking serine/threonine rich domain, an NR interaction domain containing multiple LXXLL binding motifs, C-terminal to which are transcriptional activation domain 1 (AD1), the interaction site for CREB-binding protein and p300) and transcription activation domain 2 (AD2), the latter being a site of interaction for histone methyltransferases) (Moore et al., 2010). The binding of the coactivator to NRs occurs within the hydrophobic pocket of H12 and co-crystalization studies have shown that they are stabilised by the leucine residues of the LXXLL motif with the hydrophobic pocket and by hydrogen bonding between an H3 lysine and a glutamate within the LXXLL motif (Johnson and O'Malley, 2012).

Transcriptional corepressors act as abrogaters of agonist activity or to repress target gene activity for the ligand bound NR in the absence of a ligand, e.g. for RARα/RXR heterodimers. The related co-repressors, SMRT and NCOR, bind to ERα in the presence of antagonists, rather than in the unliganded state, and *in vitro* data show that mutations in α-helices H3 and H5, inhibit this interaction (Huang et al., 2002). NCOR and SMRT are able to sit in the same AF2 binding pocket as co-activators due to displacement of the H12 α-helix by antagonists (Madauss et al., 2007; Xu et al., 2002). Blocking the actions of NCOR and SMRT with specific antibodies promotes the agonist action of the active form of tamoxifen (4-hydroxytamoxifen (4HT)) (Lavinsky et al., 1998) and 4HT acts as an agonist in fibroblasts developed from NCOR null mice (Jepsen et al., 2000). Similarly when NCOR and SMRT are over-expressed in HEPG2 cells, where agonism with 4HT is

usually seen, the agonist action of 4HT is reduced. The effects of co-repressors on the ligand independent activity (AF1, DBD) are less clear (Jackson et al., 1997; Jepsen et al., 2000; Smith et al., 1997).

NCOR and SMRT interact with nuclear receptors at the AF2 binding site via an elongated α-helix, with the consensus sequence, LxxH/IIxxxI/L, also known as the CoRNR box (Hu and Lazar, 1999). Other co-repressors, such as RIP140 and LCOR, share the same binding motif as co-activators (LxxLL) and as for co-activator recruitment, they are recruited by agonist bound receptors, e.g. estrogen bound ERα. RIP140 and LCOR exert their repressive effects by recruiting co-repressors such as C-terminal binding protein (CtBP), as well as DNA and histone methyltransferases (Perissi et al., 2010; Watson et al., 2012). As they bind in the same manner as co-activators such as SRC1 and AIB1, it is unclear as to what mechanisms determine binding of co-activators or these co-repressors. However, detailed chromatin immunoprecipitation (ChIP) studies for ERα binding at the estrogen-responsive pS2 gene demonstrated cyclical association and dissociation of ERα that was accompanied by cyclical recruitment and dissociation of co-activators and RNA polymerase II (PolII) and PolII-associated factors. These cyclical events were accompanied by histone acetylation and methylation events that accompany transcription initiation and which are required at gene promoters, for transcription to occur. Again histone acetylation and methylation were cyclical, indicating that co-activators and co-repressors are recruited to estrogen responsive genes in a cyclical manner, with the cycles of co-activator recruitment and histone modification being critical for regulation of target gene expression (Metivier et al., 2003; Reid et al., 2003).

1.2.3 ERα Ligands and Modulators

Ligand specific interaction by ERα is achieved through a combination of specific hydrogen bonds and hydrophobic residues that line the LBD. The specificity for

estrogen over other endogenous steroidal hormones relates to the extensive polar and non-polar interactions allowing estrogen to bind with sub-nanomolar affinity (Brzozowski et al., 1997). Estrogen is relatively small in comparison with the binding area (245Å versus 450Å), so the size of the ERα LBD also allows binding of other, non steroidal compounds (Brzozowski et al., 1997). The reason for the relatively large size of the binding pocket is not definitively known but it may be that there are other, as yet undiscovered, ERα ligands or modulators.

Selective ERα modulators, such as raloxifene and tamoxifen bind at the same site as estrogen but differ by displacing H12 due to their structurally distinct long side chain, which is too long to be contained within the ligand binding pocket (Figure 1.4).

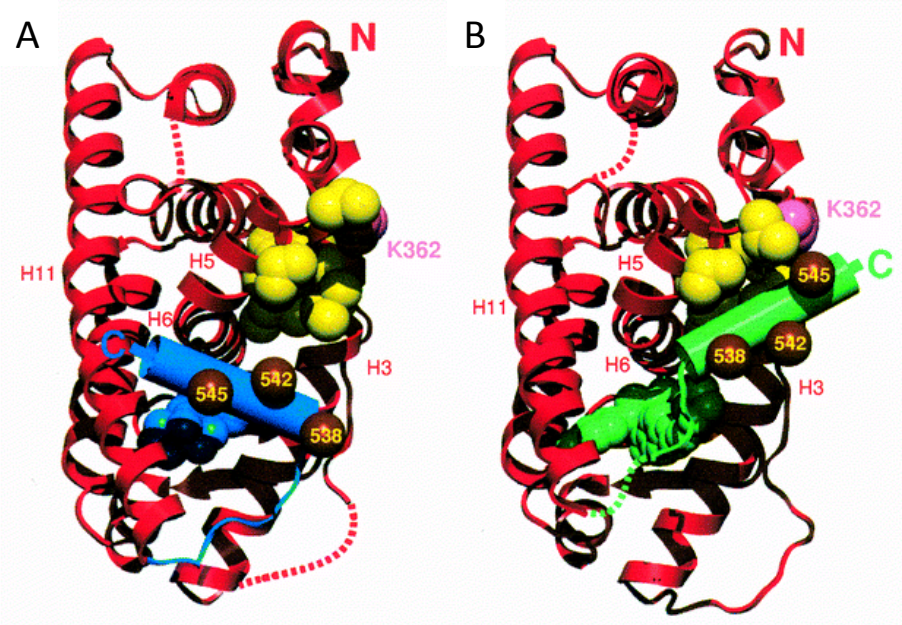


Figure 1.4 The repositioning of Helix 12 in the ER LBD by SERM Raloxifene

A. ER LBD-E2 complex and B. ER LBD-RAL complex. The ER LBD is shown in red with H12 highlighted in blue, in complex with Estrogen, and green, complexed with Raloxifene. Taken from Brzozowski et al (1997).

H12 is essential to the ability of the AF-2 to interact with co-activators. Loss or mutation in this area has been shown to result in a loss of responsiveness to ligand (Danielian et al., 1992). Although H12 is the main α-helix involved, mutational analyses also suggest that H3, H5/6 and H11 are important in ligand binding in ERα and other NRs (Henttu et al., 1997; Pakdel et al., 1993). On estrogen (E2) binding H12 sits over the binding cavity generating a groove on AF-2 enabling the binding of co-activators. This binding groove is formed by H3, H4, H5 and H12. Cofactor binding is stabilised by a charge clamp with a glutamic acid residue in H12 (Glu542) and a lysine at the C terminal end of H3 (Lys362) (Nolte et al., 1998; Pike et al., 2000). Binding of Raloxifene, displaces H12, thus changing the topography of this binding groove and enabling co-repressor recruitment (Pike et al., 2000). Tamoxifen competitively binds to the ER LBD AF2, to inhibit ERα activity in breast cancer cells. However, tamoxifen has estrogen-like (agonist) activity in many other estrogen target tissues, including bone, brain and the endometrium. This tissue selectivity of tamoxifen and related anti-estrogens has led to their being named selective estrogen receptor modulators, or SERMs. The mechanism behind this tissue diversity is multifactorial, poorly understood and and may be important in the development of endocrine resistance. One possible mechanism underlying the tissue-specific agonist or antagonist activity of SERMs is differences in relative levels of coactivators and corepressors (Shang and Brown, 2002). In agreement with this model, SRC1 coactivator levels are high in the Ishikawa (uterine carcinoma) cell line and low in MCF7 (breast carcinoma) cells where tamoxifen acts as an agonist and antagonist respectively. RNA interference mediated reduction in SRC1 levels in Ishikawa cells resulted in ERα mediated recruitment of the co-repressors NCOR/SMRT to ERα target genes and tamoxifen no longer behaved as an agonist. Knockdown of NCOR/SMRT in MCF7 cells resulted in tamoxifen behaving as an agonist (Jepsen et al., 2000). In both HepG2 and Hela cell lines the over expression/transfection of SMRT inhibits ERα basal activity and attenuates the agonism of 4HT by 70%. SRC1 over-expression does not rescue SMRT inhibition of 4HT agonism (Smith et al., 1997). A more recent study using chromatin immunoprecipitation (ChIP) with promoter microarray hybridization in breast

cancer T47D and endometrial cancer ECC1 cell lines also confirmed the above data, showing that differential co-factor recruitment altered the phenotype of tamoxifen i.e. over expression of SRC-1 or SMRT altered the transcriptional action of tamoxifen on a number of target genes (Romano et al., 2010). In nude mice transplanted with MCF7 cells and then treated over a prolonged period of time with tamoxifen resulted in a tamoxifen resistant tumour with low levels of NcoR (Lavinsky et al., 1998). Clinical data also supports this, with breast tumours with low levels of NcoR or negative for SMRT being associated with a short disease free survival (DFS) and shortened DFS and overall survival (OS), respectively (Girault et al., 2003) (Green and Carroll, 2007).

The crosstalk between cell surface receptor driven signalling pathways and transcriptional cofactors are also likely to play a role in the mechanism of action of SERMs and the development of resistance. This is still poorly delineated but can be seen in clinical outcome data. SRC1 (NCOA1) is over-expressed in 19-29% of breast tumours and high expression correlates with ERBB2 expression, lymph node positivity, disease recurrence, and poor DFS (Fleming et al., 2004a; Fleming et al., 2004b; Hudelist et al., 2003; Myers et al., 2004). *In vitro* data show that over-expression of SRC1 increases cell growth in MCF7 cells treated with estrogen (Tai et al., 2000) and knockdown decreases expression of estrogen responsive genes (Cavarretta et al., 2002), ERBB2 expression, Akt activation and CSF1 expression (Wang et al., 2009). There is less data available for SRC2 (TIF2 GRIP1 NCOA2), however expression has been shown to correlate with cyclin D1 expression in ERα+ breast tumours and *in vitro*, knockdown of SRC2 reduces estrogen induced cell proliferation and target gene expression (Cavarretta et al., 2002; Girault et al., 2003). Both SRC1 and SRC2 may act via induction of CXCL12 (Kishimoto et al., 2005). The SRC3 (AIB1, RAC3, ACTR, TRAM1, NCOA3, p/CIP) gene was originally identified by cloning genes in a region of the genome amplified in approximately 10% of breast tumours (Anzick et al., 1997). AIB1 protein expression has been reported to be elevated in 9.8% and 20% of cases in two different tumour cohorts,

with over-expression again correlating with larger tumour size, higher grade, poorer DFS and tamoxifen resistance (Anzick et al., 1997; Bouras et al., 2001; Girault et al., 2003; Hudelist et al., 2003; List et al., 2001; Osborne et al., 2003; Qin et al., 2008; Zhao et al., 2003). AIB1 and HER2, EGFR or HER3 coexpression is associated with a poor tamoxifen response (Kirkegaard et al., 2007).

Another mechanism advanced for the tissue specificity of SERMs is that the relative contribution of AF1 and AF2 in different tissues is important for agonist or antagonist activity, with AF1 activity associated with the agonist action of tamoxifen and lack of AF1 activity being linked to antagonism by tamoxifen (Mahfoudi et al., 1995). In support of this, *in vivo* studies using ERα knockout mice, mice lacking the ERα-AF1 and mice lacking AF2 have been used to demonstrate the tissue-selective importance of the two activation functions. For example, AF1 is required for estrogen responses in trabecular, but not in cortical bone (Borjesson et al., 2011) Whether AF1 activity is important in SRC1 recruitment in this context is unexplored, although SRC1 can be recruited to the ERα AF1 (Webb et al., 1998).

Fulvestrant and the related compound ICI164,384 binds to the LBD to impair ERα dimerization, promotes ERα export from the nucleus and its degradation (Dauvois et al., 1993; Parker, 1993; Parker et al., 1993). Anti-estrogens in this class have been named selective estrogen receptor downregulators (SERD) and fulvestrant-bound ERα also does not activate AF1 or AF2 (Osborne et al., 2004).

In view of the evidence of the shift in cofactor recruitment in tamoxifen resistant breast cancer the manipulation of the cofactor/ERα interaction has been identified as an attractive potential target for therapeutic benefit via the development of peptidomimetics. Treatment with LXXLL motif containing peptides would potentially block co-activator recruitment by competition (Galande et al., 2005; Leduc et al., 2003; McDonnell et al., 2000). However, peptides are difficult to

administer clinically due to proteolytic degradation (Gentilucci et al., 2010) and poor cell permeability. Work on cell permeable peptides targeting ERα-coactivator interactions began with the development of thioether side chain cyclization as a means of providing a redox stable isoteric replacement for the cystine disulphide. Peptides with disulphide linkages are potent inhibitors *in vitro*; however they are easily cleaved by intracellular glutathione (Galande et al., 2004). This work has not progressed further to date. Carraz et al designed synthetic cell-permeable LXXLL peptide probes using a nona-arginine tag and biotin to enable direct visualization with confocal microscopy, showing both direct inhibition of ERα-coactivator interaction as well as sequestration to the nucleolus in U2OS cells transiently transfected with full length ERα, thereby preventing interaction with EREs (Carraz et al., 2009). The nucleolar sequestration is an additional property of the nona-arginine tag.

Small molecule inhibitors (CBIs) targeting ERα-coactivator interactions were first published by the Katzenellenbogen laboratory using alkyl substituted pyrimidines which mimic the tether sites of the three leucines on the LXXLL coactivator binding motif with leucine like substituents. These compounds have shown high affinity in *in vitro* fluorescence anisotropy-based co-activator competition assays with Ki values in the region of 30μM (Parent et al., 2008; Rodriguez et al., 2004) and following development of a library of similar compounds an improvement of potency to Ki values 10 fold lower (Parent et al., 2008). Subsequently, there has been similar promising data with guanylhydrazone compounds (LaFrate et al., 2008; Shao et al., 2004; Zhou et al., 2007) and using compounds based on bicyclo(2.2.2)octanes (Zhou et al., 2007), pyridylpyridone scaffolds (Becerril and Hamilton, 2007) and amphipathic benzenes (Gunther et al., 2008). These studies have mostly assessed the experimental compounds at a biochemical level using the ERα LBD. Translation into cell based experiments with full length ERα has proved more challenging, with concern that the behaviour of the LBD in the context of the full length receptor may be different (Bapat and Frail, 2003).

1.2.4 Mechanisms of Resistance to Endocrine Therapy

The mechanisms of endocrine resistance have been extensively studied and are still poorly understood. Areas that have been targeted include:

- ER expression and mutations
- Cofactor expression and ratios
- Post translational modifications of ER (ER phosphorylation)
- Crosstalk between growth factors/cytokine driven signal transduction pathways.

The retention of a functional ERα in over 50% of patients tested shows that a change in ERα expression is not the main cause of endocrine resistance in the majority of patients treated with tamoxifen (Johnston et al., 1997). This is confirmed by clinical data and routine practice showing a further clinical response to second and third line hormone therapies such as faslodex and aromatase inhibitors (Dowsett et al., 2005). Mutations of ERα in in vitro data were discussed and published 15 years ago however the relative significance of these mutations in clinical specimens has taken much longer to confirm due to issues in detection methods (Fuqua et al., 2014). The Cancer Genome Atlas (TCGA) showed that significant breast cancer mutations occur in only aproximately 1-5% cases (Conway et al., 2007; Fuqua et al., 2000; Koduri et al., 2000; Stephens et al., 2012). It has since been discovered that high throughput sequencing is unable to detect K303R (lysine 303 to arginine) the somatic mutation in ERα first reported in 2000 by Fuqua et al. This mutation was shown to occur in one third of premalignant breast hyperplasia specimens and half of invasive carcinomas (Fuqua et al., 2000) and the consequential activation at S305 in ERα has been shown to occur in a preclinical model of aromatase inhibitor resistance (Barone et al., 2009). Other ERα mutations linked to endocrine resistance include Y537 (to asparginine) shown in 1/30 patients which resulted in a constitutively

active ERα with resistance to hormonal therapies. Phosphorylation at this site leads to poor clinical outcomes in patients treated with tamoxifen (Skliris et al., 2010).

Similarly Y537S mutation was found in 3/15 xenograft maintained tumour samples again showing constitutively active ERα with raised PgR levels maintaining estrogen responsiveness (Li et al., 2013) . 5/11 and 9/36 metastatic tumour samples in separate series (Robinson et al., 2013; Toy et al., 2013) are further evidence to support the frequency of this mutation. Less frequently E380 in ERα LBD (Robinson et al., 2013) and S118 (Piccart M et al., 2013; Sarwar et al., 2006). Over the last 15 years, with improvements in detection methods, it has therefore become clear that ERα mutations do play a role in mechanisms of resistance. For patients that do lose ERα, the mechanisms for this include methylation of the CpG islands in the promoter regions of ERα (Ottaviano et al., 1994).

Cofactor expression and ratios of expression in different tissue types is discussed above and certainly plays a role in the mechanism of action and acquisition of resistance to SERMs.

The phosphorylation of ERα at Ser118 in AF1 leads to ligand independent transcription of ERα regulated genes (Chen et al., 2002). This has been shown to be due to growth factor dependent activation of the MAPK/PI3K/Akt pathways. Similarly, activation via overexpression of transmembrane peptide growth factors such as EGFR and HER2 leads to cross talk with ERα signalling (Chen et al., 2002; Hutcheson et al., 2003; Knowlden et al., 2003). MCF7 cells that have been grown in estrogen deprived conditions over a sustained period of time demonstrate heightened estrogen sensitivity, ongoing transcription of ERα regulated genes and an increase in peptide growth factor activity (Hutcheson et al., 2003; Knowlden et al., 2003; Martin et al., 2003; Santen et al., 2008). Similarly in our own laboratory the transient overexpression of ERα in MCF7 cells grown in estrogen deprived conditions led to estrogen independence for growth, ongoing transcription of

estrogen regulated genes and an increase in P-AKT levels with an increased sensitivity to PI3K inhibitor (LY294002) (Tolhurst et al., 2010). The blockade of the EGFR/HER2 pathways has been shown to resensitise Her2 overexpressing xenograft models to endocrine treatment and prevent the development of endocrine resistance (Arpino et al., 2007; Gee et al., 2003; Schiff et al., 2004; Shou et al., 2004).

Our knowledge of the importance of crosstalk in the development of resistance to endocrine treatments led to disappointing initial clinical phase 1/2 trials combining endocrine therapy with an EGFR inhibitor (Gefitinib) in ERα positive patients with metastatic breast cancer, however, none of these trials selected according to EGFR/HER2 status. (Mita et al., 2005; Osborne et al., 2011). In aromatase inhibitor naïve patients with newly diagnosed metastatic breast cancer the addition of gefitinib did show a statistical advantage in PFS (8.4 months versus 14.7 months, HR 0.55) (Cristofanilli et al., 2010) and in the neoadjuvant setting two phase 2 trials have been reported (Polychronis et al., 2005; Smith et al., 2007b), with only the study that selected for EGFR status showing an improvement in the endpoint, suppression of Ki67 (Polychronis et al., 2005).

Patients with HER2 positive tumours are more likely to have increased *de novo* resistance to endocrine treatment due to the repression of ERα by activation of MAPK pathways (Oh et al., 2001). The addition of HER2 inhibitors (Trastuzumab) or a dual EGFR/HER2 inhibitor (Lapatanib) in a metastatic setting resulted in at least a doubling of PFS in two phase 3 trials (Johnston et al., 2009; Kaufman et al., 2009) and in a third clinical trial showed a non statistically significant improvement in PFS (Huober et al., 2012).

Similarly, in HER2 negative patients, combining endocrine treatment with everolimus, an MTOR inhibitor, phase 2 (TAMRAD) and phase 3 (BOLERO-2) clinical trials confirmed a significant improvement in PFS in patients treated with either tamoxifen or exemestane respectively, compared with hormone treatment

alone in patients previously exposed to endocrine treatment (Bachelot et al., 2012; Baselga et al., 2012). However another phase 3 study (HORIZON) of letrozole +/- temsirolimus or placebo in AI naive patients showed no difference in PFS (Wolff et al., 2013). Rapamycin was assessed in a phase 2 study in combination with tamoxifen and was stratified as to whether or not patients had previously received endocrine treatment. The results were not affected by prior exposure and showed a significant improvement in response rates and time to progression (Bhattacharyya, 2011). Again, a more detailed understanding of the abberrant pathways in each patient is likely to be required before significant results can be seen and there are a number of clinical studies which are ongoing, targeting PI3K/AKT/mTOR pathways in breast cancer, that will hopefully add to our understanding regarding patient selection and management (Palmieri et al., 2014).

1.3 Liver Receptor Homolog 1 (LRH-1)

1.3.1 LRH-1 is a member of the Nuclear Receptor Superfamily of Transcription Factors

LRH-1 is a member of the nuclear receptor superfamily (Figure 1.5). Specifically, LRH-1 belongs to the fushi-tarazu 1 subfamily (NR5A) of nuclear receptors (Laudet, 1997). The fushi-tarazu 1 subfamily (Ftz-F1) is characterized by a 26 amino acid Ftz-F1 box extension C-terminal to the DNA binding domain and the ability to bind DNA response elements as a monomer (Ueda et al., 1992). There are four identified members, NR5A1-4, and the evolutionary importance of members of the ftz-F1 subfamily is shown by conservation from caenorhabditis elegans (round worm) to humans (Asahina et al., 2000). LRH-1 has a number of alternative names: Pancreas hormone receptor (PHR-1), Fetoprotein transcription factor (FTF), Human B1-binding factor (hB1F) and Cyp7A1 promoter binding factor (CPF). LRH-1 orthologs are found in zebrafish, *xenopus*, chick, mouse, rat, horse and human. Human LRH-1

shares structural homology with murine LRH-1 (94% within the DNA binding domain and 89% within the ligand binding domain) and with human SF1 (NR5A1, 89% within the DNA binding domain and 65% within the ligand binding domain) (Fayard et al., 2004). The LRH-1 gene is located on chromosome 1 (C1q32.11) and codes for a 150 kilobase gene consisting of 8 exons (Zhang et al., 2001). At the mRNA level there are four identified isoforms arising from alternative splicing events (Thiruchelvam et al., 2011).

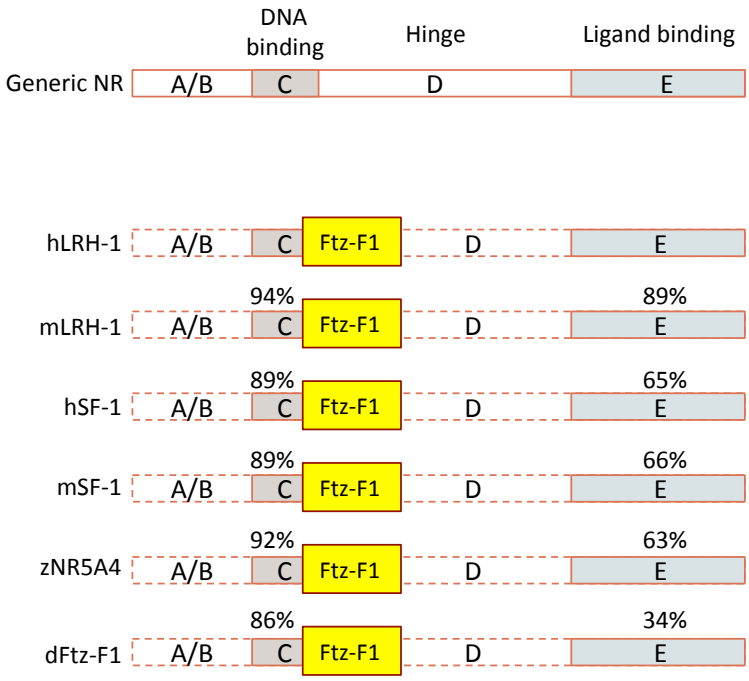


Figure 1.5 LRH-1 and the NR5A subfamily of nuclear receptor.
Canonical structure of NR is shown, together with structures of the NR5A subfamily. The location of the Ftz-F1 box between the DNA binding domain and the hinge region is highlighted. Percentage amino acid sequence identities for regions C and E are also shown, relative to human LRH-1 (hLRH-1). Mouse LRH-1 (mLRH-1), human SF-1 (hSF-1), mouse SF-1 (mSF-1), zebrafish NR5A family member (zNR5A4) and drosophila Ftz-F1 (dFTZ-F1). Not to scale. Adapted from Fayard et al (2004).

1.3.2 Crystallographic studies of the LRH-1 LBD

The crystal structure of the LRH-1 LBD has been solved (Krylova et al., 2005) (Ortlund et al., 2005), initially for murine LRH-1 and more recently human (Krylova et al., 2005; Li et al., 2003; Ortlund et al., 2005; Sablin et al., 2003). This reveals that the LBD has a characteristic protein folding, like other nuclear receptors with known ligands, with 12 α-helices, two ß-strands and H12 positioned in the active confirmation. In general, nuclear receptor LBDs are folded into three layers. An extension of H2 provides an additional fourth layer in LRH-1 (and SF1) and the main differences between human and murine crystal protein structures can be seen in the positioning of this fourth layer (Krylova et al., 2005). This extension of helix two is thought to stabilize H3, as in other liganded nuclear receptors, to provide a stable AF2 for co-activator binding (Figures 1.6 and 1.7) (Li et al., 2003) in the absence of a ligand. Initial studies showed that LBD pocket mutations did not seem to affect the functionality and activity of LRH-1 (Sablin et al., 2003). However, the presence of a conserved, hydrophobic, relatively enclosed binding pocket has provided impetus for de-orphanising LRH-1 and discovering both natural and synthetic ligands. Natural ligands have since been proposed in the form of phospholipids (Krylova et al., 2005; Ortlund et al., 2005), although the large hydrophobic binding pocket (820$Å^3$ (Sablin et al., 2003) compared with ERα, approximately 600 $Å^3$ (Brzozowski et al., 1997)) suggests a range of sized ligands could be accommodated. The binding of phospholipids is described in greater detail in section 1.3.6.

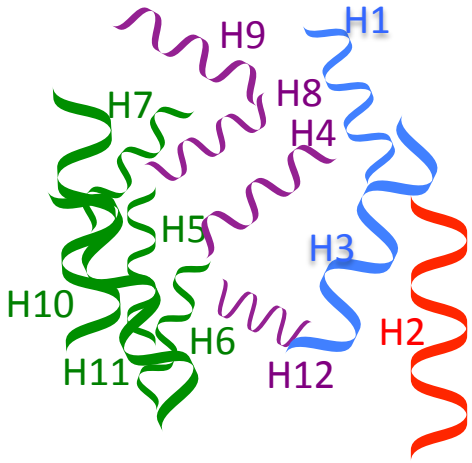


Figure 1.6 Schematic representation of the LRH-1 LBD showing the four layers formed by the 12 helices. Layer 1: green, Layer 2: purple, Layer 3: blue, Layer 4: red. Adapted from Sablin et al (2003)

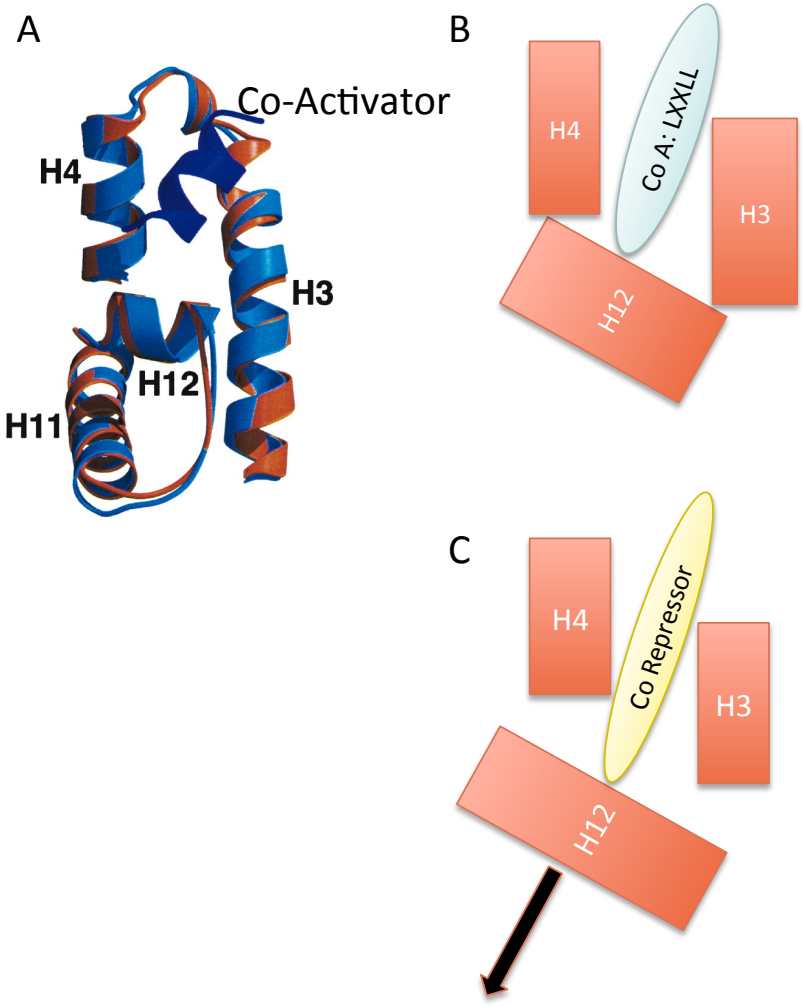


Figure 1.7 Coactivator binding to LRH-1 and RXR

A. Ribbon representation of helices 3, 4, 11 and 12 with LRH-1 shown in orange, RXR in light blue and the co-activator in royal blue. B. Schematic diagram of the binding of co-activator into the AF2 in comparison to C. showing the binding of co-repressor with displacement of H12. Adapted from Sablin et al (2003).

1.3.3 Expression and Function

LRH-1 is expressed in healthy endodermal tissues such as the liver, pancreas (Li et al., 1998; Nitta et al., 1999) and intestine (Botrugno et al., 2004), steroidogenic tissues such as adrenal (Wang et al., 2001), ovary, testis (Sirianni et al., 2002) as well as preadipocytes (Clyne et al., 2002) and embryonic stem cells (Gu et al., 2005; Heng et al., 2010; Wagner et al., 2010). It has a diverse number of functions including a key role in development, metabolism, proliferation, steroidogenesis and, more recently, a role in immune response has been identified.

1.3.3.1 Roles in Development and Stem Cells

Embryonal stem cells strongly express LRH-1. This expression has been carefully studied and mapped throughout murine embryogenesis. LRH-1 is present in all cells at the morula stage (E2.5= embryonal day 2.5) but by E3.5 is just in the inner cell mass and trophoectoderm of the blastocyst stage, limiting to the visceral endoderm by the egg cylinder stage (E5.5). Throughout gastrulation (E6.5-7.5), it is present in the endoderm and primitive mesoderm and by mid gestation (E8-15) is abundantly present in the endodermal tissues; liver, pancreas, intestine, bone and some parts of the brain. A similar pattern of expression then persists into adulthood in the liver, exocrine pancreas, ovary and intestine (Fernandez-Marcos et al., 2011; Pare et al., 2004; Rausa et al., 1999).

LRH-1 deficient mice embryos die at day E6.5 (Gu et al., 2005; Pare et al., 2004) due to a deficiency in OCT4, an important pluripotency factor in embryonic stem cells (Gu et al., 2005). OCT4 deficiency in mice embryos is also associated with lethality due to disruption of differentiation (Nichols et al., 1998). Furthermore, LRH-1 has been shown to also regulate Nanog, a gene essential for embryo development (Wagner et al., 2010).

At later stages of embryogenesis LRH-1 plays a role in liver development, regulating early expression of AFP and binding to the promoters of HNF-1α, HNF-3ß and HNF-4alpha hepatic nuclear factors involved in embryonic liver development (Fernandez-Marcos et al., 2011; Galarneau et al., 1996).

1.3.3.2 Metabolism

In the adult liver, LRH-1 plays an important functional role in bile acid homeostasis and reverse cholesterol transport. In humans, bile acids are important for the absorption of fat soluble vitamins and dietary fat from the intestine, and for the elimination of cholesterol by direct excretion into bile. Most of our understanding of the role that LRH-1 plays in this process comes from mice studies and there are significant interspecies variations in the regulation of this key process. The main difference between humans and mice models is that in mice excess cholesterol can be converted into bile acids. Humans do not have the ability to divert excess cholesterol into bile acids and therefore have a much greater tendancy to develop hypercholesterolaemia (Goodwin et al., 2003). In mice, this conversion occurs by a classical pathway that increases the synthesis of oxysterols, thereby activating LXRα and inducing Cyp7A1 (Lu et al., 2000) using LRH-1 as a competence factor. Conversion can also occur by the acidic pathway via Cyp27. Cyp8B1 is the enzyme crucial for synthesis of more hydrophobic bile acids, such as cholic acid (Fayard et al., 2004). Hydrophobic bile acids repress both Cyp7A1 and Cyp8B1, partly mediated by FXR which induces SHP, with SHP in turn repressing LRH-1 and LXR, and consequently repressing Cyp7A1 and Cyp8B1 transcription (Nitta et al., 1999).

The pancreas produces the enzyme, carboxyl ester lipase (CEL), which catalyses the hydrolysis of cholesteryl esters in the intestine, an important step in the absorption of dietary cholesterol from the intestine and the assembly and secretion of chylomicrons by enterocytes (Hui and Howles, 2002). CEL has an LRH-1 response element in its gene promotor and is co-expressed with LRH-1 in the exocrine

pancreas (Fayard et al., 2003), implicating LRH-1 in the regulation of CEL expression.

In the enterohepatic circulation at least two other enzymes/genes have been shown to be regulated by LRH-1 in the control of bile acid homeostasis; MRP3 and ABST. MRP3 (multi drug resistant protein 3, or ABCC3) is expressed in both murine and human intestine and liver. MRP3 is involved with the control of intracellular accumulation of bile acids by secretion into portal blood from enterocytes and hepatocytes (Bohan et al., 2003; Inokuchi et al., 2001). LRH-1 regulation appears to be mediated by two adjacent LRH-1 binding sites in the MRP3 gene promoter and requires TNF-α (Bohan et al., 2003; Inokuchi et al., 2001). ASBT (apical sodium-dependant BA transporter) actively transports bile acids through ileum enterocytes thereby mediating intestinal re-uptake of bile acids. Again in the mouse model, this is mediated by LRH-1 via cyp7A1.

Reverse cholesterol transport is the process by which high density lipoproteins transport cholesterol from peripheral tissue to the liver for excretion. SR-B1 (scavenger receptor type B1) and CETP (cholesteryl-ester-transfer protein) have both been identified as LRH-1 regulated genes. ABCA1 (ATP-binding-cassette transporter A1), is also known as the cholesterol efflux regulatory protein (CERP) and as its alternative name suggests, is involved with the efflux of cellular cholesterol to apolipoprotein to form high density lipoproteins (HDLs). A mutation in this gene causes Tangier's Disease in humans which results in very low levels of HDLs (Oram and Vaughan, 2000; Ordovas, 2000). Following the formation of HDLs, a process of remodeling occurs via CETP and the HDL is then circulated back to the liver via SR-B1. CETP transfers cholesteryl esters from HDL to triglyceride rich very low density lipoproteins (vLDL) and low density lipoproteins (LDLs) that are then cleared by the liver. The induction of CETP is prompted by high levels of cholesterol, mediated by LXR and potentiated by LRH-1 (Luo et al., 2001). SR-B1 mediates

hepatic uptake of cholesteryl esters from HDL, thereby facilitating cholesterol excretion. SR-B1 expression is induced by LRH-1 and decreased, as expected, in LRH-1 -/+ mice (Schoonjans et al., 2002) (Figure 1.8).

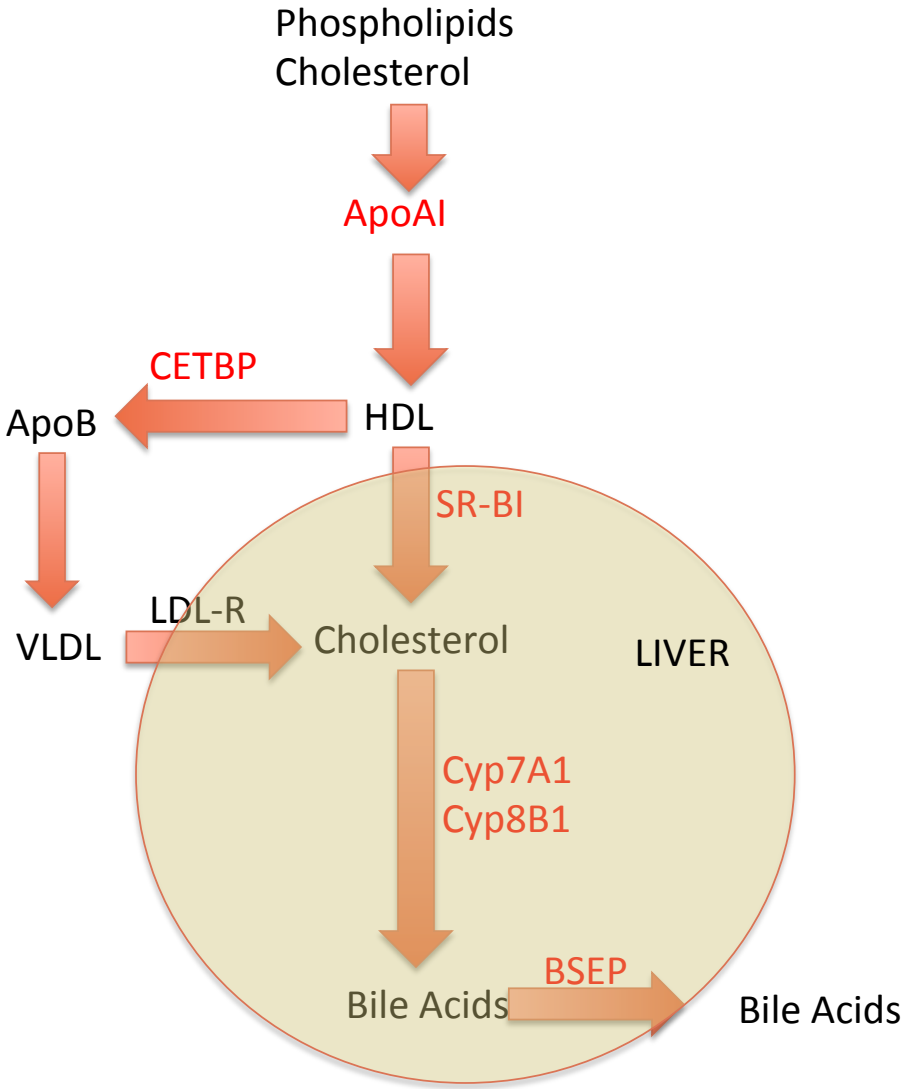


Figure 1.8 The Role of LRH-1 in cholesterol metabolism

LRH-1 is intricately involved in the metabolism of cholesterol and phospholipids. LRH-1 regulated genes are shown in red. Adapted from Lee and Moore, 2008.

1.3.3.3 Proliferation

LRH-1 is highly expressed in proliferative tissues (crypts) of the intestine, lost with differentiation and there is animal and cell based evidence showing that it is involved with coordinating intestinal cell renewal via cell cycle regulation (Botrugno et al., 2004; Mueller et al., 2006).

The role of LRH-1 in promoting cell proliferation has been demonstrated by the increased growth of two cell lines (with low basal expression of LRH-1), when transfected with both mouse and human LRH-1, and similarly in a tet inducible system. Animal models show a 20x faster growth of LRH-1 positive tumours in athymic mice injected with LTPA-hLRH-1 (murine pancreatic cells retrovirally transduced with human LRH-1) cells compared with control. The specific role of LRH-1 in the cell cycle was confirmed following an observed increase in the BrdU index of DNA synthesis. At both mRNA and protein level, growth arrested (serum starved) LRH-1 positive cells, on release from growth arrest (by addition of serum) resulted in an induction of cyclin D1 and E1 after four hours. This effect was confirmed with siRNA-mediated LRH-1 knockdown (Botrugno et al., 2004).

Within the intestine cellular proliferation occurs mainly in the crypts of Lieberkuhn. Mouse models with a heterozygous loss of LRH-1 (-/+) in the intestine have 40% reduction in mRNA in the duodenum, ileum and colon. Although no morphological differences could be detected, examination of the crypts showed that they were much shorter in the heterozygous -/+ mouse model than in wild-type mice, implying that proliferation is reduced. To confirm this Cyclin D1, cyclin E1, c-Myc, BrdU, Ki67 and H3 (marker of chromosomal condensation) were also assessed and were reduced (Botrugno et al., 2004). The action of LRH-1 in regulating proliferation in the crypts involves direct regulation of gene expression by binding of LRH-1 to DNA response elements in the cyclin E1 gene promoter and the recruitment of ß-catenin through a direct interaction between LRH-1 and ß-catenin (Botrugno et al., 2004).

Additionally, however, LRH-1 is recruited to Tcf4 binding sites in the cyclin D1 and c-Myc genes by interaction with ß-catenin. Thus, interaction between LRH-1 and ß-catenin appears to be critical, at least for promoting intestinal proliferation.

This data has been confirmed to some extent with alternative mouse models in which LRH-1 was specifically knocked out in the intestine (Lee et al., 2008). In this model, mice with no intestinal LRH-1 expression had reduced cyclin E1 and cMyc mRNA levels. However, in this model there was no detectable difference in BrdU proliferation index or Cyclin D1 levels in the LRH-1 knockout cells.

1.3.3.4 Steroidogenesis

Steroid hormones are synthesized from cholesterol. As described in section 1.3.4.2, LRH-1 plays an important role in reverse cholesterol transport and therefore contributes indirectly to the many cellular functions of cholesterol including steroid hormone biosynthesis. LRH-1 also plays a direct and critical role in reproduction. It is expressed in the granulosa and luteal cells of the ovary and mice lacking LRH-1 in granulosa cells are sterile due to anovulation (Duggavathi et al., 2008). This is thought to be due to dysregulation of the prostaglandin and hyaluronan pathways and key regulators in the progesterone pathway because of reduced expression of direct LRH-1 targets such as StAR and Cyp11A1 (cholesterol-side-chain-cleavage protein) (Duggavathi et al., 2008; Sirianni et al., 2002; Stocco, 2001). StAR controls the movement of cholesterol to Cyp11A1, the rate limiting enzyme in the conversion of cholesterol to pregnenolone (Stocco, 2001). HSD3B2 (3β-hydroxysteroid dehydrogenase type II), which converts pregnenolone in the corpus luteum to progesterone is also regulated by LRH-1 (Peng et al., 2003). Progesterone can be catalysed by 17α-hydroxylase into androgens such as testosterone which in turn are converted, in the ovarian follicle, to estrogen by Cyp19 (aromatase) (Fayard et al., 2004). Cholesterol is delivered to steroidogenic tissues by SR-B1, which is LRH-1 regulated (section 1.3.4.2). Cyp19 is widely expressed in both ovarian granulosa and

in luteal cells and CYP19 expression follows the onset of expression of LRH-1, suggesting that Cyp19 expression is regulated by LRH-1 (Hinshelwood et al., 2003) (see also section 1.3.6.1).

With further regard to steroidogenesis, LRH-1 has also been implicated in the regulation of extra-adrenal glucocorticoid production in the intestine. The intestine synthesises and secretes glucocorticoids in a paracrine manner to regulate local immune cell homeostasis (Noti et al., 2009). This was discovered by injecting mice with a CD3 antibody, triggering T-cell activation, which induced a counter regulatory immune response in intestinal epithelial cells, strongly inducing expression of cyp11A1 and cyp11B1. Cyp11A1 is the enzyme responsible for the steroidogenic cholesterol side chain cleavage enzyme p450scc that converts cholesterol to pregnalone. Cyp11B1 (11ß-hydroxylase) catalyses the conversion of deoxycorticosterone into corticosterone. This response appears to be limited to the basal compartment of the intestinal mucosa (Cima et al., 2004) where the crypts are located and where LRH is predominantly expressed. LRH-1 has been shown to be essential for local production of corticosterone via regulation of Cyp11A1 and cyp11B1 (Mueller et al., 2006).

1.3.3.6 Immune response

LRH-1 negatively regulates the acute phase response proteins in the liver. LRH-1 heterozygous knockout mice injected with lipopolysaccharide (LPS), a membrane component of gram-negative bacteria which induces a cytokine response and therefore an acute phase response, resulted in the worsening of inflammation by excess expression and protein secretion of serum amyloid A, haptoglobin and C reactive protein (CRP) via IL1β and IL6 (Kim et al., 2003; Venteclef et al., 2011). The treatment of human hepatocytes with the LRH-1 agonist GSK8470 (Whitby compound 5A) (Whitby et al., 2006) (Whitby et al., 2011) repressed the acute phase response (Venteclef et al.). The mechanisms by which LRH-1 is thought to regulate

this process is unclear, but evidence so far indicates that LRH-1 inhibits the CCAAT-enhancer-binding proteins (C/EBP) signalling pathway (Venteclef et al., 2006) and regulates IL-1 receptor antagonist (IL-1RA) gene expression, a well described anti-inflammatory protein known to modulate inflammatory responses both *in vitro* and *in vivo* (Venteclef and Delerive, 2007). The C/EBPs are a family of leucine zipper transcription factors involved in the control of inflammation and native immunity (Poli, 1998). All of the acute phase response genes inhibited by LRH-1 had C/EBP DNA binding sites within their promoter regions and and transfection experiments showed that LRH-1 negatively regulates the acute phase response gene expression by antagonising the C/EBP signalling pathway (Venteclef et al., 2006). This has since been postulated to occur by the SUMOylation of LRH, whereby ligand binding triggers the stabilisation of the SUMOylated LRH-1 pool which then interacts with co-repressor complex and prevents the dissociation of the co-repressor complex from gene promoters of acute phase response genes (Venteclef et al.).

Extra-adrenal glucocorticoid synthesis regulated by LRH-1 in the intestine, (see previous section), also adds to the role of LRH-1 in the immune system (Coste et al., 2007; Mueller et al., 2006).

1.3.4 LRH-1 is expressed in Breast Cancer and Breast Cancer Associated Stroma

There is increasing evidence implicating LRH-1 in breast cancer. An immunolocalisation study looking at 88 invasive primary breast cancer specimens showed that 43.2% (38 out of 88) and 27.8% of DCIS specimens (5 out of 18) expressed LRH-1 (Miki et al., 2006). This study confirmed data from a prior study showing elevated mRNA levels of LRH-1 and aromatase in adipocytes adjacent to breast carcinoma and carcinoma cells. The immunolocalisation studies of LRH-1 in breast cancer also revealed that LRH-1 positivity is significantly associated with ERα status in breast tumours (Miki et al., 2006).

1.3.4.1 LRH-1 regulation of Aromatase gene expression

In pre-menopausal women estrogen production mainly takes place in the ovaries. However in post-menopausal women, the major source of estrogen is due to the conversion of circulating androgens to estrone or estradiol in peripheral tissues, such as adipose tissue and in estrogen target tissues such as breast, brain, endothelium and skin (Figure 1.9). The key step in conversion of androgens to estrogens is mediated by the aromatase enzyme (CYP19).

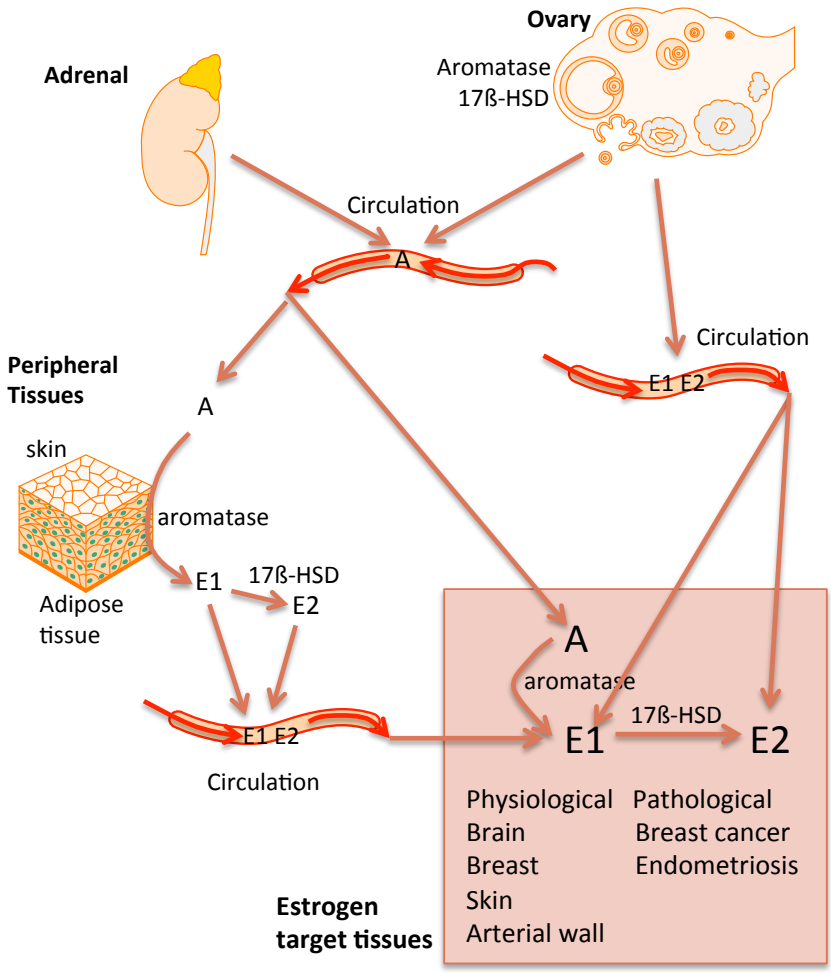


Figure 1.9 The Origins of Estrogen in Women

Estradiol (E2) is produced by direct secretion from the ovaries in reproductive-age women. It is also produced by the conversion of adrenal and ovarian androstenedione (A) to estrone (E1) in peripheral tissues and in estrogen target tissues. Estrone is converted to estradiol (E2) by the enzymes aromatase and 17β-hydroxysteroid dehydrogenase (17β-HSD). Adapted from Bulun et al (2005).

Immunostaining studies have shown that aromatase is expressed in cancer-associated fibroblasts (pre-adipocytes), stromal and parenchymal cells in breast cancer and is thought to act to produce estrogen which drives breast cancer growth and proliferation in both an autocrine and paracrine manner (Knower et al., 2013; Miki et al., 2006; Miki et al., 2007; Zhou et al., 2005). The induction of CYP19, and thus the protein aromatase, occurs through the use of alternative promotors in different tissues. For example in the ovary, where CYP19 expression is largely driven by follicle stimulating hormone (FSH) activated signalling, CYP19 expression occurs through the use of promoter II. By contrast, in the placenta CYP19 is regulated in response to retinoids via promoter 1.1 and in bone and adipose tissue, expression mainly occurs through the use of promoter 1.4 (Figure 1.10) (Clyne et al., 2002). The mechanism of regulation of aromatase in pre-adipocytes adjacent to breast carcinomas differs compared with pre-adipocytes in normal breast tissue stroma. The promoter usage changes from 1.4 in normal breast tissue stroma to the use of promoters II, 1.3 and to a small extent, promoter 1.7 in breast cancer associated pre-adipocytes (Figure 1.11) (Agarwal et al., 1996; Harada et al., 1993; Sebastian et al., 2002; Zhao et al., 1996).

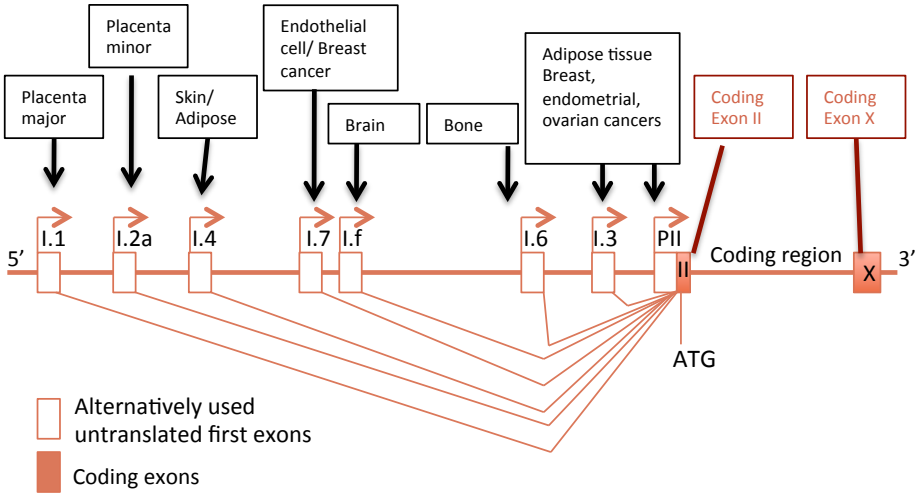


Figure 1.10 The CYP19 (Aromatase) gene. Tissue specific activation and expression of aromatase protein occurs via alternative splicing of a number of promoters. Adapted from Bulun et al (2005).

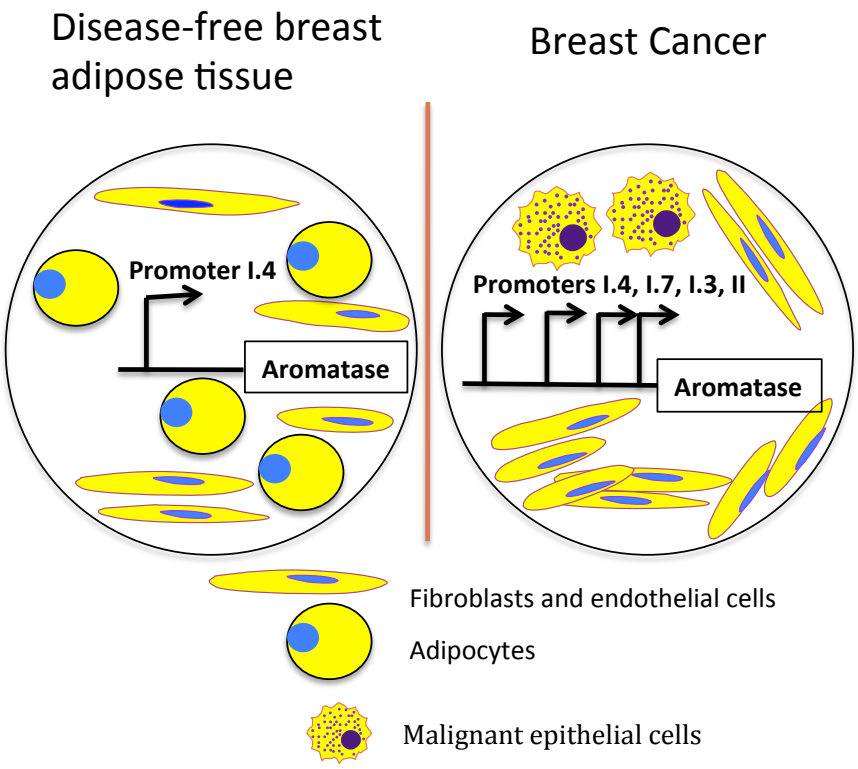


Figure 1.11 Regulation of aromatase gene expression in the breast. The promoter use for aromatase expression changes in malignant epithelial cells compared with benign endothelial cells, fibroblasts and surrounding adipose tissue. In non malignant breast tissue total aromatase mRNA levels are low with promoter I.4 predominantly used whereas in estrogen receptor positive breast cancer total mRNA aromatase levels are higher and useage changes to II, I.3, I.7 and I.4. Adapted from Bulun et al (2005).

LRH-1 is also expressed in cancer associated fibroblasts, shown in experiments at an mRNA level and also by confirmatory quantitative IHC in an independent cell line panel (Knower et al., 2013). LRH-1 knockdown and chromatin immunoprecipitation studies show LRH-1 directly binds to a response element in aromatase promoter II with LRH-1 knockdown resulting in a decrease in total aromatase mRNA and forskolin/PMA mediated aromatase expression (Chand et al., 2011; Wu et al., 2011). This confirms previously published studies using the mouse preadipocyte cell line (3T3-L1) and primary cultures from human breast adipose tissue (Clyne et al., 2004; Clyne et al., 2002). Adenoviral overexpression of LRH-1, in the rat testis, leads to large increases in mRNA aromatase levels, again with confirmation of direct binding of endogenous LRH-1 to aromatase PII by ChiP (Sierens et al., 2010).

1.3.4.2 LRH-1 is an ERα-regulated gene in breast cancer cells

LRH-1 is expressed in ERα-positive breast cancer cell lines and in MCF-7 cells its expression was ERα-regulated ((Annicotte et al., 2005), a finding subsequently confirmed in our own laboratory (Thiruchelvam et al., 2011).

In our studies, a tetracycline-regulated dominant-negative ERα, PLZF-ERα, in which the DNA and ligand binding domains of ERα were fused C-terminal to the transcriptional repression domains of the PLZF transcription repressor (Figure 1.12), resulted in tetracycline-dependent inhibition of MCF-7 cell growth (Buluwela et al., 2005). PLZF-ERα was used, since a naturally occurring t(11;17) translocation in acute promyelocytic leukaemia (APL) fuses the transcriptional repressor, PLZF (promyelocytic leukaemia zinc finger) with the DBD and LBD coding regions of the RARα (retinoic acid receptor α) gene, resulting in silencing of retinoic acid regulated genes (Chen et al., 1993).

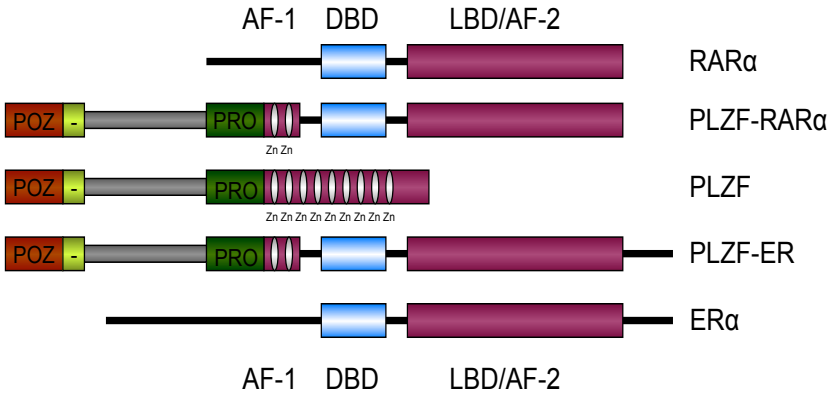


Figure 1.12 A schematic representation of the PLZF-ERα fusion protein.

PLZF-RARα is the protein resulting from the t(11;17) translocation naturally occurring in acute promyelocytic leukaemia (APL). The analogous portion of ERα has replaced RAR fused to PLZF. The POZ domain is required for mediating the recruitment of the Sin3A HDAC complex and nine zinc fingers.

Gene expression microarray analysis of this line identified 1,627 estrogen-regulated genes, numbers similar to those reported by other studies. However, only 149 of these genes were additionally repressed upon PLZF-ERα expression, suggesting that these estrogen regulated genes are especially important for the growth of MCF-7 cells in response to estrogen. One of these 149 genes was LRH-1. This study identified an ERα binding site located 10 kb upstream of the major LRH-1 gene transcription start site in MCF-7 cells.

Importantly, these studies use siRNA mediated LRH-1 silencing to demonstrate that LRH-1 is required for estrogen-stimulated growth of MCF-7 cells (Annicotte et al., 2005; Thiruchelvam et al., 2011). Moreover, LRH-1 was shown to regulate ERα expression through binding to LRH-1 binding sites in the ERα gene promoter (Thiruchelvam et al., 2011), identifying a positive feedback loop in which ERα stimulates LRH-1 expression and LRH-1 in turn up-regulates ERα. Subsequent LRH-1 ChIP-seq in MCF-7 cells demonstrated that LRH-1 is required for the recruitment of ERα to its binding sites, indicative of co-operativity between LRH-1 and ERα at ERα target genes in breast cancer cells (Lai et al 2013). In addition to its importance for the growth of ERα-positive breast cancer cells, LRH-1 has also been shown to promote breast cancer cell motility and invasion (Chand et al., 2012).

1.3.5 LRH-1 Ligands

1.3.5.1 LRH-1 and SF-1 are Ftz-f1 subfamily members of the nuclear receptor superfamily that bind Phospholipids

LRH-1 and SF-1 have been classed as orphan nuclear receptors due to the lack of identified ligands. However, clues to potential ligands were provided by crystallographic determination of their LBDs. These structures were generated from expression of the LBDs in bacterial cells and the structures showed the presence of bacterial phospholipids in the ligand-binding pocket of both murine (although only a very small proportion ~10%) and human LRH-1 LBDs (Krylova et al., 2005; Li et al., 2005; Ortlund et al., 2005; Sablin et al., 2009; Sablin et al., 2003; Sablin et al.,

2008; Wang et al., 2005b). Mutations in the LRH-1 LBD, that reduced phospholipid binding to the LBD, inhibited coactivator recruitment and transcriptional activity (Li et al., 2005; Ortlund et al., 2005). What is not clear from these studies is whether the phospholipids are ligands for these receptors, or if the phospholipids are required simply for maintaining the structural integrity of the LBD. However, a recent publication shows that phosphatidylcholines (PC), in particular dilauroyl phosphatidylcholine (DLPC) and diundecanoyl phosphatidylcholine (DUPC), stimulate LRH-1 activity and displace bacterial phospholipids from the LBD (Lee et al., 2011; Ortlund et al., 2005). These PCs are dietary lipids, which decrease hepatic steatosis and serum glucose levels in mouse models of insulin resistance (Lee et al., 2011) and which may therefore be *bona fide* ligands for LRH-1. A subsequent publication confirmed that DLPC (PC 12:0-12:0, a medium chain phosphatidylcholine) acts as an LRH-1 agonist, resulting in increased binding of LRH-1 with the coactivators SRC1 and TIF2, whilst having no effect on recruitment of PGC1α by LRH-1 and abolishing the interaction of LRH-1 with SHP. The same study generated LRH-1 LBD lacking phospholipids in the LBD by denaturation/renaturation (apo LRH-1) and found that apo-LRH-1, but not the DLPC-bound LRH-1 LBD interacted with high affinity with the transcriptional corepressor SMRT (Musille et al., 2012).

The large size of the LRH-1 ligand binding pocket and the visualization of bacterial phospholipids on crystallography has led to the hypothesis that there are other endogenous ligands for LRH-1 and SF-1, such as sphingolipids.

LRH-1 expression is up regulated by sphingosine-1-phosphate (S1P) in MCF7 cells in a PGE2 dependent manner by stimulating the recruitment of LRH-1, CREB, C/EBP and PolII to the LRH-1 promoter (Hadizadeh et al., 2008).

Sphingosine and lyso-sphingomyelin have been shown to act on SF1 by increasing the recruitment of SMRT and decreasing the SF1 dependent transcription of CYP17

reporter constructs (Urs et al., 2006), however, sphingosine had no effect on proliferation or transcription in SF1 positive cells (Doghman et al., 2009).

Sphingomyelin is a structural component of all cell membranes. Hydrolysis of sphingomyelin produces ceramide, which can be additionally hydrolysed to sphingosine. Structurally sphingosine is a sphingolipid comprising of a long-chain sphingoid base backbone, a polar head group and an amide linked long chain fatty acid. The phosphorylation of sphingosine by two iso-enzymes, sphingosine kinase 1 and 2 (SK1 and SK2) produces sphingosine-1-phosphate (S1P). S1P is known to act via a multitude of cell signalling pathways especially via GPCRs (Maceyka et al., 2012) inducing cell proliferation, prolonging cell survival and promoting the release of pro-angiogenic cytokines. In murine xenograft models, using a monoclonal antibody against S1P, tumor invasion is substantially reduced (Visentin et al., 2006). Overexpression of S1P in NIH3T3 and HEK293T cell lines results in cellular transformation with increased cell growth and serum independent survival (Pitson et al., 2005). Elevated levels (2 fold or more) of sphingosine kinase mRNA have been identified in a range of tumours compared with matched adjacent non cancerous tissue (French et al., 2003). More recently S1P has been confirmed in in vitro studies to be important for tumour progression and tumour induced haemaniogenesis and lymphangiogenesis in breast cancer (Nagahashi et al., 2012).

Sphingolipids are important in the progression of cancer however there is little direct evidence, as yet, for their direct role as ligands for LRH-1 and SF-1.

1.3.5.2 Atrazine

Atrazine is a widely used herbicide, which causes demasculinization, feminisation and reproductive abnormalities on fish, amphibians and mammals. It has been shown to activate aromatase in an SF-1 dependent manner (Fan et al., 2007a; Fan et al., 2007b; Suzawa and Ingraham, 2008). The mechanism of this activation has not been confirmed.

An initial study demonstrated that activation by atrazine does not occur by binding to the SF-1 LBD, but suggested, via mutational studies, that it does occur by direct binding to the DBD. The same study demonstrated proof of a physical interaction between SF-1 and atrazine by using a 27Mhz quartz crystal microbalance measuring the decrease in frequency with increasing physical mass following the addition of recombinant SF-1 to immobilized atrazine (in comparison with a positive control: phospholipid and negative control). In this paper no activation of other members of the NR5A family was seen, notably LRH-1.

A subsequent paper by Suzawa et al confirmed that the activation of aromatase by SF-1 in response to atrazine but also showed activation by LRH-1. It confirms that this does not involve the binding of Atrazine to the SF-1 ligand binding domain, as it does not activate a Gal4-SF-1 LBD fusion construct but also does not increase DNA binding of SF-1. Similarly, it was unable to displace bound phospholipid (phophatidyl glycerol) or an exchanged PIP3 ligand present in the LBD and atrazine also stimulated SF-1 LBD pocket mutants. Suzawa et al hypothesise that atrazine acts indirectly by increasing the intracellular production of cAMP, phosphorylation of SF-1 and by generating SF-1 ligands (Suzawa and Ingraham, 2008).

1.3.5.3 Inverse agonists SF-1

As described above, the SF-1 LBD is structurally extremely similar to the LRH-1 LBD (65% amino acid sequence identity). Using a Receptor Selection and Amplification Technology (R-SAT) screening approach, a cell-based functional assay that allows the monitoring of receptor-dependent proliferative responses, which is a technique previously validated and used for other receptor types such as tyrosine kinases and GPCRs, screening of 280,000 compounds with drug like characteristics identified a SF-1 inverse agonist 4-(heptyloxy)phenol AC-45594 (IC50 = 50-100nM). Analogues with different alkyloxy chain lengths showed that compound activity was constrained by a 6-10 carbon length chain (Del Tredici et al., 2008). This alkyl chain, is noted, by the authors, to be a feature in other potential SF-1 ligands such as

phosphatidylinositol (Krylova et al., 2005; Ortlund et al., 2005; Wang et al., 2005b) and sphingosine (Urs et al., 2006).

Madoux et al screened 64,908 compounds from the National Institute of Health's molecular libraries Small Molecule Repository with a transactivation luciferase reporter cell-based assay using a chimeric SF-1 construct in which the SF1 LBD was fused to the GAL4 DBD (Madoux et al., 2008). This screen identified two isoquinolinones with IC_{50} values of 255nM and 760nM, as inhibitors of SF-1. Their inhibitory activity was confirmed in a reporter gene assay using full-length SF1 (IC_{50} = 16 and 30nM). Moreover, these compounds were selective for SF-1 over LRH-1 Subsequent work developed two analogues with improved potency and selectivity against other nuclear receptors (Roth et al., 2008).

The proliferative effects of these two classes of compound were tested in H295R adrenocortical carcinoma cells positive for SF1 and in SW-13 cells that do not express SF-1. The alkyloxyphenol compounds had significant off-target effects and decreased growth in both cell lines, whereas the isoquinolones were active only in the SF1-positive cells (Doghman et al., 2009). However, the activity of these isoquinolones was not reproduced by another study (Whitby et al., 2011).

1.3.5.4 Synthetic small molecule agonists of LRH-1 and SF-1

Whitby et al published the first synthetic small molecule agonists for LRH-1 and SF-1. The lead compound, 5A (GSK8470) has a cis-bicyclo(3.3.0)oct-2-ene skeleton. The functionality of this compound was tested using a LRH-1 responsive SHP gene promoter driving the firefly luciferase gene. Co-transfection of LRH-1 and the reporter gene showed a modest stimulation of LRH-1 by compound 5A and established an EC_{50} of 1μM. Moreover, compound 5A stimulated expression of the endogenous SHP gene in the liver HepG2 cells and in primary hepatocytes (Whitby et al., 2006). The problems with this compound related to acid instability, biological variability and nuclear receptor promiscuity, as it activates LRH-1, SF-1 and to a lesser extent ERα. Since then, Whitby et al have developed a new series of LRH-1

agonists. Of the new series, compound RJW101 was selective for LRH-1 but with poor potency, whilst compound RJW100 activated both LRH-1 and SF1. Other compounds described were selective for SF-1 (Whitby et al., 2011). This publication also reported a crystal structure of the human LRH-1 LBD with compound 5A, which shows that compound 5A sits within the binding pocket, occupying a similar volume as the terminal 12 carbon atoms in both chains of the phospholipid. The binding pocket was seen to contract to about 5Å, indicating that the LRH-1 ligand binding pocket is extremely flexible and takes up a conformation appropriate to the size of the bound molecule (Whitby et al., 2011).

1.3.6 LRH-1 Co-Factors

1.3.6.1 LRH-1 Co-Activators

LRH-1 coactivators include PGC1α, SRC1, SRC2 and SRC3, FXR and MBF-1. PGC1α is important for the potentiation of transcriptional activity of LRH-1 in hepatocytes, progesterone production in ovarian granulosa cells and has been implicated in the regulation of aromatase in preadipocytes (Clyne et al., 2002; Safi et al., 2005; Shin and Osborne, 2008; Yazawa et al., 2010). SRC1 and SRC2 have both been shown to be co-activators for LRH-1, although the binding of SRC1 appears to be via an alternative mechanism than the classical LXXLL binding region, and involves a glutamine rich domain of SRC1 and the helix1 and AF2 regions of LRH-1. SRC-1 and SRC-2 interact with LRH-1 in a mammalian 2 hybrid assay and in GST pull down assays, to potentiate its activity (Xu et al., 2004).

Another co-activator identified with an alternative binding mechanism is MBF-1, which does not have an LXXLL motif but interacts with the Ftz-F1 box in the DBD. It seems to act as a bridging factor by binding to TATA box binding protein (TBP) or to the transcription factor IID (TFIID) complex (which includes TBP) (Brendel et al., 2002).

FXR is a nuclear receptor, predominantly expressed in the liver and intestine. It is a key regulator of enterohepatic bile acid metabolism. ChIP-seq and co-immunoprecipitation experiments have shown that FXR and LRH-1 function together to co-regulate expression of target genes (Chong et al., 2010). Similarly LRH-1 has been shown to be required for maximal activation of the fatty acid synthase (FAS) gene by the nuclear receptor LXR (Matsukuma et al., 2007). LXR is a nuclear receptor that acts as a cholesterol sensor in the liver and has at least 26 direct gene targets relating to bile acid, lipid and glucose metabolism, as well as playing a role in inflammation and immune responses (Calkin and Tontonoz, 2012).

These alternative binding mechanisms and functions of LRH-1 have led to suggestions that LRH-1 functions as a competence factor i.e by binding to other nuclear receptors and transcriptional complexes to promote gene expression (Lazarus et al., 2012). The co-operative action of ERα and LRH-1 in breast cancer cells, which we have recently established (Lai et al 2013), fits into this model of LRH-1 action.

1.3.6.2 LRH-1 Co-Repressors

LRH-1 co-repressors include SHP, DAX-1, PIASγ and PROX-1. SHP and DAX-1 are both orphan nuclear receptors that lack a DNA binding domain and share 41% structural homology in the LBD (Lee and Moore, 2002). They have both been identified as co-repressors of LRH-1 that act by competitive inhibition of co-activator binding (Zhang et al., 2000). The binding of SHP to LRH-1 has been demonstrated in mammalian two hybrid assays, and GST pull-down experiments (Lu et al., 2000). Studies also suggest a second mechanism of action via a C-terminal autonomous repression function in SHP. Point mutations within this region of SHP lead to abrogation of LRH-1 mediated transactivation (Lee and Moore, 2002; Nishigori et al., 2001; Seol et al., 1997). SHP has two motifs that closely resemble LXXLL motifs (ILYTLL = ID1 and ILKKIL – ID2 (Johansson et al., 2000; Li et al.,

2005)) in the AF-1 region. These two motifs were studied in an in vitro Alpha Screen using purified human LRH-1 LBD, showing preferential binding to LRH-1 over coactivator-derived LXXLL motifs (Li et al., 2005). The crystal structure of the LRH-1 LBD and SHP ID1 shows a conformational change in the topology of the LRH-1 co-activator binding site allowing high affinity SHP binding.

Full length DAX-1 binds to the LRH LBD in *in vitro* GST pull down assays. Crystal structures of the Dax-1/LRH-1 LBD complex reveal that binding occurs as a trimeric structure and subsequent analyses have shown this to be a Dax-1 homodimer and a LRH-1 monomer. There do not appear to be any conformational changes seen in the LRH-1 LBD on Dax-1 binding. Mutational analyses have confirmed that the first Dax-1 protein binds in the co-activator groove via a repression helix and the N-terminal part of H9, with the sequence PCFXXLP. The second Dax-1 is positioned just outside the LRH-1 ligand binding pocket but binds to the LRH-1 LBD using the same region in Dax-1 as the first Dax-1 molecule i.e. the repression helix and PCFXXLP motif (Sablin et al., 2008).

PIASγ (Protein inhibitor of activated STAT) represses LRH-1 mediated transactivation of CYP11A1 in luciferase assays. Mutant constructs confirm that this requires the PIASγ repression domain 1 (RD1) rather than repression domain 2 (RD2) (Hsieh et al., 2009). PIASγ can act as an E3 SUMO ligase and enhances substrate SUMOylation, causing repression of activity, however in the LRH-1 SUMOylation deficient mutant (K289R) repression of CYP11A1 expression occurred to the same level as the wild type indicating that the PIASγ induced repression of LRH-1 is not associated with LRH-1 SUMOylation. Mammalian two-hybrid and co-immunoprecipitation studies confirm previous publications showing that the interaction of SRC1 with LRH-1 is via the LRH-1 AF2 region (Xu et al., 2004) and went on to show that co-transfection of PIASγ with VP16–SRC-1 and Gal4–$LRH_{191-560}$

resulted in complete abrogation of the interaction, suggesting that PIASγ competes with SRC1 (Hsieh et al., 2009).

PROX-1 as a potential cofactor for LRH-1 was initially identified as a nuclear receptor interacting protein in a yeast-2-hybrid screen (Johansson et al., 1999). Subsequently it has been confirmed in mammalian cells and in vitro as a direct interaction with LRH-1 via the entire LRH-1 LBD (aa 317- 560) and a portion of PROX-1 containing two LXXLL motifs within amino acids 48-132 (Steffensen et al., 2004). The importance of PROX-1 for LRH-1 function is yet to be determined, although high expression of PROX-1 is seen in many LRH-1 target tissues such as liver and pancreas, with lower levels in the ovary and small intestine. (Steffensen et al., 2004)

1.3.7 Post-translational modifications of LRH-1

Potential means of regulating LRH-1 activity, other than ligands and cofactors include post-translational modifications, particularly phosphorylation and sumoylation (see above). Activation of the ERK1/2 MAPK pathway has been shown to lead to phosphorylation of Ser-238 and Ser-243 in the LRH-1 hinge domain. This leads to stimulation of transactivation by LRH-1. Mutation of these serines to alanine eliminates the PMA induced phosphorylation of LRH-1 and decreases transactivation. Conversely, mutation to aspartate (i.e. mimicking the effects of phosphorylation) increases LRH-1 activity (Lee et al., 2006).

Sumoylation occurs in the hinge region of LRH-1 and results in repression of transcriptional activity by the localization of LRH-1 in the transcriptionally inert promyelocytic leukaemia protein bodies (Chalkiadaki and Talianidis, 2005). Forskolin and Cholera toxin both inhibited the accumulation of LRH-1 in nuclear bodies, suggesting that the cAMP signalling pathway is involved in the regulation of LRH-1 sumoylation (Yang et al., 2009).

However, the importance of these post-translational modifications in the context of co-factors and potential ligands was queried by the findings that the agonists DLPC and DUPC continued to activate mutant LRH-1 constructs i.e. LRH-1 derivatives that have inactive LRH-1 responses to phosphorylation and sumoylation respectively (Lee et al., 2011). This has been interpreted to mean that the LRH-1 LBD and potential ligands are of greater regulatory importance than post-translational modifications (Lazarus et al., 2012).

1.4 Aims

Estrogens are known to promote breast cancer development and progression. Estrogen actions are largely mediated by ERα and endocrine agents (anti-estrogens, aromatase inhibitors) are used to inhibit ERα activity in breast cancer cells. These therapies have contributed considerably to the falls in breast cancer mortality over the last 2-3 decades. However, many patients do not respond to these therapies, whilst many patients become resistant following a period of response. Endocrine resistance therefore represent a clinically important problem. Unfortunately, the mechanisms underlying endocrine resistance remain largely unclear. Studies to understand mechanisms underlying endocrine resistance are therefore urgently needed. Additionally, it is important to identify new therapeutic targets that could be used for the treatment of endocrine resistant breast cancer.

Previous studies in the group have led to the development of breast cancer cells that grow in an estrogen-independent manner (Tolhurst et al., 2010). MCF-7 cells represent the most commonly used breast cancer cell line model of ERα-positive and estrogen-responsive breast cancer. MLET5 cells represent a clonal line, established following long-term of MCF-7 cells in the absence of estrogen. Despite continued expression of ERα, MLET5 cell growth is only partially inhibited by the anti-estrogens, tamoxifen and fulvestrant.

Other studies in the laboratory identified the nuclear receptor LRH-1 and showed that LRH-1 regulates the growth of ERα-positive breast cancer cells (Thiruchelvam et al 2011). Subsequent studies also demonstrated that LRH-1 is required for the recruitment of ERα to its gene targets.

The aims of this project, therefore, were two-fold. In the first part, I aimed to use the MLET5 model of endocrine resistant breast cancer to identify genes whose expression is altered in the development of estrogen-independence and which might therefore be candidate genes involved in the emergence of endocrine resistance in these cells.

In the second part, I investigated the potential role of LRH-1 in breast cancer cells, by analysis of LRH-1 target genes following gene expression microarray analysis of MCF-7 cells in which LRH-1 expression was silenced using RNA interference. I also developed an assay to screen libraries of compounds for the identification of LRH-1 inhibitors, towards the identification of lead compounds that could be developed towards clinical evaluation.

2 Materials and Methods

2.1 Materials

2.1.1 Chemicals and materials

General chemicals and reagents were supplied by BDH, Sigma-Aldrich (Poole, UK) and VWR (Leicestershire, UK). Molecular biological reagents such as DNA ladders, random hexamers and reverse transcriptase were obtained from Fermentas, Helena Biosciences Europe (Sunderland, UK). Kits for DNA and RNA preparation were obtained from Qiagen (West Sussex, UK). Semi-quantitative and Sybr-green Real-time PCR reagents and primers were obtained from Primer Design (Southampton, UK). Taqman Real-time PCR reagents and primers were obtained from Applied Biosystems (Cheshire, UK). Lipofectamine RNAiMAX transfection reagent (Invitrogen, UK) was used for siRNA transfection. Double-stranded RNA oligonucleotides (siRNA) were purchased from Dharmacon (Fisher Scientific, Loughborough, UK). FuGENE HD transfection reagent, used for reporter transfections, was obtained from Roche-applied science (Burgess Hill, UK). The Dual-Glo Luciferase Assay System was used for determining luciferase reporter gene activities (Promega, Hants, UK). His-tagged protein purification was carried out over HisTALON™ Gravity columns from Clontech. For the *in vitro* LRH-1 inhibitor assay, AlphaScreen Histidine (Nickel Chelate) Detection kit was obtained from PerkinElmer (Buckinghamshire, UK). Coomassie blue, for protein staining, was performed using Simply Blue™ Safe Stain from Invitrogen (Paisley, UK).

2.1.2 Cell culture reagents

Cells were maintained at 37°C in a humidified air atmosphere supplied with 5% CO_2. Cell culture manipulations were carried out in a NuAIRE class II, ducted laminar flow safety cabinet (NUAIRE DH Autoflow, Oxon, UK). Dulbecco's Modified Eagle's Medium (DMEM) with L-Glutamine–Penicillin–Streptomycin solution (200 mM L-glutamine, 10,000 U penicillin and 10 mg steptomycin/mL in 0.9% NaCl, sterile-filtered, adding 10 ml per litre or 5 ml per 500 ml DMEM) and 10X trypsin solution were supplied by Sigma-Aldrich (Poole, UK). Phenol red-free DMEM was purchased

from Invitrogen, UK. Fetal calf serum (FCS) and Dextran-coated, charcoal-treated FCS (DSS) were purchased from First Link (Birmingham, UK). 17β-estradiol (E2) and 4-hydroxytamoxifen (OHT) were obtained from Sigma-Aldrich (Dorset, UK). Raloxifene and Faslodex (ICI 182 780) were obtained from Tocris (UK). Etoposide was obtained from Invitrogen (Paisley, UK).

2.1.3 Cell Lines

The MCF-7, MDA-MB-231 and COS-1 cell lines were obtained from the American Type Culture Collection (ATCC) (LGC promochem, Middlesex, UK). The MLET lines were developed in this laboratory by transient over-expression of ERα using adenoviral gene transduction, followed by selection over 6 months for clones that grew in estrogen-free culture conditions (Tolhurst et al 2011). The clones were expanded and three cell lines, MLET 1, MLET2 and MLET5 were obtained. Microsatellite genotyping confirmed lineage from MCF7cells (Tolhurst et al., 2010). All cell lines were tested every three months for mycoplasma and genotyped on an annual basis (LGC Standards, Teddington, UK).

MCF-7: Human breast adenocarcinoma cell line expressing ERα and LRH-1
COS-1: SV40 transformed African Green Monkey kidney cells negative for ERα and LRH-1 expression.
MDA MB 231: Human breast carcinoma cells negative for ERα and LRH-1.
MLET1: negative for ERα expression.
MLET2: negative for ERα expression.
MLET5: ERα-positive cells (Tolhurst et al., 2010)

2.1.4 Antibiotics

Antibiotics, for bacterial work, were obtained from Sigma-Aldrich (Dorset, UK) as solids.
Ampicillin: dissolved in ddH_2O at 100mg/ml and stored at -20°C. Used at a final concentration of 100 μg/ml.

Chloramphenicol: dissolved in ethanol at a concentration of 25mg/ml and stored at -20°C. Used at a final concentration of 34 μg/ml.

2.1.5 Sundries

Cell culture and general laboratory plastics were obtained from Triple Red (Oxon, UK) and Corning (supplier Appleton Woods, Birmingham, UK). Eppendorf tubes were purchased from Anachem (Bedfordshire, UK). Sterilin plates were purchased from Barloworld Scientific (Staffordshire, UK). Kodak BioMax light film was supplied by Sigma-Aldrich (Poole, UK). White, opaque 384 well plates (OptiPlate™-384) for use in the Alphascreen assay were obtained from PerkinElmer (Buckinghamshire, UK). For western blotting NuPAGE Novex 4-12% Bis-Tris pre-cast protein gels were obtained from Invitrogen (Paisley, UK).

2.1.6 Bacterial media and plates

L-Broth (LB) (Luria-Betani)	LB capsules (16g bacto-tryptone, 10g bacto-yeast extract, 5g NaCl). Adjusted to pH7.0, made up to 1 litre with double-distilled, deionized H_2O (DDW). Autoclaved and stored at 4 ^oC.
LB Plates	LB agar 11.1g in 300mls DDW autoclaved to sterilise then cooled to 50^oC prior to the addition of appropriate antibiotics. The molten LB-agar was then poured into Sterilin Petri dishes, allowed to set and stored inverted at 4^oC. Prior to use, the plates were left inverted in an incubator oven at 37^oC for 30 minutes to dry.

SOC Medium	2% Tryptone, 0.5% yeast extract, 10mM NaCl, 2.5mM KCl, 10mM $MgCl_2$, 10mM $MgSO_4$, 20mM glucose. Purchased from Invitrogen (Paisley, UK). Stored at room temperature.
Terrific Broth	12g/L Casein enzymic hydrolysate, 24g/L yeast extract, 2.2g/L Monopotassium phosphate, 9.4g/L Dipotassium phosphate, 0.4% Glycerol. Made up to 1L with DDW. Final pH 7.2. Purchased from Invitrogen (Paisley, UK). Stored at 4 ^oC.

2.1.7 General stock solutions

Solutions were prepared in distilled de-ionised water (DDW). Solutions were autoclaved if appropriate and stored at room temperature, unless stated otherwise.

TBE (x10)	89mM Tris base 89mM Boric acid 2mM Na-EDTA pH 8.0.
Phosphate buffered saline (PBS) (10x) Stored at 4^oC	136mM NaCl 3mM KCl 8mM Na_2HPO_4 1.5mM KH_2PO_4
TE Buffer	10mM Tris-HCl 1mM Na EDTA pH 8.0
2x Laemmli Buffer	4% SDS 20% Glycerol 0.1% Bromophenol Blue 0.1M Tris-HCl pH 6.8 0.2M DTT (added immediately prior to use)
NuPAGE MOPS SDS 20x running buffer (Invitrogen)	50mM MOPS 50mM Tris Base 0.1% SDS 1mM EDTA (diluted to 1x prior to use pH7.7)

2.1.8 Antibodies

Antigen	Company	Antibody Species of Origin	Raised against amino acids	Dilution Used
β Actin	Abcam ab8226	Mouse monoclonal	1-100	1:200,000
GAPDH	Abcam ab9484	Mouse monoclonal		1:200,000
His tag	Abcam ab14923	Rabbit polyclonal		1:1000
LRH-1	Sigma HPA017067	Rabbit polyclonal	393-531	1:1000
Bcl2	Abcam ab692	Mouse monoclonal	41-54	1:1000
Bad	Santa Cruz sc-8044	Mouse monoclonal	1-168	1:200
Bik	Santa Cruz sc-10770	Rabbit polyclonal	1-160	1:200
Bid	Santa Cruz sc-11423	Rabbit polyclonal	1-195	1:200
HRP-conjugated goat anti-Mouse igG	DakoCytomation, Ely, UK	Goat polyclonal		1:2500
HRP-conjugated goat anti-rabbit IgG	DakoCytomation, Ely, UK	Goat polyclonal		1:2500

2.1.9 Real time RT-PCR Primers

Gene	Company	Approach	Sequence/Assay ID no.
ERα	Primer Design	Sybr green	AAGAAAGAACAACATCAGCAGTAAA TCTTTGGATGACCTAGCCTCTC
PgR	Primer Design	Sybr green	GAGTCACCTTGCCCCTTCA GCCTTTTATGCTTGCCTGTAAA
PS2	Primer Design	Sybr green	CCCCCGTGAAAGACAGAATT ACGTCGATGGTATTAGGATAGAAG
GREB1	Primer Design	Sybr green	ATAAGAGAATCCACAATAGAGACCTT CTCTCATCAGTTTCAGTGCCATTT
CD36	Primer Design	Sybr green	TGTAGAAACCACTTTAATCATATCCA CCAGGACAGCACCAATGAC
IGFL1	Primer Design	Sybr green	TGGAGAAAGAGGCTGGTGTT GAATGAAGTGGGCAGTTGAGT
TM4SF1	Primer Design	Sybr green	TGTATTGGCTGCTCTCATTGG CCGAGGGAATCAAGACATAGTG
Calb2	Primer Design	Sybr green	ATCCTGCCAACGAAGAGAA CGATGTAGCCACTCCTGTCT
BCL2	Primer Design	Sybr green	GAGGTCACGGGGGCTAATT GAGGCTGGGCACATTTACTG
BCL6	Primer Design	Sybr green	GGACTGTGAAGCAAGGCATT GGAGACGATTAAGGTTGAGAAGA
NUPR1	Primer Design	Sybr green	CTTATTCCCGCTGACTGAGT TAGCTTTCTTTTCTGGGGGATC
SOCS2	Primer Design	Sybr green	TTTTATCAGAATGCCTTGCCTTC GGTTCCTTCCCACTTCTTCAG
DR6	Primer Design	Sybr green	GCCTTGACTGACCGAGAATG CTTACACCGCACATCCTCAG

ANXA1	Primer Design	Sybr green	GAGCCCCTATCCTACCTTCAA CTTCATCCACACCTTTAACCATTAT
BAD	Primer Design	Sybr green	CCTGGTGGGATCGGAACTT TGGGAACGGGTGGAGTTTC
BID	Primer Design	Sybr green	CTGTAAACTTCCAATTTCTAGCCATA GTCCAACTGCTCTTTCATCTTTT
BIK	Primer Design	Sybr green	TGAAGTAAGACCCCTCTCCAG CCAAAGAATCGAAGTCCTCCAT
IGFBP3	Primer Design	Sybr green	ATATGGTCCCTGCCGTAGAG TAAAATCCCTTCTTGTCACAGTTG
PPARG	Primer Design	Sybr green	GAATAAAGATGGGGTTCTCATATCC AACTTCACAGCAAACTCAAACTT
NR5A2	Primer Design	Sybr green	GATCACACCAACGACAGGAG AATCGGCTAACAATCAACATTAGAG
NR5A1	Primer Design	Sybr green	GGTGCATGGTCTTCAAGGAG GCGGTAGATGTGGTCGAAC
SCNN1A	Primer Design	Sybr green	CTGCCAGAGAACTCCTATGC TCAATTTTGGGGAAGACAAGATG
BCAS1	Primer Design	Sybr green	AGAGATTATAAAGTCCAAGGAAGTAGA GTTTCGCTTCTGTGGGTTCA
CYP1B1	Primer Design	Sybr green	CACTGGAAACCGCACCTC AGCACCGACAGGAGTAGC
CYP1A1	Primer Design	Sybr green	CAAGGTGTTAAGTGAGAAGGTG AGCACCGACAGGAGTAGC
LCOR	Primer Design	Sybr green	GCCACTAATAGCCAGCACCAA TGAATTTAGTAGTTATCGTGAAGA
ACOX2	Primer Design	Sybr green	CCAGAATGAGCGTTATAAGGC CGTCTCCAGAAAGGGCTCT
BIRC3	Primer Design	Sybr green	GCTTCAAGACACTTCAAGATACAC GCTGCTCAGGATTAACTAGAACA
PMP22	Primer Design	Sybr green	TACTCCTACGGTTTCGCCTAC ACATAGATGACACCGCTGAGAA
TACC1	Primer Design	Sybr green	GCCATGACCGTTATGAGGAAA CATTCTGCCCAGTATATTCTCTTG
GPERv2	Primer Design	Sybr green	ACCAACATCTGGACGGCAG CACACCGGCATGGTGCATC

GPERv3	Primer Design	Sybr green	GGGAAGAGGCCACCAACATC GCTGCAGGAGGTGTACCTCTG
GPERv4	Primer Design	Sybr green	CGGGTCTCTTCCTCTCTCTAGC GCCCATCAGGCTGGAGGTG
SLC9A6	Primer Design	Sybr green	TCCAGACCAAGACCGTAGAAG CTTTACTCGCCTCTTGCTCTC
PCP4	Primer Design	Sybr green	CACCAAATTCAACCATCATCTGT TTGCTATGCGTGTGTGGATT
GFRA1	Primer Design	Sybr green	TGAGAGGCGAGAAACTAGCA AGCGGACTAACTGGCGAAT
ADCY1	Primer Design	Sybr green	CTGTCCGAGAAAAGTTGTGTAAG AGTGAGTTGTATTGTGCGAGAA
RAMP3	Primer Design	Sybr green	AACGAGACAGGCATGTTGG GGACAGGTTGCACCACTTC
MYB	Primer Design	Sybr green	CCTTAGCCACTGGAGACTGTA AGAACTGCGAGGGAGAGAAG
GAPDH	Primer Design	Sybr green	N/A sequence kept in house
GAPDH	Applied Biosystems	Taqman	Hs99999905_m1
ESR1	Applied Biosystems	Taqman	Hs00174860_m1
GREB1	Applied Biosystems	Taqman	Hs00536409_m1
pS2	Applied Biosystems	Taqman	Hs00170216_m1
PgR	Applied Biosystems	Taqman	Hs00172183_m1

2.1.10 Compounds

Estrogen (17ß-estradiol) was prepared in ethanol at a concentration of 10 mM and used at a final concentration of 10nM. 4-Hydroxy Tamoxifen (OHT), Raloxifene, Faslodex (ICI 182, 780) were prepared in ethanol or DMSO at a concentration of 100mM and used at a final concentration of 100 nM unless stated otherwise. Mr. Andrew Bayly (AB), Mr. Jullien Rey (JR) and Dr Timothy O'Riordan (TJC) made

experimental compounds under the supervision of Professors' Alan Spivey and Anthony Barrett in the chemistry department at the Imperial College London South Kensington campus. Experimental compounds were solubilised in DMSO.

2.1.11 Coactivator Peptides

Biotinylated coactivator peptides, for use in the in vitro Alpha Screen, were synthesized by Cambridge Research Biochemicals (Cambridge, UK). Peptide sequences have previously been described (Li et al., 2005; Whitby et al., 2006).

SRC2
Biotin-AHX-LYS-GLU-LYS-IS-LYS-ILE-LEU-HIS-ARG-**LEU-LEU-**GLN-ASP-SER-SER-SER-PRO-NH2

SRC2 mutant
Biotin-AHX-LYS-GLU-LYS-HIS-LYS-ILE-LEU-HIS-ARG-**ALA-ALA-**GLN-ASP-SER-SER-SER-PRO-NH2

PGC1-alpha
Biotin-AHX-ALA-GLU-GLU-PRO-SER-LEU-LEU-LYS-LYS-**LEU-LEU-**LEU-ALA-PRO-ALA-ASN-THR-NH2

PGC1-alpha mutant
Biotin-AHX-ALA-GLU-GLU-PRO-SER-LEU-LEU-LYS-LYS-**ALA-ALA**-LEU-ALA-PRO-ALA-ASN-THR-NH2

Biotinylated his
Biotin-AHX-HIS-HIS-HIS-HIS-HIS-HIS-NH2

NB: AHX = aminohexanoic acid - a hydrocarbon chain used as a 'spacer' between biotin and the peptide to reduce steric hindrance with the subsequent binding of biotin to streptavidin http://www.crbdiscovery.com/technical/peptides/biotinylation.php

2.1.12 Equipment

RNA concentration and purity was measured using an ND-1000 spectrophotometer and by running 2µg on 1.5% agarose gel with 0.1ul/ml SYBR Safe DNA gel stain in 1x TBE buffer and visualizing using an ultraviolet illuminator, UVIpro Platinum Gel Doc System (UVItec, UK). Optical densities for SRB assays were measured using a Tecan Sunrise Optical Plate Reader (Tecan-UK, Reading, UK). Optical densities for bacterial cultures and for protein lysate concentration (BCA) were determined, at 600nm and 562nm respectively on a Shimadzu UV-1201 UV-VIS spectrophotometer (Milton Keynes, UK). Luminescence for luciferase reporter assays was measured using a Packard Top Count microplate luminometer or Tecan Sunrise Optical Plate Reader (Tecan-UK, Reading, UK). The Alpha signal for the Alpha Screen was detected on a PHERAstar^{plus} (BMG LabTech, Aylesbury, UK). Western Blot protein transfer was carried out using the iBlot Dry Blotting System (Invitrogen, Paisley, UK). Compounds were prepared by weighing solid powder on a Pioneer Precision Balance (Ohaus, NJ, USA) and pH of buffers was checked and adjusted appropriately using an Ultra BASIC pH/mV Meter UB10 (Denver Instrument, NY, USA). Semi quantitative PCR/reverse transcription was carried on a GeneAmp 9700 PCR machine (Applied Biosystems, UK) and qRT-PCR on an ABI 7900HT fast Real-time PCR system (Applied Biosystems, UK).

2.2 Methods

2.2.1 Cell culture

MCF-7 cells were routinely maintained in DMEM supplemented with 10% FCS and 1% (v/v) P/S/G, in a humidified incubator supplied with 5% CO_2 at 37°C. MLET1, MLET2 and MLET5 cells were routinely maintained in phenol-red free DMEM medium supplemented with 10% DSS and 1% P/S/G. Cells were passaged at approximately 80% confluency by washing in 1x trypsin (Trypsin in 0.02% EDTA) and then leaving in 1x trypsin for 5 minutes, or until cells detach, in the incubator as above. The detached cells were thoroughly pipetted to ensure an even monolayer on re-seeding.

To freeze cells down for storage, cells at approximately 80% confluency in a T150 flask were washed twice with pre-warmed PBS, trypsinised and recovered cells were centrifuged at 1300 rpm for three minutes to forms a cell pellet. The cell pellet was resuspended in 4.5mls of freeze media (90% FCS and 10% DMSO) and aliquoted in 1.5mls into 1.8ml cryovials and stored at -80°C for 24 hours before being placed in liquid nitrogen storage tanks.

To revive frozen stocks, the cryovials were removed from liquid nitrogen storage, tubes cleaned with 100% ethanol and placed at 37°C water bath for 1 minute. Cell suspensions were diluted in 25mls of culture medium in a 50ml falcon tube and centrifuged at 1300rpm to remove the remaining freeze media. The cell pellet resuspended in 7 mls of medium, seeded in a T25 tissue culture flask and grown at 37°C with 5% CO_2 as above.

For growth experiments in which the effects of estrogen and anti-estrogens were determined, cells were cultured in phenol red free DMEM supplemented with 10% DSS for three days before the experiments.

2.2.2 Sulphorhodamine B (SRB) growth/toxicity assay

The SRB was carried out as described (Skehan et al., 1990). Briefly, the cells were cultured in either phenol-red free DMEM supplemented with 10% DSS and antibiotics for 3 days (growth experiments) or DMEM supplemented with 10% FCS and antibiotics (off target effect experiments). Cells were seeded ($1x10^4$) in flat-bottomed 96-well plates, in medium (100 µl/well) as above. Culture medium, supplemented with ligands, was added after 48 hours and cell growth was assessed using the sulphorhodamine B (SRB) assay over a 12-day period. Culture medium supplemented with ligands as appropriate, was changed every three days. The cells were fixed by adding 100µl ice-cold 40% trichloroacetic acid (TCA) to each well and incubated at RT for 1 hour. The wells were then washed five times in distilled water and 100 µl of 0.4% SRB (Sigma, UK) prepared in 1% acetic acid was added for 30 minutes. Following this, the wells were washed five times with 1% acetic acid and

allowed to air-dry. The bound dye was then solubilised by adding 100µl of 10mM Tris-base to the wells and placed on a plate shaker for 10 minutes at room temperature. The absorbance of the dye was read at 492nm on a Tecan Sunrise Optical Plate Reader (Tecan-UK, Reading, UK).

2.2.3 Total RNA preparation

Two million cells were plated in 10cm plates for 24 hours prior to the addition of ligand and then harvested 16 hours later. Cell culture medium was completely removed and cells were washed twice with ice-cold PBS and collected by cell scraping following the addition of lysis buffer from the RNeasy mini preparation kit (Qiagen Ltd, UK). Total RNA was extracted using this kit according to manufacturer's instructions and RNA concentration determined at 260nm and 280 nm and by running 2µg on 1.5% agarose gel with 0.1µl/ml SYBR Safe DNA gel stain in 1x TBE buffer and visualizing using an ultraviolet trans-illuminator.

2.2.4 cDNA by Reverse Transcription

cDNA were prepared from total RNA using thin-walled PCR tubes, with the reagents listed below added in the following order:

- 4µl 5x RT buffer (250mM Tris-HCl, 200mM KCl, 30mM $MgCl_2$), containing 50mM DTT (Fermentas, Helena Biosciences Europe, UK) pre-warmed to 37^{o}C for 30 minutes
- 2µl 10mM dNTP stock (Fermentas, Helena Biosciences Europe, UK)
- 1 µl (200ng) random hexamers $p(dN)_6$ (Fermentas, Helena Biosciences Europe, UK)
- 2 µg RNA
- Sterile DDW to a total volume of 19µl
- 1 µl Reverse transcriptase (RevertAid Moloney Murine Leukaemia Virus (M-MuLV) (200U/µl) (Fermentas, Helena Biosciences Europe, UK)

The reaction was incubated at 42°C for 1 hour in a thermal cycler and heat inactivated at 95°C for 5 minutes. The cDNA was then diluted 1:10 with sterile water and 2µl of diluted cDNA subsequently used as a template for each PCR and real time PCR reaction.

2.2.5 Polymerase chain reaction (PCR)

25µl PCR reactions were set up in 0.2 ml PCR tubes, containing:

- 12.5 µl of PCR master mix (2x Pre-Aliquoted ReddyMix™ (Abgene, UK))
- 1.0 µl of sybr green primers (forward and reverse combined = 300nM final concentration)
- 2 µl cDNA
- DDW to make up a total volume of 25 µl

The PCR mixture was centrifuged briefly, prior to loading onto a GeneAmp 9700 PCR machine (Applied Biosystems, UK). PCR was carried out over 22-40 cycles using the following conditions:

- Initial Denaturing 94°C, 5 minutes, 1 cycle
- Denaturing 94°C, 30 seconds
- Annealing X°C, 30 seconds (X = annealing temperature)
- Extension 72°C, 1 minute
- Final Extension 72°C, 4 minutes, 1 cycle

2.2.6 Real-time RT-PCR

Real-time RT-PCR was carried out according to manufacturer's protocols on an Applied Biosystems ABI 7900HT fast Real-time PCR system using Taqman Gene Expression assays from Applied Biosystems or Sybr green primers from Primer Design. Appropriate master mix was obtained from Applied Biosystems. Each PCR

reaction was carried out in triplicate, in a Microamp™ fast optical 96-well reaction plate (ABI, UK).

For Taqman reactions (40 cycles):

- Denaturing 95° - 20 seconds
- Annealing 95° - 1 second
- Extension 60° - 20 seconds

For Sybr green reactions (40-50 cycles):

- Denaturing 95° - 10 minutes
- Annealing 95° - 15 seconds
- Extension 60° - 1 minute
- Melt Curve 95° - 15 seconds
  50° - 15secs
  95° - 15secs

2.2.7 Preparation of Protein lysates for Western Blotting

Cells were twice washed in pre-warmed PBS (37°C) before 500 µl of pre-heated hot lysis buffer (composition as per section 2.1.7) (100°C) was added to the cells in wells. The cells were scraped and transferred to 1.5ml Eppendorf tubes. The collected lysates were heated to 100°C for 5 minutes, cooled on ice and stored at -80°C.

2.2.8 Western Blotting

MCF7 and MLET5 cell were seeded ($1x10^6$), in 10 cm plates, in DMEM containing FCS and lysed after 48 hours in hot lysis buffer. For experiments in which estrogen and/or anti-estrogens were added to the cells, the cells were incubated in phenol red-free DMEM containing 10% DSS for 72 hours prior to seeding. The ligands were

added 24 hours after seeding and the cells harvested as above after a further 24 hours.

Protein lysates were heated at 100°C for 5 minutes and vortexed prior to loading on a Nu-PAGE Bis-Tris SDS-PAGE pre-cast gradient gel (4-12%). The gel was prepared and assembled in the Xcell *Sure Lock*™ Mini Cell as per the manufacturer's instructions (Invitrogen, UK). The gel running apparatus was filled with NuPAGE MOPS SDS 1x running buffer, the protein marker and samples loaded, and run at 200V constant for 35 minutes.

The resolved protein gels were transferred onto a nitrocellulose membrane for immunodetection using an iBLOT dry transfer unit. The membrane was then incubated with blocking buffer (5% Marvel in PBS with 0.05% Tween-20) for 1 hour at room temperature to prevent non-specific binding of the antibody. After removal of blocking buffer, the primary antibody diluted by the appropriate amount (see Section 3.1.8) in blocking buffer, was added to the membrane and the membrane was incubated for 1.5 hrs at room temperature on a shaking platform. The membrane was then washed 3 times for 15 minutes in PBS containing 0.05% Tween-20, prior to the addition of the appropriate HRP-conjugated secondary antibody in blocking buffer and incubation for 1 hour at room temperature, with shaking. The membrane was once again washed in wash buffer for a total of 1 hour with four changes of buffer.

SuperSignal West Pico Chemoluminescent Substrate (Pierce Biotechnology, UK) was added, as per manufacturers instructions, followed by autoradiography using Kodax Biomax Light film (Sigma, UK) and the film developed with a Konica SRX-1001A X-ray developer.

2.2.9 Plasmid Preparation for Luciferase Reporter Assays

pci-LRH-1 and SF-1-LUC were gifts from Dr Donald McDonnell (Duke University, USA). The renilla luciferase reporter gene was RLTK (Promega, UK). The ERα expression plasmid (pSG5-HEG0) and ERE-3-Luc reporter gene have been described

(Thomas et al., 2008).

2.2.9.1 Bacterial Cell Transformation

40 µl Subcloning Efficiency™ DH5α™ Competent Cells (Invitrogen, Paisley, UK) were added to 0.1 µg of plasmid DNA and incubated on ice for 30 minutes in 1.5 ml Eppendorf tubes. After 30 minutes the tube was heated to 42° in a water bath for 45 seconds. The mixture was then incubated on ice for 2 minutes and 600 µl SOC medium added followed by incubation in shaker incubator 200rpm at 37° for 1 hour. The cells were centrifuged for 20 seconds at 13,000 rpm, 900µl medium was removed, the remainder was gently pipetted to resuspend the cells and 50µl spread on LB-agar plates containing ampicillin(50µg/ml) and incubated overnight at 37°.

2.2.9.2 Plasmid Preparation

A single colony was added to 4 mls LB medium containing ampicillin to a final concentration of 50µg/ml, and placed in a shaking incubator (200 rpm) at 37°C for 6-8 hours. 500µl of the medium was added to 200mls LB media containing antibiotic as above and placed in a shaking incubator for at 37°C for 18-24hrs. Plasmid DNA was prepared using Qiagen columns (Qiagen, UK), according to the manufacturer's methods and quantified by measuring nucleic acid concentration and purity on ND-1000 spectrophotometer.

2.2.10 Reporter Assays

$5x10^4$ COS-1 cells were plated in each well of 24-well plates, in 1 ml DMEM lacking phenol red and containing 10% DSS. After 24 hours the medium was changed for serum free OptiMEM (Invitrogen, UK) and the cells were transfected with:

- pCI-LRH-1 (full length LRH-1) 50ng per well
- SF1-LUC (SF-1- promoter-Luciferase) 100ng per well

- pRL-TK (internal control Renilla) 100ng per well
- BSM (blue script carrier DNA) 150ng per well

Or

- pSG5 HEG0 (ERα) 10ng per well
- ERE-3-LUC (ERα-promoter-Luciferase) 100ng per well
- pRL-TK 100ng per well
- BSM 190ng per well

The transfection mix was made up to a concentration of 0.02µg/µl with OptiMEM (Invitrogen, UK). Fugene HD transfection reagent (Roche, UK) was added to the DNA/Optimem mix as 5 volumes of Fugene HD to 2 µg of DNA. The transfection mix was vortexed and left at room temperature for 15 minutes before adding 20µl to each well.

Five hours following transfection the compounds to be tested were added. As the compounds were prepared in DMSO, an equal volume of DMSO was added to control wells. The cells were lysed, and the Firefly and Renilla luciferase activities determined after 24 hours, using the Dual-Glo Luciferase Assay System (Promega, UK). Transfection efficiency was normalized using renilla reporter activity. Luciferase readings represent the mean of three individual transfections, and error shown as SEM.

2.2.11 siRNA Transfection

MCF-7 cells, maintained in DMEM supplemented with 10% FCS, or cultured in phenol red free DMEM supplemented with 10% DSS, and MLET5 cells, cultured in DMEM lacking phenol red and containing 10% DSS for 3 days, were transfected with double-stranded RNA (dsRNA) oligonucleotides using the reverse transfection method with Lipofectamine RNAiMAX.

For this, the (dsRNA) oligonucleotides, purchased as ON-TARGETplus SMARTpool siRNA or Non-targeting siRNA (Dharmacon, USA), were transfected with Lipofectamine RNAiMAX (Invitrogen, UK), according to the manufacturer's protocol. Briefly, the following components were gently added to each 10cm tissue culture plate, mixed and left to wait for 20-30 minutes:

- 500µl phenol-red free DMEM
- 40µl Lipofectamine RNAiMAX (Invitrogen, UK) – kept on ice
- 40µl siRNA – kept on ice (20µM stock)

10ml of $2x10^6$ cell suspension was added to the siRNA (made up in DMEM supplemented with 10% FCS and 2mM/ml L-Glutamine (Gibco, UK)) and the plate gently rocked for 1 minute to allow mixing. The cells were then incubated for 48 hours before harvesting to prepare RNA or protein. RNA was prepared after 48 hours, as described (section 3.2.3).

For SRB growth assay experiments, $1x10^4$ cells were plated in each well of 96 well plates and growth was assayed over a 5-day period (section 3.2.2). To determine the effect of gene silencing by siRNA on cell numbers, the following was prepared in a 24 well plate and the reagents were thoroughly mixed and left for 20-30 minutes:

- 250µl phenol-red free DMEM
- 5µl Lipofectamine RNAiMAX (Invitrogen, UK) – kept on ice
- 5µl siRNA – kept on ice (20µM/ml stock).

10µl of the siRNA mixture was then added to each well of a 96 well plate (5 reactions were performed per condition). Following this, a 200µl cell suspension (made up in DMEM supplemented with 10% FCS and 3mM L-Glutamine (Gibco, UK)) containing 1 x 10_4 cells was added to each well containing the siRNA mix. For growth experiments in which E_2 was added, a similar method was followed except that the medium used was phenol red-free DMEM containing 10% DSS. E_2 (10 nM

final concentration) was added to the medium 24 hours after transfection.

2.2.12 siRNA Oligonucleotides

SiRNAs were purchased from Dharmacon.

SiRNA LRH-1 OnTargetPlus Smartpool comprised SiRNAs with the following sequences:

♯1 5'-CAUAAUGGGCUAUUCAUAU-3'

♯2 5'-AGAGAAAUUUGGACAGCUA-3'

♯3 5'-GGAGUGAGCUCUUAAUCCU-3'

♯4 5'-GAAGCCAUGUCUCAGGUGA-3'

SiGenome non-targeting siRNA (Dharmacon) had sequences:

5'-UAAGGCUAUGAAGAGAUAC-3'

5'-AUGUAUUGGCCUGUAUUAG-3'

5'-AUGAACGUGAAUUGCUCAA-3'

5'-UGGUUUACAUGUCGACUAA-3'

2.2.13 Gene Expression Microarray Analysis

Total RNA (10μg per condition), produced as described in 3.2.3, were sent on dry ice to the Centre for Microarray Resources, Department of Pathology, Cambridge University. The RNA samples were amplified and labeled, using Illumina TotalPrep RNA Amplification kit (Ambion, USA), with biotinylated nucleotides. The RNA was amplified with the incorporation of biotin followed by hybridization to the array. Hybridisaton data was obtained using Illumina BeadStudio software to delineate and quantify the hybridization signal for each bead. The raw data and image files were provided for further analysis.

Functional analysis of the data was performed on-line using Gene Ontology (http://www.geneontology.org) and DAVE (http://david.abcc.ncifcrf.gov/gene2gene.jsp) databases.

2.2.14 His tagged LRH-1 LBD Expression and Purification

2.2.14.1 Transformation into bacterial cells

40 µl competent Rosetta 2 (DE3 pLysS) Competent Cell bacteria (Novagen, Merck KGaA, Darmstadt, Germany,) was added to 0.1 µg of pMALCH10T-LRH-1-LBD plasmid DNA (a kind gift from Dr Eric Ortlund, Emory University, USA (Ortlund et al., 2005)) and transformations were performed as in section 3.2.9 using antibiotics 100 µg/ml ampicillin and 34 µg/ml chloramphenicol.

2.2.14.2 Growth and Induction of Protein Expression

A single bacterial colony was picked from the LB-agar plate above and grown for 6 hours in 1 ml of Terrific Broth (TB Invitrogen, Paisley, UK) containing 100 µg/ml ampicillin and 34 µg/ml chloramphenicol. This culture was then expanded into 100mls of TB with ampicillin and chloramphenicol and grown at 37°C in a shaker incubator overnight. The baseline OD was measured prior to further expansion into 500mls of TB with antibiotics until the OD measured 0.8-1.0 (A_{600}). At this point the temperature was dropped to 32°C and 0.1mM IPTG added to induce protein expression for 4 hours. The bacterial culture was then harvested by centrifugation at 5000rpm, 4°C, weighed and frozen at -80°C overnight.

2.2.14.3 Purification

The frozen pellet was defrosted and resuspended in 4mls per gram Buffer A with 0.1mM DNAase, Protease Inhibitor Cocktail and 0.2% Triton X100. The pellet was sonicated for 1-2 minutes until the cells appeared to be lysed and the sonicated suspension centrifuged at 4°C, 15000 rpm for 60 minutes. The supernatant was then removed, transferred to a new cold tube, and stirred on ice for 5 minutes followed by further centrifugation for 60 minutes as above.

The HisTALON™ Gravity columns (Clontech, UK) were prepared according to the manufacturer's protocol. The supernatant was added to the column and

flowthrough collected. The flowthrough was passed over the column three times to ensure histidine tagged binding to cobalt resin. The column was washed with 8 mls of buffer A, followed by 7 mls buffer B (with 5mM Imidazole). The purified protein was eluted from the column using 250mM Imidazole in elution buffer. The imidazole was removed from the purified protein by dialysis.

Buffer A	5mM Imidazole 150mM NaCl pH 7.4 20mM Tris 5% Glycerol + protease inhibitor cocktail and DNAase
Buffer B	5mM Imidazole pH 7.4 100mM NaCl 20mM Tris 5% Glycerol + protease inhibitor cocktail
Elution Buffer	250mM Imidazole pH 7.4 150mM NaCl 20mM Tris + protease inhibitor cocktail
Dialysis Buffer	150mM NaCl pH 7.4 20mM Tris Glycerol 5%
After Elution/Dialysis	DTT 2mM EDTA 0.5mM

2.2.14.4 Dialysis

The dialysis containers were thoroughly washed and autoclaved with dialysis buffer. The dialysis cassettes (Slide-a-Lyzer, 10K MWCO, ThermoScientific, UK) were pre-hydrated in dialysis buffer for 1-2 minutes followed by insertion of the sample

via a beveled needle and syringe as per manufacturer's instructions. Excess air was removed to ensure maximal buffer exchange and a buffer volume of 200-500x size of sample used. The sample was dialysed for 2 hours at room temperature followed by a change of buffer and further dialysis at room temperature for 2 hours and subsequent final change of buffer and the dialysis at 4°C overnight. Following recovery of the dialysed sample, DTT and EDTA were added, prior to freezing at -80°C. Analysis of protein concentration was carried out using a Pierce BCA (bicinchonic acid) protein Assay (Thermo Fisher Scientific UK Ltd, Leicester) or by measuring UV absorbance at 580nm.

2.2.15 Cleavage and re-purification of His tagged LRH-1 LBD

Cleavage of the LRH-1 LBD from the histidine tagged maltose binding protein was achieved using a TEV protease (AcTEV Protease, Invitrogen, UK).

Component	Amount/Volume
His tagged LRH-1 LBD	100µg
20X TEV buffer	37.5µl
AcTEV Protease	5µl
DDW	to 750µl

The reaction mixture was incubated at room temperature for 6 hours on a gentle shaker platform.

The sample was re-purified using the cobalt metal affinity column, as described above, to enable removal of the his-tagged protein and the AcTEV protease. A further purification step was included to remove the MBP bound protein using a MBP Trap column (Dextrin Sepharose High Performance/MBPTrap HP, GE Healthcare, UK) as per manufacturer's methods. The resulting sample was

concentrated using Amicon Ultra 3K MWCO centrifugal filter (Millipore (UK), Watford) and purity assessed using SDS/PAGE analyses.

2.2.16 Alpha Screen protocol

The total volume per well for each alpha screen reaction is 25 µl. Conditions were performed in triplicate and a Z score calculated to ensure experimental validity (Zhang et al., 1999). Z score of 0.45 or above was considered acceptable.

Z= 1-(((3x stdev A)+(3x stdev B)/ (Mean A)-(Mean B))

A = High control i.e DMSO treated

B = Low Control i.e background signal

5µl of the intermediate concentrations of his tagged LRH-1 LBD protein and 5µl of biotinylated PGC1α coactivator peptide (both 5x more concentrated than final concentration required) were added to each well of 384 well plate required. A negative control was included by substituting the peptide for 5µl of 1x alpha buffer. Experimental compounds were prepared by initially diluting in DMSO to mM concentration range, followed by an intermediary dilution into 1x alpha buffer (1:200 = 5µl into 995µl of 1x alpha buffer), with a DMSO control as baseline positive interaction between the protein and the peptide. 5µl of the intermediary compound dilution range was then added to the appropriate wells (i.e. a further 1:5 dilution). The histidine (nickel chelate) acceptor bead, 1:50 preparation from the supplied stock concentration, was finally added and a plate seal applied to prevent evaporation. The plate was briefly spun (15 secs) before incubation in the dark, at room temperature on a shaker platform for 30 minutes.

Following the initial incubation, the streptavidin donor bead, also 1:50 preparation from the stock concentration, was added in muted light, the plate sealed and covered and incubated under the same conditions for 60 minutes.

The plate was read using a Pherastar plus with the appropriate Alpha Screen optic module to allow excitation at 630nm and detection of emission at 520-620nm.

10x Alpha Screen buffer	250mM Hepes 1M NaCl pH 7.4
1x Alpha Screen buffer	25mM Hepes 0.1mM NaCl 0.1% BSA pH 7.4

2.2.17 Fluorescence activated cell sorting (FACS) Analysis

100,000 cells per well were seeded in six well plates in DMEM containing 10% FCS. After 48 hours the cells were treated with 1nM-100μM etoposide (Sigma-Aldrich) or DMSO and incubated for a further 48 hours. After this time, the cells were harvested by trypsinisation, centrifugation for 5 minutes and washing in 5 mls ice-cold PBS before a further 5 minute centrifugation and gently resuspending in 1 ml ethanol at 4°C for 1 hour. The cells were then washed twice with 5mls ice cold PBS as above and resuspended in 100μl PBS containing 100μg/ml RNAase (Sigma-Aldrich) and 1ml 50μg/ml propidium iodide (PI) (Sigma-Aldrich) and incubated in the dark at

4°C for 1 hour. The samples were filtered through 70 μm muslin gauze, to remove cell clumps, into FACS cell sorting tubes (Becton Dickinson). The labeled cells were acquired using the RXP cytomics software on a Beckman Coulter Elite ESP and the data analysed with Flow Jo v7.2.5 (Tree Star, Inc).

For dual labeling with Annexin V the cells were harvested by trypsinisation, centrifugation and washed twice in ice-cold PBS containing 2% (w/v) bovine serum albumin (Sigma-Aldrich). The cells were labeled with fluorescein-isothiocyanate (FITC) coupled Annexin V and PI using the Annexin V-FITC apoptosis detection kit I (BD Pharmingen) as per the manufacturers instructions for 15 minutes at room temperature. The labeled cells were acquired and analysed an hour later as described above.

3. Results

3.1 Gene Expression Profiling of MCF-7 and the MCF-7 derived, Estrogen-Independent MLET Cells

The MCF-7 cell line was generated from a pleural effusion from a patient with breast cancer (Brooks et al., 1973; Horwitz et al., 1975). MCF-7 cells express ERα and require estrogen for their growth. Hence, culturing in the absence of estrogen in the culture medium results in a block in growth and treatment with anti-estrogens also inhibits their growth. MCF-7 cells also express the progesterone receptor (PgR), a classic ERα target gene (Horwitz et al., 1975). As such, MCF-7 cells have become the prototypical cell line model of ERα-positive breast cancer. Searching for publications with the terms "MCF7" and "breast cancer" (26 June 2014) yielded 16,786 publications in Pubmed (http://www.ncbi.nlm.nih.gov/pubmed/). Evaluation of signaling pathways in MCF-7 has identified key ERα regulated genes, using among other methodologies gene expression microarray analysis (Frasor et al., 2003). The identification of global ERα binding sites using chromatin immunoprecipitation followed by hybridization of immunoprecipitated DNA to genomic tiling arrays or by high throughput DNA sequencing (ChIP-seq) (Carroll et al., 2006), as well as numerous studies have begun to determine the molecular mechanisms by which ERα regulates gene expression (Metivier et al., 2006). Within this laboratory, Dr Robert Tolhurst utilized MCF-7 cells for the investigation of the processes by which MCF-7 cells could be engineered for estrogen-independent growth, thus allowing possible mechanisms of endocrine resistance to be evaluated. The initial rationale behind this work stemmed from observations that ectopic ERα expression in ERα negative breast cancer cell lines inhibits cell growth (Jiang and Jordan, 1992; Lazennec and Katzenellenbogen, 1999; Zajchowski et al., 1993) however, conditional overexpression increased the growth of MCF7 cells in the absence of ligand (Fowler et al., 2004; Lazennec and Katzenellenbogen, 1999). This suggested that ERα overexpression may be a mechanism of cellular adaptation to estrogen deprivation (Tolhurst et al., 2010). Previous studies investigating the development

of estrogen-independence in MCF-7 cells have frequently observed ERα upregulation during the early stages of progression from estrogen-dependence to estrogen-independence (Chan et al., 2002). Dr Tolhurst infected MCF-7 cells with an adenovirus encoding ERα to achieve transient ERα over-expression in MCF-7 cells that were cultured in the absence of estrogen. Adeno-ERα infected cells showed ligand-independent activation of ERα target genes and ligand-independent growth (Tolhurst et al., 2010). ERα over-expression fell over a 3-6 week period, concomitant with loss of detectable adenoviral genome sequences. At this stage the cultures underwent a "crisis" with loss of cells over the next 2 months, with outgrowth of distinct clones over a further 3-month period. One of the clones that grew out was named MLET5. Repeat experiments generated two other lines (MLET1, MLET2), although these differed from MLET5 cells in being representative of derived cultures, rather than being distinct clones as in the case of MLET5 (Tolhurst, 2006).

MLET1, MLET2 and MLET5 grew in an estrogen-independent manner, with growth being uninhibited by treatment with the anti-estrogens tamoxifen, raloxifene or fulvestrant (Tolhurst, 2006; Tolhurst et al., 2010). Gene expression analysis determined that MLET5 continues to express ERα and the ERα target genes PgR and pS2 were also expressed (Tolhurst et al., 2010). By contrast, MLET1 and MLET2 did not express ERα, PgR or pS2 (Tolhurst, 2006). As previously mentioned most ERα-positive breast cancer remain ERα-positive following onset of resistance to tamoxifen and frequently these patients respond to fulvestrant or an aromatase inhibitor, indicating the continued importance of ERα in endocrine resistant breast cancer (Howell et al., 2002; Johnston et al., 1995; Osborne et al., 2002). About 30% of ERα-positive breast cancer do, however, progress to ERα-negative breast cancer (Johnston et al., 1995). Thus, this panel of MCF-7-derived resistant cells represents interesting models for investigation of the molecular changes that may drive acquired endocrine resistance. Investigating the gene expression profiles of these lines using gene expression microarray analysis should provide important insights

into mechanisms of acquired resistance. Gene expression microarray analysis was carried out for MCF-7, MLET1, MLET2 and MLET5 cells. The aim was to identify genes whose expression is altered in the development of estrogen-independence and which might therefore be candidate genes involved in the emergence and/or maintenance of endocrine resistance in these cells.

For these experiments, cells were seeded in an estrogen-depleted cell culture medium consisting of phenol red-free DMEM, supplemented with 10% dextran-coated charcoal-stripped foetal calf serum (DSS). Twenty-four hours after seeding, culture medium was changed for fresh estrogen-depleted medium in control cultures, or for fresh estrogen-depleted medium supplemented with 10nM 17ß-estradiol, in cultures treated with estrogen. Cultures were harvested 16 hours later to extract RNA, with three replicate cultures being processed for each cell line and treatment. The extracted RNA was quantified and quality controlled by gel electrophoresis and RT-PCR analysis for GAPDH. RNA samples were subsequently sent to the Centre for Microarray Resources, Department of Pathology, Cambridge University, for hybridization to Illumina HumanWG-6 BeadChip Expression Arrays (http://www.illumina.com/) and the resulting raw and normalised expression data obtained in a format that allowed further analysis using GeneSpring software (Agilent). Bioinformatics analysis was carried out under the supervision of Dr Ross Thomas, Imperial College London.

The normalised gene expression microarray data set was analysed to remove background noise/non-significant genes. In order to identify differentially expressed genes, replicates were then grouped to give a mean and a standard error and subjected to statistical analysis using a parametric t-test. For this, variances were assumed to be equal as the lines were closely related and expected to show only a small proportion of genes with differential expression under the different conditions. The cut off for the test were p-values (confidence value). For example,

for a p-value of 0.1, only 1 out of 100 genes would be assumed to be a false positive. The differentially expressed genes that had a p-value of 0.05 or less would then be subjected to filtering based on fold changes. Probes with the same name represent different isoforms.

3.1.1 Principal component analysis (PCA) of gene expression microarray data

A PCA analysis of these gene sets was carried out by Dr Meng-Lay Lin and used to generate a three dimensional view of the clustering of the parental MCF7 cell line with MLET 1, 2 and 5 in the presence and absence of estrogen (Figure 3.1). This included all probes after the initial filtering (which removed probes with absent information and the bottom 20%), with a significant ($p<0.05$) differential fold change ≥1.5. This analysis shows that estrogen treatment results in considerable alteration in gene expression profiles, such that the estrogen treated and control profiles segregate in the PCA analysis. The three replicates for the estrogen or control treated cells cluster, as expected. MLET5 cells similarly show segregation of the estrogen treated versus control treated cells, indicative of considerable change in gene expression following estrogen addition. MCF-7 and MLET5 cells also locate differently in the PCA map, indicating that there are considerable differences in gene expression between the two lines. There was very little difference in gene expression profiles between MLET1 and MLET2 cells in the absence or presence of estrogen, evidenced by the tight clustering evident in the PCA analysis. Moreover, MLET1 and MLET2 gene expression profiles clustered them tightly together, which may be due to loss of ERα signaling, and/or extremely similar additional gene expression profiles for the two independently derived cultures. Similar results were obtained if a cut-off of ≥2-fold expression difference was used in the PCA analysis (Dr M-L Lin and Dr S Ali, personal communication). Since, the majority of endocrine resistant breast cancers remain ERα positive, I have not further characterised the ERα-negative MLET1 and 2 cell lines but have concentrated here on comparison

between the ERα-positive and estrogen-responsive MCF7 and the ERα-positive but estrogen-independent MLET5 cells.

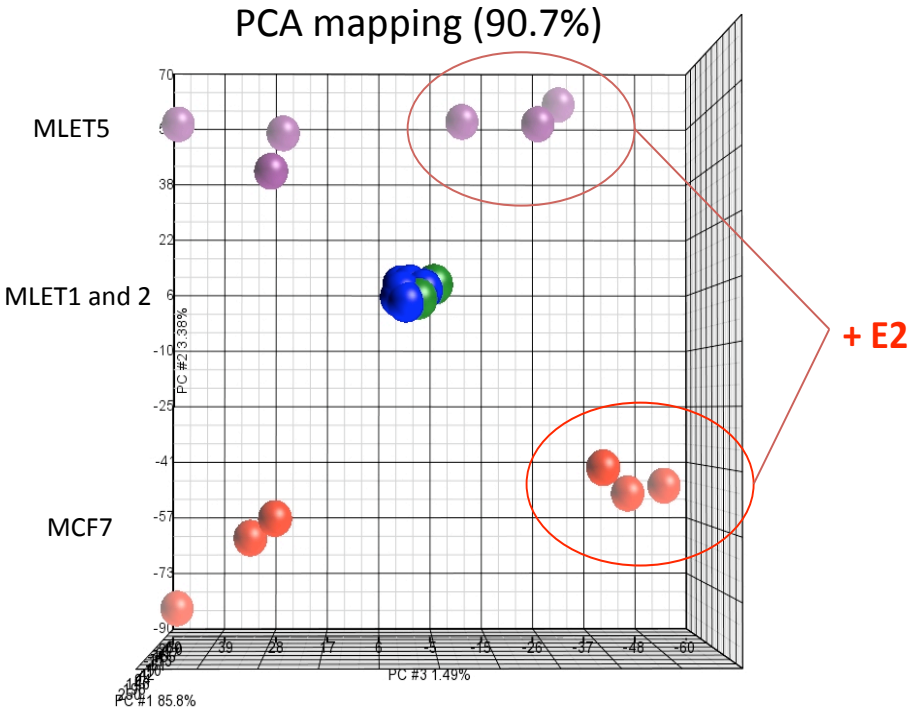


Figure 3.1 Principal Component Analysis (PCA) of Gene Expression Microarray Data Sets

Gene expression microarray profiling was carried out using the Illumina HT29 bead array. PCA analysis of normalized data carried out using Partek, is shown. This analysis was performed in our laboratory by Dr Meng-Lay Lin. Each globe represents one of the biological replicates for the MCF-7 (red), MLET1 (green), MLET2 (blue) and MLET5 (purple) samples. The MLET1 and MLET2 samples +/- estrogen mapped very closely. The estrogen (+E2) treated samples for MCF-7 and MLET5 are highlighted. The other samples were vehicle (ethanol) treated.

3.1.2 Estrogen regulated genes in MLET5 and MCF7

Two hundred and eleven genes were estrogen-regulated in MCF7 at ≥2 fold (Figure 3.2). Of these, 33% (69 genes) (shown in table 3.1) were also estrogen regulated (≥2 fold) in MLET5 cells (Figure 3.2A). This gene list includes previously characterized estrogen-regulated genes such as PgR, GREB1 and CXCL12 and highlights the functionality of ERα in MLET5, despite the estrogen-independent growth of the line. The number of genes showing estrogen regulation in MLET5 cells is lower than that in the parental MCF7 cells. This may be due to increased expression of many of the estrogen-regulated genes in the absence of estrogen in MLET5 cells. Many ERα target genes are estrogen repressed (Figure 3.2B). The expression of GREB1 and RAMP3 genes was increased ≥2-fold in MLET5 and MCF-7 cells respectively (a ratio of 0.6 and 0.7), whilst CXCR4 and TGFB3 genes were down-regulated ≥2-fold in MLET5 and MCF-7, respectively (ratio 0.5 and 0.9). Hence, there is a similar blunting of the estrogen responsive gene expression for genes whose expression is stimulated by estrogen and those genes whose expression is inhibited by estrogen, in MCF-7 cells.

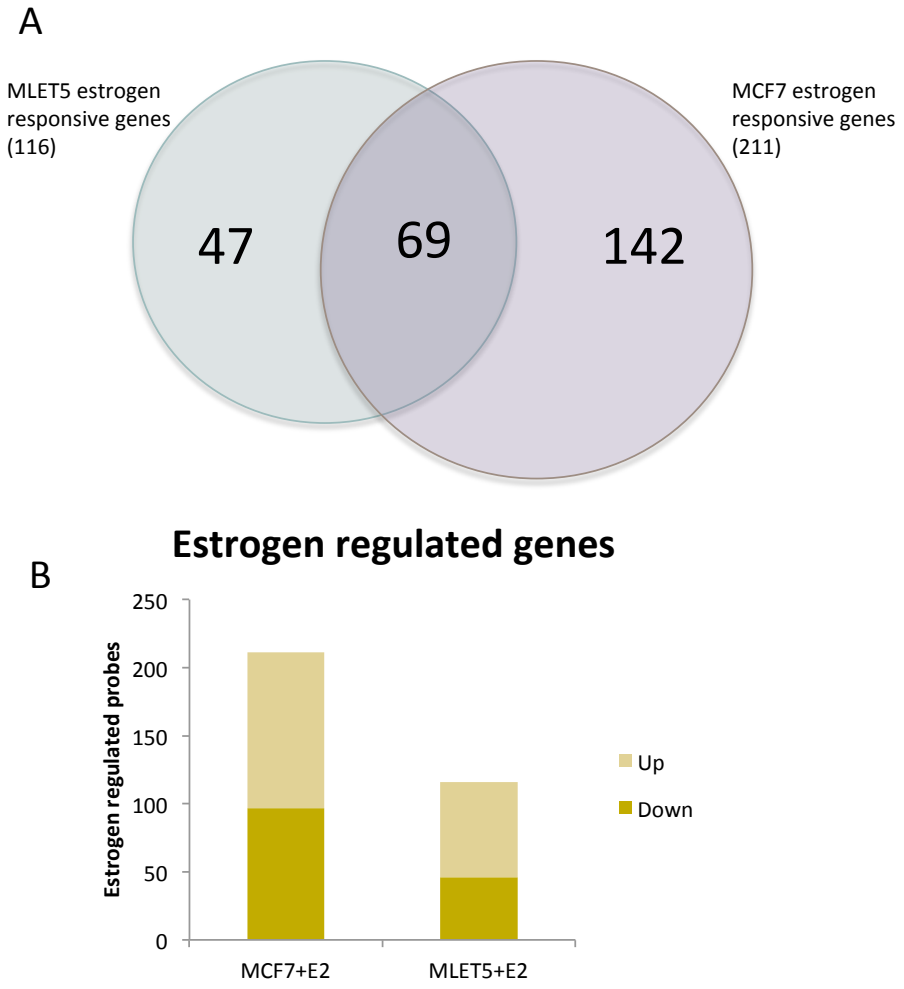


Figure 3.2 33% of differentially regulated genes in MLET5 remain estrogen regulated.

(A) Venn diagram of microarray analysis showing the overlap of genes with a ≥2 fold change in expression ($p<0.05$) between MCF-7 and MLET5 cells treated with estrogen versus (vehicle treated) control cells. This demonstrates that approximately 33% of estrogen regulated genes in MCF7 cells are also estrogen regulated in MLET5 cells by 2 fold or more. (B) Bar chart showing a division of estrogen up and down regulated genes between MLET5 and MCF7 with a fold change ≥2 or more ($p<0.05$)

Probe ID	Gene Symbol	MCF-7 E2 v MCF-7 NL	P value	MLET5 E2 v MLET5 NL	P value
2640681	GREB1	10.3	0.001	6.2	0.033
2260156	PDZK1	9.5	0.001	7.7	0.035
4670202	CXCL12	7.2	0.001	4.2	0.030
6940286	CXCL12	5.9	0.001	4.4	0.031
5550187	IGFBP4	5.7	0.001	5.2	0.030
4150474	KRT13	5.7	0.001	3.5	0.045
3140465	PKIB	5.7	0.001	3.6	0.033
50347	H19	5.0	0.001	2.7	0.035
1190735	PRSS23	4.8	0.001	4.1	0.034
4570400	SEMA3B	4.5	0.001	3.3	0.029
940370	FLJ30058	4.4	0.001	2.3	0.030
6840647	RAPGEFL1	4.3	0.001	3.5	0.028
6130239	SGK	4.0	0.000	2.8	0.030
4610551	PGR	4.0	0.001	4.7	0.030
1300326	SFXN2	3.9	0.001	2.6	0.039
4280762	SEC14L2	3.9	0.001	2.1	0.033
7210286	MYB	3.9	0.002	2.2	0.030
4390338	CELSR2	3.8	0.001	2.7	0.028
1430519	TPD52L1	3.6	0.001	2.7	0.028
5360687	RAMP3	3.6	0.002	2.5	0.030
7160274	NPY1R	3.6	0.002	3.7	0.030
2350482	CXCL12	3.3	0.002	2.7	0.041
5700341	SOX3	3.2	0.001	2.3	0.045
4670025	OLFM1	3.2	0.001	2.2	0.030
1740040	FOXC1	3.2	0.002	2.5	0.030
3310204	RERG	3.1	0.001	2.8	0.030
6450148	IL17RB	2.9	0.001	2.2	0.030
5260209	SGK3	2.9	0.001	2.2	0.030
6560162	PTGES	2.8	0.001	4.5	0.033
3370026	PCP4	2.7	0.001	4.5	0.033
3060044	MYEOV	2.6	0.001	2.1	0.033
5080576	CALCR	2.6	0.001	2.5	0.038
5890717	SUSD3	2.6	0.002	3.2	0.048
5720681	TIPARP	2.5	0.002	2.1	0.033
990128	GFRA1	2.4	0.002	2.7	0.030
2350243	UGT2B17	2.4	0.001	2.5	0.041
1110441	ADAMTS9	2.3	0.001	2.4	0.030
1690386	NT5DC3	2.3	0.002	2.1	0.030
20349	FKBP4	2.3	0.001	2.2	0.030
1010731	C1QTNF6	2.3	0.005	3.8	0.030
4560561	TUBA3E	2.2	0.001	2.5	0.037
2760092	FAIM3	2.2	0.001	3.4	0.030
6280168	NEIL2	2.1	0.001	2.0	0.033
5290215	HSPB8	2.1	0.002	2.3	0.040
2760168	KCNK6	2.1	0.001	2.1	0.030
2450414	SERPINA1	2.1	0.002	2.2	0.032
7550072	HS.388347	2.0	0.002	2.4	0.030
3610372	PLAC1	2.0	0.002	3.1	0.036

Table 3.1A Estrogen-responsive genes up-regulated in MLET5 (n=69 genes n=72 probes) p=<0.05 Fold Change ≥ 2

Probe ID	Gene Symbol	MCF-7 E2 v MCF-7 NL	P value	MLET5 E2 v MLET5 NL	P value
3940082	FAM83A	0.5	0.001	0.5	0.033
3940376	FAM107B	0.5	0.001	0.5	0.042
4890360	BLNK	0.5	0.003	0.4	0.037
2190113	KRTHB6	0.5	0.002	0.5	0.033
6420386	EFNA1	0.5	0.005	0.4	0.030
7400523	TGFB3	0.5	0.002	0.4	0.033
2260148	NELL2	0.5	0.001	0.5	0.032
6380563	YPEL3	0.4	0.001	0.4	0.033
4860689	TFPI	0.4	0.006	0.4	0.045
6220554	HS.25318	0.4	0.001	0.4	0.033
510543	ABCC3	0.4	0.001	0.5	0.031
4920576	ST8SIA4	0.4	0.002	0.5	0.030
1980458	RND3	0.4	0.001	0.5	0.040
2900450	PUNC	0.4	0.001	0.5	0.036
5570672	CLDN9	0.4	0.003	0.4	0.037
5810047	MGC59937	0.4	0.001	0.4	0.038
4670717	PGM5	0.4	0.001	0.3	0.039
5860477	EDG3	0.4	0.003	0.5	0.048
10673	HS.510367	0.3	0.001	0.3	0.045
2570129	PGM5	0.3	0.001	0.3	0.033
5820689	EFEMP1	0.3	0.001	0.4	0.031
4390634	TNS3	0.3	0.001	0.4	0.033
4540768	SALL4	0.3	0.001	0.3	0.042
7380056	TP53INP1	0.2	0.001	0.4	0.039

Table 3.1B Estrogen-responsive genes down-regulated in MLET5 (n=69 genes n=72 probes), p=<0.05 Fold Change ≥ 2.

In order to validate the findings of the microarray analysis I looked at gene expression by quantitative real time RT-PCR in MCF-7 and MLET5 cells, following the addition of estrogen (E), 4-Hydroxytamoxifen (4HT) or Faslodex (ICI 182, 780; ICI) (Figure 3.3). Cells were harvested 16 hours after addition of ligand. This time point was chosen following time course experiments, conducted within this laboratory, demonstrating that 16 and 24 hours was optimal for good induction of gene expression following the adition of estrogen (Simak Ali and Paul Thiruchelvam personal communication). To improve the likelihood of inducing direct targets I used the 16 hour time point.

ERα mRNA levels were elevated in MLET5 cells compared with expression levels in MCF7 cells (Figure 3.3), which is in agreement with results with long-term estrogen deprived LTED MCF-7 models, which commonly report elevated ERα levels (Martin et al., 2003). ERα expression in MCF-7 cells was not significantly different following estrogen, 4HT or ICI treatment. ERα expression in MCF-7 cells was similarly unaffected by ligand in MLET5 cells, with the exception of ICI treatment; the reasons for this increase in ERα expression in MLET5 following ICI addition, is unclear.

Interestingly, expression of the ERα target genes, PgR and GREB1, was also elevated in MLET5 relative to the MCF-7 cells, although estrogen stimulation of their expression was still evident. These results are in agreement with the estrogen regulation observed for the microarray data. With anti-estrogen treatments, the two genes differed in their response in the two lines. Expression of both genes was stimulated by estrogen and strongly inhibited by ICI. In the presence of 4HT, however, GREB1 was repressed but PgR expression was stimulated, relative to the no ligand control. The differences in response to 4HT are presumably a reflection of differences in 4HT-mediated recruitment of ERα to the promoters/enhancers of the PgR and GREB1 genes in these cells. A more detailed analysis of a larger series of ERα target genes might help in addressing these differences. Notwithstanding,

estrogen and anti-estrogen regulation of the expression of well-regulated ERα target genes appears, by and large, to be intact in MLET5 cells.

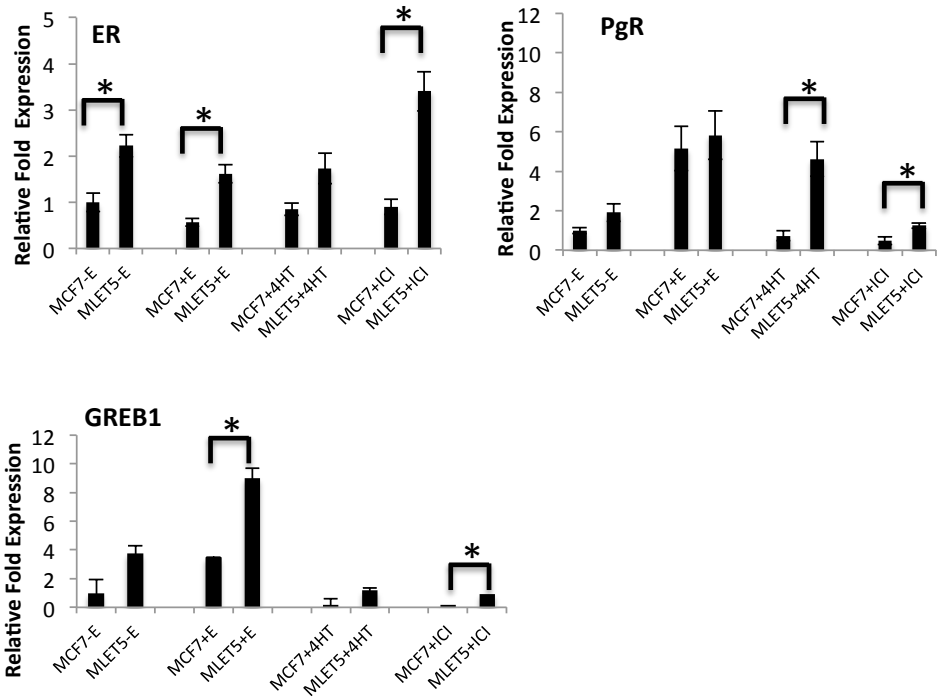


Figure 3.3 Validation of the expression of estrogen regulated genes

Q-RT-PCR expression analysis of estrogen regulated genes using primers for GAPDH, ESR, PgR and GREB1. RNA samples were prepared from MCF-7 and MLET5 cells, 16 hours after the addition of ligand. Expression is shown following normalization against GAPDH expression. For each gene, fold expression in MCF-7 cells treated with ethanol control was taken as 1 and all other samples are shown relative to this. The mean values are shown in the bar chart, n=3. The errors bars represent the standard errors of the mean (SEM). Statistically significant results ($p<0.05$) are marked with *.

3.1.3 Estrogen independent activation of gene expression in MLET5

I next examined the total number of genes that are differentially expressed between MCF-7 and MLET5 cells. Eight hundred and eighty six genes were differentially regulated in vehicle treated MLET5 compared with vehicle treated MCF7 (Figure 3.4A). The majority of these genes (567/869 = 65%) were also differentially regulated in the estrogen-treated MCF7 and MLET5 cells. To determine if this gene set includes estrogen-responsive genes whose expression becomes estrogen-independent in MLET5 cells, this gene set was compared with estrogen-responsive genes in MCF7 cells (Figure 3.4B). Ten percent (86 genes) of the differentially regulated genes in MLET5 versus MCF-7 are strongly estrogen-regulated genes in MCF7 cells. This includes GREB1, CXCL12, MYB, MYC, IGFL1, RET and TNFRSF21 (DR6) (list shown in supplementary data). Within this overlap group some genes remain estrogen regulated, such as GREB1, CXCL12, MYB, MYC, IGFL1 and RET, although expression levels in the absence of estrogen is elevated for these genes. Other genes show no estrogen regulation in MLET5 cells and appear therefore to have become estrogen independent e.g. TNFRSF21 (DR6), TMPRSS4, SMAD3.

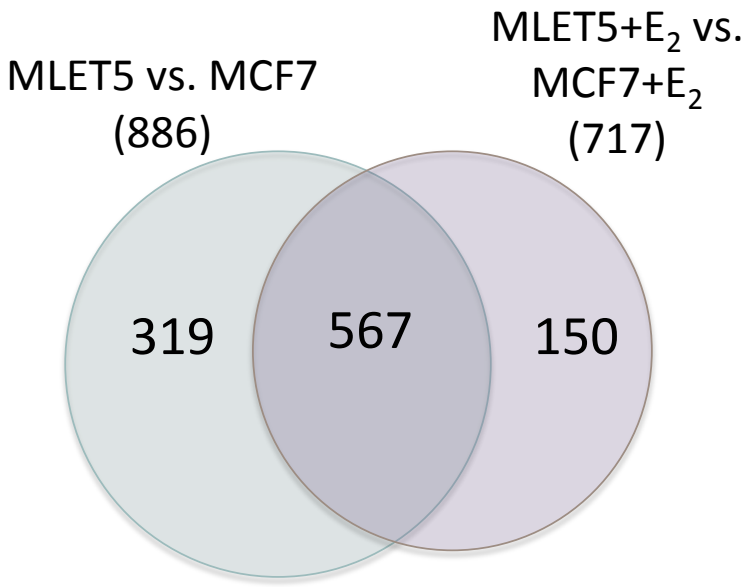


Figure 3.4A Differentially regulated genes in MLET5 versus MCF7 (≥2 Fold, $p<0.05$) Venn diagram of microarray analysis shows 886 genes are differentially regulated ≥2 fold ($p<0.05$) in the absence of estrogen and 717 in the presence of estrogen between MLET5 and MCF7 samples. 567 genes are differentially regulated in both the vehicle treated and estrogen treated samples.

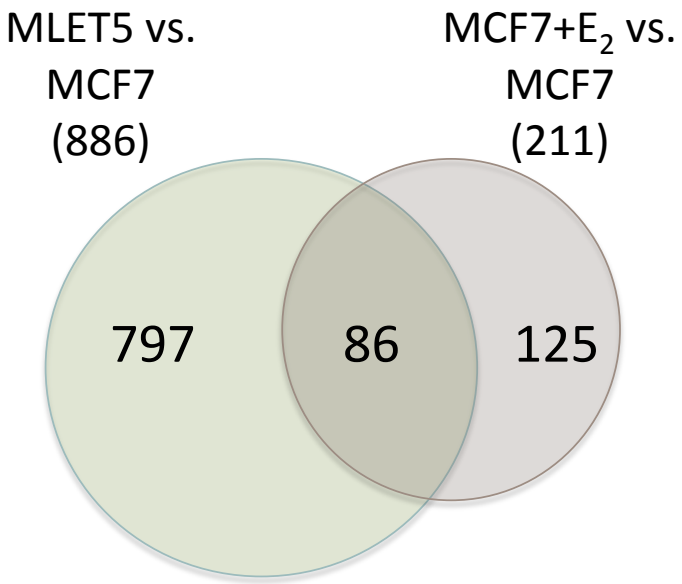


Figure 3.4B. Estrogen Independent activation of genes in MLET5

Venn diagram of microarray analysis showing the overlap of genes with a ≥2 fold change in expression ($p<0.05$) between vehicle treated MLET5 versus MCF7 cells (886), and the overlap with genes with a ≥2 fold estrogen regulation in MCF7 ($p<0.05$) .

Estrogen-responsive genes, whose expression becomes estrogen-independent and which are highly expressed in the absence of estrogen in MLET5 cells, may be interesting candidates for exploration as potential mediators of estrogen independence in endocrine resistant breast cancer. In this context, several genes demonstrated considerable up-regulation in MLET5 cells. Interestingly, of the top four genes up-regulated in MLET5 (Figure 3.5A), three were genes whose expression is repressed by estrogen in MCF7 cells (IGFL1, TM4SF1, CD36) and only one that was estrogen-stimulated in MCF7 cells (CALB2).

IGFL1, (IGF-like gene 1) is structurally related to the IGF super-family of growth factors. A study using qPCR has demonstrated expression in the ovaries and spinal cord, and, using BLAST analysis of GenBank human EST database, in fetal skin, normal breast, head and neck tumours, squamous cell carcinoma, uterine tumour and carcinoma cell lines (Emtage et al., 2006). The biological activity of IGFL1 remains to be defined but may be similar to the IGF growth factor family. In MLET5 cells IGFL1 is significantly up-regulated by approximately 3 fold, compared with MCF7 cells in the absence and presence of estrogen, and retains the estrogen repression seen in MCF7 cells (Figure 3.5B).

TM4SF1, is a trans-membrane protein that is associated with cancer growth (Hellstrom et al., 1986), motility (Chang et al., 2005) and invasion (Kao et al., 2003; Lekishvili et al., 2008). More recently it has been shown to play a key role in angiogenesis (Shih et al., 2009) and in vitro and xenograft models have shown its promise as a potential therapeutic target (Lin et al., 2014). TM4SF1 is significantly up-regulated in MLET5 cells by approximately 10 fold compared with MCF7 cells in the absence and presence of estrogen and again retains the estrogen repression seen in our MCF7 cells (Figure 3.5B).

CALB2 is a Ca^{2+} buffering protein, which has been used as a marker in malignant mesothelioma to differentiate from adenocarcinomas (Husain et al., 2009) and is under investigation as a potential therapeutic target (Blum and Schwaller, 2013). However a recent study confirms that it is also expressed on 15% of breast carcinomas, although more likely to be associated with ERα negative, high grade, basal –like phenotype (Powell et al., 2011). In this experiment, CALB2 was significantly up-regulated in MLET5 cells (approximately 3 fold) compared with MCF7, in the absence of estrogen. It is also up-regulated in response to estrogen in MCF7 cells and retains this response in MLET5 (Figure 3.5B).

CD36 is a trans-membrane receptor that is expressed on epithelial cells, platelets, phagocytes, adipocytes, hepatocytes and myocytes. It has been shown to play a role as a negative regulator of angiogenesis via thrombospondin 1 (Jimenez et al., 2000) and 2 by inducing apoptosis via loss of mitochondrial membrane potential and activation of caspase-3 (Koch et al., 2011). More recently the loss of CD36 has been linked to increased collagen deposition and increased breast tissue density, which may play a role in breast carcinogenesis (DeFilippis et al., 2012; Seewaldt, 2012). Uray et al demonstrated that hormone dependent cell lines, MCF7 and T47D, down regulate CD36 in response to estrogen and Faslodex prevents the loss of CD36 which may contribute to its mechanism of action (Uray et al., 2004). This supports the data I show for CD36, with strong up-regulation in MLET5 cells compared with MCF7 cells, in the absence and presence of estrogen (by approximately 500 fold) and estrogen inhibition (approximately two fold) is seen in both MLET5 and MCF7 cell lines, as documented in the literature (Uray et al., 2004) (Figure 3.5B).

Following treatment with the selective estrogen receptor modulator, 4-HT and the pure estrogen antagonist, Faslodex (ICI), the three estrogen repressed genes (IGFL1, TM4SF1 and CD36) show a significant increase in expression compared with MCF7 cells – as expected from the increased basal expression. CALB2, as an estrogen

stimulated gene, following treatment with 4-HT and Faslodex show values similar to untreated MCF7 and MLET5 cells ((Figure 3.5B).

A

	Probe ID	Gene Symbol	MLET5 NL v MCF-7 NL FC	MLET5 E2 v MCF-7 E2 FC	MLET5 E2 v MLET5 NL FC	MCF-7 E2 v MCF-7 NL FC
1	3990167	CD36	89.2	78.3	0.7	0.8
2	3390468	TM4SF1	20.9	41.0	0.3	0.2
3	2490021	IGFL1	20.6	32.2	0.6	0.4
4	4260433	CD36	45.3	31.9	0.7	0.9
5	6130364	CALB2	20.2	23.4	1.6	1.4

B

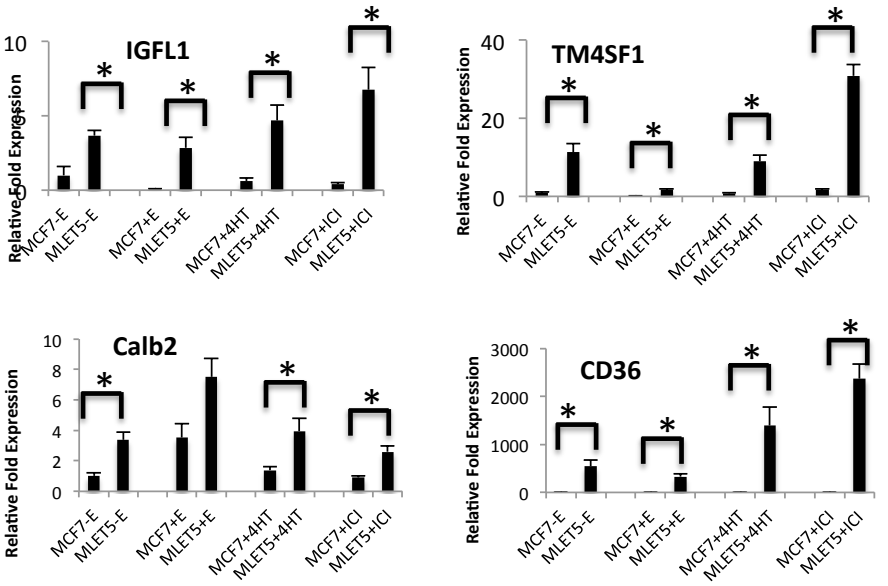


Figure 3.5 Validation of the expression of the top four genes with the greatest up-regulation between MLET5 and MCF7

(A) The table shows the genes demonstrating the greatest fold difference in expression between MCF-7 and MLET5 from the microarray analysis. The p values are all <0.05 except for CD36, shaded in grey where p=0.104. (B) Q-RT-PCR expression analysis was carried out on these four genes. RNA samples were prepared from MCF-7 and MLET5 cells, 16 hours after the addition of ligand. Expression is shown following normalization against GAPDH expression. For each gene, fold expression in MCF-7 cells, in the absence of ligand, is taken as 1 and all other samples are shown relative to this. Each Q-RT-PCR was performed in triplicate using three independent RNA samples. The mean values are shown in the bar chart. The errors bars represent the SEM. Statistically significant results ($p<0.05$) are marked with *.

3.1.4 Functional Group Analysis of MLET5 Differential Gene Expression

The above-described real-time RT-PCR analysis provides evidence confirming the gene expression microarray profiles. In order to identify signaling pathways that are altered in MLET5, pathway analysis was performed of the differentially expressed genes shown in MLET5 using DAVID online software (http://david.abcc.ncifcrf.gov/gene2gene.jsp). This revealed "Development", "Adhesion", "Differentiation and Death" and "Motility" amongst the most highly enriched functional groups. This program uses enrichment scores based on published data as a statistical likelihood of association. The initial five groups with a strong association or enrichment score appeared to be loosely linked in terms of functional grouping (Table 3.2). As one of the highest scoring GO functional groups, I investigated the potential involvement of "Differentiation and Death" or apoptosis genes. Examination of the differentially expressed genes identified 95 genes whose expression placed them in the apoptosis pathways and whose expression was significantly altered in MLET5 cells, relative to expression profiles in MCF-7 cells. Foremost amongst these genes were BCL2 (anti-apoptotic), which was up-regulated in MLET5 cells and related genes, BAD (up-regulated) and BIK (down-regulated) (Hur et al., 2004)(Figure 3.6A).

	Enrichment score	**Number of genes**
Cluster 1: Development	10.3	
Developmental process		208
Anatomical structure development		150
Organ development		98
System development		122
Multicellular organismal development		149
Multicellular organismal process		193
Cluster2: Adhesion	8.07	
Biological adhesion		68
Cell adhesion		68
Cell adhesion		37
Cluster3: Differentiation and death	4.05	
Cell differentiation		114
Cellular developmental process		114
Cell development		81
Cell death		56
Death		56
Apoptosis		52
Programmed cell death		52
Regulation of apoptosis		35
Regulation of programmed cell death		35
apoptosis		20
Cluster 4: Motility	3.81	
Localisation of cell		35
Cell motility		35
Cell migration		22
Cluster 5: Negative regulation	3.78	
Negative regulation of cellular processes		73
Negative regulation of biological processes		74
Negative regulation of metabolic processes		29
Cluster 6: Development	3.58	
Tissue development		31
Ectoderm development		17
Epidermis development		15

Table 3.2 Functional group analysis of genes differentially regulated in MLET5, compared with MCF7 cells, using DAVID (http://david.abcc.ncicrf:gov/gene2gene.jsp)

A

Probe ID	Gene Symbol	MLET5 NL v MCF-7 NL FC	MLET5 E2 v MCF-7 E2 FC	MLET5 E2 v MLET5 NL FC	MCF-7 E2 v MCF-7 NL FC
3850082	BCL2	5.7	5.8	1.7	1.7
50563	BCL6	2.9	2.7	0.9	0.9
5860181	NUPR1	2.1	2.2	0.8	0.7
1070307	SOCS2	0.2	0.4	0.9	0.6
5090195	TNFRSF21	0.1	0.3	1.1	0.5
150630	ANXA1	0.1	0.2	0.9	0.6
3170280	BAD	2.6	2.5	0.8	0.9
4540551	IGFBP3	2.6	1.7	0.5	0.8
2600091	BIK	0.4	0.4	0.6	0.6
10133	BID	0.5	0.6	1.1	0.8

Figure 3.6A Validation of expression of genes involved in apoptosis in MCF7 and MLET5 cells

Fold change in expression of Bcl2, Bcl6 and NUPR1 (anti-apoptotic); SOCS2, DR6, ANXA1, BAD, IGFBP3, BIK and BID (pro-apoptotic) from microarray analysis of MLET5 versus MCF7 and MCF7+E versus MCF7 ($p=<0.05$).

I investigated the expression of a number of the above highlighted genes that are estrogen-regulated in MCF7 cells and members of the intrinsic pathway of apoptosis (BCL2, BID, BIK and BAD). Also chosen for investigation were SOCS2, TNFRS21 and IGFBP3 as they are involved in signalling pathways that modulate cell survival/apoptosis (Butt and Williams, 2001; Cano et al., 2011; Faderl et al., 2003; Klima et al., 2011; Sen et al., 2012; Zeng et al., 2012), as well as two transcription factors, BCL6 and NUPR1 linked with apoptosis/cell survival (Cano et al., 2011; Walker et al., 2014) that are up-regulated in MLET5 cells. Interestingly, none of these genes demonstrated loss of estrogen regulation indicative of the loss of ERα regulation in the microarray datasets. Q-RT-PCR confirmed the findings of the microarray data (Figure 3.6B).

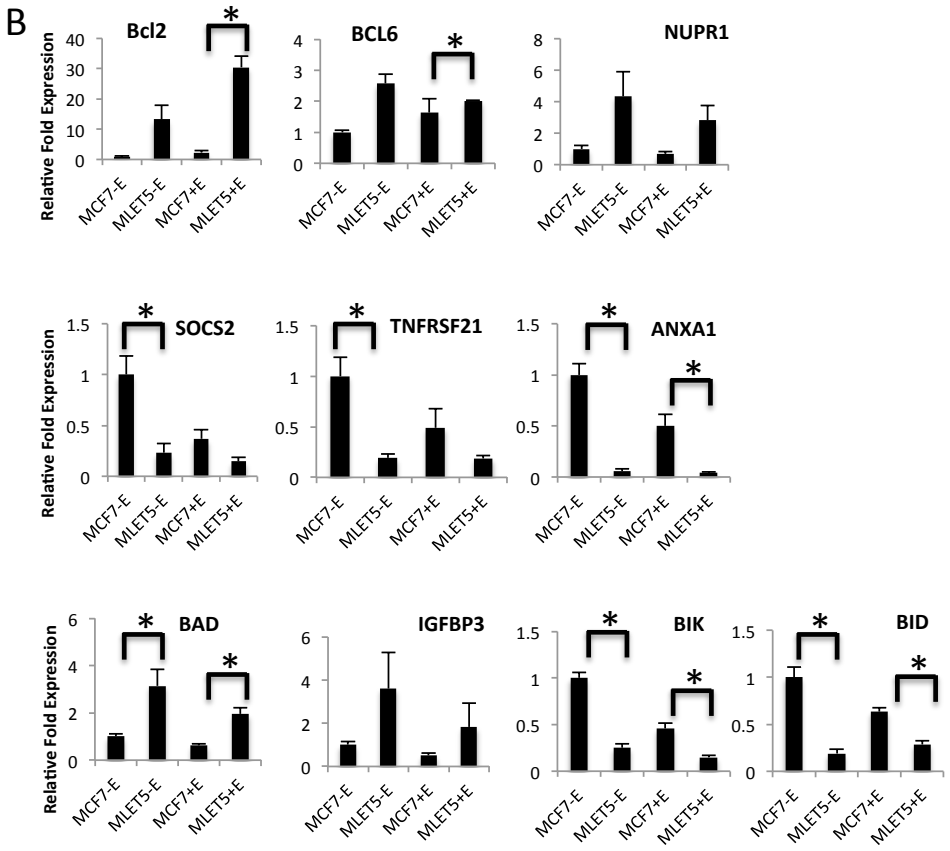


Figure 3.6B Validation of expression of genes involved in apoptosis in MCF7 and MLET5 cells

Q-RT-PCR expression analysis of genes identified in microarray analysis of MLET5 vs. MCF7 involved with apoptosis. RNA samples were prepared from MCF-7 and MLET5 cells, 16 hours after the addition of ligand (10nM E2 or ethanol control). Expression is shown following normalisation against GAPDH expression. For each gene, fold expression in MCF7 cells in the absence of ligand is taken as 1 and all other samples are shown relative to this. Each Q-RT-PCR was performed in triplicate using three independent RNA samples. The mean values are shown in the bar chart and the error bars represent the standard error of the mean (SEM).

Bcl2 is a known estrogen-stimulated gene (Su et al., 2014) and its expression was elevated 12-fold increase in MLET5 cells compared with levels of expression in MCF-7 cells (Figure 3.6B). Estrogen treatment further elevated Bcl2 levels, the level of stimulation being similar to that observed in MCF-7 cells. Bcl2 is the founding member of the Bcl2 family of anti-apoptotic proteins and functions by preventing programmed cell death (Vaux et al., 1988). It was initially identified due to a chromosomal translocation t(14;18) found in 85% of follicular lymphomas and 20% of diffuse large B cell Non Hodgkin Lymphomas (DLBC NHL) (Tsujimoto et al., 1985). There are three sub families within the Bcl2 family, BH1-4 (containing Bcl2, Bcl-XL), BH123 proteins (containing Bax and Bak) and BH3 only proteins (containing BAD, BIK and BID). The BH3 only proteins are the largest subclass of Bcl2 family proteins, which act, in the main, by inhibiting anti-apoptotic Bcl2. It is thought that the balance between levels of the pro- and anti-apoptotic Bcl2 family members determines if a cell undergoes apoptosis (Korsmeyer et al., 1993). The mechanism by which the BH3 proteins cause apoptosis has historically been thought to be due to displacement of anti-apoptotic Bcl2 or Bcl2XL from Bax and Bak by competitive binding. However, there is also evidence that direct interaction with Bax or Bak can induce activation of caspases and therefore apoptosis (Leibowitz and Yu, 2010), and post-translational modification of Bcl2 family members also being important in determining the balance between apoptosis and survival (Danial, 2008).

Expression of the pro-apoptotic BAD was elevated 2-fold in MLET5 cells, whereas expression of the pro-apoptotic BIK and BID genes was reduced in MLET5 (Figure 3.6B). Phosphorylation of BAD at S155, S112 and S136 has been shown to decrease its pro-apoptotic ability (Datta et al., 2000; Tan et al., 2000) and contribute to cancer cell survival (Virdee et al., 2000). This may occur for two reasons; firstly, S155 lies

within the BH3 anti-apoptosis factor hydrophobic binding site, although has been shown to be dependant on the two other sites of phosphorylation, S112 and S136 in mutational studies therefore may be the rate limiting step in a tiered phosphorylation system (Danial, 2008). Secondly, the location of the majority of phosphorylated BAD changes from mitochondrial to sequestration within the cytosol (Hirai and Wang, 2001; Zha et al., 1996). Non-phosphorylated BAD dimerizes BCL-XL and BCL2 displacing BAX which is then free to initiate an increase in mitochondrial membrane permeability and apoptosis (Moses et al., 1990). A previous study (Virdee et al., 2000) has shown an increase in the percentage of pBAD relative to total BAD in cancer cell lines (breast, ovary and lung) compared with immortalized normal cells (Stickles et al., 2015). It would therefore have been of value to assess pBAD in conjuntion with total BAD.

BIK and BID are also members of the BH3 family of pro-apoptotic proteins. Bik acts indirectly via BCL-XL to trigger BAX-dependant apoptosis (Chinnadurai et al., 2008; Gillissen et al., 2003; Rashmi et al., 2008) and has been implicated in playing a role in the development of lung and breast carcinomas(Vijayalingam et al., 2010). BID is thought to be related both structurally and functionally to the BH123 (or multi BH proteins) by its ability to function, once cleaved by caspase-8 or other proteases initiated by death receptors, at the mitochondrial membrane and induce permeabilization via Bax +/- Bak. (Billen et al., 2008).

ANXA1 promotes apoptosis by associating directly with the p65 subunit of NF-kB thereby preventing binding to target DNA sequences (Zhang et al., 2010). The mechanism for this prevention is not yet fully known but cell work shows ANXA1 induced inhibition of NF-kB results in a change in associated signalling molecules such as BCl2 and survivin (Shen and Tergaonkar, 2009). ANXA1 expression has been shown to be up-regulated in response to estrogen via the activation of cAMP-responsive element binding protein and the estrogen receptor and this published data suggests it may act as a tumour suppressor gene in breast cancer (Ang et al., 2009). This correlates with an associated loss of expression seen previously in

association with breast cancer development and progression (Shen et al., 2006). In this experiment ANXA1 expression was reduced 10-fold in MLET5 cells compared with MCF7 cells, with repression in response to estrogen (Figure 3.6B).

TNFRS21 (DR6), also acts through NF-kB to promote apoptosis (Kasof et al., 2001). Although a full understanding of this mechanism is not yet known, studies suggest that one mechanism may be via S5a, a subunit of the 26S proteasome enzyme complex which in turn binds polyubiquitin to target proteins for removal (Wang et al., 2005a; Wang et al., 2014). TNFRS21 expression, like that of ANXA1, is inhibited by estrogen in MCF7 cells and expression was significantly reduced in MLET5 cells (Figure 3.6B).

Suppressor of cytokine signaling 2 (SOCS2) has pro-apoptotic actions via the JAK/STAT pathway. It is known to inhibit growth hormone action and SOCS2 null mice exhibit gigantism (Favre et al., 1999; Metcalf et al., 2000). Intriguingly, cell line data (HEK293, ERα positive embryonic kidney cells) shows that the effects of SOCS2 on Growth Hormone (GH) are mixed, with suppression of action at low concentrations and enhanced action at higher concentrations (Favre et al., 1999). In my experiment, expression of SOCS2 was reduced approximately 5 fold in MLET5 cells and shows a repression of expression following treatment with estrogen (approximately 2 fold) by qPCR at 16 hours. This is in contrast to published data for alternative cell lines, HEK293 (Leung et al., 2003) and HuH7 cells (Leong et al., 2004). This contrasting result may be attributed to their measurement of SOCS-2 expression at time points up to 4 hours after estrogen treatment with a peak fold difference of approximately 1.8 at 2 hours.

BCL6 is a transcriptional repressor that inhibits apoptosis by recruiting co-repressor complexes, such as SMRT and NCoR (Ahmad et al., 2003; Huynh and Bardwell, 1998). It has been shown to be elevated in approximately 50% of breast

tumour samples and the majority of breast tumour derived cell lines (Walker et al., 2014). In this experiment, BCL6 was elevated in MLET5 with no significant estrogen response in either MCF7 or MLET5.

NUPR1, is up-regulated in metastatic breast cancer and has been shown to play a role in cellular growth inhibition (Bratland et al., 2000; Ree et al., 2000). It was significantly down regulated (14.2 fold) in a p23 over-expressing MCF7 cell line that has been shown to exhibit increased invasiveness whilst maintaining estrogen dependent proliferation (Simpson et al., 2010). It has been implicated in chemo-resistance, in pancreatic and breast cancer, possibly via p21 and activation of the anti-apoptotic Bcl-xL, (Chowdhury et al., 2009; Clark et al., 2008; Vincent et al., 2012) but also in contributing to adriamycin-induced apoptosis in mouse embryonic fibroblasts (MEFs) (Vasseur et al., 2002). The role of NUPR1 in the progression of pancreatic cancer was shown more recently to be via the alternative RelB-dependent NFkappaB pathway (Hamidi et al., 2012). Further evidence for the role of NUPR1 in apoptosis was shown by the knockdown of NUPR1 in non small cell lung cancer xenograft models in nude mice which significantly inhibited cell proliferation and arrested cells in G0 phase of the cell cycle with an increase in apoptosis shown by flow cytometry experiments (Guo et al., 2012). Despite the conflicting role of NUPR1 there is certainly strong evidence that it plays a part in apoptosis across a variety of tumour types, including breast cancer, although it is likely to be a multifunctional protein, which would explain this disparity of results. In this experiment it is up-regulated approximately 4 fold in MLET5 cells compared with MCF7 and estrogen repressed consistent with published data (Sarvari et al., 2010).

IGFBP3 functions as a tumour suppressor gene by inhibiting cell growth and inducing apoptosis (Baxter, 2014). The mechanism for this can be independent of p53 and IGF (Furstenberger and Senn, 2002; Rajah et al., 1997) although p53 has also been shown to induce expression of IGFBP3 (Grimberg, 2000). The initial work

was performed in prostate cancer cell lines, and it has subsequently been confirmed in breast cancer cells (T47D) that IGFBP3 up-regulation leads to an increase in the pro-apoptotic proteins Bax and BAD and a down regulation of the anti-apoptotic Bcl2 and Bcl-xL (Butt et al., 2000; Butt and Williams, 2001). Conversely IGFBP3 has also been shown to be over-expressed in a variety of cancers, including breast cancer and has been associated with both favourable and poor prognosis (Figueroa et al., 1993; Mu et al., 2009; Ren et al., 2007; Shao et al., 1992; Yu et al., 1996). In this experiment, IGFBP3, was up-regulated (3 fold) in MLET5 cells with a repression in expression following treatment with estrogen (Figure 3.6B).

Therefore, with the exception of BAD, whose expression was elevated in MLET5 cells, expression of known pro-apoptotic genes was reduced in MLET5 cells, whereas expression of anti-apoptotic genes was elevated, indicating that development of endocrine resistance in MLET5 involves altered programming of cell survival pathways, perhaps as a result of progression through the growth crisis brought about by prolonged culturing in estrogen-depleted medium. The reprogramming may have resulted from the transient over-expression of ERα used in the generation of MLET5 cells. NUPR1 and IGFBP3 are interesting genes whose definitive role and mechanism of action in the context of breast cancer are yet to be determined.

It was particularly interesting to see changes in expression of several genes in the Bcl2 family. To determine if the differences in levels of mRNA expression of these genes is also observed at the protein level Western blotting was carried out. The levels of BCL2 and BAD were increased, whilst BID and BIK levels were lower in MLET5 cells (Figure 3.7). BAD is pro-apoptotic, as are BIK and BID. Increase in levels are therefore counter to the other results, which show increase in expression of anti-apoptotic genes, but reduced levels of pro-apoptotic genes. It should be noted, however, that levels of BCL2 mRNA were 15-35 fold higher in MLET5 compared with MCF7 cells, compared with only an increase of 2-3 fold in the case of

BAD. Taken together with the reduction in BID and BIK levels, the large increase in BCL2, is likely to outweigh the modest increases in levels of BAD protein.

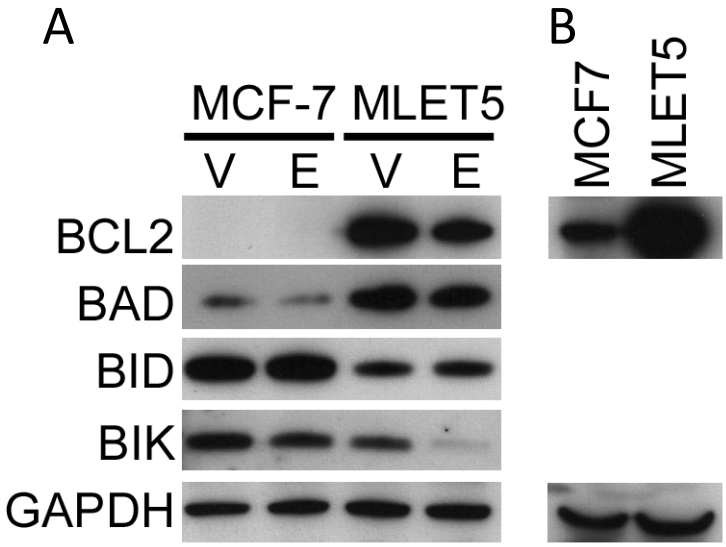


Figure 3.7 Altered protein expression of genes associated with apoptosis in MLET5 cells

(A) MCF7 and MLET 5 cells were cultured in estrogen depleted media and harvested 24 hours following the addition of 10nM E2 (E) or an equal volume of ethanol as vehicle treated control (V). Western blot shows protein expression of BCL2, BAD, BID, BIK and GAPDH. (B) Western blotting and long exposure of MCF7 and MLET5 (no ligand) lysates to show expression of BCL2 in MCF7 and MLET5 cells.

The above data suggest that during the derivation of MLET5 cells, gene expression changes have selected for pro-survival programmes. This would predict that MLET5 cells are likely to be more resistant to agents that promote apoptosis than MCF7 cells. To investigate this, growth and cell cycle analysis was carried out assessing the response of both MCF7 cells and MLET5 cells to the widely used chemotherapeutic agent Etoposide. Etoposide (VP16-213) is derived from the American mandrake and acts by inhibiting the enzyme topoisomerase II, which is involved in cleaving DNA so that it can unwind during cell division. Etoposide stabilizes the DNA-Topoisomerase II complex and results in DNA double strand breaks, thereby promoting apoptosis (D'Arpa et al., 1990; Ju et al., 2006; Zhao et al., 2012). MCF7 and MLET5 cells were treated with a titration of dosages from 100μM to 1nM, with a DMSO vehicle treated control. Cell growth was then assessed using the SRB assay (Figure 3.8A). MCF7 and MLET5 cell growth was inhibited with GI_{50} of 5.59 and 19.28 μM, respectively, indicating that MLET5 cells are resistant to etoposide. FACS analysis following treatment of cells with 100μM etoposide for 24 hours resulted in accumulation of cells in the sub-G1 peak, with 60% and 20% of the cells being in the sub-G1 peak in the case of MCF7 and MLET5, respectively (Figure 3.8B). This suggests that MLET5 cells are resistant to apoptosis promoted by etoposide. To confirm that the sub-G1 cells are indeed undergoing apoptosis, cells were treated with increasing concentrations of etoposide, fixed and immunostained for annexin V and propidium iodide (PI). FACS analysis showed a dose-dependent increase in cells undergoing apoptosis in MCF7 cells, whereas even with 100μM etoposide, less than 10% of MLET5 cells underwent apoptosis. (Figure 3.8C).

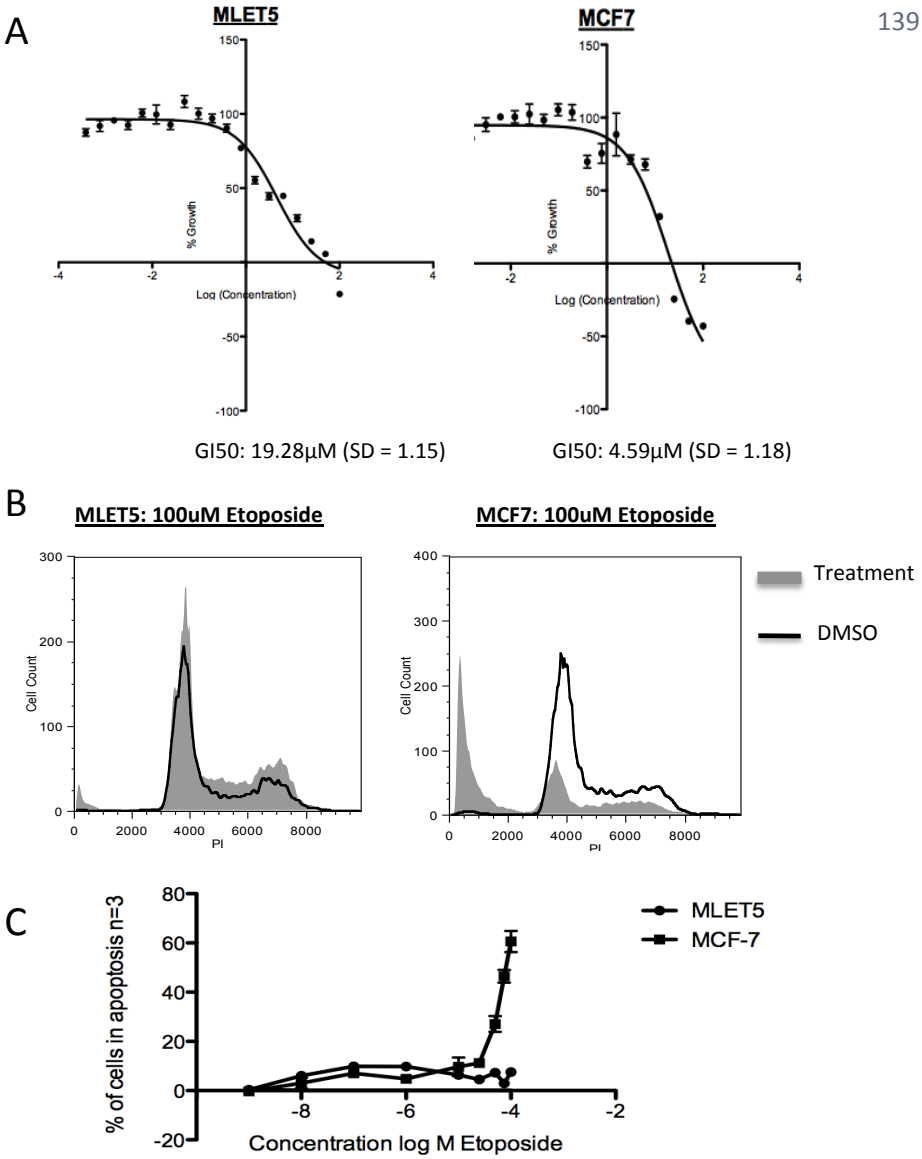


Figure 3.8 MLET5 cells are resistant to apoptosis

(A) MCF7 and MLET5 cells were treated with Etoposide (1nM to 100µM) for 48 hours and cell growth assessed using the SRB assay (n=3, error bars represent SEM). GI_{50} values were determined as the concentration of Etoposide that inhibited growth by 50%: Y=100/(1+10^((X-LogIC50))) (SD = standard deviation). (B) MCF7 and MLET5 cells were treated as above and stained with PI prior to FACS. Shown are the comparative FACS profiles for 100µM Etoposide. (C) Cells were stained with an antibody for annexin V and propidium iodide (PI). The average percentage of cells that stained positive for annexin V (n=3).

3.2 LRH-1

As described in the Introduction, previous work in the laboratory has identified liver receptor homologue 1 (LRH-1; NR5A2) as an estrogen regulated gene in breast cancer cells. LRH-1 has been shown to regulate aromatase expression and ERα expression in breast cancer cell lines and siRNA mediated LRH-1 knockdown causes growth inhibition in LRH1- expressing cells (Clyne et al., 2004; Clyne et al., 2002; Thiruchelvam et al., 2011). These findings indicate that LRH-1 plays an important role in breast cancer and that inhibition of LRH-1 activity may provide a new therapeutic strategy for the treatment of ERα-positive breast cancer. LRH-1 does not appear to be differentially regulated between MLET5 and MCF7. We have therefore performed further microarray studies assessing the role of LRH-1 on gene expression in MCF7 cells.

3.2.1 Microarray analysis of LRH-1 siRNA mediated gene knockdown

In order to identify LRH-1 target genes in breast cancer cells, we used siRNA mediated LRH-1 knockdown in MCF-7 cells, followed by preparation of RNA and gene expression microarray analysis, as described for MCF-7 and MLET5 above. In order to identify LRH-1 siRNAs for this study, MCF-7 cells were transfected with a pool of 4 siRNA and individually with each of the 4 siRNAs in the pool. Cells were harvested 24 hours after transfection and RNA and protein was prepared. LRH-1 mRNA levels were reduced 80-90% following transfection with the pool of 4 LRH-1 siRNAs (Figure 3.9A) and LRH-1 protein was undetectable in this transfection (Figure 3.9B). Similar levels of reduction in LRH-1 mRNA was observed for siLRH-1 #2, #3 and #4, with no reduction in LRH-1 levels for siLRH-1 #1. All four siRNAs reduced LRH-1 protein, again siLRH-1 #1 being the least efficient. Previous work has shown that LRH-1 knockdown results in reduction in ERα levels. Similar results were obtained for siRNA #2 and #3. Therefore, siLRH-1 #2 and #3 were chosen for gene expression microarray analysis.

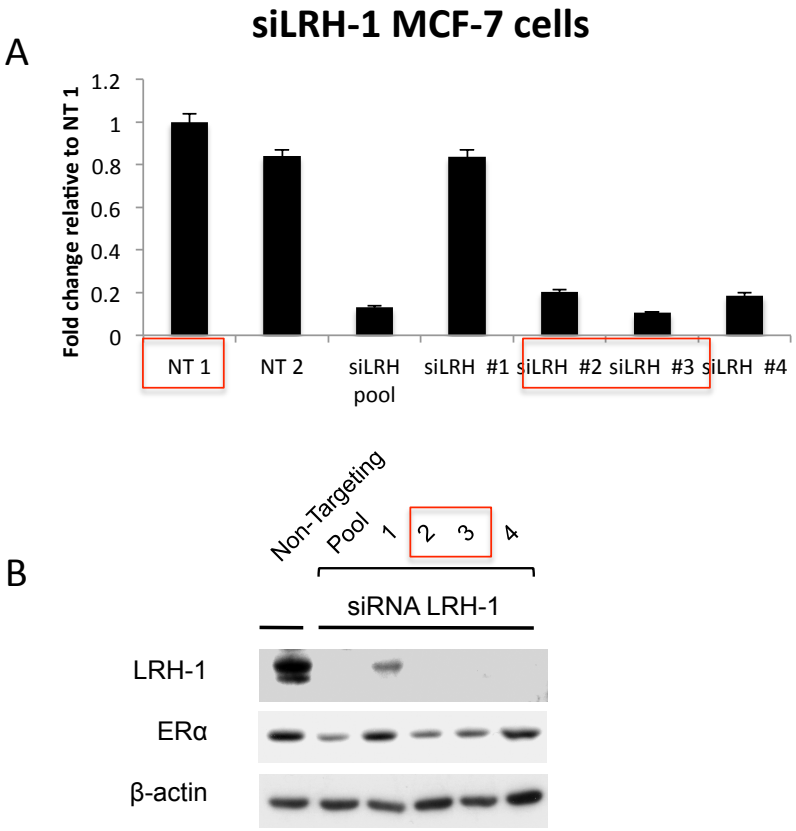


Figure 3.9 LRH-1 siRNA knockdown

(A) Q-RT-PCR expression analysis of LRH-1 siRNA knockdown using non targeting siRNA #1, non targeting siRNA #2, LRH-1 siRNA pool, LRH-1 siRNAs #1-4. RNA samples were prepared from MCF-7. LRH-1 expression is shown following normalization against GAPDH expression. Fold expression in non targeting 1 was taken as 1 and all other samples are shown relative to this. Each Q-RT-PCR was performed in triplicate using two independent RNA samples. The mean values are shown in the bar chart. The errors bars represent the SEM. (B) Western blot taken from Thiruchelvam et al 2011. Samples marked with red box indicate samples sent for microarray analysis.

RNA was prepared from four biological replicates for MCF-7 cells transfected with a non-targeting siRNA (control) and siLRH-1 #2 and #3. These RNA preparations were quality controlled and sent to the Centre for Microarray Resources, Department of Pathology, Cambridge University, for hybridization to Illumina HumanHT/12 version 3 BeadChip Expression Array (http://www.illumina.com/). The resulting raw and normalised expression data was obtained in a format that allowed further analysis using GeneSpring software (Agilent). Bioinformatics analysis was carried out under the supervision of Dr Ross Thomas, Imperial College London.

Quantile normalization was performed and the normalised gene expression microarray data set was analysed to remove background noise/non-significant probes. This was performed by setting detection flags as 'present' for $p<0.01$, which equated to 12,589 probes in at least two replicates of any of the three conditions. Data shown in the heat map relate to all the significantly expressed probes ($p<0.01$) with a fold change ≥1.5 (Figure 3.10). The siRNA LRH-1 #2 and #3 treated samples are shown in comparison with the non-targeting siRNA. Down-regulated probes are depicted in blue and the up-regulated genes in yellow. The difference in the samples with LRH-1 knockdown in comparison with the non-targeting control sample is clearly visible.

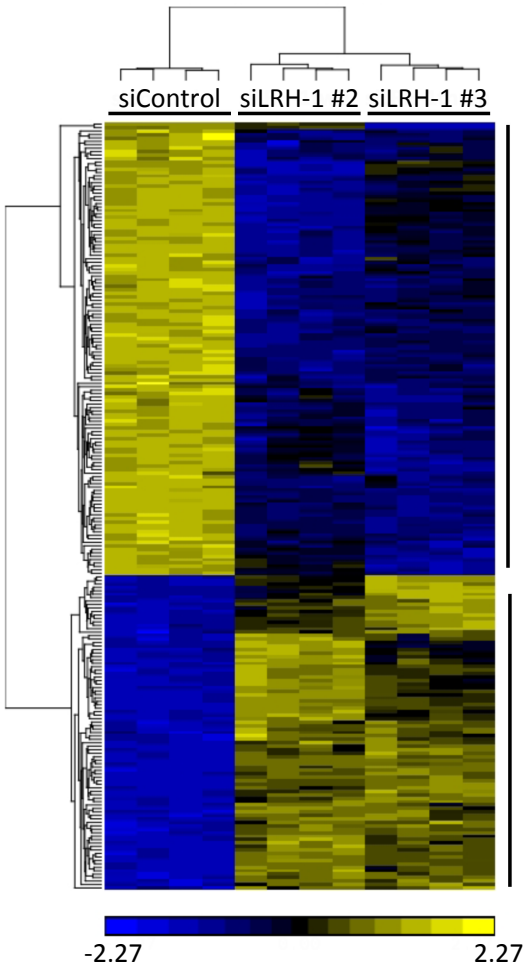


Figure 3.10 Gene expression profiling of LRH-1 knockdown in MCF-7 cells.

Microarray analysis was carried out using the Genespring software with four independent RNA preparations. Heat map of the genes differentially regulated by siRNA 2 and siRNA 3. Significant differentially expressed genes ($p<0.01$, FDR corrected) and with a differential fold change ≥1.5.

To compare conditions, parametric, unpaired t-tests were used with a Benjamini and Hochberg false discovery rate with a corrected p-value <0.05. The information shown in the Venn diagrams relates to genes (Figure 3.11). One hundred and fifteen genes were up-regulated for both LRH-1 siRNAs (Figure 3.11A). These genes are likely to be repressed by LRH-1, since LRH-1 knockdown results in increase in their expression relative to the non-targeting control. The overlap of down-regulated genes for the two siRNAs is 126 (Figure 3.11B) and these genes are likely to be activated by LRH-1. A pathway enrichment analysis of these genes (115+126) using the DAVID online tool (http://david.abcc.ncifcrf.gov/) shows the top 5 clusters (Figure 3.12A), with Cluster 1, being 'Response to estrogen', the remaining clusters also favouring pathways involved in hormonal regulation. The subcategories included in Cluster 1 are listed in Figure 3.12B. The probes included in this list are shown in Figure 3.13A and include ERα, SOCS2, BCL2, GATA3, CYP1A1 and CYP1B1 for which the real time validation is shown in Figure 3.13B.

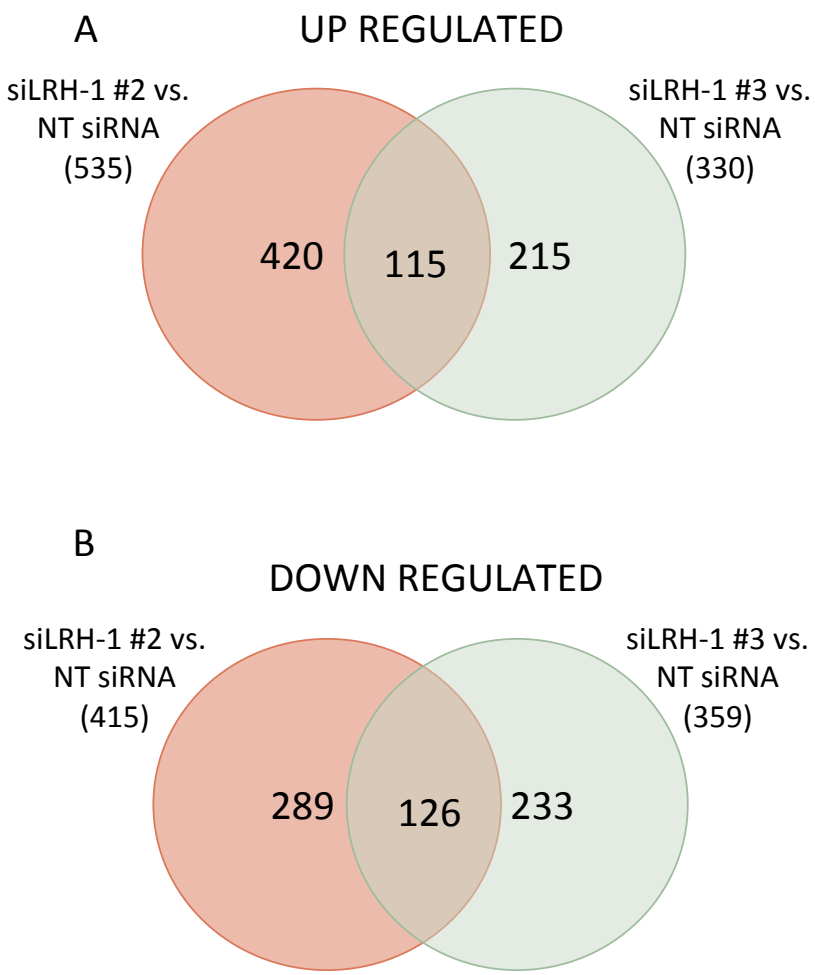


Figure 3.11 Overlap of genes between LRH-1 SiRNA 2 and 3 with significant differential regulation of 1.5 fold or more (p=<0.05)

Venn diagrams of the microarray results for LRH-1 SiRNA knockdown showing the overlap of two data sets of genes from SiRNA 2 and 3. Data sets shown are genes with a ≥1.5 fold up regulation (A) and down regulation (B) in expression ($p < 0.05$).

A

Cluster	Enrichment Score	Description
1	2.44	Response to estrogen
2	2.20	Aldehyde metabolic process
3	1.78	Cell adhesion
4	1.73	Sex differentiation
5	1.50	Cell motility

B

Cluster 1: Response to estrogen	P value	Probes	Fold enrichment
Response to endogenous stimuli	0.002	14	2.8
Response to estrogen stimulus	0.002	7	5.4
Response to hormone stimulus	0.002	13	2.9
Response to steroid hormone stimulus	0.003	9	3.8
Response to organic substance	0.003	19	2.1
Response to peptide hormone stimulus	0.042	6	3.1

Figure 3.12 Pathway enrichment analysis for LRH-1-regulated genes. Shown are the top 5 entries of the list of enriched pathways retrieved using DAVID online tool (http://david.abcc.ncifcrf.gov/) for the 241 (126+115) LRH-1-regulated genes (268 probes) common to both LRH-1 siRNAs (A). The terms included in cluster 1: Response to estrogen are listed in B.

A

Gene Symbol	FC si2 vs NT	P-value	FC si3 vs NT	P-value
ADCY1	0.2	0.000	0.4	0.002
CALCR	0.4	0.000	0.5	0.000
SOCS2	0.4	0.000	0.4	0.000
ADCY1	0.4	0.001	0.5	0.001
SOCS2	0.5	0.001	0.5	0.001
KCNJ8	0.5	0.000	0.6	0.000
BCL2	0.5	0.002	0.4	0.001
ESR1	0.5	0.001	0.6	0.000
CAV1	0.6	0.003	0.3	0.000
TFF3	0.6	0.000	0.5	0.000
MGP	0.6	0.000	0.2	0.000
GATA3	0.7	0.002	0.6	0.001
MGP	0.7	0.023	0.2	0.000
BCL2	0.7	0.043	0.6	0.005
MGST1	1.4	0.008	1.4	0.003
IDH1	1.5	0.003	1.8	0.001
EDEM3	1.6	0.006	1.5	0.008
IDH1	1.7	0.000	2.4	0.000
MGST1	1.7	0.000	1.7	0.002
TNFRSF1A	1.7	0.033	1.6	0.020
BTG2	1.7	0.008	1.8	0.007
GAL	1.9	0.001	1.5	0.014
CYP1A1	2.2	0.000	1.7	0.002
PPARG	2.2	0.000	1.8	0.003
CYP1B1	2.3	0.001	2.1	0.001

Figure 3.13A List of probes included in Cluster 1, Response to estrogen, of the DAVID Pathway enrichment analysis for LRH-1-regulated genes.

B

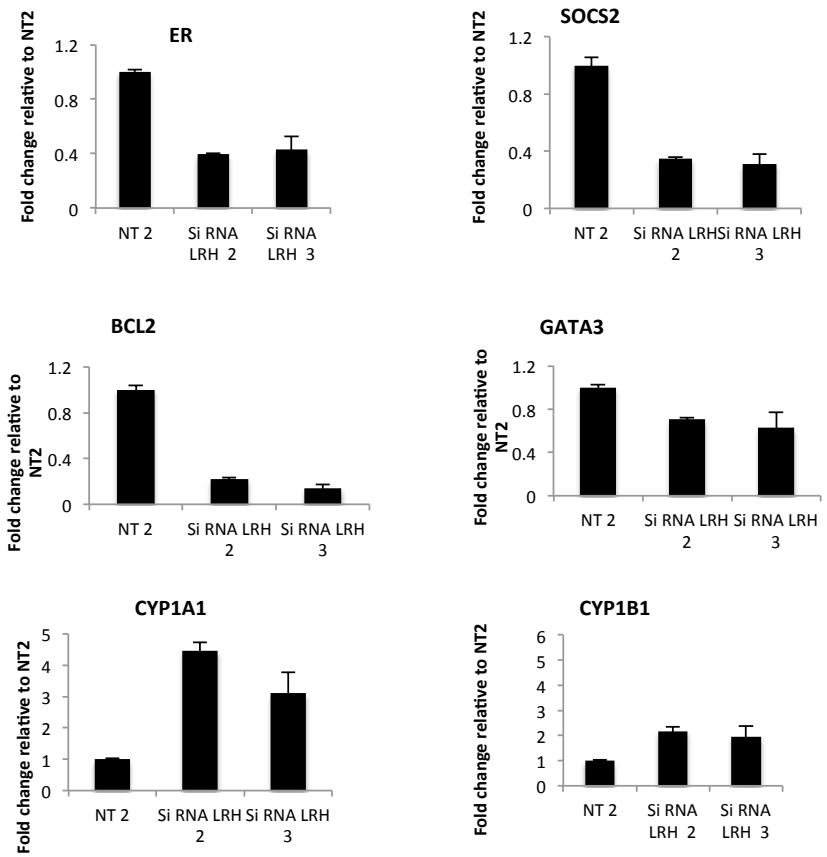


Figure 3.13B Q-RT-PCR expression analysis of ER, SOCS2, BCL2, GATA3, CYP1A1 and CYP1B1.

Q-RT-PCR was used to validate microarray data for select genes from the Cluster 1, Response to estrogen, of the DAVID Pathway enrichment analysis for LRH-1-regulated genes. . Expression is shown following normalisation against GAPDH expression. For each gene, fold expression in MCF7 cells treated with NT SiRNA is taken as 1 and all other samples are shown relative to this. Each Q-RT-PCR was performed in triplicate using three independent RNA samples.

ERα regulation by LRH-1 has been shown by both our laboratory and other groups (Chand et al., 2012; Thiruchelvam et al., 2011). Interestingly, GATA3 regulates ERα expression in breast cancer cells (Shang and Brown, 2002) and LRH-1 and GATA3 co-operatively regulate a luciferase reporter gene containing the ERα promoter (Thiruchelvam et al 2011). Moreover, ERα and GATA3 regulate LRH-1 expression (Annicotte et al., 2005; Bouchard et al., 2005; Thiruchelvam et al., 2011). The possibility that LRH-1 regulates GATA3 expression provides an interesting feed forward loop in which ERα, LRH-1 and GATA3 co-regulate the expression of the other genes in breast cancer cells.

No direct links between SOCS2, BCL2 and LRH-1 have been described as yet however, as discussed in the previous section anti-apoptotic, ERα represses expression of the pro-apoptotic SOCS2 gene and stimulates BCL2 expression.

CYP1A1 and CYP1B1 are both enzymes known to play a role in the catabolism of estrogen (2-hydroxylation and 4-hydroxylation respectively) and, certainly CYP1B1, has been implicated in the development of breast and endometrial carcinogenesis and is also regulated by estradiol (Lee et al., 2003; Tsuchiya et al., 2005), so regulation of their expression by LRH-1 in MCF-7 cells may be of particular importance for ERα-positive breast cancer. Interestingly, LRH-1 has been directly implicated in regulating aromatase expression in the ovary and in breast cancer-associated stroma (see section 1.3.6). Therefore, LRH-1 may play a significant role in estrogen biosynthesis in breast cancer by regulating estrogen availability at several levels.

In view of the results of the pathway enrichment analysis indicating a strong role for estrogen response by LRH-1, and its ability to regulate ERα expression, it was therefore of interest to determine what proportion of genes regulated by LRH-1 are also estrogen regulated. To do this I compared the LRH-1 regulated genes identified in the LRH-1 siRNA microarray with estrogen-regulated genes identified in the microarray analysis described in section 3.1.2 (Figure 3.14).

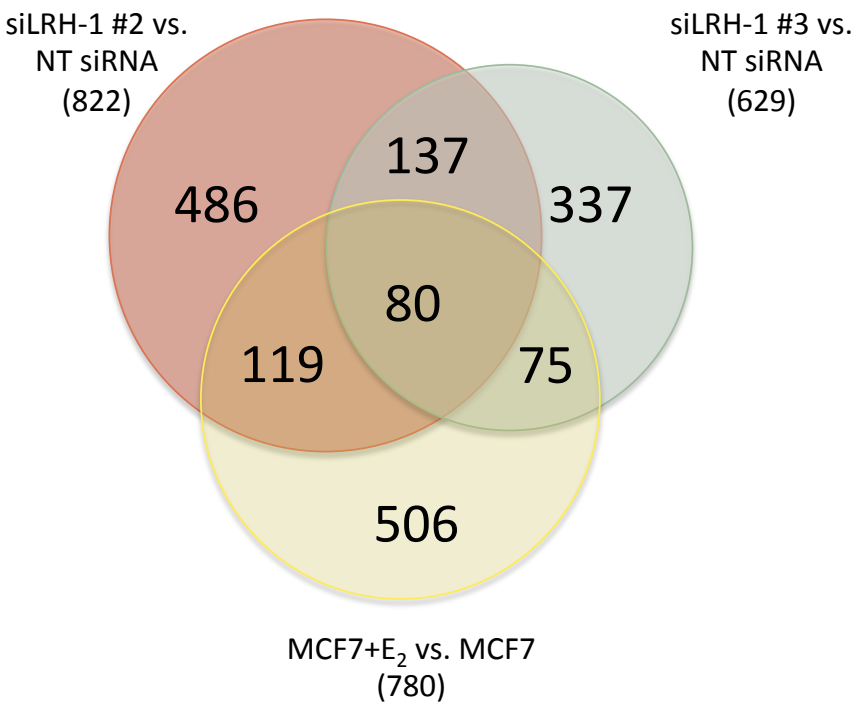


Figure 3.14 Estrogen regulation of differentially expressed genes in LRH-1 siRNA

Venn diagram of the microarray results for LRH-1 siRNA knockdown showing the overlap of genes from LRH-1 siRNA #2 and siRNA #3 with a ≥1.5 change in expression ($p < 0.05$) and the third data set, showing estrogen regulated genes in MCF7 (also with a ≥1.5 fold ($p < 0.05$)).

Symbol	P-value	Fold Change siLRH #2 vs NT	P-value	Fold Change siLRH #3 vs NT	P-value	FC MCF7+E2 vs MCF7
CXCL12	0.000	0.4	0.002	0.5	0.001	7.2
CXCL12	0.000	0.4	0.001	0.5	0.001	7.2
FLJ30058	0.000	0.4	0.000	0.4	0.001	4.4
AGR3	0.000	0.3	0.000	0.6	0.001	4.3
SGK	0.000	0.5	0.000	0.4	0.000	4.0
PGR	0.000	0.4	0.001	0.5	0.001	4.0
MYB	0.002	0.5	0.000	0.3	0.002	3.9
RAMP3	0.000	0.2	0.000	0.4	0.002	3.6
RAMP3	0.001	0.4	0.003	0.5	0.002	3.6
RBM24	0.000	0.4	0.000	0.5	0.001	3.6
OLFM1	0.001	0.5	0.000	0.6	0.001	3.2
HEY2	0.000	0.3	0.002	0.5	0.001	3.1
MGP	0.000	0.6	0.000	0.2	0.003	2.8
MGP	0.023	0.7	0.000	0.2	0.003	2.8
PCP4	0.000	0.3	0.000	0.3	0.001	2.7
CALCR	0.000	0.4	0.000	0.5	0.001	2.6
DEPDC6	0.000	0.5	0.001	0.6	0.001	2.6
HS3ST3A1	0.001	0.4	0.001	0.4	0.001	2.5
GFRA1	0.000	0.2	0.000	0.4	0.002	2.4
GFRA1	0.000	0.3	0.002	0.4	0.002	2.4
RAB31	0.000	0.5	0.000	0.4	0.002	2.3
FAIM3	0.001	0.6	0.002	0.6	0.001	2.2
PCDH19	0.004	0.6	0.004	0.6	0.001	2.1
GOLSYN	0.004	0.6	0.002	0.5	0.002	2.0
PLAC1	0.001	0.6	0.000	0.3	0.002	2.0
SLITRK4	0.002	0.6	0.004	0.6	0.001	1.9
SEPT5	0.003	0.5	0.001	0.4	0.002	1.9
LOC647784	0.000	0.4	0.001	0.6	0.004	1.9
BIRC3	0.003	2.0	0.027	1.8	0.002	1.8
ACOX2	0.004	2.0	0.000	3.9	0.001	1.8
ASCL1	0.005	0.7	0.000	0.2	0.005	1.8
GAL	0.001	1.9	0.014	1.5	0.013	1.8
MAFB	0.000	0.4	0.000	0.4	0.004	1.8
KCNF1	0.002	0.5	0.001	0.4	0.012	1.7
LONRF2	0.000	0.6	0.002	0.6	0.001	1.7
BCL2	0.002	0.5	0.001	0.4	0.001	1.7
NR5A2	0.001	0.5	0.011	0.7	0.001	1.7
NR5A2	0.005	0.6	0.015	0.6	0.001	1.7
ADCY1	0.000	0.2	0.002	0.4	0.005	1.7
ADCY1	0.001	0.4	0.001	0.5	0.005	1.7
H2AFJ	0.000	0.6	0.002	0.6	0.003	1.7
TMEM26	0.000	0.5	0.000	0.6	0.002	1.6
HCK	0.006	0.6	0.008	0.6	0.002	1.5
SULF2	0.001	0.5	0.003	0.5	0.021	1.5

Table 3.3A. List of estrogen stimulated probes (n=80 genes) differentially regulated 1.5 fold or more for both LRH-1 siRNAs. Probes highlighted in red are shown in Figure 3.15, highlighted in blue are shown in Figure 3.16

Symbol	P-value	Fold Change siLRH #2 vs NT	P-value	Fold Change siLRH #3 vs NT	P-value	FC MCF7+E2 vs MCF7
SLC11A2	0.001	1.5	0.000	2.1	0.007	0.7
CLSTN2	0.001	0.6	0.002	0.6	0.001	0.7
AHNAK	0.011	0.6	0.004	0.6	0.032	0.7
GPNMB	0.014	1.7	0.006	2.0	0.004	0.6
CAPN9	0.001	2.2	0.000	3.5	0.005	0.6
CAPN9	0.000	2.3	0.000	4.2	0.005	0.6
MGST1	0.000	1.7	0.002	1.7	0.004	0.6
PACSIN1	0.001	0.5	0.003	0.6	0.006	0.6
FAM174B	0.015	1.8	0.001	2.4	0.007	0.6
VSIG2	0.000	2.9	0.001	2.5	0.006	0.6
KRT81	0.000	2.9	0.001	2.1	0.014	0.6
CEACAM6	0.000	4.3	0.000	4.3	0.004	0.6
TPK1	0.000	2.2	0.000	3.8	0.003	0.6
KIAA1199	0.003	1.7	0.002	1.8	0.003	0.6
SERPINB1	0.003	1.8	0.004	1.7	0.003	0.6
SCNN1A	0.001	2.3	0.000	7.8	0.007	0.6
BIK	0.001	1.8	0.000	2.2	0.006	0.6
BNIPL	0.000	0.4	0.005	0.6	0.001	0.6
INHBB	0.000	3.2	0.006	1.5	0.007	0.6
SLC29A3	0.003	1.9	0.000	2.1	0.002	0.6
SOCS2	0.000	0.4	0.000	0.4	0.002	0.6
SOCS2	0.001	0.5	0.001	0.5	0.002	0.6
SGCG	0.001	0.4	0.000	0.4	0.003	0.6
ST3GAL1	0.000	3.4	0.002	2.2	0.009	0.6
CNN2	0.001	2.6	0.004	1.6	0.002	0.6
KCNJ8	0.000	0.5	0.000	0.6	0.001	0.6
NRP1	0.000	2.5	0.002	2.2	0.001	0.6
EMP1	0.000	1.6	0.001	1.5	0.003	0.6
RAP1GAP	0.004	1.7	0.000	2.6	0.003	0.5
TACC1	0.005	0.7	0.000	0.5	0.004	0.5
PMP22	0.000	0.4	0.000	0.4	0.003	0.5
PMP22	0.014	0.6	0.002	0.4	0.003	0.5
PMP22	0.001	0.6	0.002	0.5	0.003	0.5
SAT1	0.001	2.1	0.001	1.9	0.008	0.5
KRT86	0.000	1.8	0.001	1.6	0.002	0.5
NELL2	0.000	0.3	0.000	0.4	0.001	0.5
ALDH3A1	0.000	1.9	0.000	2.5	0.005	0.4
LIMA1	0.003	1.5	0.002	2.2	0.001	0.4
ABCC3	0.004	1.9	0.000	2.6	0.001	0.4
RND3	0.000	3.1	0.003	1.8	0.001	0.4
DDIT4	0.000	1.9	0.001	1.5	0.001	0.4
C9orf169	0.004	1.5	0.000	2.5	0.001	0.4
EPAS1	0.000	3.6	0.004	2.0	0.002	0.4
BCAS1	0.001	2.5	0.001	2.6	0.002	0.3
BCAS1	0.000	3.3	0.000	3.7	0.002	0.3
TNS3	0.000	2.4	0.001	1.7	0.001	0.3
TP53INP1	0.001	2.0	0.005	1.8	0.001	0.2
TP53INP1	0.000	2.2	0.003	2.0	0.001	0.2

Table 3.3B. List of estrogen repressed probes (n=80 genes) differentially regulated 1.5 fold or more in both LRH-1 siRNAs. Probes highlighted in red are shown in Figure 3.15, highlighted in blue are shown in Figure 3.16

As these two array sets were separate experiments performed at separate times only the probes common to both Genespring analysis files have been included. The result of this analysis shows that approximately 25% of genes with differential expression (≥1.5 fold change, $p<0.05$) for either of the LRH-1 siRNAs and 37% of the genes common to both LRH-1 siRNAs are significantly estrogen regulated. ERα, GATA3, CYP1A1 and CYP1B1 fall below the 1.5 fold cut-off, however down regulated genes include SOCS2, BCL2 (shown in Table 3.3 and previously in Figure 3.13B) and several other genes also previously shown to be estrogen-regulated, such as PMP22 (Simpson et al., 2010), TACC1 (Ghayad et al., 2009; Vendrell et al., 2004), SGK1, CXCL12 (Boudot et al., 2011; Sauve et al., 2009) GFRA1 (Esseghir et al., 2007), PgR (Horwitz et al., 1978), MYB (Drabsch et al., 2007; Gudas et al., 1995) and RAMP3 (Hong et al., 2004) (Watanabe et al., 2006) (shown in Table 3.3 and Figure 3.15). Significantly over-expressed genes, and therefore potentially LRH-1 repressed genes, within this group of estrogen regulated genes include BCAS1, SCNN1A and ACOX2 (Table 3.3 and Figure 3.16). These three genes are not known to be estrogen regulated in breast cancer cells. BCAS1 is a gene found to be over expressed in some breast cancers, breast cancer cell lines and in the tamoxifen resistant xenograft MaCa 3366/TAM, although it was not found to affect growth rate or anchorage independent growth in NIH-3T3 cells and is therefore surmised not to behave as a standard proto-oncogene (Beardsley et al., 2003; Becker et al., 2005; Collins et al., 1998). SCNN1A has been identified as a target gene for ERRα (Tremblay et al., 2010) and is important in the regulation of sodium transport, an area of increasing interest within cancer cells especially with regard to invasive potential (Gillet et al., 2009). ACOX2 is involved in bile acid regulation by oxidising the CoA esters of 2-methyl-branched fatty acids and the bile acid intermediates di and tri-hydroxycoprostanic acids, an insufficiency would therefore lead to an increase in bile acids (Johansson et al., 2011; Yeh et al., 2006). It has also been shown to have the ability to transform African green monkey cells (CV-1) transfected with ACOX2 (CV-ACOX-4)(Chu et al., 1995), due to its ability to produce hydrogen peroxide (Reddy et al., 1986) in

response to the fatty acid, linoleic acid. Interestingly hydrogen peroxide, as a stress factor, also activates NFkappaB transcription factor (Schreck et al., 1991).

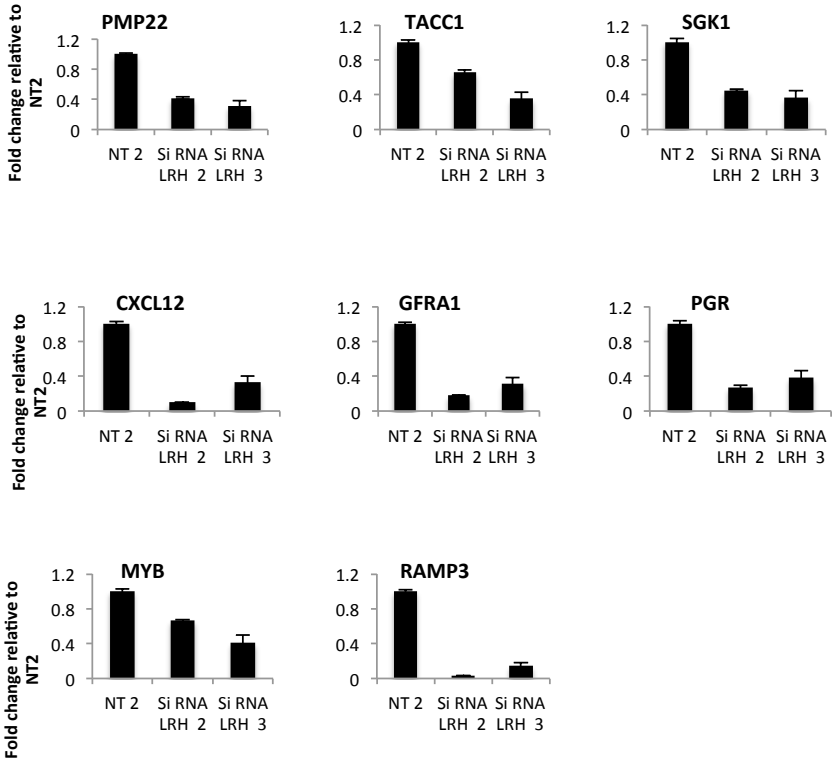


Figure 3.15 Q-RT-PCR expression analysis of down regulated genes identified in the microarray analysis of siRNA LRH-1 versus Non Targeting (NT) SiRNA and shown to be estrogen regulated (highlighted in red in Table 3.3)

Primers for PMP22, TACC1, SGK1, RAMP3, CXCL12, PgR, GFRA1, MYB and GAPDH were used to validate microarray data. Expression is shown following normalisation against GAPDH expression. For each gene, fold expression in MCF7 cells treated with NT siRNA is taken as 1 and all other samples are shown relative to this. Each Q-RT-PCR was performed in triplicate using three independent RNA samples. The mean values are shown in the bar chart and the error bars represent the SEM.

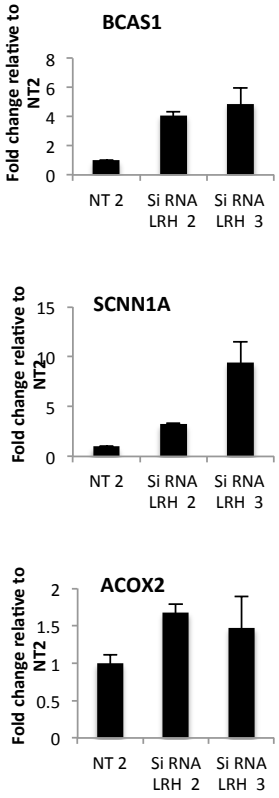


Figure 3.16 Q-RT-PCR expression analysis of over-expressed genes identified in the microarray analysis of LRH-1 siRNAs versus Non Targeting (NT) siRNA and shown to be estrogen regulated (highlighted in blue in Table 3.3)

Primers for ACOX2, BCAS1, SCNN1A and GAPDH were used to validate microarray data. Expression is shown following normalisation against GAPDH expression. For each gene, fold expression in MCF7 cells treated with NT SiRNA is taken as 1 and all other samples are shown relative to this. Each Q-RT-PCR was performed in triplicate using three independent RNA samples. The mean values are shown in the bar chart and the error bars represent the SEM.

Figure 3.17 shows two other genes; LCoR and GPER, variants 2, 3, and 4. These genes were not shown, in this experiment, to be either significantly estrogen regulated (GPER) or estrogen regulation fell below the 1.5 fold cut off (LCOR) however in view of their significant differential regulation, may be of potential importance in the role/function of LRH-1.

LCoR (Ligand dependent corepressor) is a known nuclear receptor corepressor which functions through the recruitment of C-terminal binding proteins (CtBPs) and histone deacetylases (HDACs) to its N-terminal and central domains, respectively (Calderon et al., 2012; Fernandes et al., 2003). Unlike many nuclear receptor co-repressors, which are recruited to the LBD via coRNR boxes to un-liganded or antagonist bound receptors, LCoR is recruited to agonist-bound NR, via LXXLL type motifs. This experiment showed LCOR was up-regulated approximately 1.5 fold in SiRNA LRH-1 versus MCF7.

GPER is a seven trans-membrane receptor (7TMR) belonging to the G-protein-coupled receptor family (GPCR). It has been associated with poor prognosis and metastases in breast (Filardo et al., 2006), ovarian (Smith et al., 2009) (Yan et al., 2013) and endometrial (Smith et al., 2007a) cancer. GPER binds estrogen leading to activation of the MAPK and PI3K pathways (Lin et al., 2009). Its role in breast cancer remains controversial, with studies analyzing the association between expression, as determined by immunohistochemistry, and survival in patients with inflammatory breast cancer showing that the presence of both ERα and GPER (24%) is associated with an improved overall survival ($p<0.03$) and conversely the absence of both being associated with poor prognosis ($p<0.03$). In this study 19% of specimens expressed ERα only, whereas 46% expressed GPER suggesting that estrogen signalling without ERα may be important in these patients (Arias-Pulido et al., 2010). More recently, a knockdown of GPER in breast cancer cell lines (MDA-MB-435 and HCC1806) negative for ERα, PgR and HER2 abolished the proliferative effects of 17-β estradiol and 4-hydroxytamoxifen (Girgert et al., 2012), suggesting that pharmacological inhibition of GPER maybe of therapeutic benefit in this group of patients. Our results show that knocking down LRH-1 leads to a significant

reduction in the three variants of GPER suggesting that GPER may be an LRH-1 target gene. Together with the potential regulation of estrogen catabolism genes (CYP1A1 and CYP1B1), ERα, GATA3, as well as the evidence from other laboratories for LRH-1 regulation of aromatase expression in breast cancer associated stroma, the finding that LRH-1 regulates GPER, an estrogen binding protein that mediates non-genomic effects of estrogen, these findings provide increasing evidence that LRH-1 plays an important role in the estrogen driven development and progression of breast cancer.

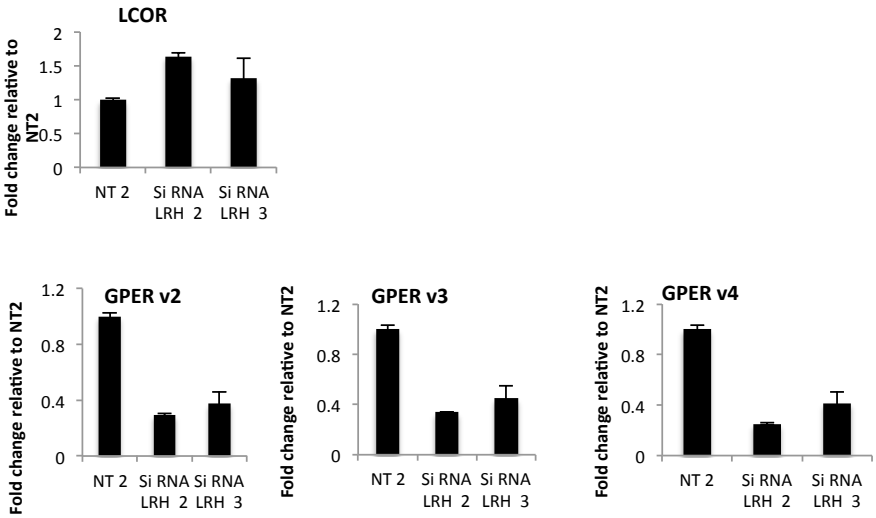


Figure 3.17 Q-RT-PCR expression analysis of genes identified in the microarray analysis of LRH-1 siRNAs versus Non Targeting (NT) siRNA

Primers for LCOR, GPER V2-4 and GAPDH were used to validate microarray data. Expression is shown following normalisation against GAPDH expression. For each gene, fold expression in MCF7 cells treated with NT siRNA is taken as 1 and all other samples are shown relative to this. Each Q-RT-PCR was performed in triplicate using three independent RNA samples. The mean values are shown in the bar chart and the error bars represent the SEM.

3.3 Approaches for the design and synthesis of small molecule antagonists of LRH-1

Synthetic agonists and antagonists have been designed for many nuclear receptors. A full list is beyond the scope of this thesis, however, include ERα: tamoxifen (Harper and Walpole, 1967), raloxifene (Gottardis et al., 1990), faslodex (ICI 182,780) (Wakeling, 1991; Wakeling et al., 1991), the androgen receptor: bicalutamide (Lunglmayr, 1989), flutamide (Prout et al., 1975; Sogani et al., 1975), metribolone (R1881)(Andersen et al., 2010; Ghanadian et al., 1978), enzalutamide (Tran et al., 2009), ARN-509 (Clegg et al., 2012) , EPI-001 (Andersen et al., 2010) , the progesterone receptor: mifepristone (RU486) and derivative compounds such as ulipristal acetate, asopisnil and telapristone acetate (Chabbert-Buffet et al., 2005) GR: mifepristone (Bourgeois et al., 1984), prednisone and related compounds, dexamethasone and fludrocortisones (Brattsand et al., 1982; Gessi et al., 2010), PPARα: GW6471, GW409544 (Xu et al., 2001; Xu et al., 2002), PPARδ: GW501516 (Oliver et al., 2001), PPARγ: rosiglitazone and pioglitazone (Erdmann et al., 2007; Kahn et al., 2006; Viberti et al., 2002), Vitamin D receptor: synthetic analogues of alfacalcidol and 1,25-$(OH)_2$D3 (Carlberg et al., 2012), LXR: LXR-623, YT32 and GW6340 (De Boussac et al., 2013; Kaneko et al., 2003; Katz et al., 2009; Yasuda et al., 2010).

Thus, the small molecule (e.g. steroid hormones) mediated activation of this large family of transcription factors appears to make this family amenable to the development of synthetic compounds that activate or inhibit their activities. This makes it possible to consider the development of synthetic small molecule modulators of LRH-1 that act by binding to its ligand binding domain.

The solution of the LRH-1 LBD, by crystallography, together with the identification of potential ligands (phospholipids) and the (albeit) weak synthetic agonists already

described, provide potential for approaches to rationally design small molecule inhibitors of LRH-1, which would act by binding to the LRH-1 LBD, to inhibit its activation. Our collaborators in the Department of Chemistry at Imperial College London (Professor A. Spivey, Professor A Barrett) and in the Department of Chemistry, Emory University (Professor J Snyder) used several approaches to aid rational design of potential LRH-1 binding compounds towards identification of LRH-1 antagonists. Each of these approaches is briefly described below (and shown in Figure 3.18), followed by the results of screening compounds arising from these diverse in silico strategies.

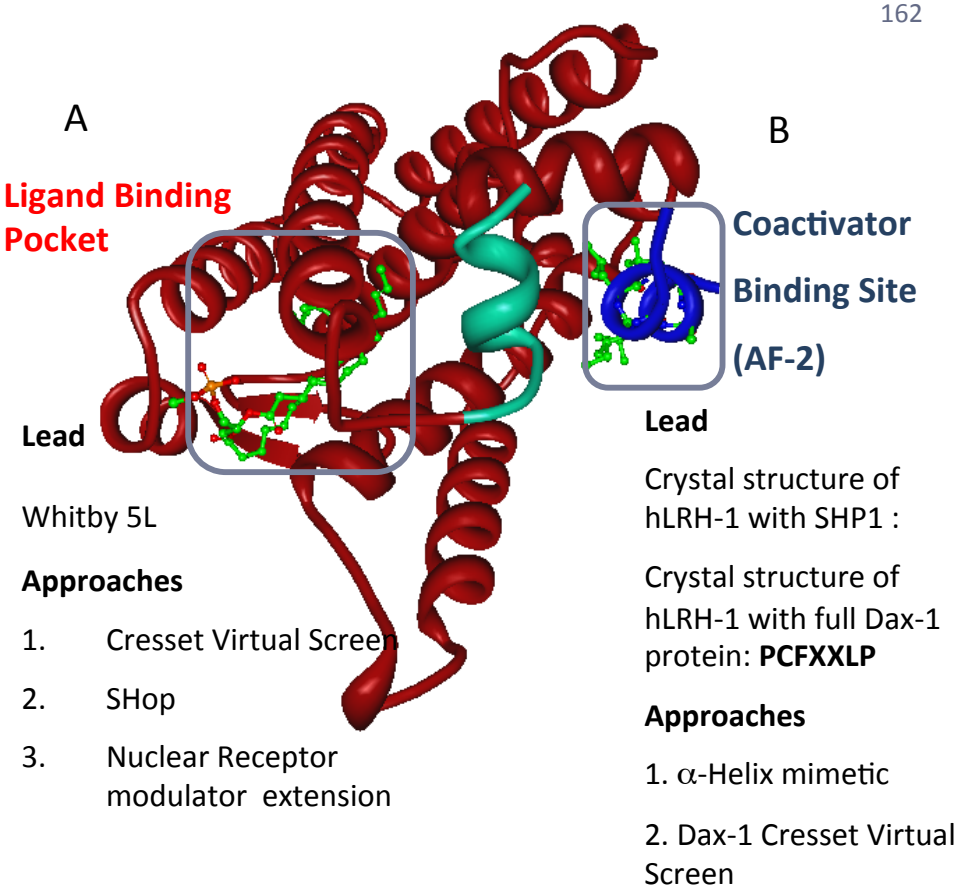


Figure 3.18 The LRH-1 LBD crystal structure.

Shown is the LRH-1 ligand binding domain structure. In green is helix 12. The positioning of helix 12 is ligand regulated (AF2) and critical for agonist and antagonist conformations by co-activator recruitment, shown in blue. Also shown is the compound 5L (Whitby et al 2006) as a green skeleton in (A) and Dax-1 as a green skeleton on (B). The scheme above outlines the approaches for the design of small molecule antagonists of LRH-1. (A) 3 approaches targeted the Ligand Binding Pocket; Compound 5L was used as the starting compound for a (1)Cresset Virtual Screen and (2) SHoP. (3) used Nuclear Receptor Modulator extensions in docking studies. (B) Approaches targeting the AF2 co-activator binding site included (1) design of α-Helix mimetics based on the analysis of the SHP NR box peptides binding residues with LRH-1 and (2) a Dax-1 Cresset virtual screen.

3.3.1 Space filling approaches for identifying compounds that are similar to phospholipids and synthetic LRH-1 agonists

One avenue of computational identification of compounds that potentially target the protein of interest is to use modeling algorithms, in which screening is performed for compounds that have similar electrostatic charge and space filling as a selected reference compound. Two computational approaches, using software developed by the Cresset group and scaffold hopping (SHoP) were used by our collaborator, Professor Alan Spivey (Department of Chemistry, Imperial College) to identify commercially available compounds that have similar space filling and electrostatic properties as the most potent LRH-1 agonist reported at that time (Whitby et al., 2006) (compound 5L, 5L, a *cis*-bicyclo(3.3.0)-oct-2-ene (Figure 3.19). One reason for attempting to identify alternative compounds rather than using compound 5L (or related compounds) was because the published compounds require an extremely complex synthetic route and are very unstable ((Whitby et al., 2011); Richard Whitby personal communication). Alternative compounds that are easier to synthesise and to derivatize for analogue generation might yield new and more facile chemical starting points for modification to generate potent LRH-1 antagonists.

The Cresset methodology utilises the ability of structurally different compounds to bind to the same biologically active site by redefining a compound based on its 'field point' data including electrostatic, steric and hydrophobic fields. The hypothesis of this approach is that it is not the three dimensional structure which is important but the way that molecules interact via their electrostatic and Van der Waal forces and that compounds with similar field patterns will have similar binding properties. Four field types are described and assigned a colour; electrophilic (red), nucleophilic (blue), van der Waals attractive (yellow) and hydrophobic (orange).

The size and position of these field points on a 3D image can then be used to match with compounds having similar chemical properties (Cheeseright et al., 2006).

Using this technique and the published agonist, compound 5L (Whitby et al., 2006) 200 commercially available compounds (similarity 0.76-0.82), of which 102 could be purchased, were identified (Figure 3.19A).

Another Cresset virtual screen approach was carried out, in order to identify compounds with similar electrostatic and space filling properties as the LRH-1 interacting α-helical motif present in Dax-1, was also used to identify compounds that might act as co-activator binding inhibitors (CBIs). (Figure 3.18). This screen was facilitated by the availability of the LRH-1 Dax-1 crystal structure (Sablin et al., 2008). Using this approach a peptide portion of DAX-1, observed to bind to LRH-1 and having the sequence, PCFXXLP, was then modeled to identify commercially available compounds. Twelve of the top 30 hits were purchased for screening.

3.3.2 Scaffold Hopping (SHoP) Software for compound identification

The second technique we utilised, SHoP or Scaffold hopping, is a method of preserving the three dimensional interaction properties of a compound whilst changing the structural skeleton. The properties that are taken into consideration include geometrical features, such as distance and dihedral angles, and the scaffold shape, in conjunction with the alignment independent GRID molecular interaction field (MIF) (Bergmann et al., 2007). Using this technique and again the published agonist 5L (Whitby et al., 2006), 9 templates were identified (similarity 0.79-0.91). One of these templates was synthesized (THP1) for testing (Figure 3.19B).

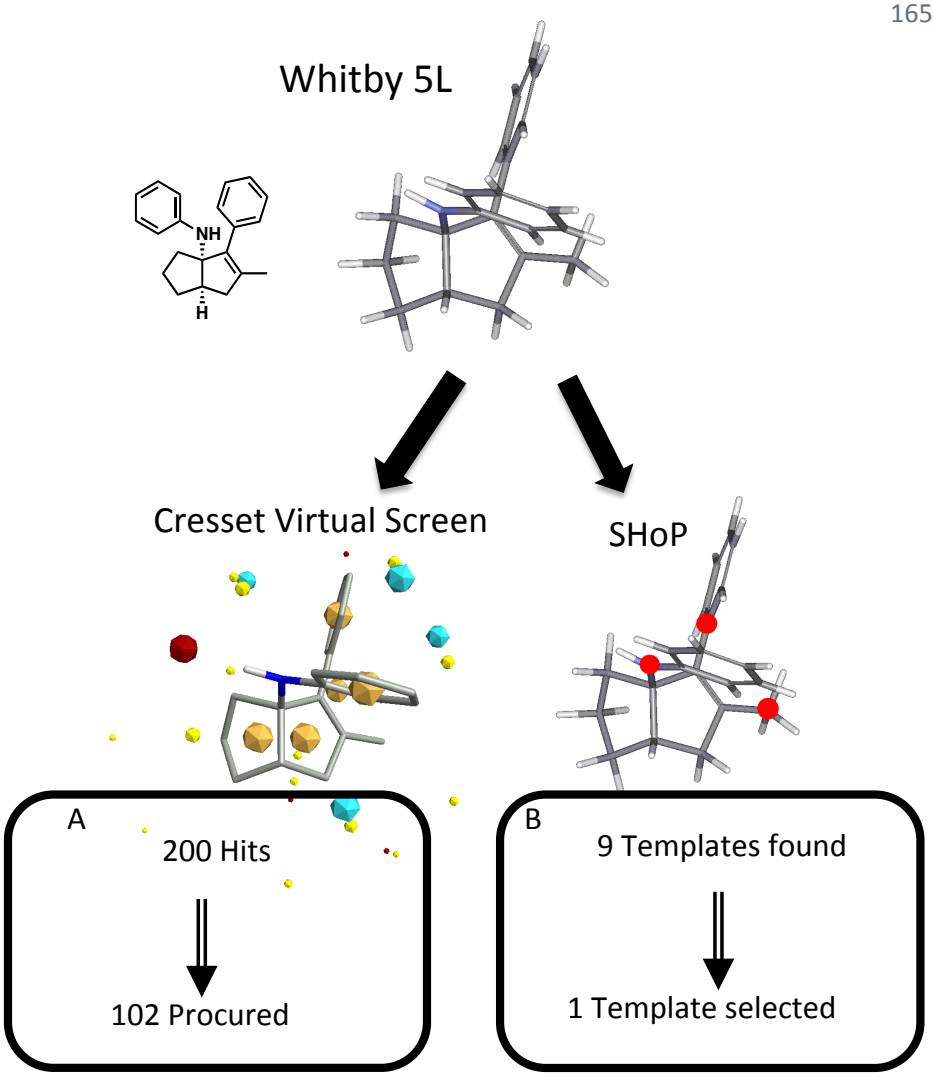
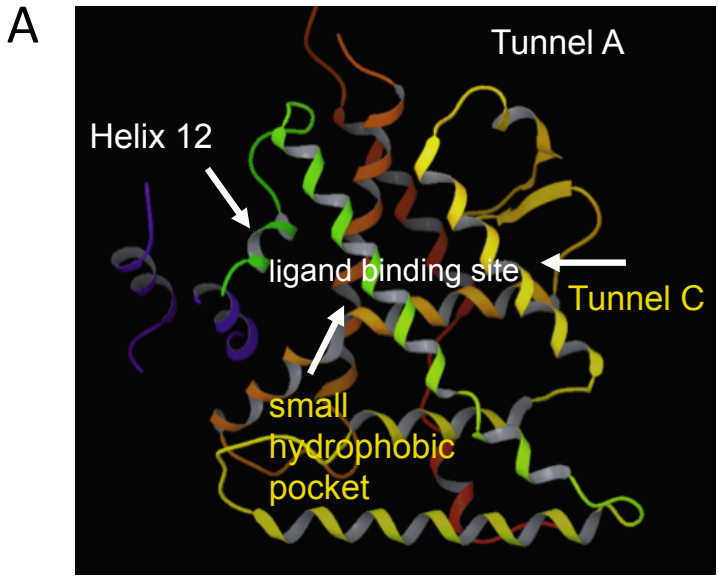


Figure 3.19 Computer Aided Drug design: 2 approaches based on the structure of the LRH-1 agonist Whitby compound 5L

(A) Shows the space-filling approach utilising the ability of structurally different compounds to bind to the same site based on their electrostatic and Wan der Waal interaction properties. Cresset screening of compound 5L, against databases of millions of compounds identified 200 compounds with a predicted similarity (r values 0.76-0.82). Of these 102 compounds could be procured commercially. (B) Shows the Scaffold hopping method of using the 3 dimensional interaction properties of a compound whilst changing it's structural skeleton. Using this technique 9 templates were identified and 1 compound chosen for synthesis.

3.3.3 Nuclear Receptor Modulator Extension

Three-dimensional computational modeling of the LBD in nuclear receptors can be used to identify potential chemical starting points for compounds that bind/dock in the LBD (Figure 3.20A) and can then be theoretically modulated to influence their activity (nuclear receptor modulator extension). The area of work described in this section, was performed by our collaborators, Professor J Snyder at Emory University, Atlanta, and Professor Anthony Barrett, with the chemistry department at Imperial College, South Kensington campus. The publication of the crystal structure of LRH-1 (X-ray available PDB code = 1YOK (Krylova et al., 2005)) allowed the use of computer modeling to dock chemical scaffolds into the LRH-1 LBD. It was reasoned that compounds that could prevent helix 12 in the LBD from taking up position in the activated LBD structure, would act as LRH-1 antagonists. Towards this end, Professor Snyder looked at other known nuclear receptors and identified antagonists, primarily the tamoxifen bound ERα, the raloxifene bound ERα and the steroid antagonist bound FXR LBD. This approach compared the docking of these antagonists in the ERα and FXR LBD and modeled them in to the LRH-1 LBD structure. Prof Snyder's modeling identified three potential docking positions within the nuclear receptor LBDs, which they named A, C and H, to which antagonist binding could occur in LRH-1 (Figure 3.20B). Of these, position 'H' looked the most promising position for an antagonist, as this would potentially allow interference with the position of helix 12 (e.g. Leu532, grey). Using the three compounds Raloxifene (Figure 3.21), tamoxifen (Figure 3.22) and the core of an FXR steroidal antagonist (Figure 3.23) and fitting these to the LRH-1 LBD, it was possible to build chemical scaffolds onto these compounds to generate compounds that may act as LRH-1 LBD binding compounds with inhibitor activities.



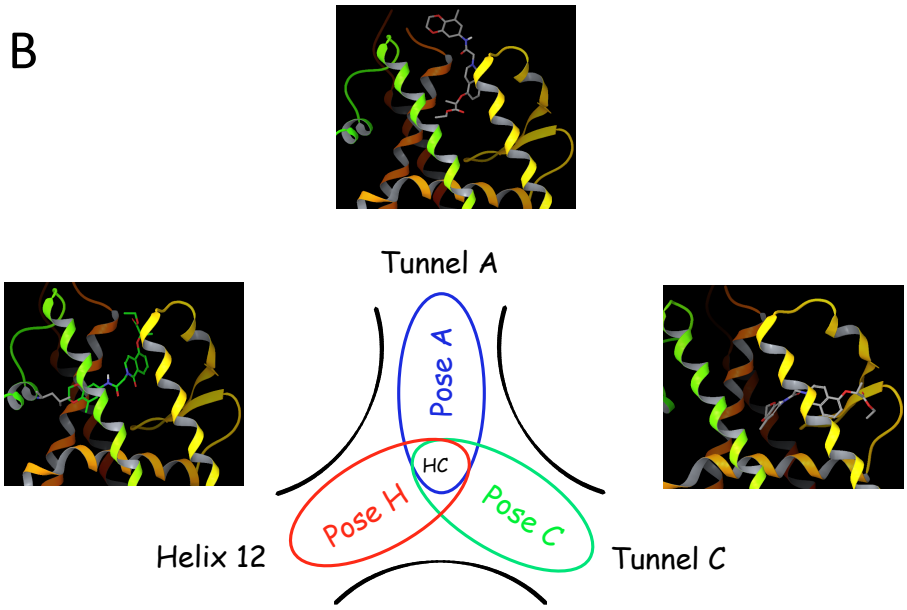


Figure 3.20 Nuclear Receptor modulator extension

(A) Using the hLRH-1 crystal structure (1YOK) the docking of known NR modulators (Steroidogenic Factor 1, Estrogen Receptor α and Farnesoid X Receptor) was investigated. The receptor structure differences were examined and ligands tailored for LRH-1. (B) shows 3 potential antagonist docking positions in poses A, C and H.

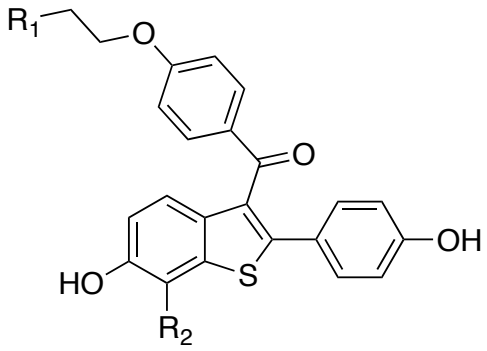


Figure 3.21A Raloxifene

The structure of Raloxifene. R_1 and R_2 denote positions at which addition of side groups could generate LRH-1 binding compounds with inhibitory activities.

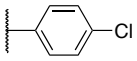
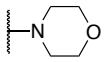
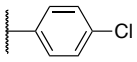
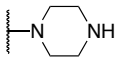
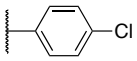
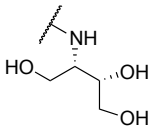
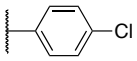
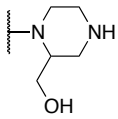
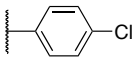
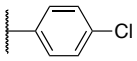
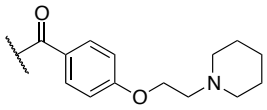
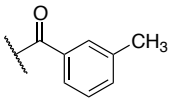
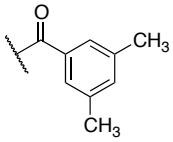
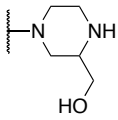
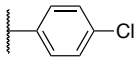
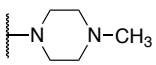
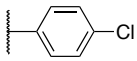
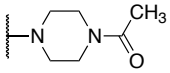
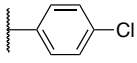
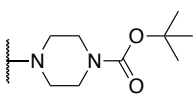
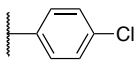
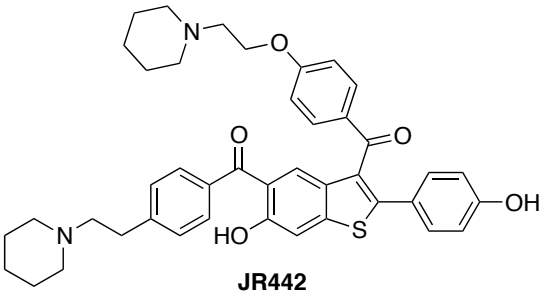
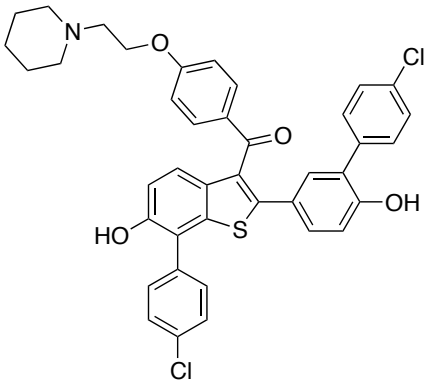
Compound	R_1	R_2
JR476 **JR700**		
JR689		
JR705		
JR786		
JR797		
JR776		
JR430		
JR505		
JR530		
JR802		
JR711		
JR714		
JR716		

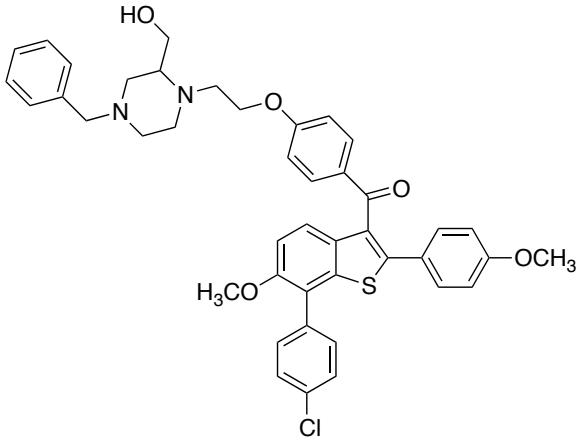
Figure 3.21B Raloxifene Analogues



JR442



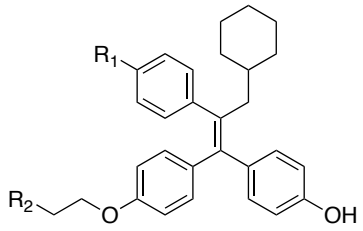
JR476 (2)



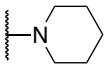
JR782

Figure 3.21C Raloxifene Analogues: Compounds from intermediate synthesis steps

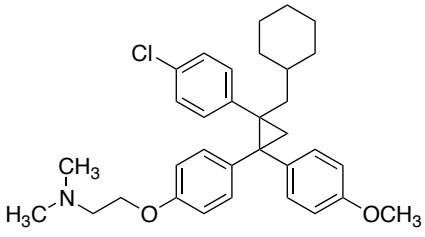
A



B

Compound	R_1	R_2
JR455		
JR449		
JR462		
JR469		
JR494		

C



JR566

Figure 3.22 Tamoxifen and analogues

The structure of tamoxifen (A). R_1 and R_2 denote positions of side chains in analogues (B). An additional compound produced from the synthesis steps of (B) is shown in (C).

3.3.4 Coactivator binding Inhibitors (CBIs)

The alternative method of targeting the co-factor binding domain, other than the Cresset approach detailed above, was the use of a rational structure. Transcriptional co-activator proteins bind to the nuclear receptor LBD through a charge clamp in the LBD interacting with the alpha helical motifs having the consensus sequence LXXLL in co-activator proteins. Some co-repressors, such as SHP also bind LRH-1 through an LXXLL type motif. (Li et al., 2005; Ortlund et al., 2005; Sablin et al., 2008). Using an approach already described for the design and development of novel CBIs for ERα (LaFrate et al., 2008), a scaffold was designed based on the LRH-1 binding region alpha helix in SHP that has the sequence ILYTLLS (Krylova et al., 2005).

Described below is the screening strategy and results for the compounds designed using the approaches outlined above.

3.4 Screening Assays for compounds with LRH-1 activity

3.4.1 Cell-based LRH-1 regulated luciferase reporter gene assay for screening of selected compounds

Initially the compounds were screened using a cell-based assay in which LRH-1 was co-transfected in COS-1 cells with an LRH-1 responsive firefly luciferase reporter gene (Thiruchelvam et al., 2011), allowing scoring of compounds by measuring firefly luciferase activity as a surrogate for LRH-1 transcriptional activity. Antagonists would be expected to inhibit LRH-1 activity and thus reduce luciferase output, whereas agonists would stimulate reporter gene activity.

To validate this approach, and develop the basis for experiments with our designed compounds, LRH-1 was co-transfected with an LRH-1 responsive firefly luciferase

reporter gene (SF-1-luc) in the African Green Monkey kidney fibroblast derived COS-1 cells (Figure 3.24A). This is a cell line commonly used for transfection studies because it is possible to achieve good transfection efficiencies. Figure 3.24B shows that LRH-1 stimulated reporter gene activity over the vector (pcDNA) control. Addition of the LRH-1 agonists compounds 5A and 5L, reported by Whitby et al (2006), stimulated reporter gene activity in a dose-dependent manner with a maximum stimulation of LRH-1 of 3 and 6-fold respectively at a concentration of 20μM, relative to the DMSO control.

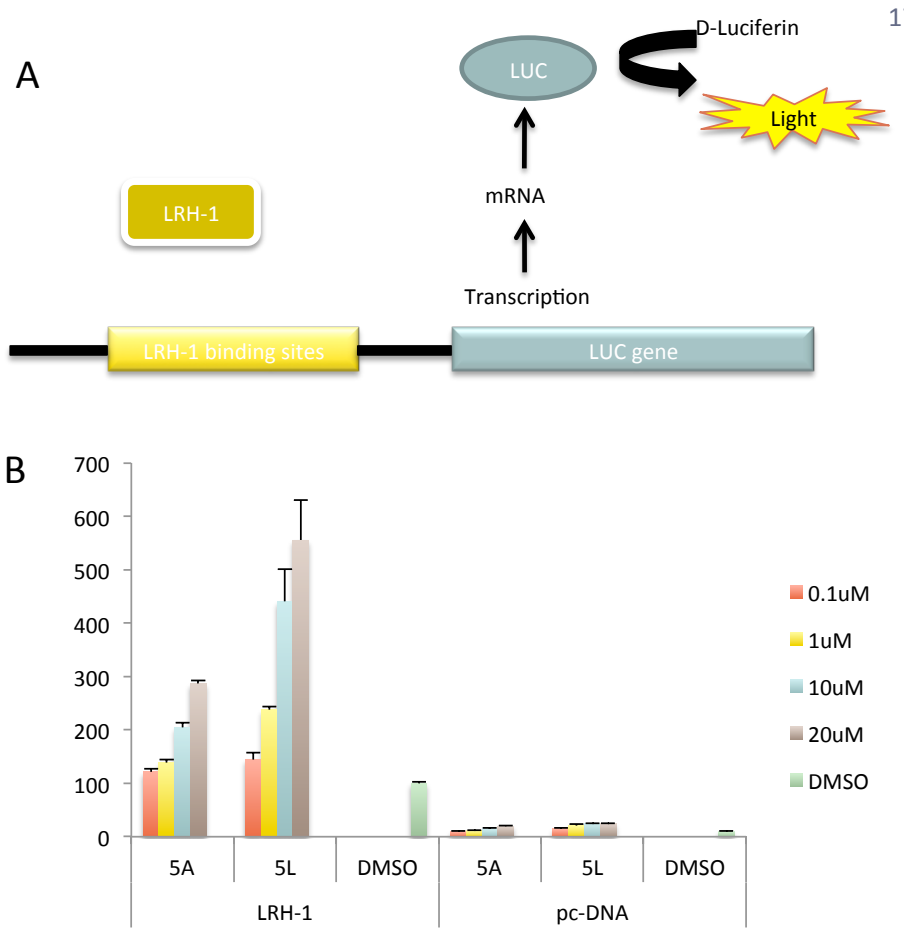


Figure 3.24 Cell based screening system for compounds targeting LRH-1

Co-transfection of LRH-1 and the LRH-1 responsive firefly luciferase gene results in the transcription of the LUC gene. Reporter activity is measured by addition of the firefly luciferase substrate D-luciferin to transfected cell lysates. Light output is measured using a luminometer. (A) Schematic view of the LRH-1 luciferase gene reporter assay. (B) COS-1 cells were transfected with LRH-1-LUC and the renilla luciferase reprter RLTK. Compounds were added 5 hours following transfection and cells harvested after a further 24 hours. Firefly luciferase activities were normalised against Renilla activity and are expressed as a percentage relative to the DMSO control. The bar chart shows mean activities for 3 independent experiments and the error bars represent the SEM.

A total of 157 compounds arising out of the different *in silico* screening approaches were initially screened using the cell-based reporter gene assay. For ease of comparison, a summary of the number of compounds derived from each discovery strategy, the positives obtained and reiterative synthesis and screening of analogues is presented in the flowchart in Figure 3.25. The results for compounds in each category are described in detail in the sections below.

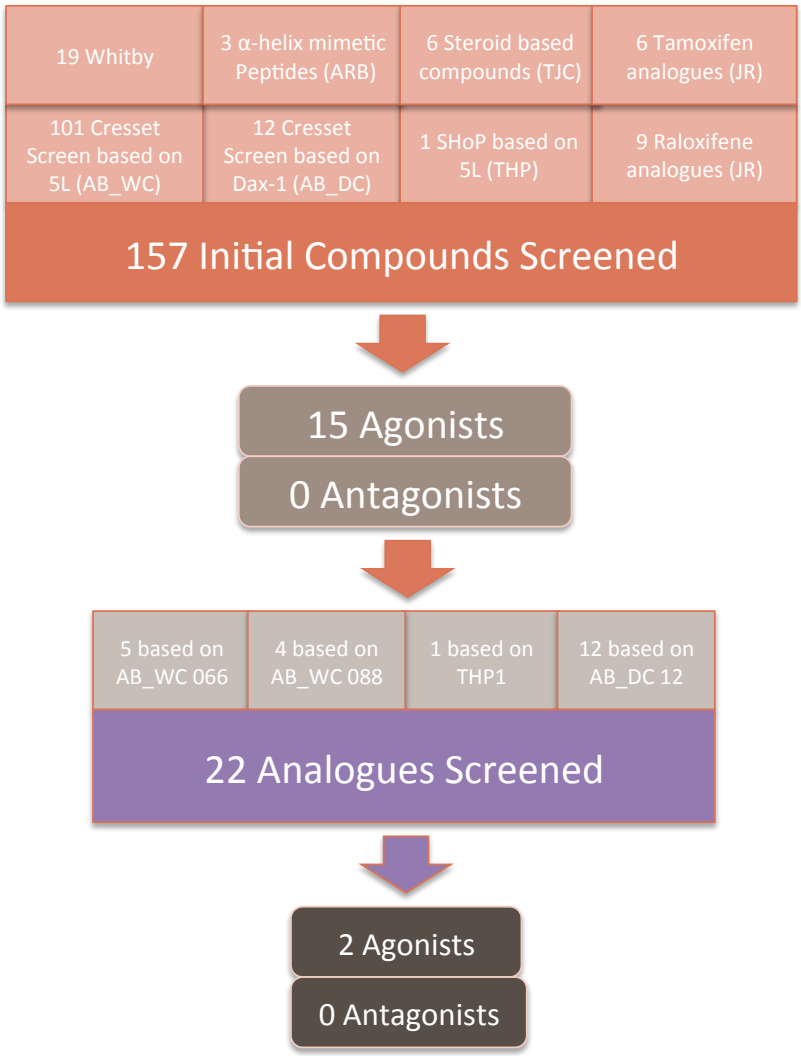


Figure 3.25 Cell Based screening Strategy

The flow chart shows the cell based screening process. 157 initial compounds were assessed using the co-transfection of LRH-1 and the LRH-1 responsive firefly luciferase gene into COS-1 cells. Each compound grouping is shown in a separate blue box. Of these compounds, 15 were seen to have potential agonist activity and 22 analogues were screened from the 4 compounds selected, AB_WC 066 and AB_WC 088 (from the Cresset screen based on Whitby compound 5L), THP1 (from the SHoP approach based on 5L) and AB_DC12 (from the Cresset screen based on Dax-1). Two potential LRH-1 agonists were identified.

3.4.1.1 'Whitby' Compound Series

The published series of LRH-1 and SF1 agonists were identified through screening of the LRH-1 LBD in a co-activator binding assay (Whitby et al., 2006). Some of the compounds stimulated the highly related SF-1, but did not stimulate LRH-1. This may mean that these compounds do not bind LRH-1. Alternatively, one or more of these compounds may bind LRH-1 and inhibit its activity i.e. may be LRH-1 antagonists, an activity that was not assayed for in the publication. To test this possibility, compounds from the 'Whitby' series that activated SF-1 but did not stimulate LRH-1 were tested in the LRH-1 reporter assay looking for a lack of activity, or inhibition of LRH-1 activity below the level of the control (DMSO) treated cells. As previously observed (Figure 3.24B), compounds 5A and 5L stimulate LRH-1, with greater activity observed for compound 5L than for compound 5A (Figures 3.24B and 3.26A). All other compounds either stimulate reporter gene activity, or do not affect reporter activity. It is interesting to note that compound 5Y was a good LRH-1 activator despite showing no activity in a TIF2 coactivator peptide/LRH-1 FRET based binding assay (Whitby et al., 2006). It is possible that compound 5Y stimulates LRH-1 activity through a different mode of action, for example by promoting the dissociation of co-repressors rather than stimulating co-activator recruitment.

For the compounds that did not affect the LRH-1 reporter gene activity, we wondered if they may have antagonistic activity that was not seen above the constitutively active conformation of LRH-1 in the absence of a synthetic ligand (possibly due to the presence of naturally occurring phospholipids). To further test if any of the compounds that failed to stimulate LRH-1 activity might be LRH-1 inhibitors, transfections were performed, with co-treatment of these compounds (5i, 5O, 5X), with compound 5A (Figure 3.26B) assessing for any abrogation of 5A mediated stimulation of LRH-1 activity. However, none of these compounds

significantly reduced LRH-1 activation by compound 5A, suggesting that they do not bind LRH-1.

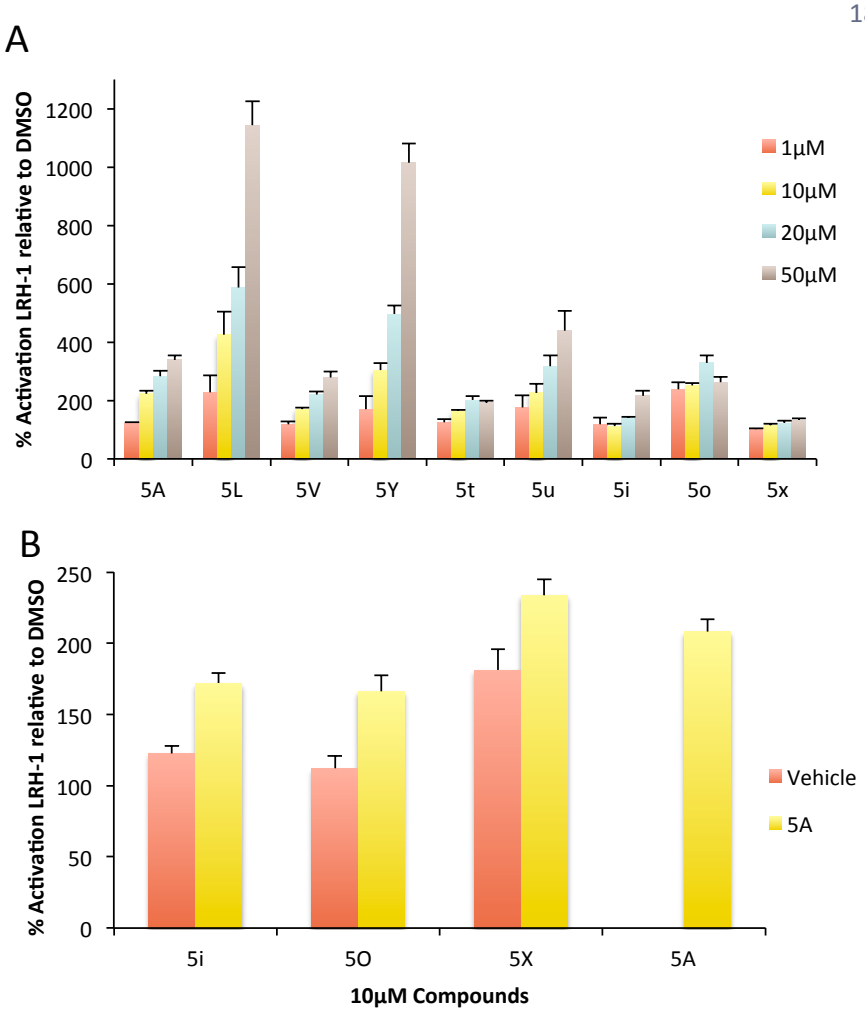


Figure 3.26 Effects of Whitby 5A analogues on LRH-1 transcriptional activity

(A) COS-1 cells were transfected with LRH-1, and the LRH-1-luc and renilla luc reporter genes. Compounds were added 5 hours following transfection and luciferase activities were determined after a further 24 hour. Bar charts show mean LRH-1-luc reporter activities following normalization against renilla-luc. Reporter activity for the DMSO (vehicle) control was taken 100% and all other activities shown relative to this. Error bars show SEM. (B) COS-1 cells were processed as in (A), except that compound 5A was added at a concentration of 10μM, as appropriate.

3.4.1.2 Compounds derived from "Cresset" screening

The LRH-1 reporter gene assay was used for screening of the compounds predicted from the "Cresset" software screen for compound 5L-like electrostatic and space filling properties (section 3.3.1). All compounds were added to a final concentration of 25μM. Of the compounds highlighted by the "Cresset" screen, 101 could be purchased commercially. Of these, 93 compounds stimulated LRH-1, compared to the vehicle control (Figure 3.27). Of these, 14 compounds showed activities greater than those observed with compound 5A. Eight out of the 101 compounds reduced LRH-1 activity.

The top 5 LRH-1 activators (98, 66, 20, 39 and 88) were tested at a range of concentration. None of the compounds stimulated LRH-1 activity at 0.1 μM or at 1μM concentrations (Figure 3.28), but all compounds stimulated LRH-1 activity at 25 μM, with compounds 66 and 98 showing strong stimulation also at 10 μM.

In addition to activating LRH-1 the closely related indole C-3 benzothioethers, compounds 66 and 88 also activated ERα (Figures 3.29-3.31), as did compound 98. Moreover, all three compounds reduced the activity of the renilla luciferase reporter gene (used as a control for transfection efficiency) at the active doses. This suggested that the compounds may be toxic at the active doses, leading to a reduction in transcription and hence renilla luciferase activity. Cell growth assays demonstrated inhibition of MCF7 cells at the active doses (10μM and 25μM) (Figures 3.29D, 3.30D, 3.31D). Since these compounds activate LRH-1 and ERα, it would be expected that they would stimulate, rather than inhibit, MCF7 growth. This suggests that compounds 66, 88 and 98 inhibit MCF7 cell growth through off-target effects. The compounds similarly inhibited the growth of the LRH-1 and ERα negative MDA-MB-231 cells, further confirming off-target effects on cell growth.

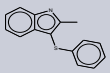
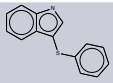
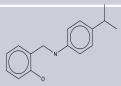
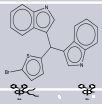
AB_WC	% Activation
98	1243
66	1228
20	982
39	923
88	822
85	627
69	572
70	436
89	403
21	399
22	397
55	391
59	334
86	333
5A	312
79	312
95	310
61	306
18	303
78	301
24	300
28	291
72	284
34	277
35	276
30	275
80	273
84	272
96	269
63	262
91	256
3	256
16	254
76	253

AB_WC	% Activation
8	252
31	245
5	239
67	232
6	216
71	215
17	214
26	199
62	196
65	195
23	190
36	190
100	189
73	188
9	182
7	182
14	181
99	179
37	178
57	174
94	171
32	167
82	165
29	163
25	162
50	162
45	161
4	155
38	153
56	152
64	150
2	150
75	148
93	147

AB_WC	% Activation
87	145
81	144
51	142
46	142
33	138
53	130
58	130
19	128
90	128
83	128
40	127
74	125
42	120
92	120
49	119
44	117
43	116
15	115
27	115
1	114
47	114
60	113
77	105
52	103
12	103
101	102
11	100
41	100
97	99
13	98
10	97
48	96
102	83
54	79

Figure 3.27 AB_WC Compound Screen (001-102)
COS-1 cells were transfected with LRH-1, LRH-1-luc and renilla-luc. Cells were treated with compounds identified from Cresset screening using compound 5A. Shown are the mean activities for each compound (n=3) for all compounds used at a final concentration of 25μM. Compounds that activated LRH-1 as better than compound 5A are shown in blue rectangles, compounds that inhibited LRH-1 are shown in orange.

A

Compound Number	Verbal Label	Structure	MW
AB_WC066	indole C-3 benzothioether		239.33
AB_WC088	indole C-3 benzothioether		225.3
AB_WC098	N-tolyl-2-thiophenylthiazolene		261.39
AB_WC020	4-Isopropylaniline		241.33
AB_WC039	Methythiophenobisindole		407.32
5A	Bicyclo-octene		

B

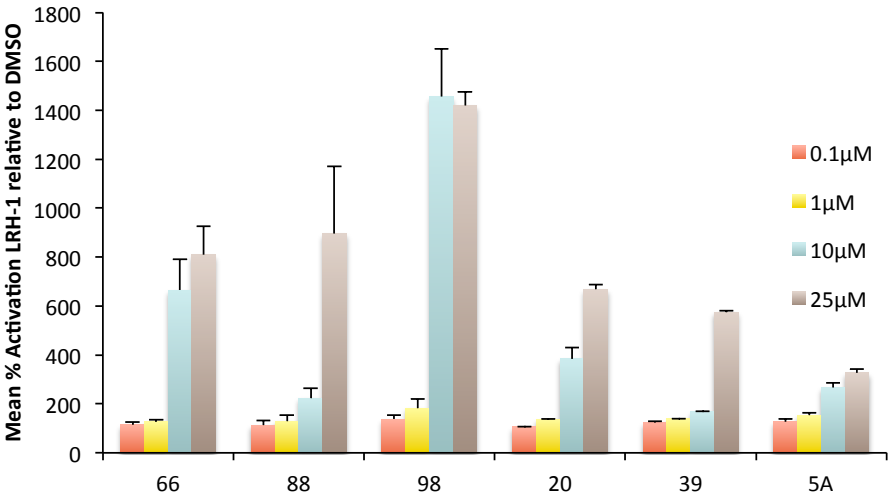


Figure 3.28 Determination of dose dependent activation of LRH-1 by AB_WC compounds

(A) Table showing compounds and structures. (B) COS-1 cells were transfected with LRH-1, and the LRH-1-luc and renilla luc reporter genes. Compounds were added 5 hours following transfection and luciferase activities were determined after a further 24 hour. Bar charts show mean LRH-1-luc reporter activities (n=4) following normalization against renilla-luc. Reporter activity for the DMSO (vehicle) control was taken 100% and all other activities shown relative to this. Error bars show SEM.

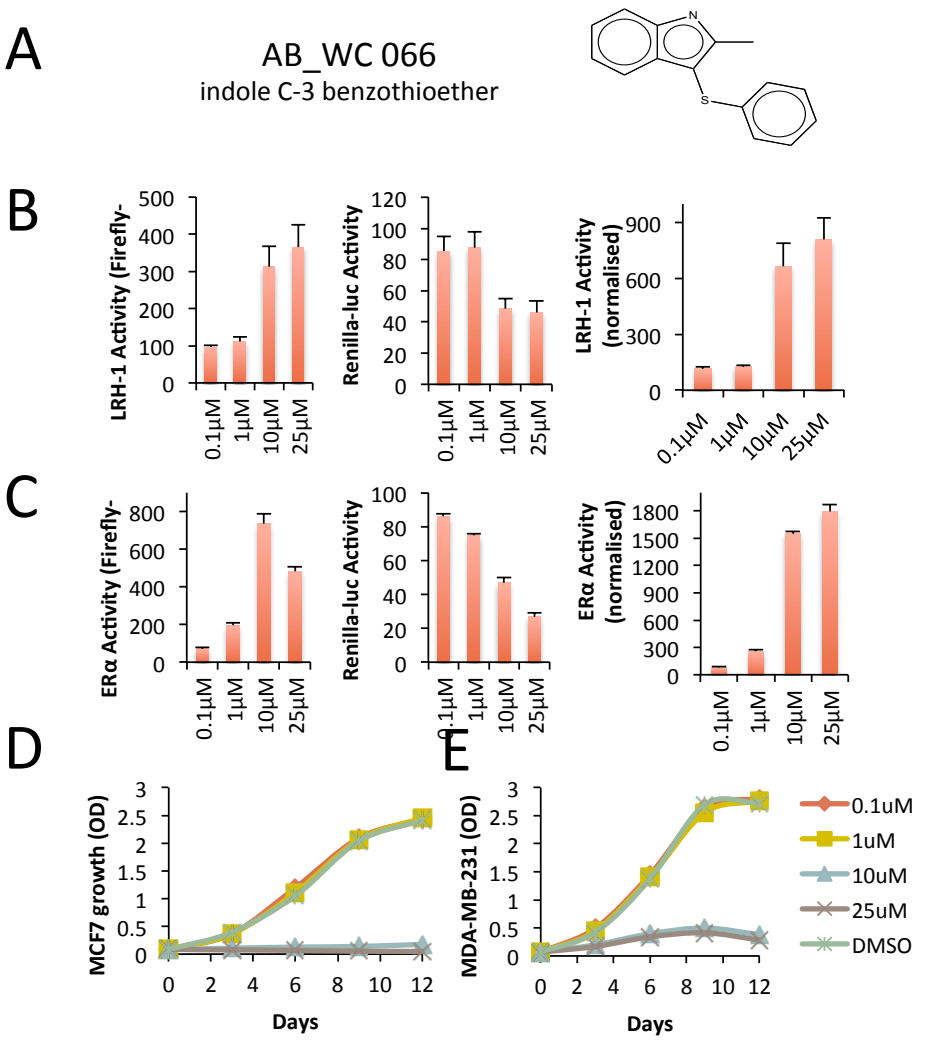


Figure 3.29 AB_WC 066 stimulates LRH-1 and ERα activity

(A) AB_WC066 is shown. COS-1 cells were transfected with LRH-1 and LRH-1-luc (B) or ERα and ERE-luc (C). AB_WC066 was added at the concentrations indicated. The bar charts show the mean reporter gene activities relative to DMSO control (n=3). Error bars represent SEM. Firefly-luc/renilla-luc ratios were determined to normalise for transfection efficiency. However, the large reduction in renilla activities at larger doses of AB_WC066 indicate 'toxicity'. MCF7 (D) and MDA-MB-231 (E) cells were grown over 12 days in the presence of AB_WC066 at the concentrations indicated. Cell numbers were estimated using the SRB assay and line graphs show the optical density at OD= 600 nm (n=6)

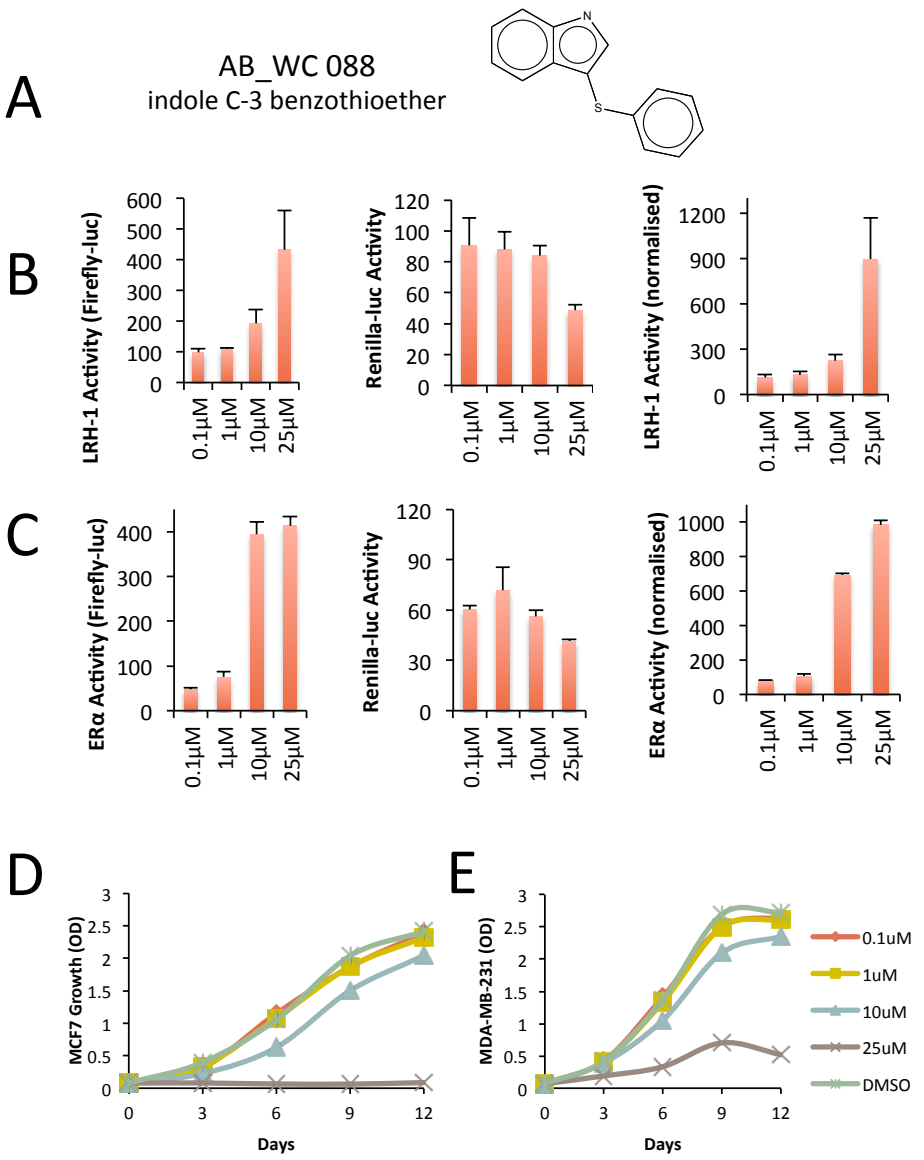


Figure 3.30 AB_WC 088 stimulates LRH-1 and ERα activity

(A) AB_WC088 is shown. COS-1 cells were transfected with LRH-1 and LRH-1-luc (B) or ERα and ERE-luc (C). AB_WC088 was added at the concentrations indicated. The bar charts show the mean reporter gene activities (n=3) relative to DMSO control. Error bars represent SEM. Firefly-luc/renilla-luc ratios were determined to normalise for transfection efficiency. MCF7 (D) and MDA-MB-231 (E) cells were grown over 12 days in the presence of AB_WC088 at the concentrations indicated (n=6).

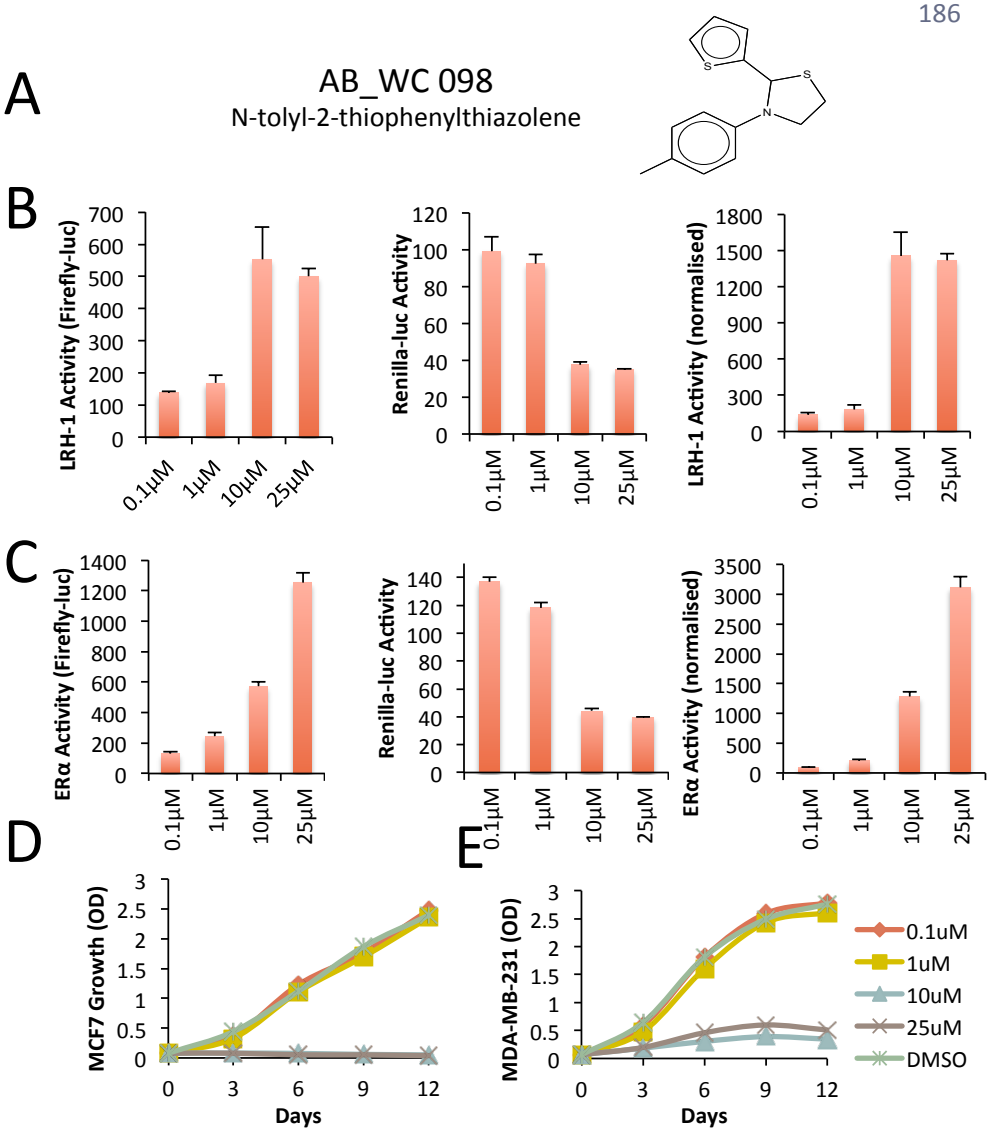


Figure 3.31 AB_WC 098 stimulates LRH-1 and ERα activity

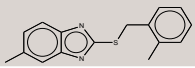
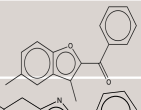
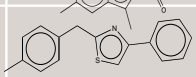
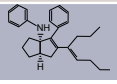
(A) AB_WC098 is shown. COS-1 cells were transfected with LRH-1 and LRH-1-luc (B) or ERα and ERE-luc (C). AB_WC098 was added at the concentrations indicated. The bar charts show the mean reporter gene activities (n=3) relative to DMSO control. Error bars represent SEM. Firefly-luc/renilla-luc ratios were determined to normalise for transfection efficiency. Again, the large reduction in renilla activities at larger doses of AB_WC098 indicate 'toxicity'. MCF7 (D) and MDA-MB-231 (E) cells were grown over 12 days in the presence of AB_WC098 at the concentrations indicated (n=6).

We re-examined the reporter gene data for all the compounds to identify weaker LRH-1 activators, which show activity at lower doses. Of the 101 compounds, three (AB-WC 057, 61 and 79) activated LRH-1 at 1μM concentrations (Figure 3.32). Of these AB_WC 057 was also evaluated against ERα, which it activated (Figure 3.33C), although there was no notable effect on renilla luciferase activity. In growth assays, AB_WC 057 did not stimulate MCF-7 cell growth in estrogen-depleted conditions despite stimulating ERα and LRH-1 activities in the reporter gene assay, implying that the ERα and LRH-1 stimulation by AB_WC 057 is extremely weak. There was also no affect on MDA_MB_231 cell growth, so AB_WC 057 does not appear to be deleterious for cell growth.

Additional chemistry was carried out (Prof Spivey group) to generate analogues of the related indole C-3 benzothioethers, compounds 66 and 88. Nine compounds were tested and of these compounds 107, 111 and 112 stimulated LRH-1 activity, with no detectable activity for the remaining compounds (data not shown).

Compound AB_WC 107 appeared, in additional reporter gene assays to inhibit renilla activity at the active doses, with some evidence of activation of ERα, indicative of off-target and non-specific growth inhibitory effects at the active doses (Figure 3.34). Similar results were obtained for compound 111 (Figure 3.35). Interestingly compound AB-WC 112, which stimulated LRH-1 and ERα (Figure 3.36) promoted MCF7 cell growth at a concentration of 10μM, although this effect was lost at 25μM, likely due to off-target 'toxicity', since the growth of MDA-MB-231 cells was also inhibited at this concentration. These results indicate that the C-3 benzothioether scaffold could be use to generate LRH-1 agonists. However, LRH-1 selectivity is clearly a problem with the compounds tested to date.

A

Compound Number	Verbal Label	Structure	MW
AB_WC057	Benzimidazole		268.37
AB_WC061	Benzofuran		250.29
AB_WC079	Thiazole		265.37
5A	Bicyclo-octene		

B

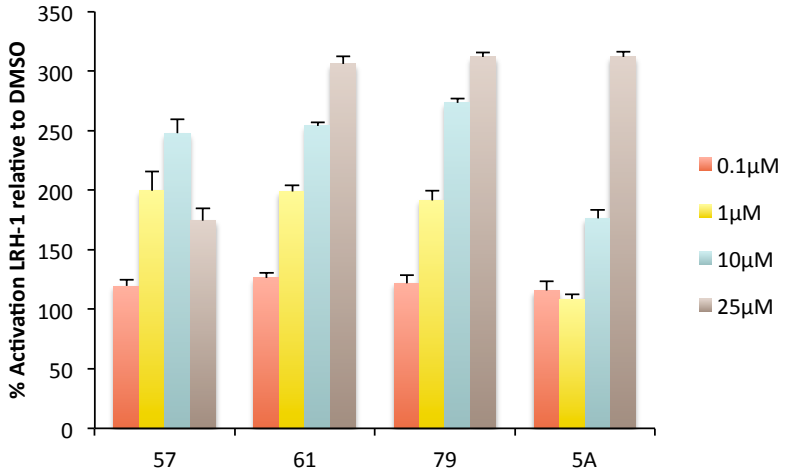


Figure 3.32 Determination of dose dependent activation of compounds AB_WC057, 061 and 079

(A) Table showing compounds and structures (B) COS-1 cells were transfected with LRH-1, and the LRH-1-luc and renilla luc reporter genes. Compounds were added 5 hours following transfection and luciferase activities were determined after a further 24 hour. Bar charts show mean LRH-1-luc reporter activities following normalization against renilla-luc. Reporter activity for the DMSO (vehicle) control was taken as 100% and all other activities shown relative to this. Error bars show SEM. From the initial 101 AB_WC Cresset compounds screened these 3 showed the greatest agonism at 1µM without the large reduction in Renilla activity indicating cellular tolerability.

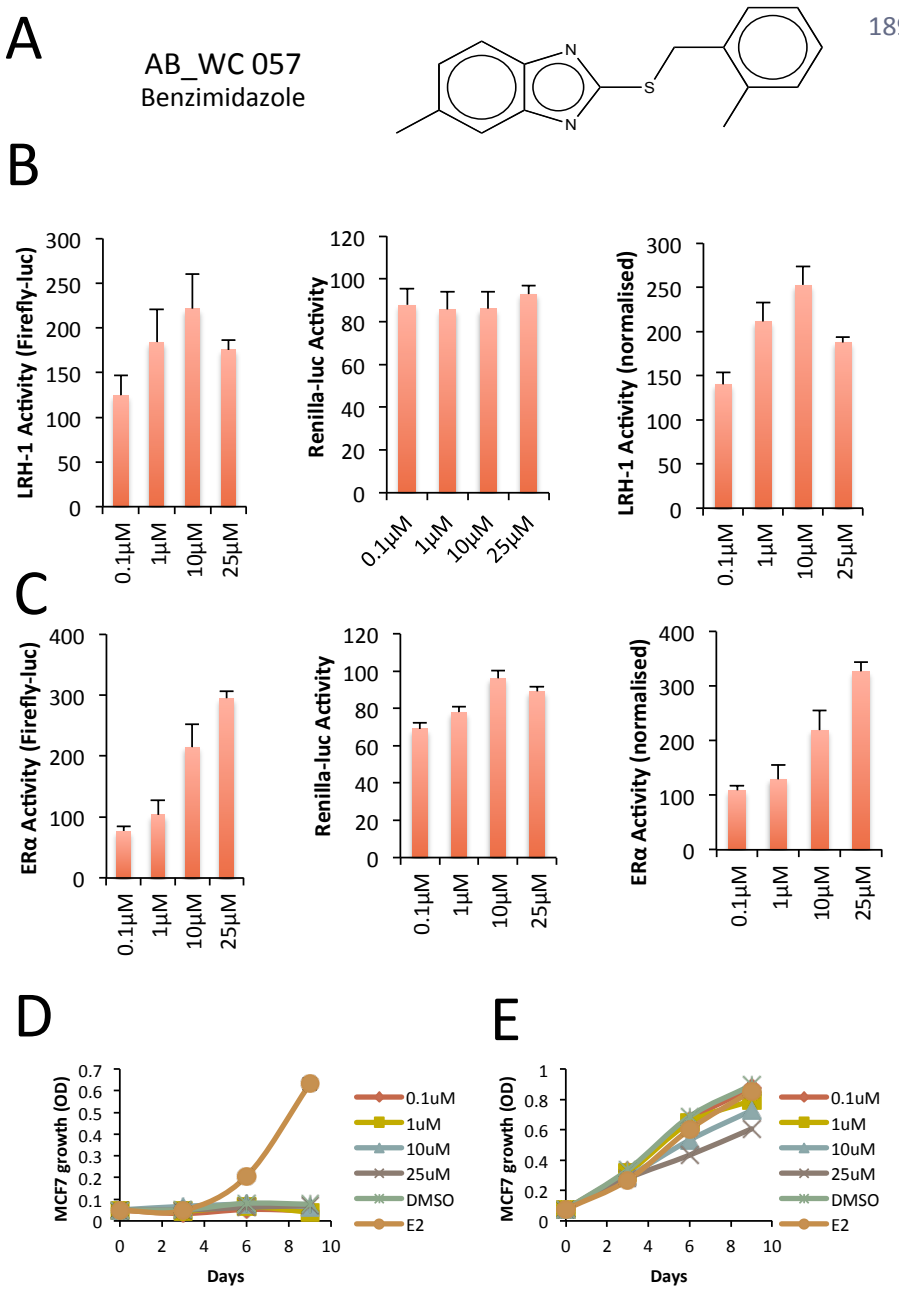


Figure 3.33 AB_WC 057 stimulates LRH-1 and ERα activity

(A) AB_WC057 is shown. COS-1 cells were transfected with LRH-1 and LRH-1-luc (B) or ERα and ERE-luc (C). AB_WC057 was added at the concentrations indicated. The bar charts show the mean reporter gene activities (n=3). Error bars represent SEM. Firefly-luc/renilla-luc ratios were determined to normalise for transfection efficiency. MCF7 (D) and MDA-MB-231 (E) cells were grown over 9 days in the presence of AB_WC057 at the concentrations indicated (n=6).

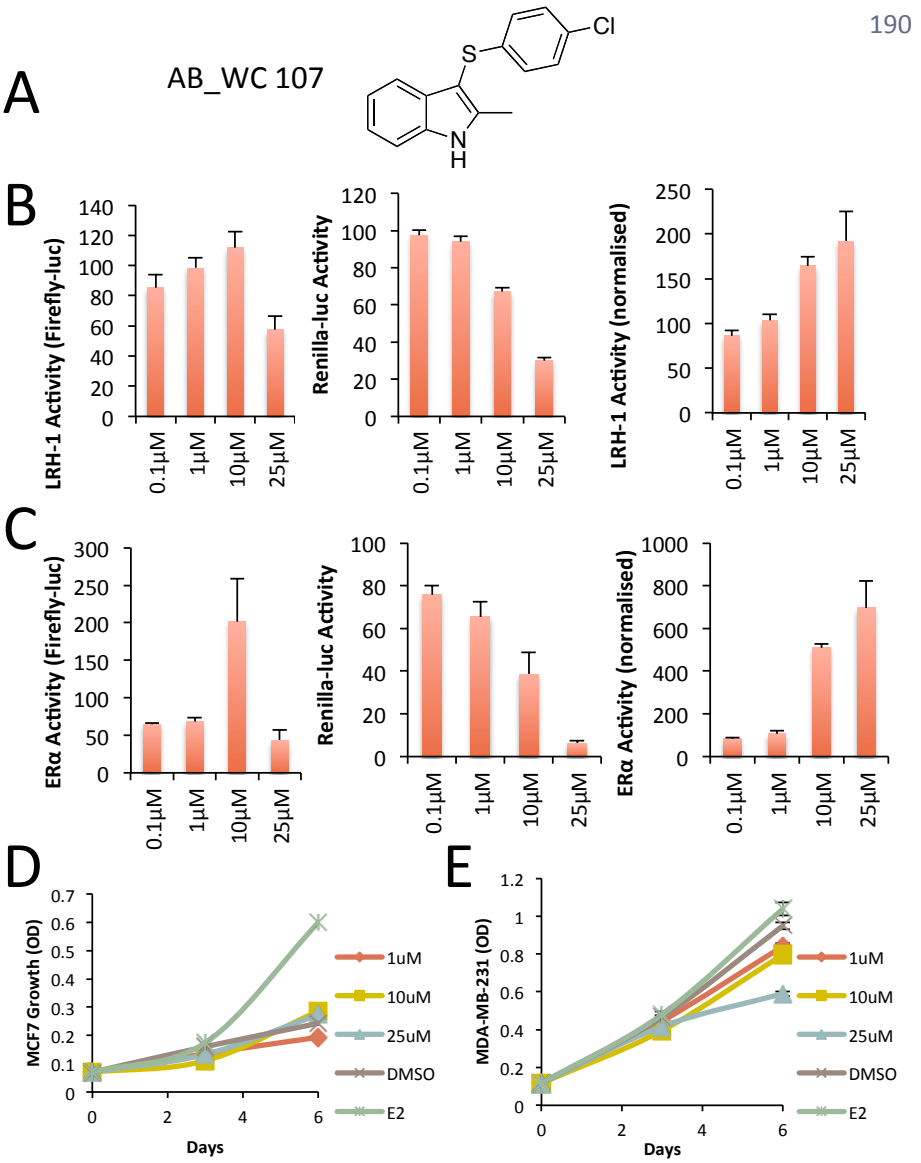


Figure 3.34 AB_WC 107 shows no effect on LRH-1 and stimulates ERα activity at 10uM but does not show any effect on growth

(A) AB_WC 107 is shown. COS-1 cells were transfected with LRH-1 and LRH-1-luc (B) or ERα and ERE-luc (C). AB_WC 107 was added at the concentrations indicated. The bar charts show the mean reporter gene activities (n=3). Error bars represent SEM. Firefly-luc/renilla-luc ratios were determined to normalise for transfection efficiency. MCF7 (D) and MDA-MB-231 (E) cells were grown over 6 days in the presence of AB_WC 107 at the concentrations indicated (n=6).

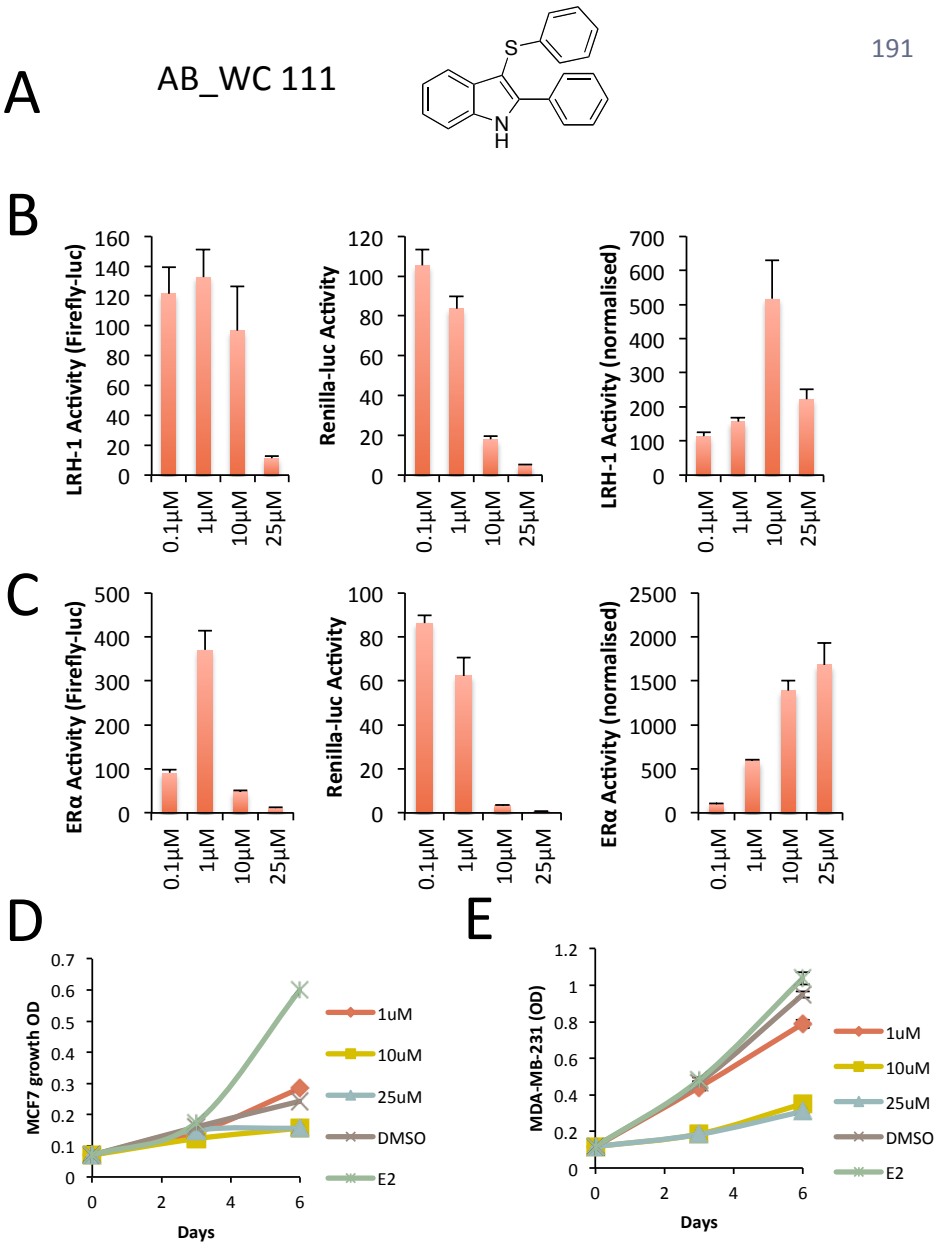


Figure 3.35 AB_WC 111 stimulates LRH-1 and ERα activity but does not show any effect on growth

(A) AB_WC 111 is shown. COS-1 cells were transfected with LRH-1 and LRH-1-luc (B) or ERα and ERE-luc (C). AB_WC 111 was added at the concentrations indicated. The bar charts show the mean reporter gene activities (n=3). Error bars represent SEM. Firefly-luc/renilla-luc ratios were determined to normalise for transfection efficiency. MCF7 (D) and MDA-MB-231 (E) cells were grown over 6 days in the presence of AB_WC 111 at the concentrations indicated (n=6).

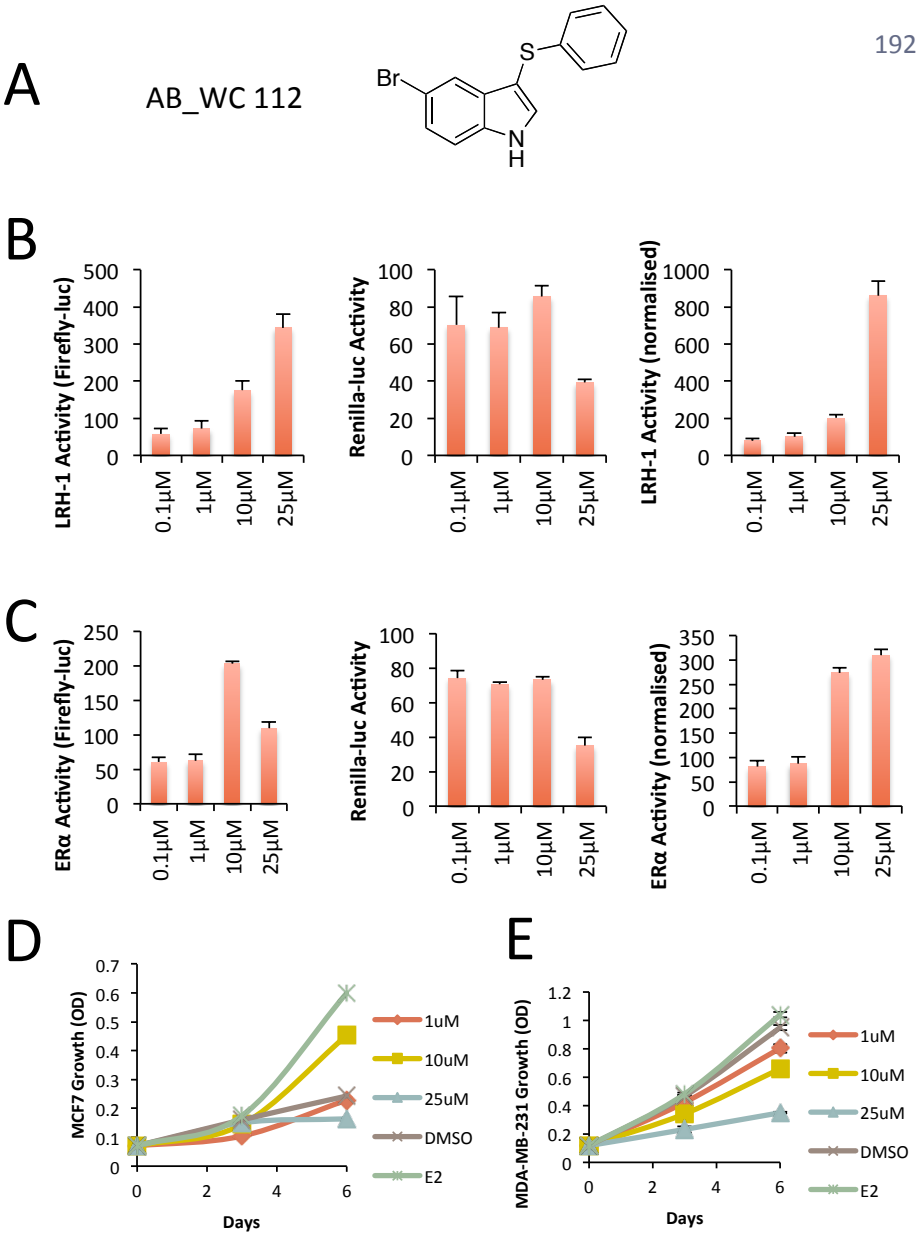


Figure 3.36 AB_WC 112 stimulates LRH-1 and ERα activity at 10µM and shows an effect on growth at 10µM

A) AB_WC 112 is shown. COS-1 cells were transfected with LRH-1 and LRH-1-luc (B) or ERα and ERE-luc (C). AB_WC 112 was added at the concentrations indicated. The bar charts show the mean reporter gene activities (n=3) relative to DMSO. Error bars represent SEM. Firefly-luc/ renilla-luc ratios were determined to normalise for transfection efficiency. MCF7 (D) and MDA-MB-231 (E) cells were grown over 6 days in the presence of AB_WC 112 at the concentrations indicated (n=6).

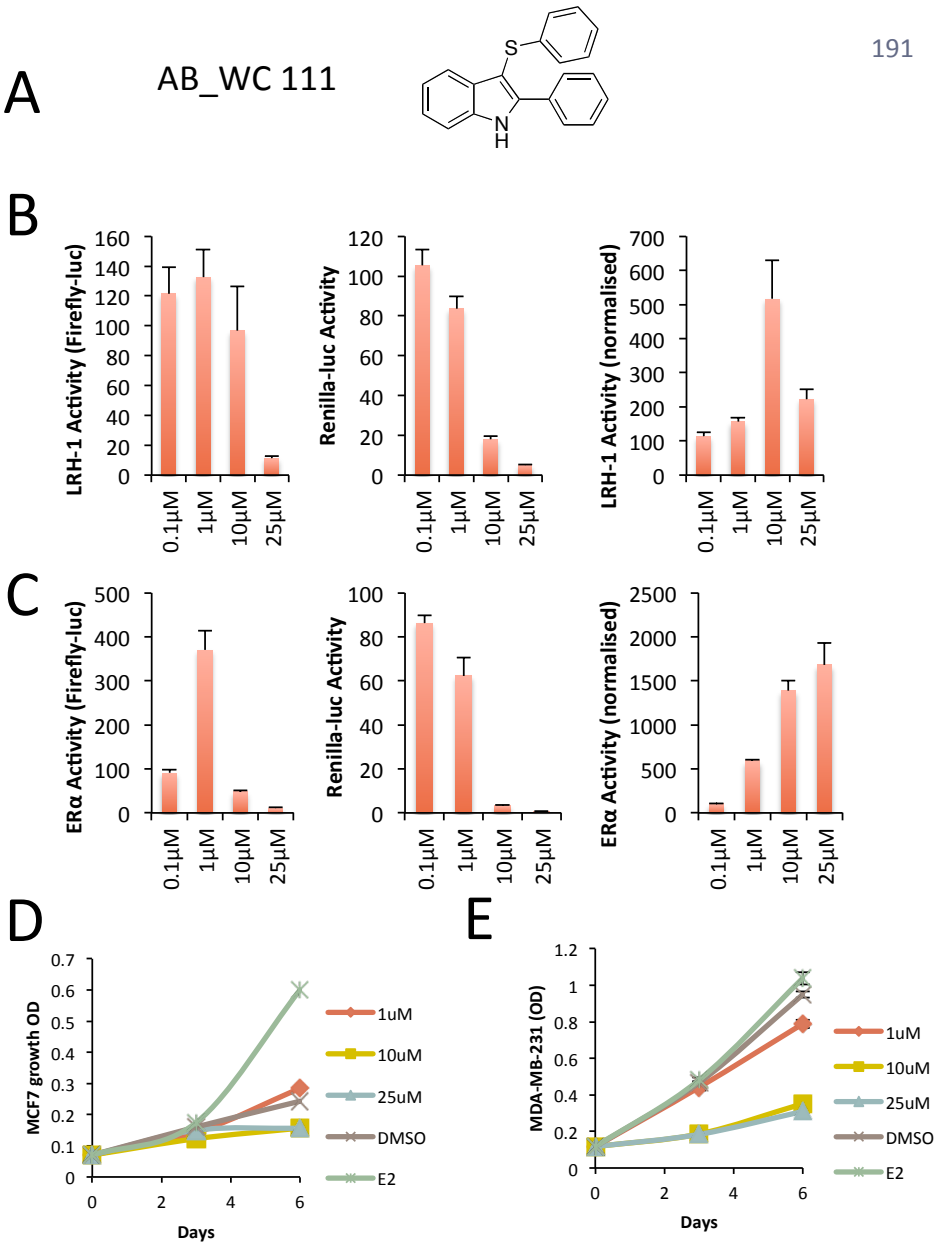


Figure 3.35 AB_WC 111 stimulates LRH-1 and ERα activity but does not show any effect on growth

(A) AB_WC 111 is shown. COS-1 cells were transfected with LRH-1 and LRH-1-luc (B) or ERα and ERE-luc (C). AB_WC 111 was added at the concentrations indicated. The bar charts show the mean reporter gene activities (n=3). Error bars represent SEM. Firefly-luc/renilla-luc ratios were determined to normalise for transfection efficiency. MCF7 (D) and MDA-MB-231 (E) cells were grown over 6 days in the presence of AB_WC 111 at the concentrations indicated (n=6).

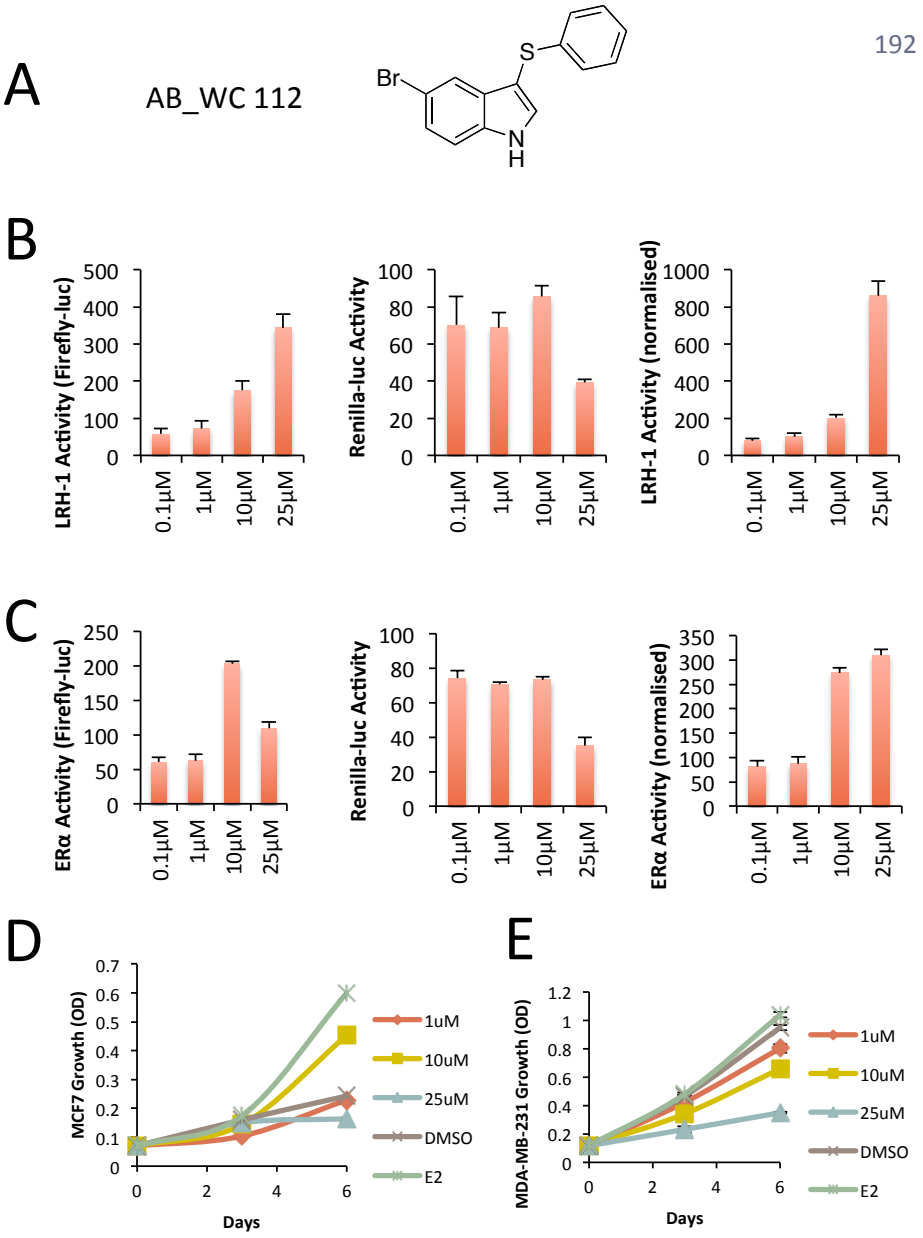
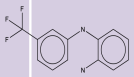
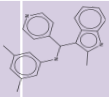
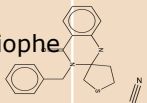
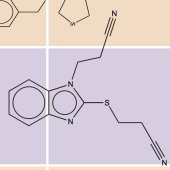
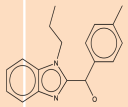


Figure 3.36 AB_WC 112 stimulates LRH-1 and ERα activity at 10µM and shows an effect on growth at 10µM

A) AB_WC 112 is shown. COS-1 cells were transfected with LRH-1 and LRH-1-luc (B) or ERα and ERE-luc (C). AB_WC 112 was added at the concentrations indicated. The bar charts show the mean reporter gene activities (n=3) relative to DMSO. Error bars represent SEM. Firefly-luc/ renilla-luc ratios were determined to normalise for transfection efficiency. MCF7 (D) and MDA-MB-231 (E) cells were grown over 6 days in the presence of AB_WC 112 at the concentrations indicated (n=6).

In terms of the compounds with potential antagonist activity from the Cresset screen there were only two compounds from the reporter screen showing an inhibition of activity below vehicle treated cells of greater than 5%, compounds 54 (17%) and 102 (21%). I chose to investigate these compounds further and also picked three other compounds (19, 44 and 101) that only weakly activated LRH-1 (Figure 3.37). Only compound 102 showed a dose dependent inhibition of LRH-1 activity. However, no reduction in activation of LRH-1 by 5A was seen indicating that LRH-1 inhibition by the compounds may be indirect (Figure 3.38).

A

Compound Number	Verbal Label	Structure	MW
AB_WC019	Benzenediamine		252.23
AB_WC044	3-methylpyridylaniline imidazole		232.23
AB_WC054	Spirotetrahydrothiophenyl quinazolinone		310.41
AB_WC101	Benzimidazole		256.32
AB_WC102	Benzimidazole		280.36

B

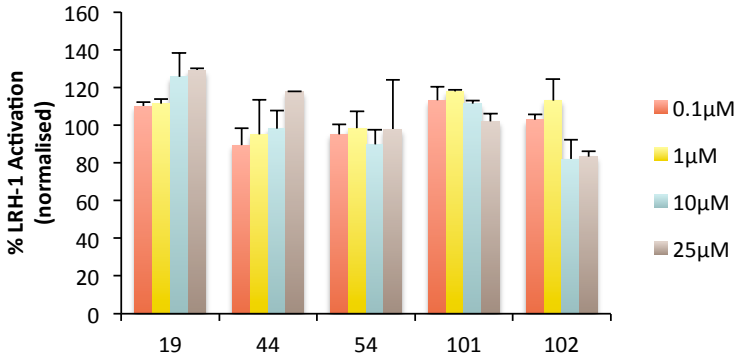


Figure 3.37 Determination of dose dependent activation/inhibition of LRH-1 by AB_WC compounds: Potential LRH-1 Antagonists

A) Table showing compounds and structures (B) COS-1 cells were transfected with LRH-1, and the LRH-1-luc and renilla luc reporter genes. Compounds were added 5 hours following transfection and luciferase activities were determined after a further 24 hour. Bar charts show mean LRH-1-luc reporter activities following normalization against renilla-luc. Reporter activity for the DMSO (vehicle) control was taken 100% and all other activities shown relative to this. Error bars show SEM.

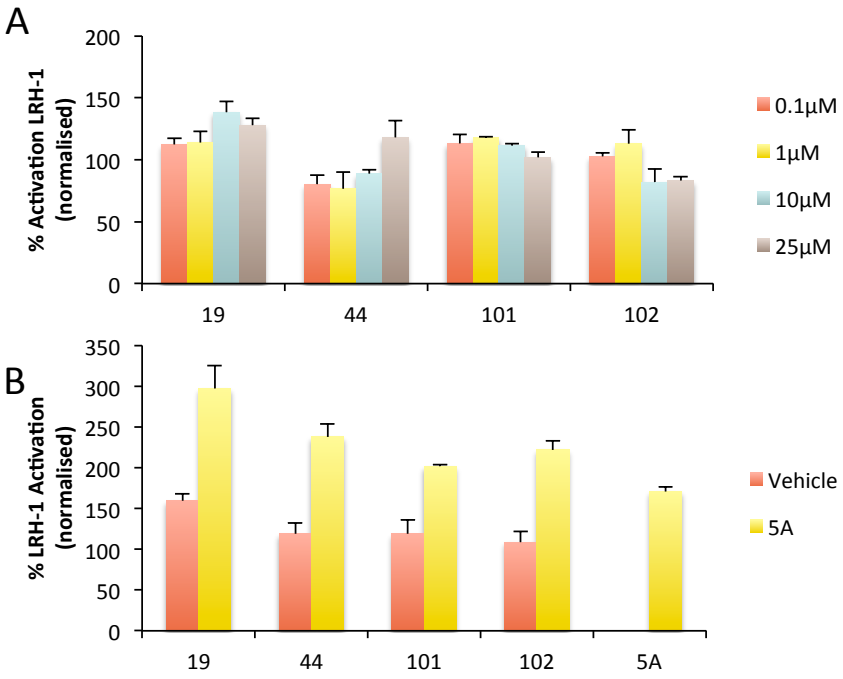


Figure 3.38 No abrogation of agonism with 5A by potential LRH-1 antagonists

(A) COS-1 cells were transfected with LRH-1, and the LRH-1-luc and renilla luc reporter genes. Compounds (10µM) were added 5 hours following transfection and luciferase activities were determined after a further 24 hour. Bar charts show mean LRH-1-luc reporter activities following normalization against renilla-luc. Reporter activity for the DMSO (vehicle) control was taken 100% and all other activities shown relative to this. Error bars show SEM. (B) COS-1 cells were processed as in (A), except that compound 5A was added at a concentration of 10µM, as appropriate.

Taken together, screening of commercially available compounds identified on the basis of an in silico screen for compounds with structural similarity to previously reported LRH-1 agonists, identified a series of compounds that strongly activated LRH-1 in a reporter gene assay. Further evaluation of these compounds is suggestive of potential binding to LRH-1, but all of the compounds that activated LRH-1 also activated ERα. Therefore, either these compounds bind widely to nuclear receptors and/or the activation is due to off-target effects, for example through modulation of protein kinase pathways or chromatin remodeling enzymes. This may explain the "toxicity" observed at higher concentrations. It is likely, therefore, that a considerable amount of chemistry design would be needed for obtaining improved, selective LRH-1 inhibitors, most likely achievable only by screening libraries of compounds related to the compounds that activate LRH-1.

With respect to the potential LRH-1 inhibitors, the effects were extremely small and are likely to be indirect. Given the very few compounds that inhibited LRH-1, as opposed to the many that activated LRH-1 it is possible that an approach for generating LRH-1 antagonists that is based on modeling of a LRH-1 agonist, may not be appropriate.

3.4.1.3 Design of LRH-1 inhibitors based on modeling of Nuclear Receptor antagonists in the LRH-1 LBD

Section 3.3.3 describes the modeling approach that was used to determine if compounds similar to available antagonists for other nuclear receptors, where structures of the antagonist bound in the LBD, are available. In particular, the anti-estrogens raloxifen, tamoxifen and faslodex in the ERα LBD were modeled in the LRH-1 LBD, to identify compounds that might be accommodated in the LRH-1 LBD. The anti-estrogens, raloxifene, tamoxifen and Faslodex, nor estrogen itself, affected the activity of LRH-1 in reporter gene assays (Figure 3.39).

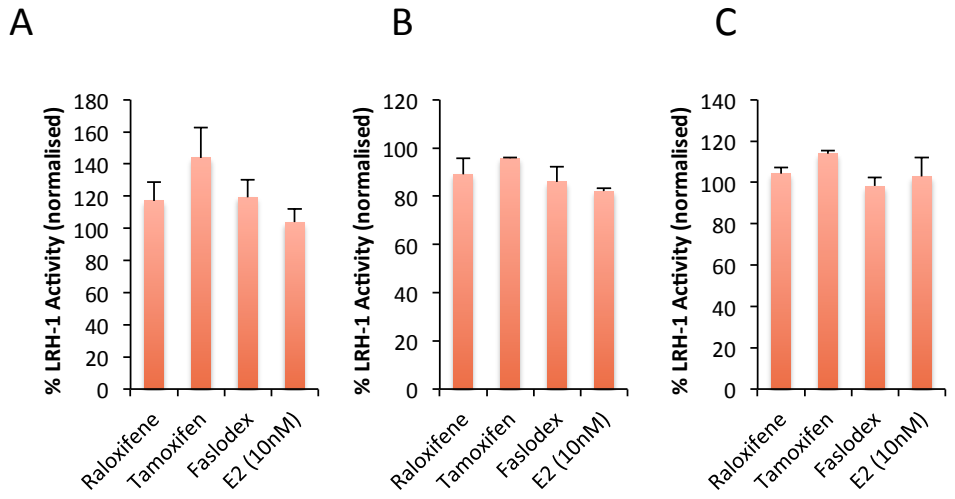


Figure 3.39 Anti-estrogens and estrogen do not affect activity of LRH-1 in COS-1 cells

LRH-1 activity was determined using the luciferase gene reporter assay. Three concentrations were assessed, (A) 0.1µM, (B) 0.5µM and (C) 1µM. The activation of LRH-1, after normalisation against Renilla, is shown after 24 hours and expressed as a percentage relative to ethanol control. The mean values are shown in the bar chart and the error bars represent the SEM. No effect on activity is seen.

A small number of compounds based on raloxifene (nine compounds), tamoxifen (six compounds) and 6 steroidal compounds based on the FXR agonist (MFA-1) (Soisson et al., 2008), were assessed using the LRH-1 responsive luciferase reporter assay. These compounds were much more difficult to solubilise in DMSO and subsequently in aqueous cell media. The starting concentration was therefore 10 μM with 1μM and 0.1μM to provide a dose titration. Again, as with the Cresset compounds, visually significant cell toxicity was seen with higher concentrations, with reduced renilla luciferase activation at 10μM doses of most compounds. At a concentration of 1μM, when no reduction on renilla luciferase activity was seen for any of the compounds (Figure 3.40) several compounds activated LRH-1, including JR430, JR476 and JR442.

Similar problems with renilla activity were observed for the tamoxifen analogues (Figure 3.41). Moreover, there was no significant activation or inhibition of LRH-1 by the tamoxifen analogues.

Finally, the FXR steroidal derived compounds also had little or no affect on LRH-1, with the exception of TJC123, which activated LRH-1 at higher concentrations (Figure 3.42).

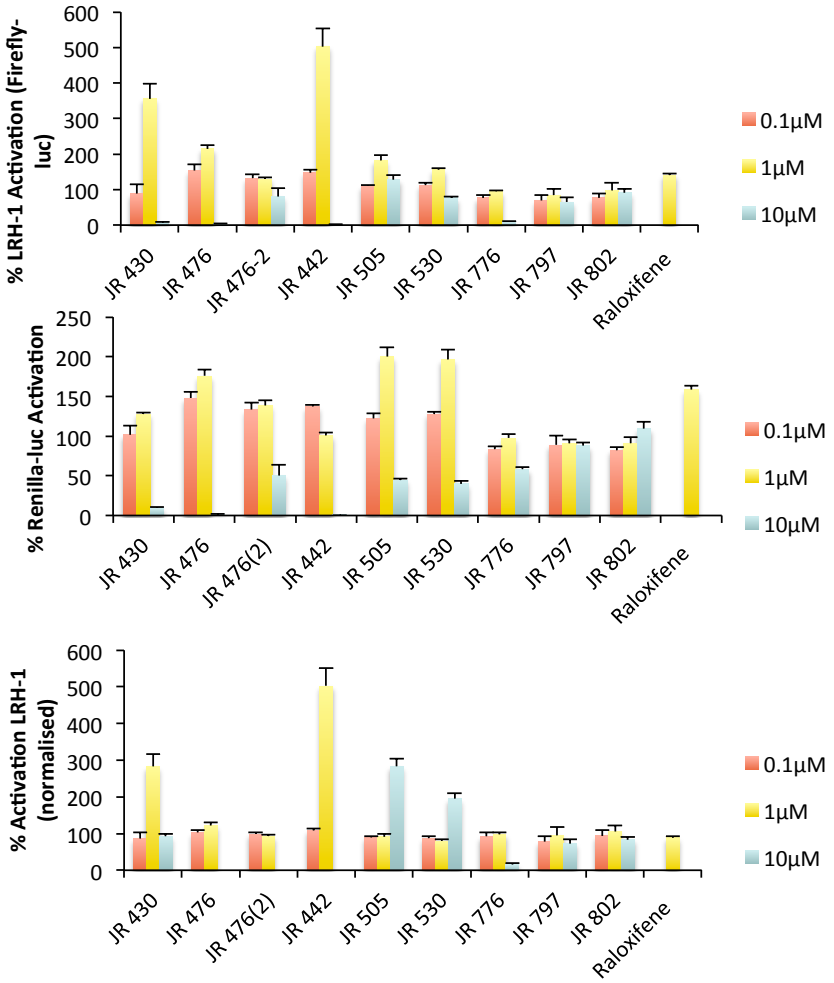


Figure 3.40 Effects of Raloxifene analogues on LRH-1 transcriptional activity

The compounds were generated from the computer aided drug design (CADD) software to fit into the large LRH-1 binding pocket and extend to disrupt the position of helix 12 and prevent co-activator recruitment. COS-1 cells were transfected with LRH-1, and the LRH-1-luc and renilla luc reporter genes. Compounds were added 5 hours following transfection and luciferase activities were determined after a further 24 hour. Bar charts show mean LRH-1-luc reporter activities following normalization against renilla-luc. Reporter activity for the DMSO (vehicle) control was taken 100% and all other activities shown relative to this. Error bars show SEM. Raloxifene was used as an additional reference at a single concentration of 1µM.

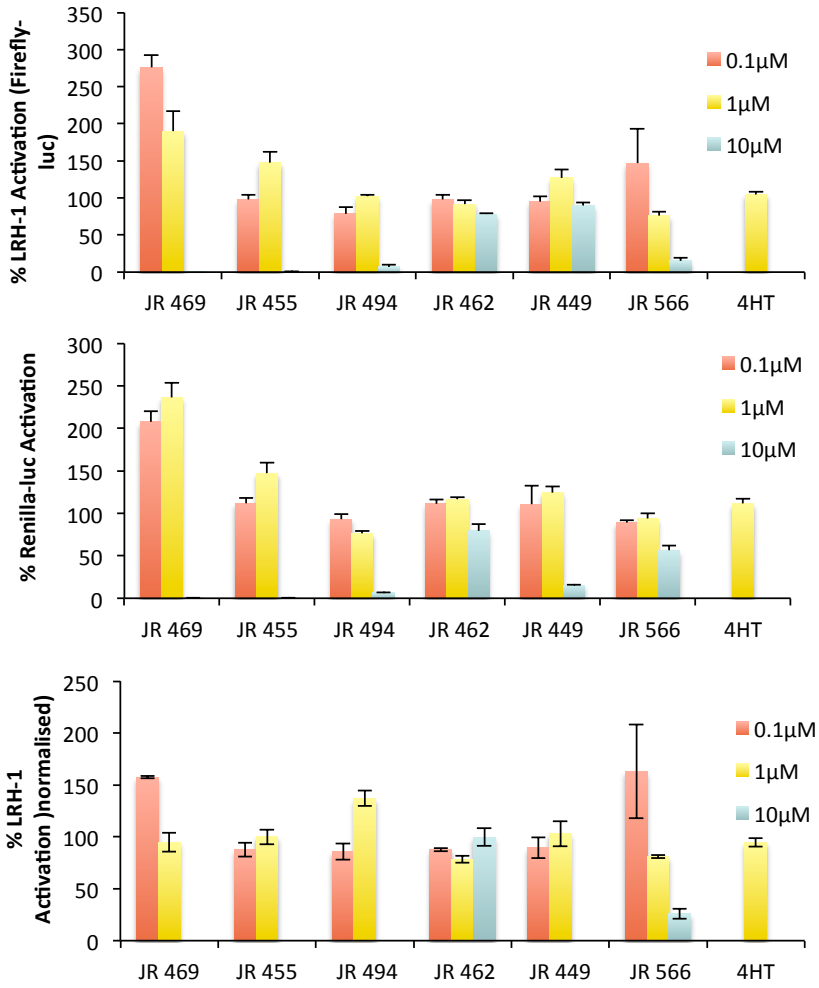


Figure 3.41 Effects of Tamoxifen analogues on LRH-1 transcriptional activity

The compounds were generated from the computer aided drug design (CADD) software to fit into the large LRH-1 binding pocket and extend to disrupt the position of helix 12 and prevent co-activator recruitment. COS-1 cells were transfected with LRH-1, and the LRH-1-luc and renilla luc reporter genes. Compounds were added 5 hours following transfection and luciferase activities were determined after a further 24 hour. 4-hydroxytamoxifen (4HT) was used as an additional reference at a single concentration of 1µM.

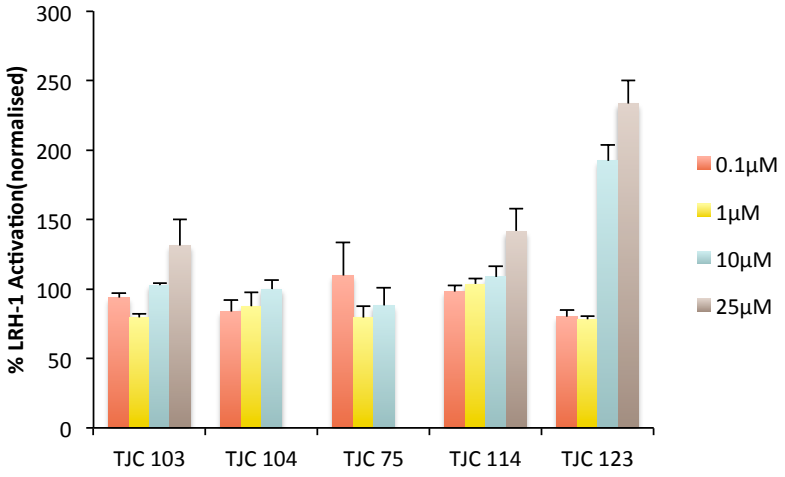


Figure 3.42 Effects of steroid based analogues on LRH-1 transcriptional activity

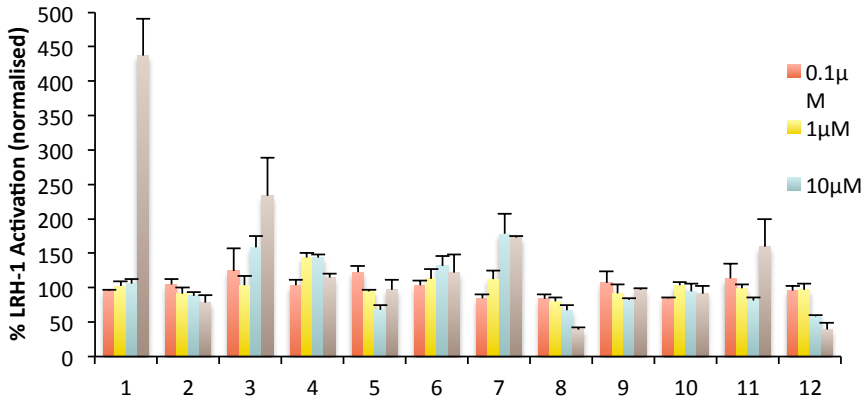
The compounds were generated from the computer aided drug design (CADD) software to fit into the large LRH-1 binding pocket and extend to disrupt the position of helix 12 and thereby prevent co-activator recruitment. COS-1 cells were transfected with LRH-1, and the LRH-1-luc and renilla luc reporter genes. Compounds were added 5 hours following transfection and luciferase activities were determined after a further 24 hour. Bar charts show mean LRH-1-luc reporter activities following normalization against renilla-luc. Reporter activity for the DMSO (vehicle) control was taken 100% and all other activities shown relative to this. Error bars show SEM. The transfected cells were treated in triplicate with four concentrations of the compounds, 0.1μM, 1μM, 10μM and 25μM except for compounds TJC 104 and 75 which was poorly soluble at 25μM dissolved in DMSO.

3.4.1.4 Cresset Screen: Dax-1 peptide

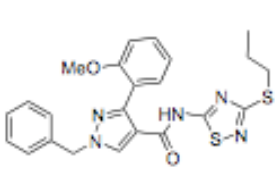
Twelve compounds arising from modeling of the DAX-1 LRH-1 interacting peptide were purchased. Of these compounds AB_DC 08 and 12 showed a dose dependent inhibition of LRH-1 activity (Figure 3.43). Compounds AB_DC 01, 03 and 11 showed apparent activation on normalised data however this was an exaggeration of decreased transfection efficiency with signs of cell toxicity.

Based on the inhibition observed with AB_DC 12, twelve analogues were synthesized, including stereo-isomers of compound AB_DC 12, AB_DC12a and AB_DC12b. However, none of these compounds inhibited LRH-1 activity (Figure 3.44).

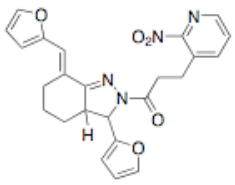
A



B



AB_DC 08



AB_DC 12

Figure 3.43 Effects of Dax-1 mimetics on LRH-1 transcriptional activity

(A) COS-1 cells were transfected with LRH-1, and the LRH-1-luc and renilla luc reporter genes. Compounds were added 5 hours following transfection and luciferase activities were determined after a further 24 hour. Bar charts show mean LRH-1-luc reporter activities following normalization against renilla-luc. Reporter activity for the DMSO (vehicle) control was taken 100% and all other activities shown relative to this. Error bars show SEM. The compounds are based on a Cresset field point analysis of peptide portion of the LRH-1 co-repressor, Dax-1. Compounds AB_DC 08 and AB_DC 12 circled in red appeared to have encouraging antagonistic properties. (B) Structures of compounds AB_DC 08 and 12.

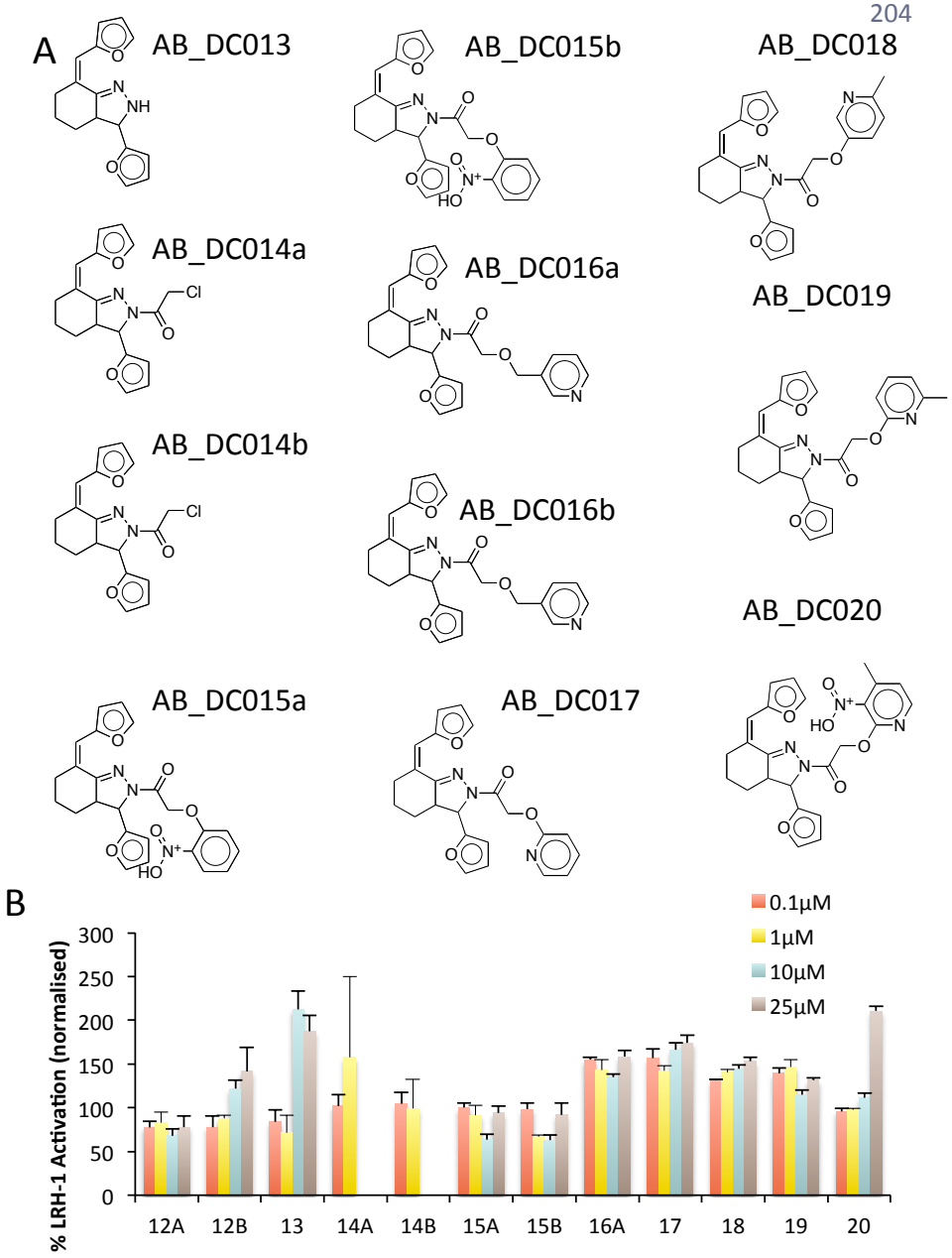


Figure 3.44 Effects of Dax-1 mimetic (AB_DC 12) analogues on LRH-1 transcriptional activity

(A) Structures of Dax-1 mimetic analogues of compound AB_DC 12 (B) COS-1 cells were transfected with LRH-1, and the LRH-1-luc and renilla luc reporter genes. Compounds were added 5 hours following transfection and luciferase activities were determined after a further 24 hour.

3.4.1.5 α-helix mimetics

Three compounds that were designed to mimic the α-helical LRH-1 interacting region in the SHP protein, (α-helical mimetics) were generated by Dr A. Bayly and Professor A. Spivey (Imperial College London) (Figure 3.45A). Compound ARB_238 did not affect LRH-1 reporter activity (Figure 3.45B). Compounds ARB_190 and ARB_260 modestly stimulated LRH-1 activity at the highest dose. The stimulation of LRH-1 activity is unexpected and may be a reflection of inhibition of co-repressor recruitment, although the α-mimetics would also be expected to prevent coactivator recruitment. Of the three compounds submitted two showed minimal agonism at 10μM up to 1.7 fold compared to vehicle treated cells (Figure 3.45B).

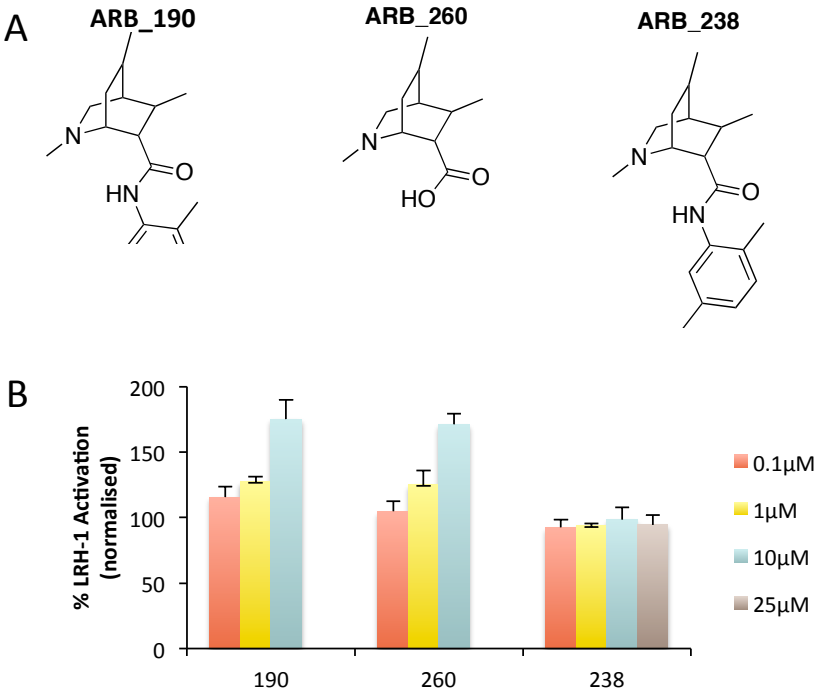


Figure 3.45 Effects of α helix mimetics on LRH-1 transcriptional activity

(A) Structures of the α helix mimetics based on the analysis of the SHP NR box peptides binding residues with LRH-1 (B) COS-1 cells were transfected with LRH-1, and the LRH-1-luc and renilla luc reporter genes. Compounds were added 5 hours following transfection and luciferase activities were determined after a further 24 hour. Bar charts show mean LRH-1-luc reporter activities following normalization against renilla-luc. Reporter activity for the DMSO (vehicle) control was taken 100% and all other activities shown relative to this. Error bars show SEM. Compounds ARB 190 and 260 show cellular toxicity and Renilla drop off at 10 and 25µM

3.4.1.6 SHoP: 5L

As described earlier (section 3.3.2), the SHoP approach for modeling the 3D interaction properties of a compound were used to identify a new compound (THP1/THP) that potentially takes the same 3D space as compound 5L and would allow further compound syntheses (Figure 3.46A). THP1 stimulated LRH-1 to a similar extent as 5L (Figure 3.46B). Based on this a number of analogues were designed and one was synthesized, THP10 (Figure 3.46C) for testing in the cell based assay. Interestingly this analogue shows LRH-1 inhibition at 1 and 10μM, compared with the vehicle treated control, although the effect was extremely small.

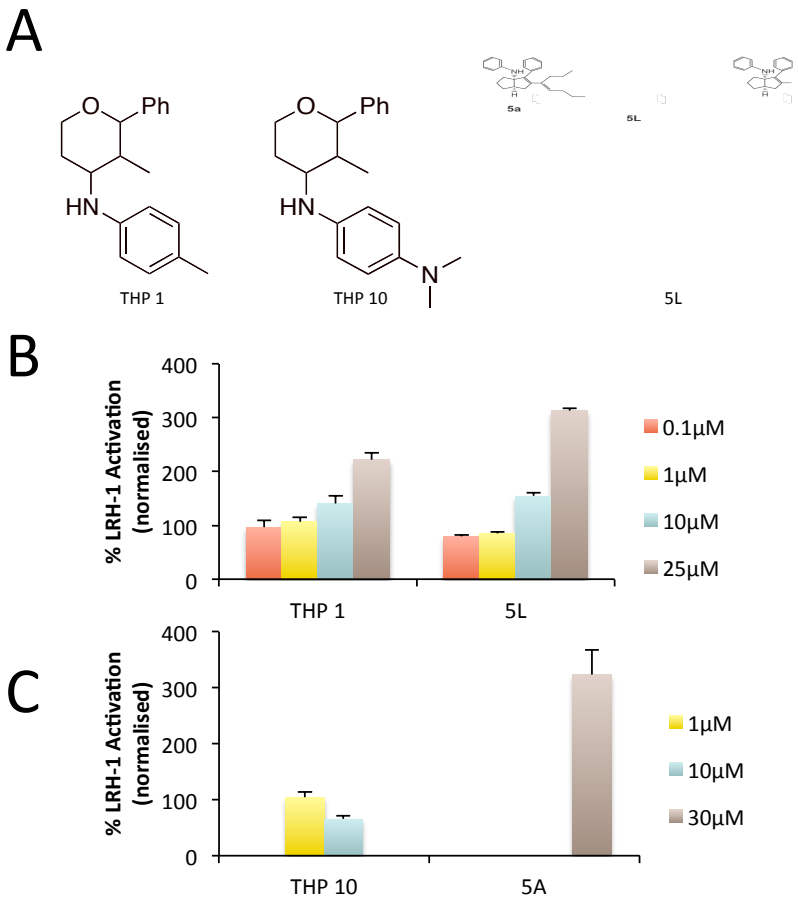


Figure 3.46 Effects of SHoP compounds on LRH-1 transcriptional activity

Compounds THP (THP1) and it's analogue THP 10, designed to act as an agonist of LRH-, were assessed in comparison with Whitby compound 5L. (A) Structures shown. COS-1 cells were transfected with LRH-1, and the LRH-1-luc and renilla luc reporter genes. Compounds were added 5 hours following transfection and luciferase activities were determined after a further 24 hour. Bar charts show mean LRH-1-luc reporter activities following normalization against renilla-luc. Reporter activity for the DMSO (vehicle) control was taken 100% and all other activities shown relative to this. Error bars show SEM. (B) THP demonstrates agonism and therefore proof of principle for SHoP. (C) THP 10 shows a promising loss of activity.

3.4.2 Development of an in vitro screen for identification of compounds that bind the LRH-1 LBD, to block co-activator recruitment

Ligand binding assays allow for direct measurement of compound binding to the ligand binding domain. Generally these assays involve the use of radioactive ligands, whose displacement by the compound of interest allows binding affinities to be determined (LaFrate et al., 2009). In the case of nuclear receptors, ligand binding to the LBD can be assessed indirectly, by measuring the ligand-dependent recruitment of transcriptional co-activators by interaction with the LBD (e.g. (Albers et al., 2006; Xu et al., 2002). Agonists would be expected to promote coactivator recruitment and conversely, antagonists will inhibit co-activator interaction. Such an assay can be performed in vivo, using protein-protein interaction assays, for example the mammalian 2-hybrid approach (Albers et al., 2006; Xu et al., 2002). As with the reporter assay used in the preceding section, there is however, the problem that off-target effects obscure identification of compounds that bind to the LRH-1 LBD. To develop an alternative approach for identifying synthetic compounds that bind to the LRH-1 LBD, I therefore developed and optimized an *in vitro* assay, using the Alpha Screen system (Glickman et al., 2002; Li et al., 2005; Taouji et al., 2009; Wu et al., 2005; Xu et al., 2002), for LBD-coactivator interaction screening of compounds. The alpha screen method allows rapid, screening of nuclear receptor LBD binding molecules that change the interaction between the LBD and co-activator or co-repressor proteins. Importantly, this assay can be scaled up for high-throughput screening of compound libraries. The method depends on the proximity of donor and acceptor beads provided by a protein-protein interaction, where one protein is coupled to the donor bead and the second to an acceptor bead. Excitation of the donor bead with a high intensity laser at 680nm generates a singlet ambient oxygen molecule on the surface of the donor bead (Figure 3.47). A photo-sensitiser present on the bead converts this ambient oxygen singlet into a more excited state with the ability to diffuse up to 200nm. If an acceptor bead is within this proximity the oxygen singlet will react with a thioxene derivative in the acceptor beads, generating chemoluminescence at 370nm and further activating a cascade of

fluorophores which emit light at 520-620nm. This light can then be detected and used as a measure of bead based proximity. If the acceptor is not within this proximity the oxygen will decay. This system has been used previously, among other indications, to look at LRH-1 LBD co-factor recruitment (Li et al., 2005; Taouji et al., 2009) and can be carried out in 384 well plate formats. Compounds that stimulate the LRH-1 LBD-coactivator interaction upon binding to the LRH-1 LBD (agonists) should increase emission at 520-620nm whilst those that inhibit the interaction will reduce the level of emission.

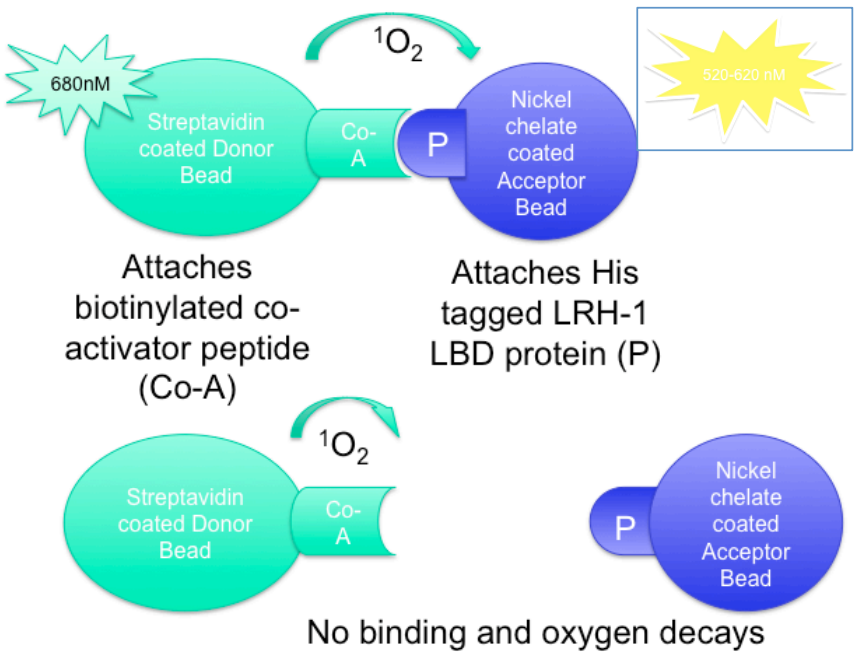


Figure 3.47 ALPHAScreen protein-peptide Interaction method

The nickel chelate coated acceptor bead is bound to the his-tagged LRH-1 LBD purified protein. The streptavidin-coated donor bead is bound to the biotinylated co-activator peptide, PGC1α.

Excitation with a high intensity laser, at 680nm, induces the formation of singlet ambient oxygen (60,000) at the surface of the donor bead. A photo-sensitiser, present on the bead, converts this to a more excited singlet state which can diffuse up to 200nm. If an acceptor bead is within this proximity the oxygen will react with a thioxene derivative generating chemo-luminescence at 370nm further activating a cascade of fluorophores in the acceptor bead and subsequently emitting light at 520-620nm. Therefore if the PGC1α is recruited to the LRH-1 LBD this will produce light which can be measured. Compounds which inhibit the recruitment and binding of PGC1α to LRH-1 LBD will decrease the light production and vice versa. This can be used as a means for detecting compounds which act as antagonists and agonists for this interaction.

A construct, expressing amino acids 291-541 of human LRH-1, cloned in frame with maltose binding protein (MBP) and a hexa-histidine (His) tag, was kindly provided by Prof Eric Ortlund (Emory University). The His-MBP-LRH-1-LBD protein construct was expressed in E. coli BL21 cells, as described in Materials and Methods, purified by incubation of the bacterial lysate with nickel beads and eluted from the beads by the addition of imidazole (Figure 3.48A). A polypeptide of approximately 75 kDal corresponding to the His-MBP-LRH-1-LBD was strongly expressed and could be purified by incubation with the nickel beads, followed by elution with imidazole. A polypeptide of about 40 kDal co-purified with His-MBP-LRH-1-LBD and likely represents His-MBP (expected molecular mass = 42 kDal). The pMALCH10 vector allows for cleavage of the His-MBP tag using enterokinase. Incubating with nickel beads and/or amylose beads (for MBP binding) would allow for recovery of the purified LRH-1-LBD. However, enterokinase treatment did not result in His-MBP-LRH-1-LBD cleavage (data not shown), I therefore dialysed the purified His-MBP-LRH-1-LBD for use in the alphascreen assay (Figure 3.48B).

Peptides containing the LRH-1 interacting regions from the coactivators PGC1α and SRC2, were those previously described (Li et al., 2005; Whitby et al., 2006) and are detailed in section 3.1.11. These were synthesized with an N-terminal biotin.

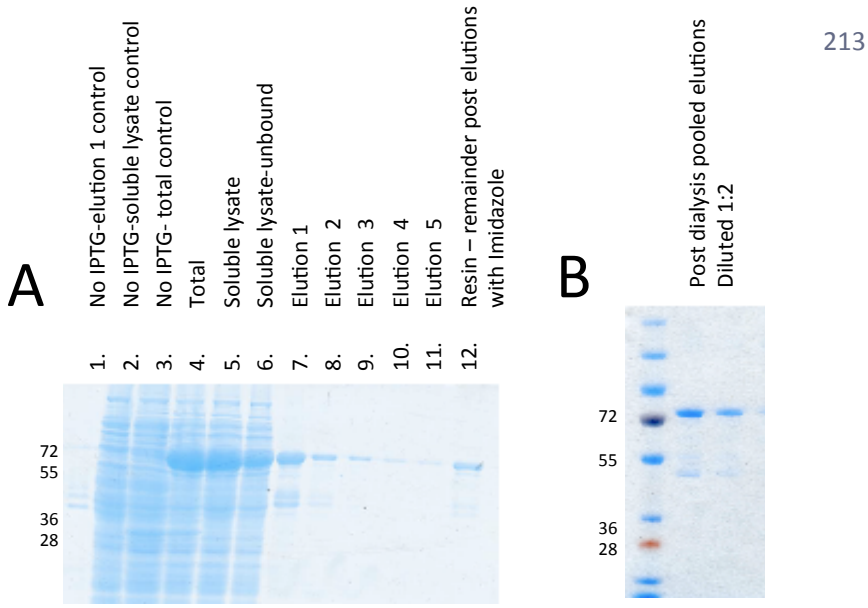


Figure 3.48 Generation and purification of His-tagged LRH-1 LBD

The pMALCH10 expression plasmid was transformed in Rosetta E. Coli bacteria and grown in terrific broth with ampicillin and chloramphenicol (see methods for full protocol). The bacteria were grown to an optical density of 0.8 then protein expression was induced by 0.1mM IPTG for 4 hours at 32°C. The cultures were harvested by centrifugation and stored at -80°C overnight. The bacterial pellet was resuspended in buffer with 0.1mM DNAase, Protease Inhibiter Cocktail and 0.2%TritonX. The pellet was sonicated until the cells were lysed, centrifuged and stirred on ice to minimise the formation of inclusion bodies and recentrifuged. The his purification using HisTALON™ gravity columns was carried out according to the manufacturers instructions and the resulting protein eluted with 250mM imidazole. (A) Shows the Coomassie Blue stained SDS-Page gel of purification process. The size (72 KDa) of the protein is consistent with a his-tagged LRH-1 and attached maltose binding fusion protein. The imidazole was then removed by dialysis with Slide-a-Lyzer, 10K MWCO cassettes (ThermoScientific, UK) to enable binding to nickel chelate beads in the Alpha Screen Assay. (C) Coomassie Blue stained SDS-Page gel with dialysed, purified, pooled elusions one and two.

3.4.2.1 Alpha Screen Optimisation

To set up the interaction assay, the His-MBP-LRH-1-LBD fusion protein (100nM) was incubated with increasing concentrations of the biotinylated PGC1α or SRC2 coactivator peptides. LRH-1 interaction with both peptides was observed, with an expected bell shaped curve with varying peptide concentration (Figure 3.49A). The bell shaped curve is due to reagent depletion or the documented 'hook effect' (www.perkinelmer.co.uk/resources/technicalresources). The optimum concentration combination was assessed by a titration of PGC1α and SRC2 against several concentrations of LRH-1 (20nM, 50nM and 100nM; Figures 3.49B and 3.49C respectively). The results showed a titratable increase in binding with increased concentration of LRH-1 LBD protein and peptide. The peak concentration or the peak of the hook effect is defined by the co-activator peptide and occurred at 137nM for both peptides with 100nM of LRH-1 (Figure 3.49A). PGC1α gave overall higher alpha signals at each concentration combination in comparison with SRC-2 (Figures 3.49B and C). At 50nM of LRH-1, the EC_{50} for PGC1α was 35nM versus 369nM for SRC2. However, using 100nM LRH-1 LBD, the values were more comparable, with EC_{50} values of 27 and 28nM, respectively.

On the basis of these experiments, a combination of 50nM LRH-1 LBD with 50nM co-activator peptide was felt to be optimum for experiments assessing compounds with agonism, i.e. an increase in the alpha signal, whereas compounds assessing antagonism, i.e. a decrease in alpha signal were felt to be better assessed using a baseline combination of 50nM LRH-1 with 100nM co-activator peptide. This would allow, in both instances, a robust 'z' score, detailed in section 3.2.16 (Zhang et al., 1999) and therefore an adequate background to signal window for experimental compounds.

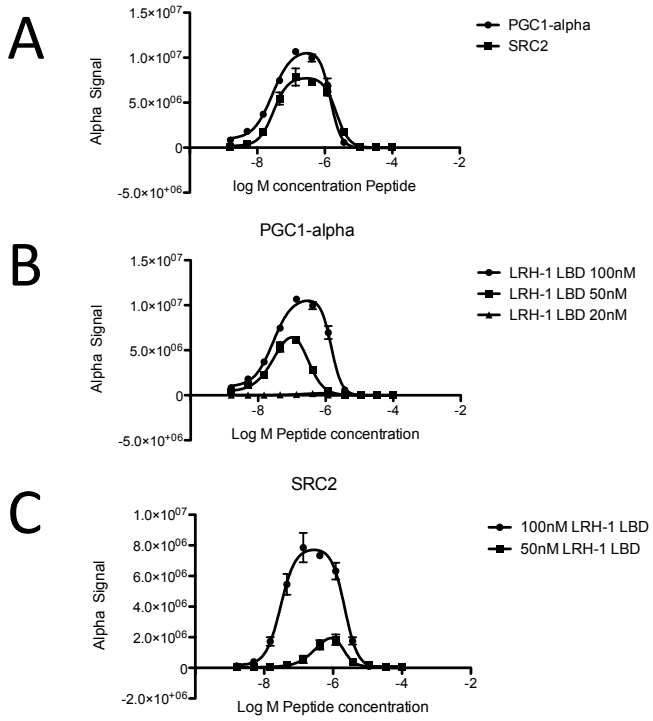


Figure 3.49 Optimisation and Validation: Co-Activator Peptides/ LRH-1 LBD

Comparison of the affinity of co-activator peptides with 100nM his tagged LRH-1 LBD protein (A). 100nM protein plus the co-activator peptide titration (ranging from 100μM to 1.6nM over 11 data points) and buffer are incubated with the nickel chelate coated acceptor beads in triplicate wells per peptide concentration on 384 well plate. Following a 30 minute incubation the streptavidin donor beads are added and the reaction further incubated for 1 hour prior to reading the plate. Statistical reliability of each experiment is assessed using a Z score and accepted if >0.45. The plate results are analysed via Prism software. The mean values of the alpha signal are shown, corrected for background signal and the error bars represent the SEM. Results show good binding by both co-activators with a marginally increased affinity of PGC1α for LRH-1 LBD over SRC2. The affinity of PGC1α (B) or SRC 2 (C) peptide with 20nM, 50nM and 100nM of his tagged LRH-1 LBD protein. Each co-activator peptide titration (ranging from 100μM to 1.6nM over 10 data points as before) is added in triplicate to 384 well plate to 20nM, 50nM and 100nM his tagged LRH-1 LBD respectively with nickel chelate acceptor beads to a total volume 20μl. Following a 30 minute incubation the streptavidin donor beads are added to a total volume of 25μl and the reaction further incubated for 1 hour prior to reading the plate. Statistical reliability of each experiment is assessed using a Z score and accepted if >0.45. Results show a titratable increase in binding with increased concentration of protein. Again, PGC1α has an increased signal with LRH-1 with an EC50 of 35nM versus 369nM at 50nM although more comparable at 100nM with EC50 27nM versus 28nM respectively.

3.4.2.2 Confirmation of the utility of the LRH-1/Coactivator Alpha Screen assay using compound 5A Whitby agonist compound 5A

To determine if the Alpha Screen assay set up can be used to screen for compounds that bind the LRH-1 LBD, we used compound 5A, (Whitby et al., 2006). The assay was performed in two ways, initially by keeping a set concentration of His-MBP-LRH-1-LBD and peptide (50nM:50nM) and adding increasing concentrations of compound 5A, or by keeping a set concentration of LRH-1 and titrating in a co-activator peptide in the presence or absence of a fixed concentration (5μM) of compound 5A. In the first assay, increasing 5A concentrations stimulated LRH-1/PGC1α interaction in a dose dependent manner, with an EC_{50}=221nM (Figure 3.50A). The second assay was performed using the SRC2 peptide. Addition of compound 5A resulted in a shift in the EC_{50} for the interaction of LRH-1 with SRC2, from 246nM to 92nM (Figure 3.50B) again demonstrating that compound 5A promotes the interaction of LRH-1 with co-activator peptides, consistent with its action as a LRH-1 agonist.

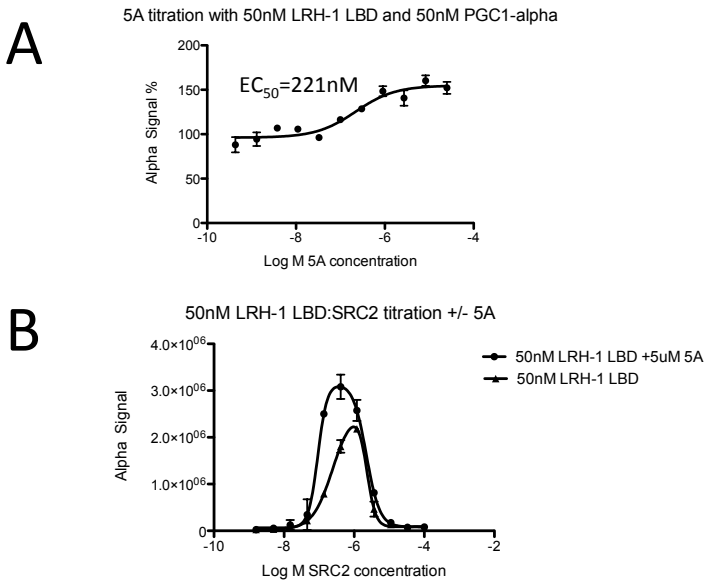


Figure 3.50 Optimisation and Validation: Increased binding with Whitby Compound 5A

(A) A final concentration of 50nM his tagged LRH-1 LBD protein, 50nM PGC1α co-activator peptide and a concentration titration of Whitby compound 5A is incubated with the nickel chelate coated acceptor beads in triplicate wells per peptide concentration on 384 well plate. Compound concentrations ranged from 25μM to 0.4nM. Following a 30 minute incubation the streptavidin donor beads were added and the reaction further incubated for 1 hour prior to reading the plate. Statistical reliability of each experiment was assessed using a Z score and accepted if >0.45. The plate results are analysed via Prism software. The mean values of the alpha signal are shown, corrected for background signal and the error bars represent the SEM. Results show agonism with 5A and an EC50 221nM. (B) The affinity of SRC 2 co-activator peptide with 50nM of his tagged LRH-1 LBD protein is assessed plus and minus 5uM compound 5A. SRC-2 peptide titration (ranging from 100μM to 1.6nM over 10 data points as before) was added in triplicate to 384 well plate to 50nM his tagged LRH-1 LBD respectively with nickel chelate acceptor beads and either compound 5A or DMSO control. Following a 30 minute incubation the streptavidin donor beads were added to a total volume of 25μl and the reaction further incubated for 1 hour prior to reading the plate. Statistical reliability of each experiment was assessed using a Z score and accepted if >0.45. The plate results were analysed via Prism software as above.

3.4.2.3 Sensitivity of the Alpha Screen to DMSO

To determine if DMSO, used to solubilise the compounds, interferes with the Alpha Screen LRH-1 LBD-Co-activator peptide interaction assay, the interaction of LRH-1 and PGC1α was tested with increasing concentrations of DMSO in the reaction. DMSO levels up to 10% (v/v) were tolerated with little or no effect on signal (Figure 3.51A). Some effect of DMSO concentration was observed for interaction between LRH-1 and SRC2, with inhibition of the alpha signal at DMSO concentrations ≥1.25% (v/v), although major inhibition by DMSO was only observed for 10% and 20% DMSO (Figure 3.51B). Since a concentration of 0.1% (v/v) DMSO was used in the reporter gene assays, and given that no interference with the in vitro assay was measurable at this concentration, all assays were performed with this concentration of DMSO.

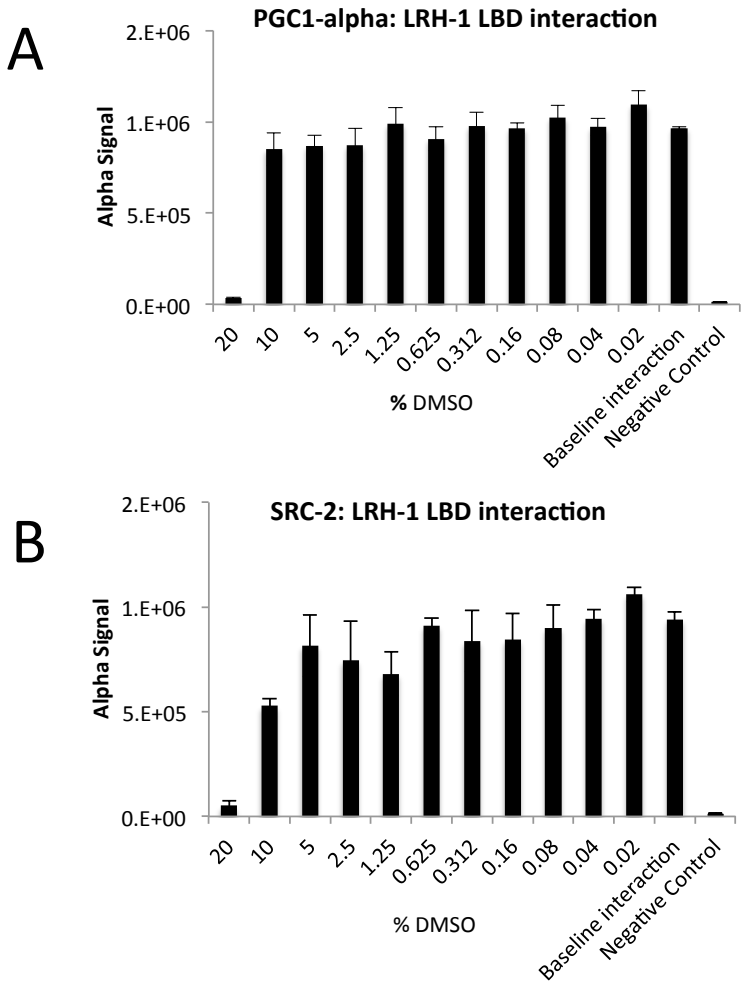


Figure 3.51 DMSO is tolerated to 5%-10% in Alpha screen assay

A final concentration of 50nM his tagged LRH-1 LBD protein, 50nM PGC1α or SRC2 co-activator peptides and a concentration titration of DMSO was incubated with the the nickel chelate coated acceptor beads in triplicate wells per peptide concentration on a 384 well plate. Final DMSO concentrations ranged from 20% to 0.02%. Following a 30 minute incubation the streptavidin donor beads were added and the reaction further incubated for 1 hour prior to reading the plate. Statistical reliability of each experiment was assessed using a Z score and accepted if >0.45. The mean values of the alpha signal are shown and the error bars represent the SEM. Results show DMSO is tolerated within the assay to 5-10% final concentration.

3.4.2.4 Alpha Screen Cascade

A total of 166 compounds were initially screened at 10μM and 65 at 1μM in the Alpha Screen assay, with 50nM LRH-1 LBD and 100nM PGC1α. A number of compounds appeared to be insoluble at 10μM, since they were cloudy and settled on being left on the bench. The results for these have therefore been shown in separate figures.

Shown in figure 3.52A and 3.52B are 110 compounds which solubilised easily. As with the cell based assay, most of the compounds from the Whitby Cresset screen look to either have very little or mild agonistic activity (alpha signal up to 150% of vehicle treated). 13 compounds showed a decrease in alpha signal equal to or greater than 50% and were assessed at 1μM. Of these 13 compounds there were 4 showing a decrease in alpha signal less than or equal to 75% and all were raloxifene and tamoxifen analogues (JR 705, JR 700, JR 560(2) and JR 469) (Figure 3.53).

Of the 56 compounds that did not solublise well at 10 μM (Figure 3.54), they were diluted 10-fold and assessed to allow their use at a final concentration of 1 μM. 8 compounds remained poorly soluble and were therefore not tested further (AB_WC 32, 84, 89, 93, 96, 98, 111 and TJC 104). At 1 μM 18 compounds showed a decrease in alpha screen signal of 75% or more including 3 AB_WC compounds (17, 39 and 103), only AB_DC 15a of the Dax Cressett screen and all of the 14 raloxifene and tamoxifen analogues (Figure 3.55). Interestingly, and acting as a further form of validation, the more recently published LRH-1 and SF-1 agonists, Whitby compounds 18A and 24 (Whitby et al., 2011) showed alpha signal activation up to 180% consistent with agonism.

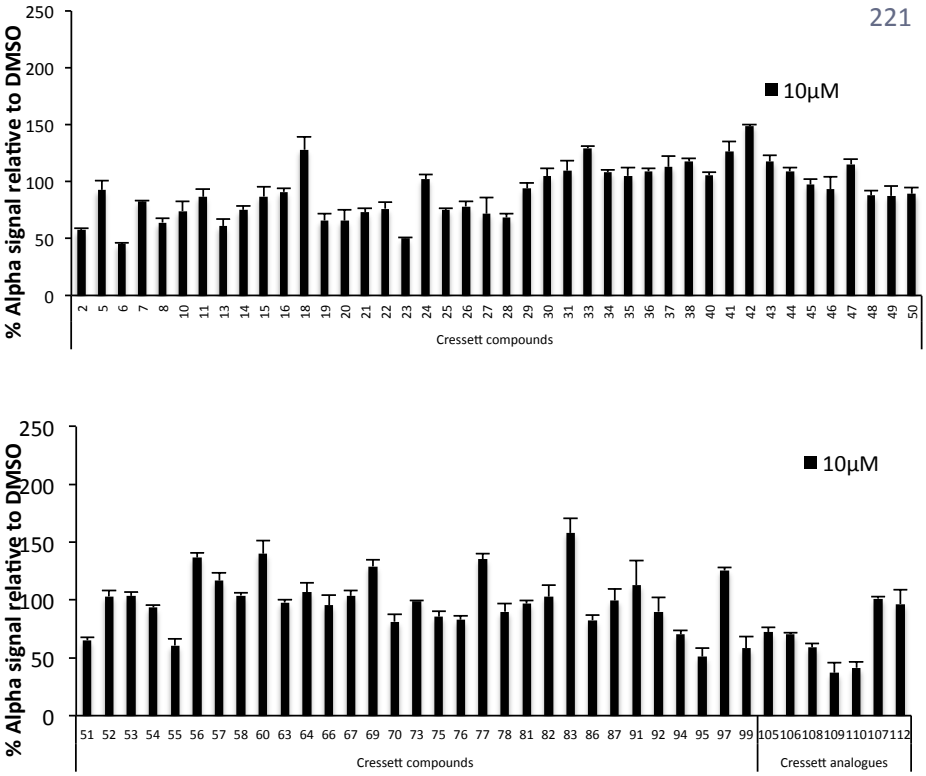


Figure 3.52A Alpha Screen assay for determining effects of soluble compounds (10μM) on interaction of the LRH-1 LBD with the PGC1α coactivator peptide

The Alpha Screen assay was performed in the presence of 10μM concentration of the compounds AB_WC001-AB_WC112. The interaction of LRH-1 LBD and coactivator peptide was determined as before. A final concentration of 50nM of His-LRH-1-LBD and 100nM biotinylated PGC1α peptide were incubated with the nickel chelate coated acceptor beads and 10μM of compounds in triplicate wells. The alpha signal is shown, correcting for background signal and expressed as a percentage relative to the DMSO control. The mean values of triplicate wells are shown and the error bars represent the SEM. Statistical reliability of each experiment is assessed using a Z score and accepted if >0.45.

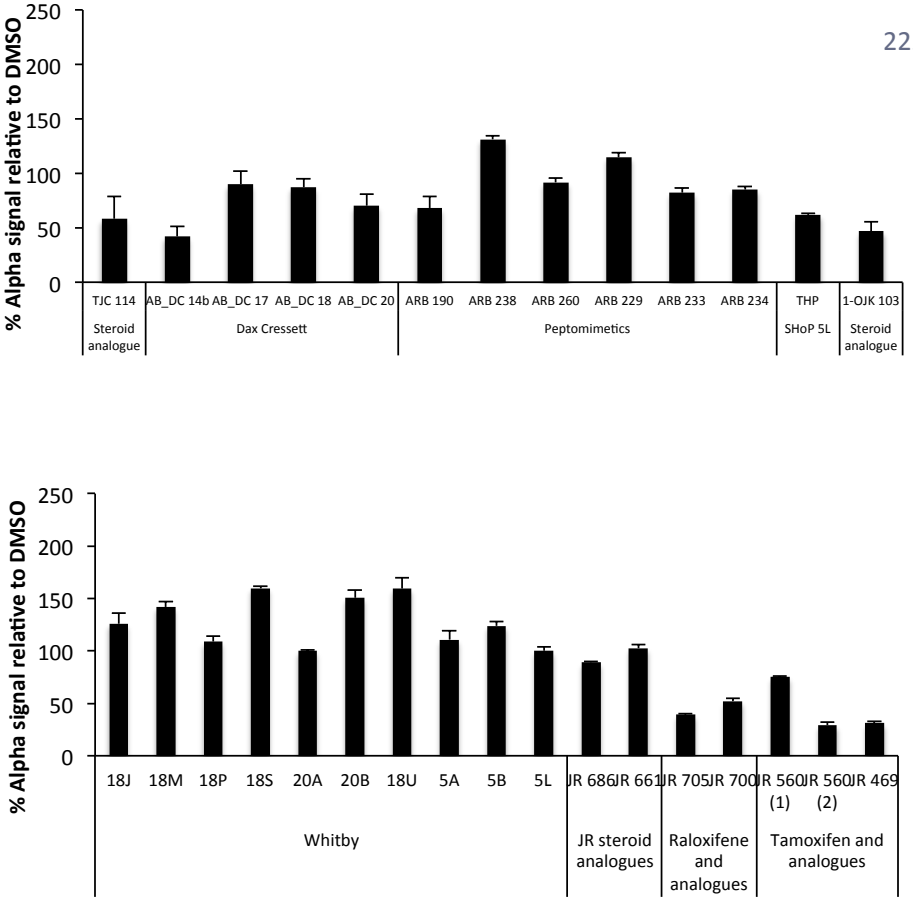


Figure 3.52B Alpha Screen assay for determining effects of soluble compounds (10μM) on interaction of LRH-1 LBD with PGC1α coactivator peptide

The Alpha Screen assay was performed in the presence of 10μM concentration of the compounds. The interaction of LRH-1 LBD and co-activator peptide was determined as before. A final concentration of 50nM of His-LRH-1-LBD and 100nM biotinylated PGC1α peptide were incubated with the nickel chelate coated acceptor beads and 10μM of compounds in triplicate wells. The alpha signal is shown, correcting for background signal and expressed as a percentage relative to the DMSO control. The mean values of triplicate wells are shown and the error bars represent the SEM. Statistical reliability of each experiment is assessed using a Z score and accepted if >0.45.

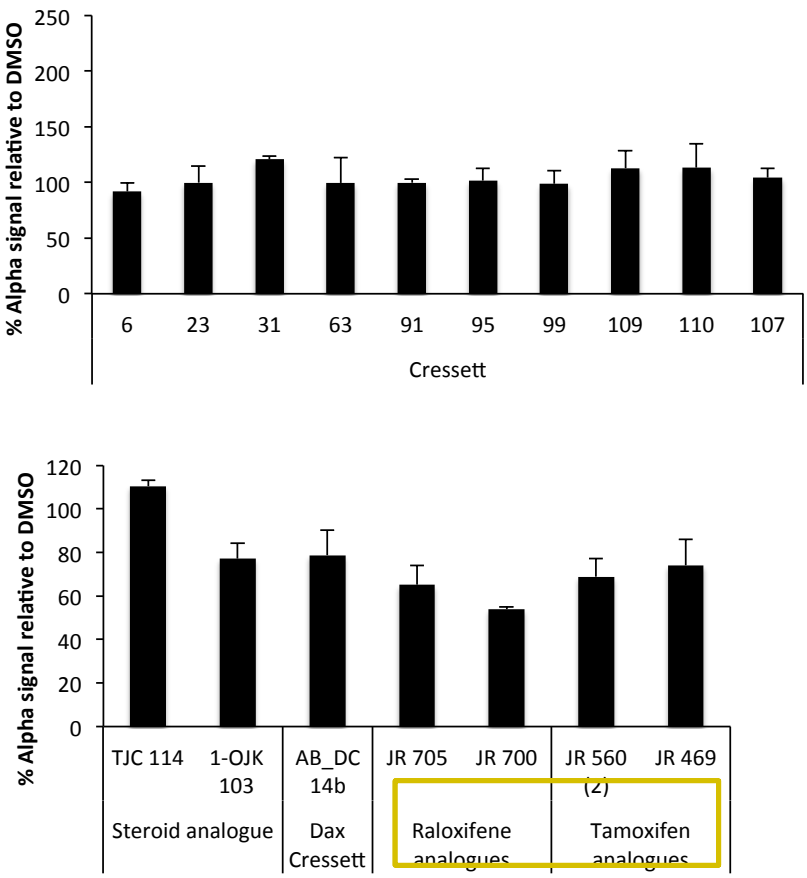


Figure 3.53 Alpha Screen assay for determining effects of soluble compounds (1μM) on interaction of LRH-1 LBD with PGC1α co-activator peptide

The Alpha Screen assay was performed in the presence of 1μM concentration of the compounds. The interaction of LRH-1 LBD and co-activator peptide was determined as before. 50nM of His-LRH-1-LBD and 100nM biotinylated PGC1α peptide were incubated with the nickel chelate coated acceptor beads and 1μM of compounds in triplicate wells. The alpha signal is shown, correcting for background signal and expressed as a percentage relative to the DMSO control. The mean values of triplicate wells are shown and the error bars represent the SEM. Statistical reliability of each experiment is assessed using a Z score and accepted if >0.45. Compounds with a percentage alpha signal of <75% are boxed.

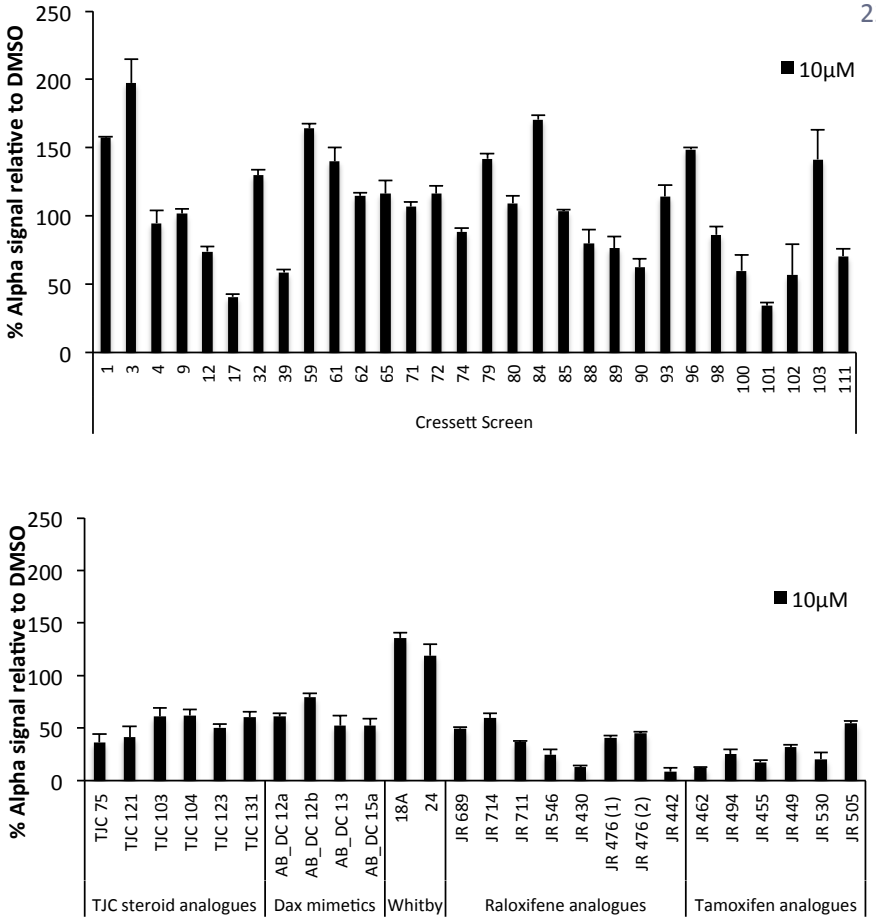


Figure 3.54 Alpha Screen assay for determining effects of poorly soluble compounds (10μM) on interaction of the LRH-1 LBD with the PGC1α co-activator peptide

The Alpha Screen assay was performed in the presence of 10μM concentration of the compounds. The interaction of LRH-1 LBD and coactivator peptide was determined as before. A final concentration of 50nM of His-LRH-1-LBD and 100nM biotinylated PGC1α peptide were incubated with the nickel chelate coated acceptor beads and 10μM of compounds in triplicate wells. The alpha signal is shown, correcting for background signal and expressed as a percentage relative to the DMSO control. The mean values of triplicate wells are shown and the error bars represent the SEM. Statistical reliability of each experiment is assessed using a Z score and accepted if >0.45.

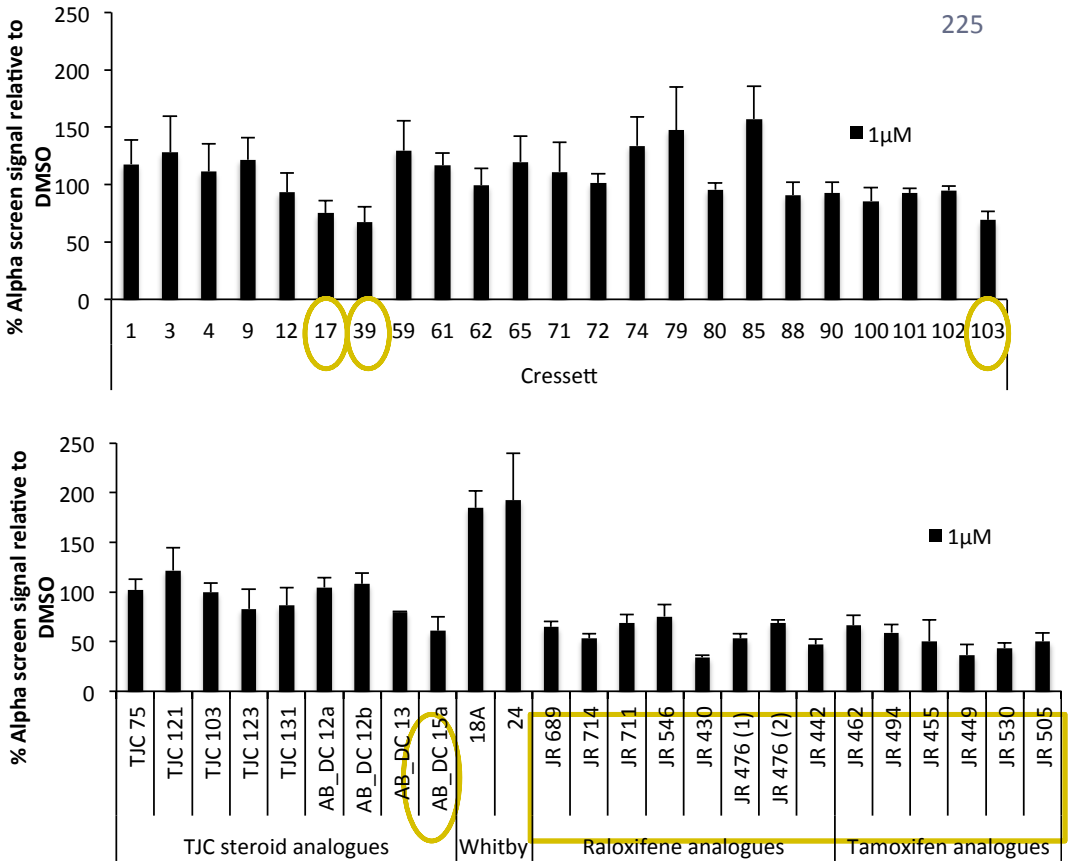
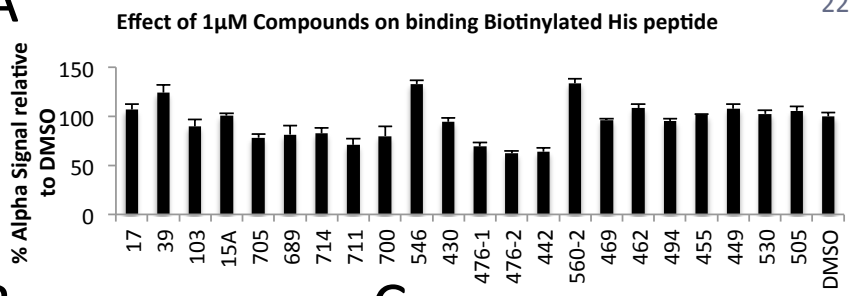


Figure 3.55 Alpha Screen assay for determining effects of poorly soluble compounds (1µM) on interaction of LRH-1 LBD with PGC1α co-activator peptide

The Alpha Screen assay was performed in the presence of 1µM concentration of the compounds. The interaction of LRH-1 LBD and co-activator peptide was determined as before. 50nM of His-LRH-1-LBD and 100nM biotinylated PGC1α peptide were incubated with the nickel chelate coated acceptor beads and 1µM of compounds in triplicate wells. The alpha signal is shown, correcting for background signal and expressed as a percentage relative to the DMSO control. The mean values of triplicate wells are shown and the error bars represent the SEM. Statistical reliability of each experiment is assessed using a Z score and accepted if >0.45. Compounds with a percentage alpha signal of <75% are circled or boxed.

From the above analyses, 22 compounds in total decreased the LRH-1/coactivator interaction. To determine the specificity of this interference with interaction, these compounds were incubated with a biotinylated hexa-His peptide. The biotinylated hexa-his peptide should be sufficient to bring together the acceptor and donor beads, so any compound that interferes with the transfer of oxygen and/or can itself be excited at 680 nm to emit at 520-560 nm, can be identified. Eight of the tested compounds inhibited the alpha signal using the biotinylated hex-his peptide, suggesting that they interfere with the assay (Figure 3.56). Compounds that did not significantly inhibit the alpha signal in this assay were re-assayed for their activities in the LRH-1 LBD/coactivator peptide assay, across a range of concentrations to generate IC_{50} values. A summary of this screening cascade sequence is shown in Figure 3.57.

A



B

Compound	Mean (%)	SEM
AB_WC 17	107	6
AB_WC 39	124	8
AB_WC 103	90	7
15A	101	3
JR 705	78	3
JR 689	81	9
JR 714	83	5
JR 711	71	6
JR 700	80	10
JR 546	133	4
JR 430	94	4
JR 476-1	69	4
JR 476-2	62	3
JR 442	64	4
JR 560-2	134	5
JR 469	96	1
JR 462	108	4
JR 494	95	2
JR 455	101	1
JR 449	108	5
JR 530	103	4
JR 505	106	4
DMSO	100	4

C

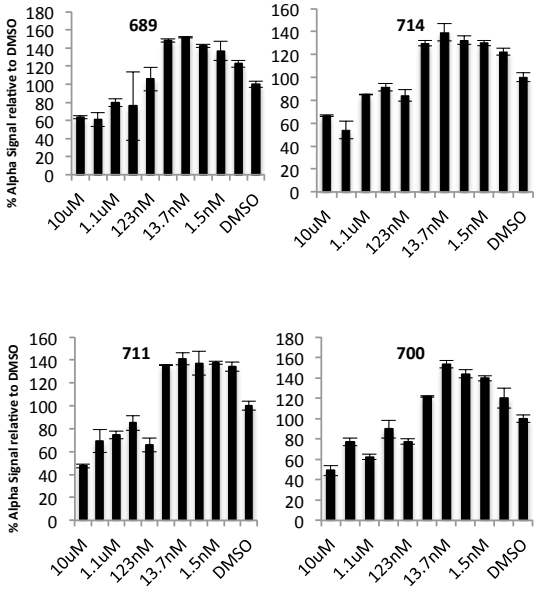


Figure 3.56 Alpha Screen assay for determining non specific binding inhibition: effects of the 22 compounds previously shown to decrease the LRH-1/co-activator peptide interaction

The Alpha Screen assay was performed in the presence of 1µM concentration of the compounds. 50nM of the biotinylated-his (BH) peptide were incubated with the nickel chelate coated acceptor beads and 1µM of compounds in triplicate wells. Following a 30 minute incubation the streptavidin donor beads were added and the reaction further incubated for 1 hour. The alpha signal is shown, correcting for background signal and expressed as a percentage relative to the DMSO control. The mean values of triplicate wells are shown and the error bars represent the SEM. Statistical reliability of each experiment is assessed using a Z score and accepted if >0.45. Shown in the bar chart in (A) and in the table (B) are the mean Alpha signals. Compounds with 85% Alpha signal or lower, were considered to have non specific binding effects. (C) 4 compounds were further assessed and rejected with dose titrations against BH.

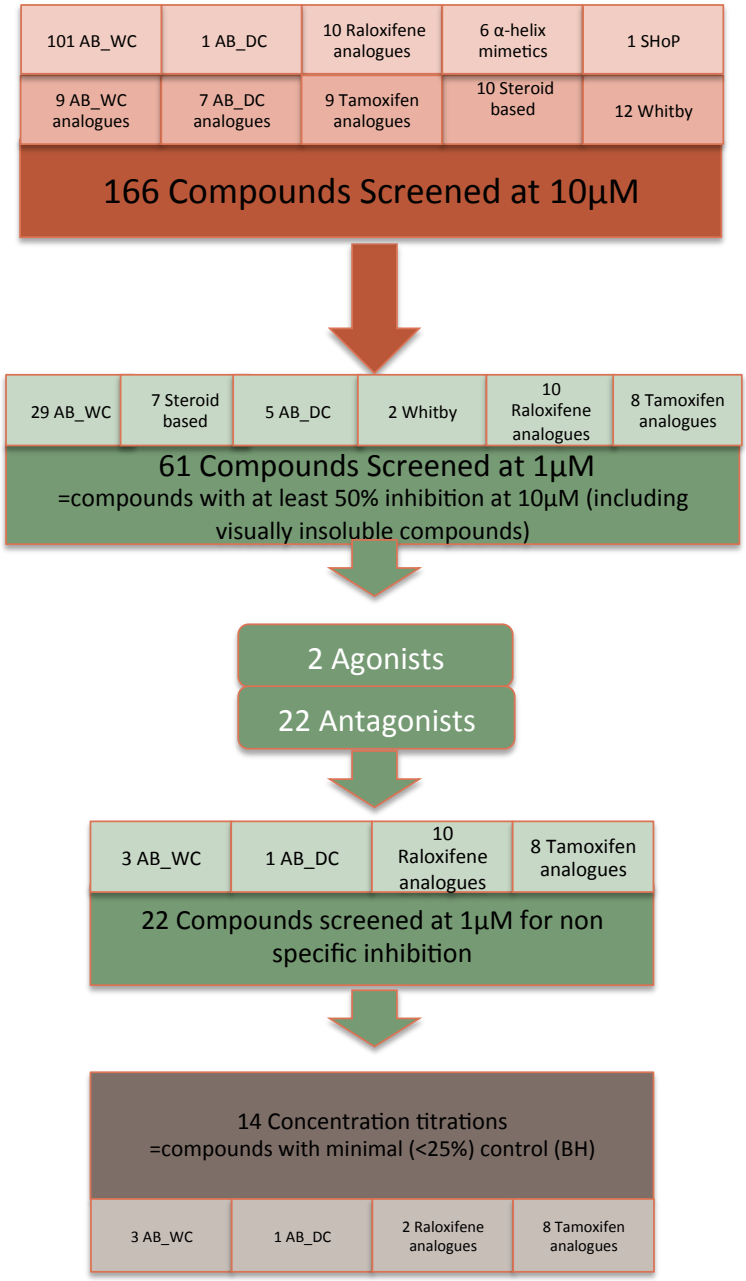


Figure 3.57 Screening cascade for in vitro Alpha Screen

A 12-point titration curve was performed for each of the 14 compounds that inhibited the LRH-1/coactivator interaction and did not interfere with the biotinylated hexa-his peptide assay. For the majority of the compounds, the IC_{50} of non-specific inhibition of alpha signal was similar to or lower than the IC_{50} for specific inhibition with LRH/Co-activator (data not shown).

Compounds JR 430 and JR 449 showed the most promising activity (Figures 3.58 and 3.59 respectively). JR430 had an IC_{50} = 3.1µM (95% CI 2.6-3.7µM) in the LRH-1 LBD/CoA Alpha screen, with an IC_{50} =7.8 µM (95% CI 7.5-8.2µM) in the biotinylated hexa-his peptide assay. Interestingly this compound also activated LRH-1 in the LRH-1 reporter gene assay. Compound JR 449 gave an IC_{50} =6.8µM (95% CI 6-7.7µM) and an IC_{50} =10.1µM in the BH peptide assay (95%CI 10-10.1µM), but did not modulate LRH-1 activity in the reporter gene assay. However, the small differences in IC_{50} values between the two assays, is of concern for taking these findings forward for further compound design.

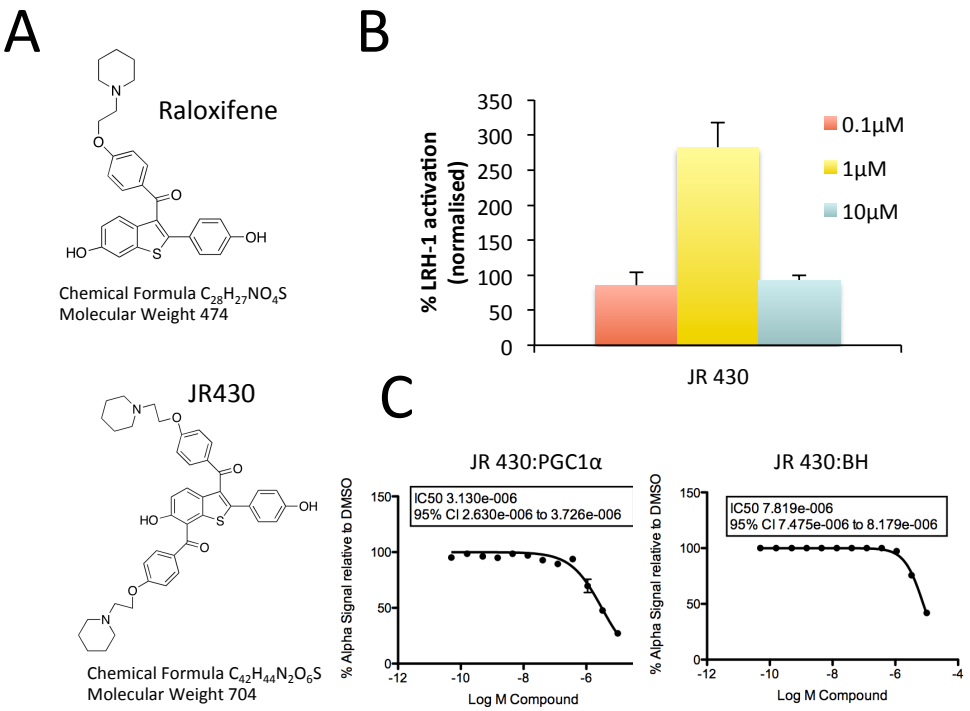


Figure 3.58 JR 430 has weak antagonism to LRH-1 and shows agonism of transcriptional activity

(A) The structure of compound Raloxifene with experimental compound JR 430. (B) Cos-1 cells were transfected with LRH-1 and the LRH-1-luc and renilla-luc reporter genes. Compounds were added 5 hours following transfection (JR430 0.1µM-10µM, Raloxifene 0.1-1µM) and luciferase activities were determined after a further 24 hours. Shown is the bar chart of mean LRH-1 luc reporter activities following normalisation against renilla-luc. Reporter activity for the DMSO (vehicle) control was taken as 100% and all other activities relative to this. Error bars show SEM. (C) The Alpha Screen analysis of the effect of compound JR 430 on the interaction with his tagged LRH-1 LBD protein with biotinylated co-activator PGC1α peptide or non specific biotinylated his (BH) peptide. 100nM of both protein and peptide or 50nM BH is incubated with the nickel chelate coated acceptor beads and a titration of compound concentrations in triplicate wells. The concentrations range from 10µM to 0.5nM over 10 data points. The mean values of triplicate wells are shown and the error bars represent the SEM. Statistical reliability of each experiment is assessed using a Z score and accepted if >0.8.

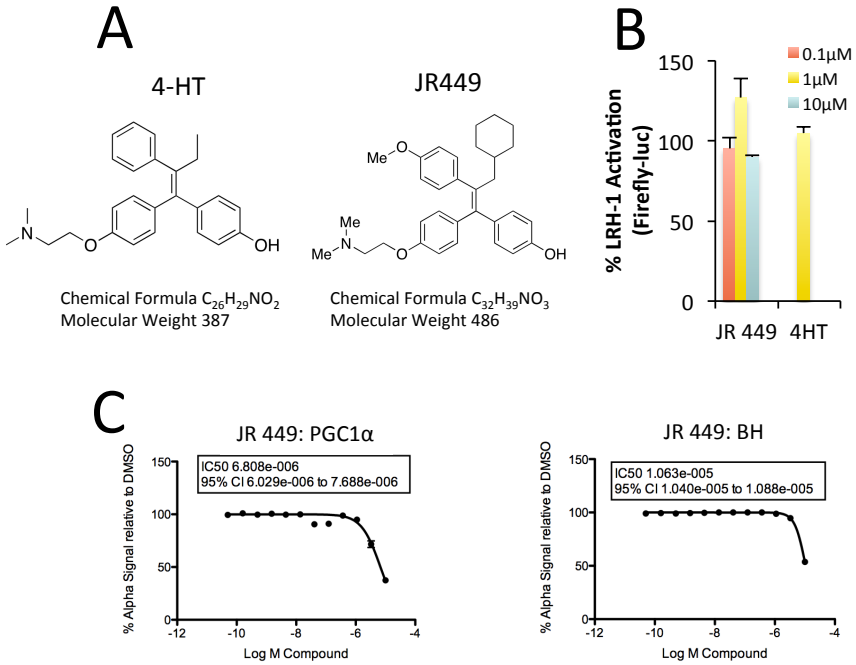


Figure 3.59 JR 449 shows weak/ no antagonism of LRH-1

(A) The structure of parent compound 4-hydroxytamoxifen with experimental compound JR 449.

(B) Cos-1 cells were transfected with LRH-1 and the LRH-1-luc and renilla-luc reporter genes. Compounds were added 5 hours following transfection (JR449 0.1µM-10µM, Tamoxifen control 1µM) and luciferase activities were determined after a further 24 hours. Shown is the bar chart of mean LRH-1 firefly-luc reporter. Reporter activity for the DMSO (vehicle) control was taken as 100% and all other activities relative to this. Error bars show SEM. Results show no effect on transcriptional activity of LRH-1. (C) The Alpha Screen analysis of the effect of compound JR 449 on the interaction with his tagged LRH-1 LBD protein with biotinylated co-activator PGC1α peptide or non specific biotinylated his (BH) peptide. 100nM of both protein and peptide or 50nM BH is incubated with the nickel chelate coated acceptor beads and a titration of compound concentrations in triplicate wells. The concentrations range from 10µM to 0.5nM over 10 data points. The mean values of triplicate wells are shown and the error bars represent the SEM. Statistical reliability of each experiment is assessed using a Z score and accepted if >0.8.

3.4.2.5 Subsequent Screening in the in vitro assay

Subsequent compounds, to those described and discussed above, were screened using the same cascade, with an adjustment in the protein concentration ratios to allow visualization of an antagonist more easily (100nM:100nM LRH). These have been kept as separate results as the strength of the baseline alpha screen values using this interaction ratio would make it difficult to see any increase in the LBD/CoActivator interaction.

A further 48 compounds were screened at 10 μM (Figure 3.60). These compounds consisted of 30 analogues of the SHoP scaffold THP, 3 analogues of AB_WC 057, 4 analogues of AB_DC 12, 3 further compounds from steroid series, 6 raloxifene analogues with different side chains to improve solubility and 1 further tamoxifen analogue. Of these, 3 raloxifene analogues, the tamoxifen analogue JR 566 and THP 10 were taken forward to 1 μM. At these concentrations, none of the compounds showed any decrease in the LBD/CoA interaction below 85% (Figure 3.61A), which was higher than that for non-specific inhibition (80 to 95%) using the BH (Figure 3.61B).

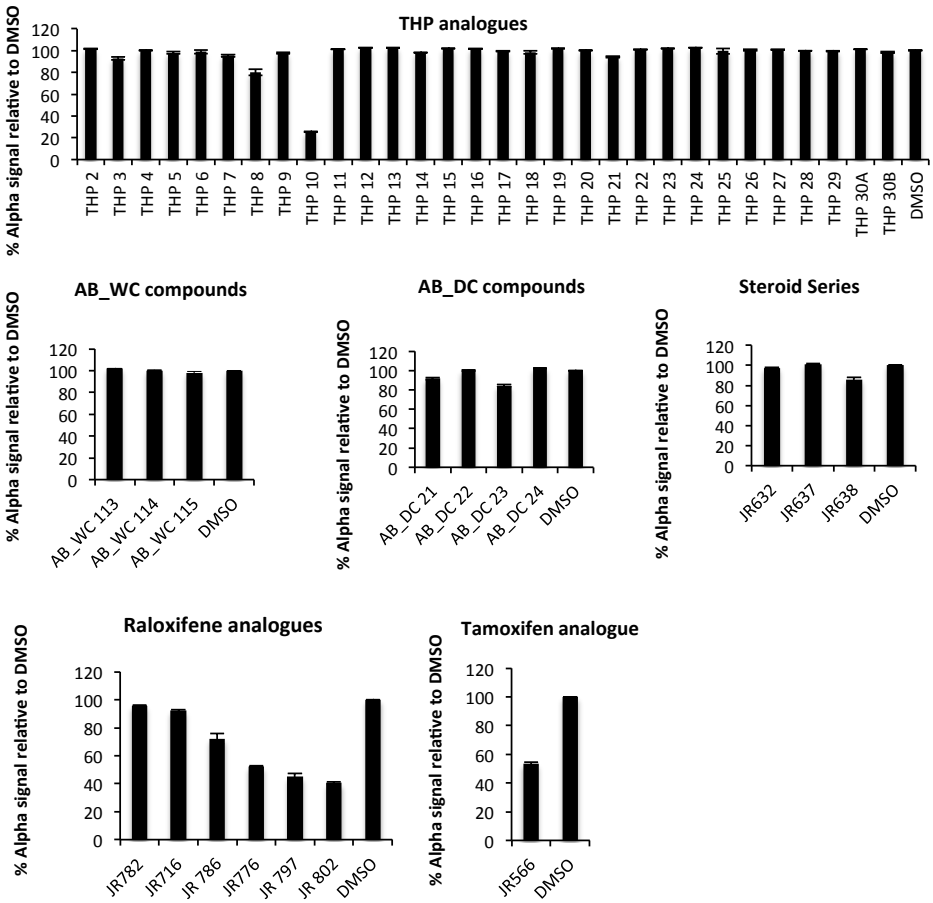


Figure 3.60 Alpha Screen assay for determining the effects of compounds on interaction of the LRH-1 LBD with the PGC1α co-activator peptide

The Alpha Screen assay was performed in the presence of 10μM concentration of the compounds. The interaction of LRH-1 LBD and co-activator peptide was determined as before. 100nM of His-LRH-1-LBD and 100nM biotinylated PGC1α peptide were incubated with the nickel chelate coated acceptor beads and 10μM of compounds in triplicate wells. The alpha signal is shown, correcting for background signal and expressed as a percentage relative to DMSO control. The mean values of triplicate wells are shown and the error bars represent the SEM. Statistical reliability of each experiment is assessed using a Z score and accepted if >0.80.

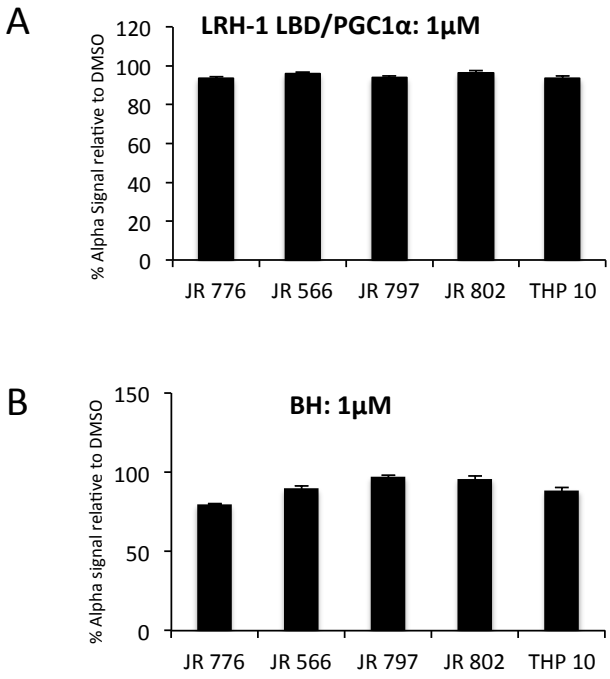


Figure 3.61 Alpha Screen assay for determining the effects of compounds on interaction of the LRH-1 LBD with the PGC1α co-activator peptide

The Alpha Screen assay was performed in the presence of 1μM concentration of the compounds. (A) The interaction of LRH-1 LBD and co-activator peptide was determined as before. 100nM of His-LRH-1-LBD and 100nM biotinylated PGC1α peptide were incubated with the nickel chelate coated acceptor beads and 1μM of compounds in triplicate wells. The alpha signal is shown, correcting for background signal and expressed as a percentage relative to DMSO control. The mean values of triplicate wells are shown and the error bars represent the SEM. Statistical reliability of each experiment is assessed using a Z score and accepted if >0.80. (B) 50nM biotinylated his (BH) is incubated with the nickel chelate coated acceptor beads and 1μM of compounds in triplicate wells. The alpha signal is shown, correcting for background signal and expressed as a percentage relative to DMSO control. The mean values of triplicate wells are shown and the error bars represent the SEM. Statistical reliability of each experiment is assessed using a Z score and accepted if >0.8

4. Discussion

4.1 Models of Endocrine Resistance, MLET5 cells

4.1.1 Gene expression analysis in MCF7 derived models of endocrine-resistant breast cancer

Gene expression microarray analysis showed that the overall number of estrogen regulated genes was lower in MLET5 than in MCF7 cells. Increased expression of ERα, PgR and GREB1 mRNA levels was evident in the absence of estrogen, reflecting the estrogen independence of MLET5 cell growth. A number of the genes that are estrogen-regulated in MCF7 cells showed altered expression in MLET5 cells, consistent with gain of estrogen-independent expression. Examples include CD36 (mildly estrogen repressed), TM4SF1 (estrogen repressed), IGFL1 (estrogen repressed) and Calb2 (estrogen stimulated) and these were the top four ranking differentially regulated genes. It would be interesting to look further at these genes as per the data discussed in section 3.1.3 which suggests they could be useful as part of a genetic signature of endocrine resistance, or novel therapeutic targets in breast cancer (TM4SF1). Estrogen independence in the expression of ERα target genes has been described for long-term estrogen-deprived (LTED) MCF7 cells, developed by Dr L-A Martin and Prof M Dowsett (Chan et al., 2002). LTED cells were generated by continuous culturing and passaging of MCF7 cells in estrogen-free media. The LTED cells go through three stages: initially no growth (quiescence) for 15 weeks, followed by growth in keeping with increasing estrogen sensitivity (hypersensitivity), then growth independent of estrogen at 50 weeks (independence). ERα expression is elevated in the estrogen hypersensitive and independent stages, as is also observed in MLET5 cells. Note that MLET5 cells are clonal, whereas the LTED phenotype is reflective of the culture and may therefore represent a mixed cell population. In LTED cells, no significant changes were seen in cofactor protein levels (SMRT, TIF-1, RIP140), but elevated ERK1/ERK2 activity led to increased ERBB2 expression and the LTED cells were sensitive to the tyrosine

kinase inhibitor ZD1839 and the MEK inhibitor U0126 (Martin et al., 2003; Martin et al., 2005). LTED cells have increased sensitivity to growth suppression by ICI 182,780 (Martin et al., 2005), indicative of a requirement for ERα. By contrast, MLET5 cells grow in the presence of tamoxifen or ICI 182,780, although their growth is slowed compared with culturing in the presence of estrogen or in the absence of ligand, implying some estrogen dependence. LTED cells generated in the Santen lab also showed emergence of increase in sensitivity to low levels of estrogen (Song et al., 2002), however, in this model there was no change in the transcription of ERα target gene regulation, although there was an increase in activation of the MAPK/mTOR/PI3K pathways (Santen et al., 2008; Song et al., 2002; Yue et al., 2003). In MLET5 cells, other work from our laboratory did not provide evidence for changes in EGFR or HER2. However, there was an increase in P-AKT activity and MLET5 cells were 5 times more sensitive than MCF7 to the PI3K inhibitor, LY294002 (Tolhurst et al., 2010). The activation of AKT by growth factors occurs in a PI3K dependant way (Franke et al., 1995). Once activated AKT then activates ERα by phosphorylation at Ser-167 or regulates apoptosis pathways. Kirkegaard *et al* have reported that the AKT/mTOR/PI3K pathway is associated with a greater risk of relapse and death in patients with ERα breast cancer treated with tamoxifen (Kirkegaard et al., 2005). A recent study looked at ERα positive primary breast cancer samples and subsequent metastatic samples. It assessed the expression of downstream activated proteins in the AKT/mTOR/PI3K pathway (p-mTOR, p-4EBP and p-p70S6K) by immunohistochemistry and showed a 45% increase in p-mTOR in metastatic samples compared with primary tumour in patients previously treated with endocrine therapy (n=34) versus patients who did not receive adjuvant endocrine treatment (n=37). A multivariate analysis confirmed a significant increase in all three proteins in patients previously treated with adjuvant endocrine therapy (Beelen et al., 2014). Preclinical studies using low dose everolimus (RAD-001), an mTOR inhibitor, and letrozole or fulvestrant reversed AKT-mediated endocrine resistance (Beeram et al., 2007).

In a clinical setting there have been a number of completed trials looking at the combination of an mTOR inhibitor with endocrine therapy with some conflicting results, suggesting that patient selection remains key. HORIZON was a negative phase III trial evaluating temsirolimus and letrozole in a first line metastatic setting, in patients who had not previously received an aromatase inhibitor (patients could have received an aromatase inhibitor adjuvantly if it was greater than twelve months prior). Hence this trial had very low numbers of patients who had received adjuvant endocrine treatment (43% in the combination arm and 40% in letrozole only arm) (Baselga et al., 2012; Wolff et al., 2013), which may explain the lack of improvement in PFS. Conversely BOLERO-2, a positive phase III trial, looked at everolimus and exemestane in metastatic, ERα positive patients who had relapsed following treatment with a non-steroidal aromatase inhibitor. This trial showed a significant improvement in PFS (10.6 months versus 4.1 months) and a recent updated analysis confirmed an ongoing improvement in PFS although the overall survival data are not yet ready (Baselga et al., 2012). Similarly TAMRAD, a phase II clinical trial in patients with metastatic breast cancer who had previously been treated with an aromatase inhibitor, looked at everolimus and tamoxifen, showing an improved clinical benefit rate (61 versus 42%) and a 55% decreased risk of death in combination treatment. In this trial, an unplanned analysis suggested patients with acquired resistance (>6 month response to an aromatase inhibitor in the metastatic setting or greater than 6 months following completion of adjuvant treatment with an aromatase inhibitor) to endocrine therapy obtained a greater benefit (Bachelot et al., 2012). In contrast to HORIZON, both BOLERO-2 and TAMRAD are assumed to have a greater proportion of patients with endocrine resistance based on the outcomes in the control groups (lack of response in the first line setting to endocrine therapy and PFS <6 months)(Paplomata and O'Regan, 2014).

PI3K inhibitors are under evaluation in clinical trials, for example PX-866, which demonstrates good tolerability and stable disease in phase I studies alone (Hong et al., 2012) and also in combination with docetaxel (Bowles et al., 2013). Similar

results have been seen with BGT226 a dual PI3K and mTOR inhibitor (Markman et al., 2012). There are various ongoing phase I studies looking at the combination of a pan PI3K inhibitor and a dual PI3K and mTOR inhibitor with letrozole and a selective class 1 PI3K inhibitor with Fulvestrant (GDC-0942).

BKM120 is a pan PI3K inhibitor which is well tolerated on its own (Bendell et al., 2012; Maira et al., 2012) and in combination with trastuzumab (Saura et al., 2014). This drug is currently undergoing assessment within BELLE-2, BELLE-3 and BELLE-4 clinical trials. BELLE-2 addresses the role of BKM120 with Fulvestrant after progression with an AI in patients with HER2 negative breast cancer. BELLE-3 addresses the role of BKM120 in patients with HER2 negative breast cancer who have had prior treatment with an mTOR inhibitor and BELLE-4 addresses the use of BKM120 in combination with paclitaxel.

Appropriate patient selection remains a key question and selecting patients who are less likely to respond to AKT/PI3K/mTOR inhibitors by analysis for PI3K mutations has been proposed (Vasudevan et al., 2009), but this still requires clinical validation.

4.1.2 Pro-survival pathways are upregulated in MLET5 cells

One of the most significantly altered cellular pathways identified from comparison of the MCF7 and MLET5 microarray datasets was apoptosis. Examination of the differentially regulated genes in this pathway showed that expression of pro-apoptotic genes (including BIK) was reduced and expression of anti-apoptotic genes, in particular BCL2, was increased in MLET5 cells. Real-time RT-PCR and Western blotting confirmed these findings, and MLET5 cells were shown to be resistant to the apoptosis inducing agent, etoposide. Interestingly, many of the differentially regulated apoptosis associated genes demonstrate estrogen-regulation in MCF-7 cells, where estrogen treatment represses expression of pro-apoptotic genes, whilst stimulating expression of anti-apoptotic genes. The best studied of these genes is BCL2, estrogen stimulation of which is well known (Su et al., 2014; Teixeira et al., 1995). Interestingly, BCL2 expression was also elevated in LTED cells,

whilst expression of BIK and BID was reduced in LTED cells, as it is in MLET5 cells. These results indicate that escape from the growth arrest engendered by estrogen withdrawal requires activation of pro-survival pathways and highlights survival pathways as potential therapeutic targets in the treatment of endocrine resistant breast cancer. Methods that have been investigated as means of targeting BCl2 include the development of antisense BCL2 and BH3 mimetics i.e. small molecules that mimic the actions of pro-apoptotic BH3-only proteins (Souers et al., 2013). Anti sense BCL2 increased the sensitivity of MCF7 cells to doxorubicin (Teixeira et al., 1995). Two BH3 mimetics, ABT-737 and the platelet sparing ABT-199 and tamoxifen were tested alone and in combination in four patient derived xenograft models, three ER-positive and one ER-negative. Of the ER-positive xenografts, two showed a partial response and one an almost complete response, but there was no response in the ER-negative xenograft. The effect of the combination of BH3 mimetic and tamoxifen was greater than tamoxifen alone, measured by reduction in tumour volume and survival. Following on from this, pAKT expression was measured and found to be much higher in the two partial response xenografts, as might be predicted as AKT modulates the expression of phophorylated BAD and suppreses its pro-apoptotic function (Vaillant et al., 2013). This causative finding was then confirmed by the dual treatment with ABT-737 and a dual PI3K/mTOR inhibitor resulting in a superior response to both single and dual therapies (Vaillant et al., 2013). BCL2 as a potential therapeutic target has recently moved into phase 1 clincal trials with BH3 mimetic ABT-199 in patients with NHL and CLL (Vaillant et al., 2013).

This indicates that treatment of endocrine resistant disease is likely to involve the targeting of several pathways to gain control of growth and prevent alternative growth (escape) pathways being activated. MLET5 cells, featuring AKT upregulation and upregulation of BCL2, may provide an important model cell line for investigating the action of drugs targeting PI3K and apoptosis pathways.

4.1.3 Future Directions

The studies described in this thesis provide evidence for the importance of the PI3K/AKT and BCL2 family in endocrine resistance and potential therapeutic approaches targeting these pathways. As described above, there is much evidence linking these pathways to ERα-positive breast cancer progression and resistance to endocrine therapies. A number of other genes whose expression is greatly changed in MLET5 cells may have potential as biomarkers and/or therapeutic targets, as discussed in section 3.1.3. Whilst I extended some of our findings to MCF-7 LTED cells from the Martin and Dowsett laboratory, it is important also to extend to further MCF7 derived models of endocrine resistance, including lines generated following culturing in the presence of anti-estrogens (Brunner et al., 1997; Lykkesfeldt et al., 1994). It is clearly also important to extend beyond MCF7 cells to resistance models generated from other ERα-positive breast cancer cell lines, e.g. T47D, ZR-75-1. Finally, recent advances allow indefinite maintenance of patient biopsies, usually by passaging in mice, the so-called patient derived xenografts (PDX). PDX from endocrine resistant breast cancer have been generated and characterised (Li et al., 2013). PDX could provide important new models for determining the importance of the genes and pathways identified here. Finally, immunohistochemical staining of large tissue microarrays (TMAs) (Abd El-Rehim et al., 2005) would provide further opportunities for validation of the differentially regulated genes identified here, should appropriate antibodies be available.

As mentioned above, MLET5 cells are characterised by ligand-independent regulation of many ERα target genes. MLET5 cells therefore provide an important resource for investigating changes in ERα activity that may be involved in development of endocrine resistance. Unlike many other LTED models, MLET5 cells are clonal and thus provide a valuable model for studying ERα interaction with transcriptional co-regulators and ERα recruitment to gene regulatory regions globally, for example with ChIP-seq using antibodies for ERα. The potential significance of such studies for understanding ERα action in breast cancer cells is highlighted by the finding that the key ERα coactivator AIB1 is frequently amplified

and/or over-expressed in breast cancer cells, whilst the related co-activator SRC-1 has been linked to the agonist activity of tamoxifen (Anzick et al., 1997; Burandt et al., 2013; Harigopal et al., 2009; Torres-Arzayus et al., 2004; Torres-Arzayus et al., 2010; Zwart et al., 2011). The co-repressors NCoR and SMRT are frequently down-regulated in breast cancer (Ciriello et al., 2013; Smith et al., 2012) and mutations in NCoR (NCoR1) have been identified in breast cancer (Stephens et al., 2012). These changes are likely to impact on regulation of gene expression by ERα, so understanding the molecular mechanisms by which ERα activity might be altered in endocrine resistance is important for understanding breast cancer progression.

4.2 Evaluation of LRH-1 target gene expression in breast cancer cells

Studies comparing MCF7 and MLET5 are helping to identify potential biomarkers and therapeutic targets. One of the ERα target genes thus identified is the nuclear receptor LRH-1. LRH-1 is potentially of great interest given its role in regulating aromatase expression in breast cancer associated stroma (Clyne et al., 2004; Clyne et al., 2002). Our previous studies demonstrated that LRH-1 is a direct ERα target gene, with ERα binding to a region 10kb upstream of the LRH-1 gene promoter (Thiruchelvam et al., 2011). LRH-1 was down regulated in MCF7 cells using a pool of four small interfering RNAs. This resulted in an inhibition of MCF-7 growth, confirmed in LRH-1 positive ZR-75-1 and T47D cell lines. Growth effects of LRH-1 were then confirmed using the, previously described, published synthetic LRH-1 activating compounds 5A, 5L and 5B with stimulation of growth effects in LRH-1 positive cell lines and again no effect in LRH-1 negative (specifically BT474 which is ERα positive but LRH-1 negative). These compounds stimulated the activity of an LRH-1 responsive reporter gene and in MCF7 cells, stimulated the expression of ERα.

This work confirmed the importance of LRH-1 for growth in breast cancer cells and its role in regulating ERα expression by direct recruitment to the ERα gene promoter. These studies further highlight LRH-1 as a potentially significant new therapeutic target and prompted us to perform gene expression microarray

analysis, in order to identify LRH-1 target genes in breast cancer, with a view to elucidating the potential mechanisms of LRH-1 function in breast cancer cells. As there were no suitable LRH-1 agonists and/or antagonists, LRH-1 target gene identification was undertaken following siRNA-mediated LRH-1 knockdown. As some siRNAs have off-target effects, we used two independent siRNA in the gene expression microarray analysis. Note that the synthetic LRH-1 agonists, whilst stimulating LRH-1 activity, only increase its activity marginally, thus bringing into question the possibility of obtaining robust microarray data, so the siRNA approach was followed.

Evidence for the importance of LRH-1 in the estrogen driven development and progression of breast cancer is seen in the analysis of LRH-1 siRNA microarray with 37% of the genes whose expression was up- or down-regulated following LRH-1 siRNA treatment, being known ERα target genes. Pathway enrichment analysis confirmed these findings and 'Response to estrogen' pathway was the top hit, with well-recognised estrogen regulated genes included in this list (GATA3, BCL2, SOCS2, CYP1A1 and CYP1B1) and importantly ERα. The regulation of ERα and ERα target genes by LRH-1 has been published both by this laboratory and others (Chand et al., 2012; Lai et al., 2013; Thiruchelvam et al., 2011). As mentioned in section 3.2.1 the cooperativity between LRH-1, ERα and GATA3 may provide a further mechanism whereby other genes important in breast cancer are regulated.

MCF7 cell do not express aromatase and therefore direct delineation of the role of LRH-1 in the regulation of aromatase (CYP19) is not advanced by this experiment. However as previously mentioned, CYP1A1 and CYP1B1 are both involved in the catabolism of estrogens, therefore LRH-1 inhibition of these genes might increase estrogen levels and strengthen the evidence for the role of LRH-1 in increasing estrogen bioavailability. Remarkably, expression of GPER, an estrogen binding protein that mediates the non-genomic effects of estrogen, was reduced upon LRH-1 knockdown. This finding adds yet another facet to the regulation of estrogen signalling in breast cancer cells by LRH-1. By upregulating GPER, LRH-1 may

promote the non-genomic actions of estrogen, in addition to regulating estrogen biosynthesis and ERα expression. A further surprise finding regarding LRH-1 function in breast cancer cells is that obtained in our laboratory recently using ChIP-seq for LRH-1 (Lai et al., 2013). Global identification of LRH-1 binding regions in MCF7 cells using ChIP-seq for LRH-1 demonstrated that a large proportion of LRH-1 binding sites are coincident with ERα binding regions. Importantly, LRH-1 promotes the recruitment of ERα to coincident binding sites.

Together, these findings demonstrate a central role for LRH-1 in estrogen signaling in breast cancer cells, which together with its other defined role in local estrogen biosynthesis, makes LRH-1 an important new therapeutic target in breast cancer.

4.3 Development of Small Molecule Inhibitors of LRH-1

As described in section 1.3.5 the first synthetic LRH-1 ligands, published by Professor Whitby's group, were agonists based on a cis-bicyclo(3.3.0)oct-2-ene skeleton (Whitby et al., 2006). A second series, by the same group, has been published, with improved stability and specificity but less potency (Whitby et al., 2011). The discovery by Professor Ortlund's group, during crystallographic examination, that phospholipids are present in the LRH-1 LBD has led to the discovery that medium chain phosphatidylcholines act as LRH-1 agonists, DLPC and DUPC, with increased binding of coactivators and inhibition of interaction of LRH-1 with SHP and the corepressor SMRT (Lee et al., 2011; Musille et al., 2012; Ortlund et al., 2005). These compounds are interesting as they bind superficially, near the mouth of the LBP, leaving a deeper unoccupied pocket (Musille et al., 2012).

To design an antagonist for LRH-1, some assumptions have been made with regard to its potential similarity to other nuclear receptors for which antagonists have been successfully discovered and designed, such as ERα. The similarities that have been assumed relate to the structural changes of a nuclear receptor in the activated format, i.e. for ERα on binding of an antagonist the adjustment in the positioning of

H12, to change the AF2 topology and allow the recruitment of co-repressors rather than co-activators.

With regards to this thesis we targeted the LBD, beginning with the published agonist compound 5L and using computational identification (Cresset and SHoP) of compounds with similar 3Dand/or electrophysiological characteristics, to search for potential antagonists. Using this approach, a number of compounds with agonist activity greater than compound 5L were identified in both the cell based and *in vitro* assays. However, these compounds were unselective, with off target cell toxicity. The poor selectivity, shown by the activation of ERα by these compounds, indicates that they are either promiscuous or activation is due to off target effects, perhaps via modulation of protein kinase pathways or chromatin remodelling enzymes. To go from these to viable selective antagonists would likely mean a considerable amount of chemistry redesign perhaps achievable only by screening libraries of compounds. Two potential antagonists were identified but these did not block the activation of LRH-1 by 5A, indicating that any inhibitory activity may be indirect or that these compounds have only a very weak affinity for LRH-1. That very few potential antagonists were identified using this technique perhaps indicates that modelling using LRH-1 agonists, as a starting structure may not be appropriate.

The most promising results from this thesis relate to the nuclear receptor modulator extension work. This technique also targeted the LBD, using the nuclear receptor modulators raloxifene and tamoxifen as templates initially for two dimensional virtual HTS of the Chem Navigator library (50+ million compounds), followed by three dimensional docking based screening of the delivered hits using the LRH-1 LBD with bound phospholipid (PDB code 1YUC). Two potential scaffolds for the development of LRH-1 antagonists were identified, a Raloxifene analogue and a Tamoxifen analogue, although both had poor potency and solubility, and molecular weights above 700 and will therefore require significant modification. The Raloxifene analogue (JR430) has been chosen for further chemistry design based on LRH-1 docking analysis suggesting that the C-7 arm of the benzothiophene

scaffold is a key feature as it is directed towards H12. Certainly compounds that moved away from this feature had little activity (JR505 and JR530). Future work will aim to develop analogues with modifications of this arm to improve potency. Ideally to enable the most effective analogues to be developed this structure would be co-crystallised with the LRH-1 LBD as this would allow 'intelligent design' of further compounds by defining the key interactions between the LRH-1 LBD and compound.

4.4 LRH1: Future direction

The limitations of the screening methods that I have employed within this thesis relate to throughput and specificity. In future, using an *in vitro* binding assay as the first step in the screening cascade would allow a more rapid throughput of compounds and could be used initially to screen for both potential LRH-1 activity and specificity by developing the same assay for a range of nuclear receptors. The *in vitro* binding assay I have set up and validated could certainly be used for such screening efforts. Confirmation of the functional effects on full length LRH-1 and other nuclear receptors could then be assessed in cell based assays. This would then be followed by growth and proliferation assays in appropriate breast cancer cell lines.

Work published by Professor Fletterick's group at the University of California in San Francisco highlights potential drawbacks in our initial approaches for identifying LRH-1 antagonists. This group, in a similar manner to us, used the structural conformation of the LRH-1 LBD from the known agonist bound conformation but with predicted adjustments based on ERα bound to tamoxifen (PDB code 3ERT)) (Benod et al., 2013). The adjustments looked at the way in which ERα antagonists have a hydrophobic core with a polar side chain protruding out of the pocket, preventing H12 from allowing the recruitment and docking of co-activators. As there have been many different positions of H12 seen in ERα this meant that the actual position of H12 was unknown in LRH-1 and H12 was therefore removed from their model. They then used a flexible ligand-sampling algorithm that superimposes

atoms of a docked molecule onto spheres matching a defined binding site. In this case there were 50 matching spheres which mimicked the inside of the LRH-1 binding pocket and subsequently were readjusted to increase sampling at the opening in the receptor's molecule surface created by deletion of H12. This model was screened using an online database (ZINC) (Irwin and Shoichet, 2005) but an additional filtering step was added at this point to improve the 'druggability' of any compounds selected by also screening out compounds using molecular weight (<400), a logP (an octanol-water partition coefficient) <4 and less than 10 rotatable bonds.

Additionally, the type of compound library used for the initial identification of potential compounds to take forward into *in vitro* assay testing might need to be considered with the potential advantages offered by compound fragment libraries. Lipinski's rule of five has been the basic guide to predicting the potential suitability of new drugs based on their pharmacokinetic properties and states that four out of the five rules should be adhered to, to ensure success of a compound in a biological system. The five rules are: no more than five hydrogen bond donors, not more than 10 hydrogen bonds acceptors, a molecular mass of less than 500 daltons and a logP not greater than 5 (Lipinski et al., 2001). Maintaining these properties during lead optimisation is challenging if the starting molecular weight of a lead compound is already 700. Hence, fragment libraries use a modified rule of three: a logP not greater than 3, a molecular mass less than 300 daltons, not more than 3 hydrogen bond acceptors, not more than 3 hydrogen bond donors and not more than 3 rotatable bonds (Congreve et al., 2003).

It would be important in the future, in view of the drive to find LRH-1 inhibitors, to further predict and assess what the downstream impact of LRH-1 inhibition would be, for example on reversal cholesterol and bile acid metabolism. As described in section 1.3, we might predict that lowering LRH-1 systemically could result in hypercholesterolaemia, requiring additional therapy with HMG-CoA reductase inhibitors (Statins). LRH-1 alone promotes bile acid production by the induction of

CYP7A1 and Cyp8B1, however increased levels of bile acids initiate a regulatory feedback mechanism to activate FXR, which in turn induces SHP, SHP then inhibits LRH-1 (Goodwin et al., 2000; Lu et al., 2000). With further regard towards the potential problems associated with decreasing LRH-1 levels systemically, its role in diabetes has been of interest. LRH-1 has previously been found to be protective against diabetes and the discovery that the LRH-1 agonist, DLPC (dilauroyl phosphatidylcholine), decreases hepatic steatosis and improves glucose homeostasis in two independent mice models of insulin resistance, (specifically lowering serum glucose levels and hepatic triglycerides), whilst increasing bile acid levels has compounded this and led to the pilot human clinical study in USA to explore the effects of DLPC in patients with pre-type 2 diabetes mellitus (Lee et al., 2011; Mellado-Gil et al., 2012). The full impact of lowering LRH-1 levels has not been fully revealed and in fact a recently published study looking at heterozygous LRH-1 knockout mice found that they are prone to obesity but without any objective worsening of glucose and lipid metabolism (Hattori et al., 2014) indicating the presence of compensatory pathways.

In view of the role of LRH-1 in ERα and aromatase regulation, LRH-1 antagonism in breast cancer may be seen in combination with existing endocrine treatments or indeed in combination with alternative pathway antagonism i.e. Akt/PI3K/mTOR inhibitors as is currently under investigation within the BELLE clinical trials. The challenge, as always will be to select out appropriate groups of breast cancer patients who are likely to benefit most from LRH-1 inhibition and to this end, there is a need for robust biomarkers of LRH-1 activity. Identifying LRH-1 target genes using microarray analysis, as described in this thesis, will surely aid biomarker development.

5. Conclusions

The MLET5 microarray analysis has confirmed the functionality of ERα in MLET5 by the presence of ERα and associated estrogen regulated genes. It has also confirmed the estrogen independence of this clonal cell line and highlights the potential of MLET5 as a model of endocrine resistant breast cancer. I have shown that one of the mechanisms of resistance in MLET5 involves an up-regulation of the pro-survival pathway involving BCL2 family members, suggesting that targeting this pathway, in addition to endocrine treatment, may provide an important strategy for overcoming endocrine resistance. Future studies should focus on confirming these findings in alternative cell lines of endocrine resistance with a view to investigating potential new therapeutic targets or biomarkers.

LRH-1 is a direct ERα target gene important for the growth of breast cancer, and work from this laboratory has confirmed that LRH-1 itself can directly regulate ERα and ERα regulated genes. Identification of LRH-1 target genes in breast cancer cells has confirmed the importance of LRH-1 in estrogen driven development and progression of breast cancer. The co-operativity between LRH-1, ERα and other genes such as GATA3 may provide a key mechanism for regulating the expression of genes required for breast cancer progression. GPER has been shown to be an LRH-1 regulated gene and further investigation of the potential non-genomic effects of GPER on estrogen regulation are required. Similarly, there will be ongoing analysis for appropriate biomarkers that could be used during future drug discovery.

The evidence from other groups showing that LRH-1 drives estrogen biosynthesis in breast cancer associated stroma, together with the demonstration here that LRH-1 is directly involved in regulation of the ERα transcriptome in breast cancer cells, together with the identification of GPER, which has been implicated in non-genomic actions of estrogen, provide compelling evidence for exploration of LRH-1 inhibitors as breast cancer therapeutics. The studies described in this thesis demonstrate that

it should be possible to develop LRH-1 selective small molecule inhibitors. However, it is also clear that successful identification of molecules for development as therapeutics, or even LRH-1 selective tool molecules, require the use of sophisticated approaches, ideally utilizing high-throughput screening of large compound libraries and/or fragment libraries, couple with co-crystallisation studies, prior to any focused chemistry approaches.

References

Abd El-Rehim, D.M., Ball, G., Pinder, S.E., Rakha, E., Paish, C., Robertson, J.F., Macmillan, D., Blamey, R.W., and Ellis, I.O. (2005). High-throughput protein expression analysis using tissue microarray technology of a large well-characterised series identifies biologically distinct classes of breast cancer confirming recent cDNA expression analyses. Int J Cancer *116*, 340-350.

Agarwal, V.R., Bulun, S.E., Leitch, M., Rohrich, R., and Simpson, E.R. (1996). Use of alternative promoters to express the aromatase cytochrome P450 (CYP19) gene in breast adipose tissues of cancer-free and breast cancer patients. J Clin Endocrinol Metab *81*, 3843-3849.

Ahmad, K.F., Melnick, A., Lax, S., Bouchard, D., Liu, J., Kiang, C.L., Mayer, S., Takahashi, S., Licht, J.D., and Prive, G.G. (2003). Mechanism of SMRT corepressor recruitment by the BCL6 BTB domain. Mol Cell *12*, 1551-1564.

Albers, M., Blume, B., Schlueter, T., Wright, M.B., Kober, I., Kremoser, C., Deuschle, U., and Koegl, M. (2006). A novel principle for partial agonism of liver X receptor ligands. Competitive recruitment of activators and repressors. J Biol Chem *281*, 4920-4930.

Ali, S., and Coombes, R.C. (2002). Endocrine-responsive breast cancer and strategies for combating resistance. Nat Rev Cancer *2*, 101-112.

Andersen, R.J., Mawji, N.R., Wang, J., Wang, G., Haile, S., Myung, J.K., Watt, K., Tam, T., Yang, Y.C., Banuelos, C.A.*, et al.* (2010). Regression of castrate-recurrent prostate cancer by a small-molecule inhibitor of the amino-terminus domain of the androgen receptor. Cancer Cell *17*, 535-546.

Ang, E.Z., Nguyen, H.T., Sim, H.L., Putti, T.C., and Lim, L.H. (2009). Annexin-1 regulates growth arrest induced by high levels of estrogen in MCF-7 breast cancer cells. Mol Cancer Res *7*, 266-274.

Annicotte, J.S., Chavey, C., Servant, N., Teyssier, J., Bardin, A., Licznar, A., Badia, E., Pujol, P., Vignon, F., Maudelonde, T.*, et al.* (2005). The nuclear receptor liver receptor homolog-1 is an estrogen receptor target gene. Oncogene *24*, 8167-8175.

Anzick, S.L., Kononen, J., Walker, R.L., Azorsa, D.O., Tanner, M.M., Guan, X.Y., Sauter, G., Kallioniemi, O.P., Trent, J.M., and Meltzer, P.S. (1997). AIB1, a steroid receptor coactivator amplified in breast and ovarian cancer. Science *277*, 965-968.

Arias-Pulido, H., Royce, M., Gong, Y., Joste, N., Lomo, L., Lee, S.J., Chaher, N., Verschraegen, C., Lara, J., Prossnitz, E.R.*, et al.* (2010). GPR30 and estrogen receptor expression: new insights into hormone dependence of inflammatory breast cancer. Breast Cancer Res Treat *123*, 51-58.

Arpino, G., Gutierrez, C., Weiss, H., Rimawi, M., Massarweh, S., Bharwani, L., De Placido, S., Osborne, C.K., and Schiff, R. (2007). Treatment of human epidermal growth factor receptor 2-overexpressing breast cancer xenografts with multiagent HER-targeted therapy. J Natl Cancer Inst *99*, 694-705.

Asahina, M., Ishihara, T., Jindra, M., Kohara, Y., Katsura, I., and Hirose, S. (2000). The conserved nuclear receptor Ftz-F1 is required for embryogenesis, moulting and reproduction in Caenorhabditis elegans. Genes Cells *5*, 711-723.

Bachelot, T., Bourgier, C., Cropet, C., Ray-Coquard, I., Ferrero, J.M., Freyer, G., Abadie-Lacourtoisie, S., Eymard, J.C., Debled, M., Spaeth, D.*, et al.* (2012). Randomized phase II trial of everolimus in combination with tamoxifen in patients with hormone receptor-positive, human epidermal growth factor receptor 2-negative metastatic breast cancer with prior exposure to aromatase inhibitors: a GINECO study. J Clin Oncol *30*, 2718-2724.
Bapat, A.R., and Frail, D.E. (2003). Full-length estrogen receptor alpha and its ligand-binding domain adopt different conformations upon binding ligand. J Steroid Biochem Mol Biol *86*, 143-149.
Barone, I., Cui, Y., Herynk, M.H., Corona-Rodriguez, A., Giordano, C., Selever, J., Beyer, A., Ando, S., and Fuqua, S.A. (2009). Expression of the K303R estrogen receptor-alpha breast cancer mutation induces resistance to an aromatase inhibitor via addiction to the PI3K/Akt kinase pathway. Cancer Res *69*, 4724-4732.
Baselga, J., Campone, M., Piccart, M., Burris, H.A., 3rd, Rugo, H.S., Sahmoud, T., Noguchi, S., Gnant, M., Pritchard, K.I., Lebrun, F.*, et al.* (2012). Everolimus in postmenopausal hormone-receptor-positive advanced breast cancer. N Engl J Med *366*, 520-529.
Baxter, R.C. (2014). IGF binding proteins in cancer: mechanistic and clinical insights. Nat Rev Cancer *14*, 329-341.
Beardsley, D.I., Kowbel, D., Lataxes, T.A., Mannino, J.M., Xin, H., Kim, W.J., Collins, C., and Brown, K.D. (2003). Characterization of the novel amplified in breast cancer-1 (NABC1) gene product. Exp Cell Res *290*, 402-413.
Beatson, G.T. (1896). On the treatment of inoperable cases of carcinoma of the mamma: suggestions for a new method of treatment, with illustrative cases. The Lancet, 104-107.
Becerril, J., and Hamilton, A.D. (2007). Helix mimetics as inhibitors of the interaction of the estrogen receptor with coactivator peptides. Angew Chem Int Ed Engl *46*, 4471-4473.
Becker, M., Sommer, A., Kratzschmar, J.R., Seidel, H., Pohlenz, H.D., and Fichtner, I. (2005). Distinct gene expression patterns in a tamoxifen-sensitive human mammary carcinoma xenograft and its tamoxifen-resistant subline MaCa 3366/TAM. Mol Cancer Ther *4*, 151-168.
Beelen, K., Hoefnagel, L.D., Opdam, M., Wesseling, J., Sanders, J., Vincent, A.D., van Diest, P.J., and Linn, S.C. (2014). PI3K/AKT/mTOR pathway activation in primary and corresponding metastatic breast tumors after adjuvant endocrine therapy. Int J Cancer *135*, 1257-1263.
Beeram, M., Tan, Q.T., Tekmal, R.R., Russell, D., Middleton, A., and DeGraffenried, L.A. (2007). Akt-induced endocrine therapy resistance is reversed by inhibition of mTOR signaling. Ann Oncol *18*, 1323-1328.
Bendell, J.C., Rodon, J., Burris, H.A., de Jonge, M., Verweij, J., Birle, D., Demanse, D., De Buck, S.S., Ru, Q.C., Peters, M.*, et al.* (2012). Phase I, dose-escalation study of BKM120, an oral pan-Class I PI3K inhibitor, in patients with advanced solid tumors. J Clin Oncol *30*, 282-290.
Benod, C., Carlsson, J., Uthayaruban, R., Hwang, P., Irwin, J.J., Doak, A.K., Shoichet, B.K., Sablin, E.P., and Fletterick, R.J. (2013). Structure-based discovery of antagonists of nuclear receptor LRH-1. J Biol Chem *288*, 19830-19844.

Bergmann, R., Linusson, A., and Zamora, I. (2007). SHOP: scaffold HOPping by GRID-based similarity searches. J Med Chem *50*, 2708-2717.
Bhattacharyya, G.e.a. (2011). Reversal of tamoxifen resistance 9hormone resistance) by addition of sirolimus (mTOR inhibitor) in metastatic breast cancer. European Multidisciplinary Cancer Congress, Stockholm, Sweden.
Billen, L.P., Shamas-Din, A., and Andrews, D.W. (2008). Bid: a Bax-like BH3 protein. Oncogene *27 Suppl 1*, S93-104.
Blum, W., and Schwaller, B. (2013). Calretinin is essential for mesothelioma cell growth/survival in vitro: a potential new target for malignant mesothelioma therapy? Int J Cancer *133*, 2077-2088.
Bohan, A., Chen, W.S., Denson, L.A., Held, M.A., and Boyer, J.L. (2003). Tumor necrosis factor alpha-dependent up-regulation of Lrh-1 and Mrp3(Abcc3) reduces liver injury in obstructive cholestasis. J Biol Chem *278*, 36688-36698.
Borjesson, A.E., Windahl, S.H., Lagerquist, M.K., Engdahl, C., Frenkel, B., Moverare-Skrtic, S., Sjogren, K., Kindblom, J.M., Stubelius, A., Islander, U.*, et al.* (2011). Roles of transactivating functions 1 and 2 of estrogen receptor-alpha in bone. Proc Natl Acad Sci U S A *108*, 6288-6293.
Botrugno, O.A., Fayard, E., Annicotte, J.S., Haby, C., Brennan, T., Wendling, O., Tanaka, T., Kodama, T., Thomas, W., Auwerx, J.*, et al.* (2004). Synergy between LRH-1 and beta-catenin induces G1 cyclin-mediated cell proliferation. Mol Cell *15*, 499-509.
Bouchard, M.F., Taniguchi, H., and Viger, R.S. (2005). Protein kinase A-dependent synergism between GATA factors and the nuclear receptor, liver receptor homolog-1, regulates human aromatase (CYP19) PII promoter activity in breast cancer cells. Endocrinology *146*, 4905-4916.
Boudot, A., Kerdivel, G., Habauzit, D., Eeckhoute, J., Le Dily, F., Flouriot, G., Samson, M., and Pakdel, F. (2011). Differential estrogen-regulation of CXCL12 chemokine receptors, CXCR4 and CXCR7, contributes to the growth effect of estrogens in breast cancer cells. PLoS One *6*, e20898.
Bouras, T., Southey, M.C., and Venter, D.J. (2001). Overexpression of the steroid receptor coactivator AIB1 in breast cancer correlates with the absence of estrogen and progesterone receptors and positivity for p53 and HER2/neu. Cancer Res *61*, 903-907.
Bourgeois, S., Pfahl, M., and Baulieu, E.E. (1984). DNA binding properties of glucocorticosteroid receptors bound to the steroid antagonist RU-486. EMBO J *3*, 751-755.
Bowles, D.W., Ma, W.W., Senzer, N., Brahmer, J.R., Adjei, A.A., Davies, M., Lazar, A.J., Vo, A., Peterson, S., Walker, L.*, et al.* (2013). A multicenter phase 1 study of PX-866 in combination with docetaxel in patients with advanced solid tumours. Br J Cancer *109*, 1085-1092.
Boyd, S. (1900). On oophorectomy in cancer of the breast. British Medical Journal *Part 2*, 1161-1167.
Bratland, A., Risberg, K., Maelandsmo, G.M., Gutzkow, K.B., Olsen, O.E., Moghaddam, A., Wang, M.Y., Hansen, C.M., Blomhoff, H.K., Berg, J.P.*, et al.* (2000). Expression of a novel factor, com1, is regulated by 1,25-dihydroxyvitamin D3 in breast cancer cells. Cancer Res *60*, 5578-5583.

Brattsand, R., Thalen, A., Roempke, K., Kallstrom, L., and Gruvstad, E. (1982). Development of new glucocorticosteroids with a very high ratio between topical and systemic activities. Eur J Respir Dis Suppl *122*, 62-73.
Brendel, C., Gelman, L., and Auwerx, J. (2002). Multiprotein bridging factor-1 (MBF-1) is a cofactor for nuclear receptors that regulate lipid metabolism. Mol Endocrinol *16*, 1367-1377.
Brooks, S.C., Locke, E.R., and Soule, H.D. (1973). Estrogen receptor in a human cell line (MCF-7) from breast carcinoma. J Biol Chem *248*, 6251-6253.
Brunner, N., Boysen, B., Jirus, S., Skaar, T.C., Holst-Hansen, C., Lippman, J., Frandsen, T., Spang-Thomsen, M., Fuqua, S.A., and Clarke, R. (1997). MCF7/LCC9: an antiestrogen-resistant MCF-7 variant in which acquired resistance to the steroidal antiestrogen ICI 182,780 confers an early cross-resistance to the nonsteroidal antiestrogen tamoxifen. Cancer Res *57*, 3486-3493.
Brzozowski, A.M., Pike, A.C., Dauter, Z., Hubbard, R.E., Bonn, T., Engstrom, O., Ohman, L., Greene, G.L., Gustafsson, J.A., and Carlquist, M. (1997). Molecular basis of agonism and antagonism in the oestrogen receptor. Nature *389*, 753-758.
Buluwela, L., Pike, J., Mazhar, D., Kamalati, T., Hart, S.M., Al-Jehani, R., Yahaya, H., Patel, N., Sarwar, N., Heathcote, D.A.*, et al.* (2005). Inhibiting estrogen responses in breast cancer cells using a fusion protein encoding estrogen receptor-alpha and the transcriptional repressor PLZF. Gene Ther *12*, 452-460.
Burandt, E., Jens, G., Holst, F., Janicke, F., Muller, V., Quaas, A., Choschzick, M., Wilczak, W., Terracciano, L., Simon, R.*, et al.* (2013). Prognostic relevance of AIB1 (NCoA3) amplification and overexpression in breast cancer. Breast Cancer Res Treat *137*, 745-753.
Butt, A.J., Firth, S.M., King, M.A., and Baxter, R.C. (2000). Insulin-like growth factor-binding protein-3 modulates expression of Bax and Bcl-2 and potentiates p53-independent radiation-induced apoptosis in human breast cancer cells. J Biol Chem *275*, 39174-39181.
Butt, A.J., and Williams, A.C. (2001). IGFBP-3 and apoptosis--a license to kill? Apoptosis *6*, 199-205.
Calderon, M.R., Verway, M., An, B.S., DiFeo, A., Bismar, T.A., Ann, D.K., Martignetti, J.A., Shalom-Barak, T., and White, J.H. (2012). Ligand-dependent corepressor (LCoR) recruitment by Kruppel-like factor 6 (KLF6) regulates expression of the cyclin-dependent kinase inhibitor CDKN1A gene. J Biol Chem *287*, 8662-8674.
Calkin, A.C., and Tontonoz, P. (2012). Transcriptional integration of metabolism by the nuclear sterol-activated receptors LXR and FXR. Nat Rev Mol Cell Biol *13*, 213-224.
Cano, C.E., Hamidi, T., Sandi, M.J., and Iovanna, J.L. (2011). Nupr1: the Swiss-knife of cancer. J Cell Physiol *226*, 1439-1443.
Carlberg, C., Molnar, F., and Mourino, A. (2012). Vitamin D receptor ligands: the impact of crystal structures. Expert Opin Ther Pat *22*, 417-435.
Carraz, M., Zwart, W., Phan, T., Michalides, R., and Brunsveld, L. (2009). Perturbation of estrogen receptor alpha localization with synthetic nona-arginine LXXLL-peptide coactivator binding inhibitors. Chem Biol *16*, 702-711.

Carroll, J.S., Meyer, C.A., Song, J., Li, W., Geistlinger, T.R., Eeckhoute, J., Brodsky, A.S., Keeton, E.K., Fertuck, K.C., Hall, G.F*., et al.* (2006). Genome-wide analysis of estrogen receptor binding sites. Nat Genet *38*, 1289-1297.
Cavarretta, I.T., Mukopadhyay, R., Lonard, D.M., Cowsert, L.M., Bennett, C.F., O'Malley, B.W., and Smith, C.L. (2002). Reduction of coactivator expression by antisense oligodeoxynucleotides inhibits ERalpha transcriptional activity and MCF-7 proliferation. Mol Endocrinol *16*, 253-270.
Chabbert-Buffet, N., Meduri, G., Bouchard, P., and Spitz, I.M. (2005). Selective progesterone receptor modulators and progesterone antagonists: mechanisms of action and clinical applications. Hum Reprod Update *11*, 293-307.
Chalkiadaki, A., and Talianidis, I. (2005). SUMO-dependent compartmentalization in promyelocytic leukemia protein nuclear bodies prevents the access of LRH-1 to chromatin. Mol Cell Biol *25*, 5095-5105.
Chan, C.M., Martin, L.A., Johnston, S.R., Ali, S., and Dowsett, M. (2002). Molecular changes associated with the acquisition of oestrogen hypersensitivity in MCF-7 breast cancer cells on long-term oestrogen deprivation. J Steroid Biochem Mol Biol *81*, 333-341.
Chand, A.L., Herridge, K.A., Howard, T.L., Simpson, E.R., and Clyne, C.D. (2011). Tissue-specific regulation of aromatase promoter II by the orphan nuclear receptor LRH-1 in breast adipose stromal fibroblasts. Steroids *76*, 741-744.
Chand, A.L., Wijayakumara, D.D., Knower, K.C., Herridge, K.A., Howard, T.L., Lazarus, K.A., and Clyne, C.D. (2012). The orphan nuclear receptor LRH-1 and ERalpha activate GREB1 expression to induce breast cancer cell proliferation. PLoS One *7*, e31593.
Chang, C., Norris, J.D., Gron, H., Paige, L.A., Hamilton, P.T., Kenan, D.J., Fowlkes, D., and McDonnell, D.P. (1999). Dissection of the LXXLL nuclear receptor-coactivator interaction motif using combinatorial peptide libraries: discovery of peptide antagonists of estrogen receptors alpha and beta. Mol Cell Biol *19*, 8226-8239.
Chang, Y.W., Chen, S.C., Cheng, E.C., Ko, Y.P., Lin, Y.C., Kao, Y.R., Tsay, Y.G., Yang, P.C., Wu, C.W., and Roffler, S.R. (2005). CD13 (aminopeptidase N) can associate with tumor-associated antigen L6 and enhance the motility of human lung cancer cells. Int J Cancer *116*, 243-252.
Cheeseright, T., Mackey, M., Rose, S., and Vinter, A. (2006). Molecular field extrema as descriptors of biological activity: definition and validation. J Chem Inf Model *46*, 665-676.
Chen, D., Washbrook, E., Sarwar, N., Bates, G.J., Pace, P.E., Thirunuvakkarasu, V., Taylor, J., Epstein, R.J., Fuller-Pace, F.V., Egly, J.M*., et al.* (2002). Phosphorylation of human estrogen receptor alpha at serine 118 by two distinct signal transduction pathways revealed by phosphorylation-specific antisera. Oncogene *21*, 4921-4931.
Chen, Z., Brand, N.J., Chen, A., Chen, S.J., Tong, J.H., Wang, Z.Y., Waxman, S., and Zelent, A. (1993). Fusion between a novel Kruppel-like zinc finger gene and the retinoic acid receptor-alpha locus due to a variant t(11;17) translocation associated with acute promyelocytic leukaemia. EMBO J *12*, 1161-1167.
Chinnadurai, G., Vijayalingam, S., and Rashmi, R. (2008). BIK, the founding member of the BH3-only family proteins: mechanisms of cell death and role in cancer and pathogenic processes. Oncogene *27 Suppl 1*, S20-29.

Chong, H.K., Infante, A.M., Seo, Y.K., Jeon, T.I., Zhang, Y., Edwards, P.A., Xie, X., and Osborne, T.F. (2010). Genome-wide interrogation of hepatic FXR reveals an asymmetric IR-1 motif and synergy with LRH-1. Nucleic Acids Res *38*, 6007-6017.
Chowdhury, U.R., Samant, R.S., Fodstad, O., and Shevde, L.A. (2009). Emerging role of nuclear protein 1 (NUPR1) in cancer biology. Cancer Metastasis Rev *28*, 225-232.
Chu, S., Huang, Q., Alvares, K., Yeldandi, A.V., Rao, M.S., and Reddy, J.K. (1995). Transformation of mammalian cells by overexpressing H2O2-generating peroxisomal fatty acyl-CoA oxidase. Proc Natl Acad Sci U S A *92*, 7080-7084.
Cima, I., Corazza, N., Dick, B., Fuhrer, A., Herren, S., Jakob, S., Ayuni, E., Mueller, C., and Brunner, T. (2004). Intestinal epithelial cells synthesize glucocorticoids and regulate T cell activation. J Exp Med *200*, 1635-1646.
Ciriello, G., Sinha, R., Hoadley, K.A., Jacobsen, A.S., Reva, B., Perou, C.M., Sander, C., and Schultz, N. (2013). The molecular diversity of Luminal A breast tumors. Breast Cancer Res Treat *141*, 409-420.
Clark, D.W., Mitra, A., Fillmore, R.A., Jiang, W.G., Samant, R.S., Fodstad, O., and Shevde, L.A. (2008). NUPR1 interacts with p53, transcriptionally regulates p21 and rescues breast epithelial cells from doxorubicin-induced genotoxic stress. Curr Cancer Drug Targets *8*, 421-430.
Clegg, N.J., Wongvipat, J., Joseph, J.D., Tran, C., Ouk, S., Dilhas, A., Chen, Y., Grillot, K., Bischoff, E.D., Cai, L., *et al.* (2012). ARN-509: a novel antiandrogen for prostate cancer treatment. Cancer Res *72*, 1494-1503.
Clyne, C.D., Kovacic, A., Speed, C.J., Zhou, J., Pezzi, V., and Simpson, E.R. (2004). Regulation of aromatase expression by the nuclear receptor LRH-1 in adipose tissue. Mol Cell Endocrinol *215*, 39-44.
Clyne, C.D., Speed, C.J., Zhou, J., and Simpson, E.R. (2002). Liver receptor homologue-1 (LRH-1) regulates expression of aromatase in preadipocytes. J Biol Chem *277*, 20591-20597.
Collins, C., Rommens, J.M., Kowbel, D., Godfrey, T., Tanner, M., Hwang, S.I., Polikoff, D., Nonet, G., Cochran, J., Myambo, K., *et al.* (1998). Positional cloning of ZNF217 and NABC1: genes amplified at 20q13.2 and overexpressed in breast carcinoma. Proc Natl Acad Sci U S A *95*, 8703-8708.
Congreve, M., Carr, R., Murray, C., and Jhoti, H. (2003). A 'rule of three' for fragment-based lead discovery? Drug Discov Today *8*, 876-877.
Conway, K., Parrish, E., Edmiston, S.N., Tolbert, D., Tse, C.K., Moorman, P., Newman, B., and Millikan, R.C. (2007). Risk factors for breast cancer characterized by the estrogen receptor alpha A908G (K303R) mutation. Breast Cancer Res *9*, R36.
Coombes, R.C., Kilburn, L.S., Snowdon, C.F., Paridaens, R., Coleman, R.E., Jones, S.E., Jassem, J., Van de Velde, C.J., Delozier, T., Alvarez, I., *et al.* (2007). Survival and safety of exemestane versus tamoxifen after 2-3 years' tamoxifen treatment (Intergroup Exemestane Study): a randomised controlled trial. Lancet *369*, 559-570.
Coste, A., Dubuquoy, L., Barnouin, R., Annicotte, J.S., Magnier, B., Notti, M., Corazza, N., Antal, M.C., Metzger, D., Desreumaux, P., *et al.* (2007). LRH-1-mediated glucocorticoid synthesis in enterocytes protects against inflammatory bowel disease. Proc Natl Acad Sci U S A *104*, 13098-13103.
Cristofanilli, M., Valero, V., Mangalik, A., Royce, M., Rabinowitz, I., Arena, F.P., Kroener, J.F., Curcio, E., Watkins, C., Bacus, S., *et al.* (2010). Phase II, randomized trial

to compare anastrozole combined with gefitinib or placebo in postmenopausal women with hormone receptor-positive metastatic breast cancer. Clin Cancer Res *16*, 1904-1914.
Cuzick, J. (2008). Aromatase inhibitors in early breast-cancer treatment: The story so far. Breast *17 Suppl 3*, S2-8.
D'Arpa, P., Beardmore, C., and Liu, L.F. (1990). Involvement of nucleic acid synthesis in cell killing mechanisms of topoisomerase poisons. Cancer Res *50*, 6919-6924.
Danial, N.N. (2008). BAD: undertaker by night, candyman by day. Oncogene *27 Suppl 1*, S53-70.
Danielian, P.S., White, R., Lees, J.A., and Parker, M.G. (1992). Identification of a conserved region required for hormone dependent transcriptional activation by steroid hormone receptors. EMBO J *11*, 1025-1033.
Darimont, B.D., Wagner, R.L., Apriletti, J.W., Stallcup, M.R., Kushner, P.J., Baxter, J.D., Fletterick, R.J., and Yamamoto, K.R. (1998). Structure and specificity of nuclear receptor-coactivator interactions. Genes Dev *12*, 3343-3356.
Datta, S.R., Katsov, A., Hu, L., Petros, A., Fesik, S.W., Yaffe, M.B., and Greenberg, M.E. (2000). 14-3-3 proteins and survival kinases cooperate to inactivate BAD by BH3 domain phosphorylation. Mol Cell *6*, 41-51.
Dauvois, S., White, R., and Parker, M.G. (1993). The antiestrogen ICI 182780 disrupts estrogen receptor nucleocytoplasmic shuttling. J Cell Sci *106 (Pt 4)*, 1377-1388.
De Boussac, H., Alioui, A., Viennois, E., Dufour, J., Trousson, A., Vega, A., Guy, L., Volle, D.H., Lobaccaro, J.M., and Baron, S. (2013). Oxysterol receptors and their therapeutic applications in cancer conditions. Expert Opin Ther Targets *17*, 1029-1038.
DeFilippis, R.A., Chang, H., Dumont, N., Rabban, J.T., Chen, Y.Y., Fontenay, G.V., Berman, H.K., Gauthier, M.L., Zhao, J., Hu, D.*, et al.* (2012). CD36 repression activates a multicellular stromal program shared by high mammographic density and tumor tissues. Cancer Discov *2*, 826-839.
Del Tredici, A.L., Andersen, C.B., Currier, E.A., Ohrmund, S.R., Fairbain, L.C., Lund, B.W., Nash, N., Olsson, R., and Piu, F. (2008). Identification of the first synthetic steroidogenic factor 1 inverse agonists: pharmacological modulation of steroidogenic enzymes. Mol Pharmacol *73*, 900-908.
den Hollander, P., Rayala, S.K., Coverley, D., and Kumar, R. (2006). Ciz1, a Novel DNA-binding coactivator of the estrogen receptor alpha, confers hypersensitivity to estrogen action. Cancer Res *66*, 11021-11029.
Doghman, M., Cazareth, J., Douguet, D., Madoux, F., Hodder, P., and Lalli, E. (2009). Inhibition of adrenocortical carcinoma cell proliferation by steroidogenic factor-1 inverse agonists. J Clin Endocrinol Metab *94*, 2178-2183.
Dowsett, M., Cuzick, J., Ingle, J., Coates, A., Forbes, J., Bliss, J., Buyse, M., Baum, M., Buzdar, A., Colleoni, M.*, et al.* (2010). Meta-analysis of breast cancer outcomes in adjuvant trials of aromatase inhibitors versus tamoxifen. J Clin Oncol *28*, 509-518.
Dowsett, M., Nicholson, R.I., and Pietras, R.J. (2005). Biological characteristics of the pure antiestrogen fulvestrant: overcoming endocrine resistance. Breast Cancer Res Treat *93 Suppl 1*, S11-18.
Drabsch, Y., Hugo, H., Zhang, R., Dowhan, D.H., Miao, Y.R., Gewirtz, A.M., Barry, S.C., Ramsay, R.G., and Gonda, T.J. (2007). Mechanism of and requirement for estrogen-

regulated MYB expression in estrogen-receptor-positive breast cancer cells. Proc Natl Acad Sci U S A *104*, 13762-13767.
Duggavathi, R., Volle, D.H., Mataki, C., Antal, M.C., Messaddeq, N., Auwerx, J., Murphy, B.D., and Schoonjans, K. (2008). Liver receptor homolog 1 is essential for ovulation. Genes Dev *22*, 1871-1876.
Ellis, M.J., Coop, A., Singh, B., Mauriac, L., Llombert-Cussac, A., Janicke, F., Miller, W.R., Evans, D.B., Dugan, M., Brady, C.*, et al.* (2001). Letrozole is more effective neoadjuvant endocrine therapy than tamoxifen for ErbB-1- and/or ErbB-2-positive, estrogen receptor-positive primary breast cancer: evidence from a phase III randomized trial. J Clin Oncol *19*, 3808-3816.
Emtage, P., Vatta, P., Arterburn, M., Muller, M.W., Park, E., Boyle, B., Hazell, S., Polizotto, R., Funk, W.D., and Tang, Y.T. (2006). IGFL: A secreted family with conserved cysteine residues and similarities to the IGF superfamily. Genomics *88*, 513-520.
Endoh, H., Maruyama, K., Masuhiro, Y., Kobayashi, Y., Goto, M., Tai, H., Yanagisawa, J., Metzger, D., Hashimoto, S., and Kato, S. (1999). Purification and identification of p68 RNA helicase acting as a transcriptional coactivator specific for the activation function 1 of human estrogen receptor alpha. Mol Cell Biol *19*, 5363-5372.
Erdmann, E., Dormandy, J., Wilcox, R., Massi-Benedetti, M., and Charbonnel, B. (2007). PROactive 07: pioglitazone in the treatment of type 2 diabetes: results of the PROactive study. Vasc Health Risk Manag *3*, 355-370.
Esseghir, S., Todd, S.K., Hunt, T., Poulsom, R., Plaza-Menacho, I., Reis-Filho, J.S., and Isacke, C.M. (2007). A role for glial cell derived neurotrophic factor induced expression by inflammatory cytokines and RET/GFR alpha 1 receptor up-regulation in breast cancer. Cancer Res *67*, 11732-11741.
Faderl, S., Harris, D., Van, Q., Kantarjian, H.M., Talpaz, M., and Estrov, Z. (2003). Granulocyte-macrophage colony-stimulating factor (GM-CSF) induces antiapoptotic and proapoptotic signals in acute myeloid leukemia. Blood *102*, 630-637.
Fan, W., Yanase, T., Morinaga, H., Gondo, S., Okabe, T., Nomura, M., Hayes, T.B., Takayanagi, R., and Nawata, H. (2007a). Herbicide atrazine activates SF-1 by direct affinity and concomitant co-activators recruitments to induce aromatase expression via promoter II. Biochem Biophys Res Commun *355*, 1012-1018.
Fan, W., Yanase, T., Morinaga, H., Gondo, S., Okabe, T., Nomura, M., Komatsu, T., Morohashi, K., Hayes, T.B., Takayanagi, R.*, et al.* (2007b). Atrazine-induced aromatase expression is SF-1 dependent: implications for endocrine disruption in wildlife and reproductive cancers in humans. Environ Health Perspect *115*, 720-727.
Favre, H., Benhamou, A., Finidori, J., Kelly, P.A., and Edery, M. (1999). Dual effects of suppressor of cytokine signaling (SOCS-2) on growth hormone signal transduction. FEBS Lett *453*, 63-66.
Fayard, E., Auwerx, J., and Schoonjans, K. (2004). LRH-1: an orphan nuclear receptor involved in development, metabolism and steroidogenesis. Trends Cell Biol *14*, 250-260.
Fayard, E., Schoonjans, K., Annicotte, J.S., and Auwerx, J. (2003). Liver receptor homolog 1 controls the expression of carboxyl ester lipase. J Biol Chem *278*, 35725-35731.

Fernandes, I., Bastien, Y., Wai, T., Nygard, K., Lin, R., Cormier, O., Lee, H.S., Eng, F., Bertos, N.R., Pelletier, N.*, et al.* (2003). Ligand-dependent nuclear receptor corepressor LCoR functions by histone deacetylase-dependent and -independent mechanisms. Mol Cell *11*, 139-150.
Fernandez-Marcos, P.J., Auwerx, J., and Schoonjans, K. (2011). Emerging actions of the nuclear receptor LRH-1 in the gut. Biochim Biophys Acta *1812*, 947-955.
Figueroa, J.A., Jackson, J.G., McGuire, W.L., Krywicki, R.F., and Yee, D. (1993). Expression of insulin-like growth factor binding proteins in human breast cancer correlates with estrogen receptor status. J Cell Biochem *52*, 196-205.
Filardo, E.J., Graeber, C.T., Quinn, J.A., Resnick, M.B., Giri, D., DeLellis, R.A., Steinhoff, M.M., and Sabo, E. (2006). Distribution of GPR30, a seven membrane-spanning estrogen receptor, in primary breast cancer and its association with clinicopathologic determinants of tumor progression. Clin Cancer Res *12*, 6359-6366.
Fleming, F.J., Hill, A.D., McDermott, E.W., O'Higgins, N.J., and Young, L.S. (2004a). Differential recruitment of coregulator proteins steroid receptor coactivator-1 and silencing mediator for retinoid and thyroid receptors to the estrogen receptor-estrogen response element by beta-estradiol and 4-hydroxytamoxifen in human breast cancer. J Clin Endocrinol Metab *89*, 375-383.
Fleming, F.J., Myers, E., Kelly, G., Crotty, T.B., McDermott, E.W., O'Higgins, N.J., Hill, A.D., and Young, L.S. (2004b). Expression of SRC-1, AIB1, and PEA3 in HER2 mediated endocrine resistant breast cancer; a predictive role for SRC-1. J Clin Pathol *57*, 1069-1074.
Fowler, A.M., Solodin, N., Preisler-Mashek, M.T., Zhang, P., Lee, A.V., and Alarid, E.T. (2004). Increases in estrogen receptor-alpha concentration in breast cancer cells promote serine 118/104/106-independent AF-1 transactivation and growth in the absence of estrogen. FASEB J *18*, 81-93.
Franke, T.F., Yang, S.I., Chan, T.O., Datta, K., Kazlauskas, A., Morrison, D.K., Kaplan, D.R., and Tsichlis, P.N. (1995). The protein kinase encoded by the Akt proto-oncogene is a target of the PDGF-activated phosphatidylinositol 3-kinase. Cell *81*, 727-736.
Frasor, J., Danes, J.M., Komm, B., Chang, K.C., Lyttle, C.R., and Katzenellenbogen, B.S. (2003). Profiling of estrogen up- and down-regulated gene expression in human breast cancer cells: insights into gene networks and pathways underlying estrogenic control of proliferation and cell phenotype. Endocrinology *144*, 4562-4574.
French, K.J., Schrecengost, R.S., Lee, B.D., Zhuang, Y., Smith, S.N., Eberly, J.L., Yun, J.K., and Smith, C.D. (2003). Discovery and evaluation of inhibitors of human sphingosine kinase. Cancer Res *63*, 5962-5969.
Fuqua, S.A., Gu, G., and Rechoum, Y. (2014). Estrogen receptor (ER) alpha mutations in breast cancer: hidden in plain sight. Breast Cancer Res Treat *144*, 11-19.
Fuqua, S.A., Wiltschke, C., Zhang, Q.X., Borg, A., Castles, C.G., Friedrichs, W.E., Hopp, T., Hilsenbeck, S., Mohsin, S., O'Connell, P.*, et al.* (2000). A hypersensitive estrogen receptor-alpha mutation in premalignant breast lesions. Cancer Res *60*, 4026-4029.
Furstenberger, G., and Senn, H.J. (2002). Insulin-like growth factors and cancer. Lancet Oncol *3*, 298-302.

Galande, A.K., Bramlett, K.S., Burris, T.P., Wittliff, J.L., and Spatola, A.F. (2004). Thioether side chain cyclization for helical peptide formation: inhibitors of estrogen receptor-coactivator interactions. J Pept Res *63*, 297-302.
Galande, A.K., Bramlett, K.S., Trent, J.O., Burris, T.P., Wittliff, J.L., and Spatola, A.F. (2005). Potent inhibitors of LXXLL-based protein-protein interactions. Chembiochem *6*, 1991-1998.
Galarneau, L., Pare, J.F., Allard, D., Hamel, D., Levesque, L., Tugwood, J.D., Green, S., and Belanger, L. (1996). The alpha1-fetoprotein locus is activated by a nuclear receptor of the Drosophila FTZ-F1 family. Mol Cell Biol *16*, 3853-3865.
Gee, J.M., Harper, M.E., Hutcheson, I.R., Madden, T.A., Barrow, D., Knowlden, J.M., McClelland, R.A., Jordan, N., Wakeling, A.E., and Nicholson, R.I. (2003). The antiepidermal growth factor receptor agent gefitinib (ZD1839/Iressa) improves antihormone response and prevents development of resistance in breast cancer in vitro. Endocrinology *144*, 5105-5117.
Gentilucci, L., De Marco, R., and Cerisoli, L. (2010). Chemical modifications designed to improve peptide stability: incorporation of non-natural amino acids, pseudo-peptide bonds, and cyclization. Curr Pharm Des *16*, 3185-3203.
Gessi, S., Merighi, S., and Borea, P.A. (2010). Glucocorticoid's pharmacology: past, present and future. Curr Pharm Des *16*, 3540-3553.
Ghanadian, R., Auf, G., Chisholm, G.D., and O'Donoghue, E.P. (1978). Receptor proteins for androgens in prostatic disease. Br J Urol *50*, 567-569.
Ghayad, S.E., Vendrell, J.A., Bieche, I., Spyratos, F., Dumontet, C., Treilleux, I., Lidereau, R., and Cohen, P.A. (2009). Identification of TACC1, NOV, and PTTG1 as new candidate genes associated with endocrine therapy resistance in breast cancer. J Mol Endocrinol *42*, 87-103.
Gillet, L., Roger, S., Besson, P., Lecaille, F., Gore, J., Bougnoux, P., Lalmanach, G., and Le Guennec, J.Y. (2009). Voltage-gated Sodium Channel Activity Promotes Cysteine Cathepsin-dependent Invasiveness and Colony Growth of Human Cancer Cells. J Biol Chem *284*, 8680-8691.
Gillissen, B., Essmann, F., Graupner, V., Starck, L., Radetzki, S., Dorken, B., Schulze-Osthoff, K., and Daniel, P.T. (2003). Induction of cell death by the BH3-only Bcl-2 homolog Nbk/Bik is mediated by an entirely Bax-dependent mitochondrial pathway. EMBO J *22*, 3580-3590.
Girault, I., Lerebours, F., Amarir, S., Tozlu, S., Tubiana-Hulin, M., Lidereau, R., and Bieche, I. (2003). Expression analysis of estrogen receptor alpha coregulators in breast carcinoma: evidence that NCOR1 expression is predictive of the response to tamoxifen. Clin Cancer Res *9*, 1259-1266.
Girgert, R., Emons, G., and Grundker, C. (2012). Inactivation of GPR30 reduces growth of triple-negative breast cancer cells: possible application in targeted therapy. Breast Cancer Res Treat *134*, 199-205.
Glickman, J.F., Wu, X., Mercuri, R., Illy, C., Bowen, B.R., He, Y., and Sills, M. (2002). A comparison of ALPHAScreen, TR-FRET, and TRF as assay methods for FXR nuclear receptors. J Biomol Screen *7*, 3-10.
Goodwin, B., Jones, S.A., Price, R.R., Watson, M.A., McKee, D.D., Moore, L.B., Galardi, C., Wilson, J.G., Lewis, M.C., Roth, M.E*., et al.* (2000). A regulatory cascade of the nuclear

receptors FXR, SHP-1, and LRH-1 represses bile acid biosynthesis. Mol Cell *6*, 517-526.
Goodwin, B., Watson, M.A., Kim, H., Miao, J., Kemper, J.K., and Kliewer, S.A. (2003). Differential regulation of rat and human CYP7A1 by the nuclear oxysterol receptor liver X receptor-alpha. Mol Endocrinol *17*, 386-394.
Gottardis, M.M., Ricchio, M.E., Satyaswaroop, P.G., and Jordan, V.C. (1990). Effect of steroidal and nonsteroidal antiestrogens on the growth of a tamoxifen-stimulated human endometrial carcinoma (EnCa101) in athymic mice. Cancer Res *50*, 3189-3192.
Green, K.A., and Carroll, J.S. (2007). Oestrogen-receptor-mediated transcription and the influence of co-factors and chromatin state. Nat Rev Cancer *7*, 713-722.
Grimberg, A. (2000). P53 and IGFBP-3: apoptosis and cancer protection. Mol Genet Metab *70*, 85-98.
Gronemeyer, H., Gustafsson, J.A., and Laudet, V. (2004). Principles for modulation of the nuclear receptor superfamily. Nat Rev Drug Discov *3*, 950-964.
Gu, P., Goodwin, B., Chung, A.C., Xu, X., Wheeler, D.A., Price, R.R., Galardi, C., Peng, L., Latour, A.M., Koller, B.H.*, et al.* (2005). Orphan nuclear receptor LRH-1 is required to maintain Oct4 expression at the epiblast stage of embryonic development. Mol Cell Biol *25*, 3492-3505.
Gudas, J.M., Klein, R.C., Oka, M., and Cowan, K.H. (1995). Posttranscriptional regulation of the c-myb proto-oncogene in estrogen receptor-positive breast cancer cells. Clin Cancer Res *1*, 235-243.
Gunther, J.R., Moore, T.W., Collins, M.L., and Katzenellenbogen, J.A. (2008). Amphipathic benzenes are designed inhibitors of the estrogen receptor alpha/steroid receptor coactivator interaction. ACS Chem Biol *3*, 282-286.
Guo, X., Wang, W., Hu, J., Feng, K., Pan, Y., Zhang, L., and Feng, Y. (2012). Lentivirus-mediated RNAi knockdown of NUPR1 inhibits human nonsmall cell lung cancer growth in vitro and in vivo. Anat Rec (Hoboken) *295*, 2114-2121.
Hadizadeh, S., King, D.N., Shah, S., and Sewer, M.B. (2008). Sphingosine-1-phosphate regulates the expression of the liver receptor homologue-1. Mol Cell Endocrinol *283*, 104-113.
Hamidi, T., Algul, H., Cano, C.E., Sandi, M.J., Molejon, M.I., Riemann, M., Calvo, E.L., Lomberk, G., Dagorn, J.C., Weih, F.*, et al.* (2012). Nuclear protein 1 promotes pancreatic cancer development and protects cells from stress by inhibiting apoptosis. J Clin Invest *122*, 2092-2103.
Harada, N., Utsumi, T., and Takagi, Y. (1993). Tissue-specific expression of the human aromatase cytochrome P-450 gene by alternative use of multiple exons 1 and promoters, and switching of tissue-specific exons 1 in carcinogenesis. Proc Natl Acad Sci U S A *90*, 11312-11316.
Harigopal, M., Heymann, J., Ghosh, S., Anagnostou, V., Camp, R.L., and Rimm, D.L. (2009). Estrogen receptor co-activator (AIB1) protein expression by automated quantitative analysis (AQUA) in a breast cancer tissue microarray and association with patient outcome. Breast Cancer Res Treat *115*, 77-85.
Harper, M.J., and Walpole, A.L. (1967). Mode of action of I.C.I. 46,474 in preventing implantation in rats. J Endocrinol *37*, 83-92.

Hattori, T., Iizuka, K., Horikawa, Y., and Takeda, J. (2014). LRH-1 heterozygous knockout mice are prone to mild obesity. Endocr J *61*, 471-480.
Heery, D.M., Kalkhoven, E., Hoare, S., and Parker, M.G. (1997). A signature motif in transcriptional co-activators mediates binding to nuclear receptors. Nature *387*, 733-736.
Hellstrom, I., Horn, D., Linsley, P., Brown, J.P., Brankovan, V., and Hellstrom, K.E. (1986). Monoclonal mouse antibodies raised against human lung carcinoma. Cancer Res *46*, 3917-3923.
Heng, J.C., Feng, B., Han, J., Jiang, J., Kraus, P., Ng, J.H., Orlov, Y.L., Huss, M., Yang, L., Lufkin, T.*, et al.* (2010). The nuclear receptor Nr5a2 can replace Oct4 in the reprogramming of murine somatic cells to pluripotent cells. Cell Stem Cell *6*, 167-174.
Henttu, P.M., Kalkhoven, E., and Parker, M.G. (1997). AF-2 activity and recruitment of steroid receptor coactivator 1 to the estrogen receptor depend on a lysine residue conserved in nuclear receptors. Mol Cell Biol *17*, 1832-1839.
Hinshelwood, M.M., Repa, J.J., Shelton, J.M., Richardson, J.A., Mangelsdorf, D.J., and Mendelson, C.R. (2003). Expression of LRH-1 and SF-1 in the mouse ovary: localization in different cell types correlates with differing function. Mol Cell Endocrinol *207*, 39-45.
Hirai, I., and Wang, H.G. (2001). Survival-factor-induced phosphorylation of Bad results in its dissociation from Bcl-x(L) but not Bcl-2. Biochem J *359*, 345-352.
Hong, D.S., Bowles, D.W., Falchook, G.S., Messersmith, W.A., George, G.C., O'Bryant, C.L., Vo, A.C., Klucher, K., Herbst, R.S., Eckhardt, S.G.*, et al.* (2012). A multicenter phase I trial of PX-866, an oral irreversible phosphatidylinositol 3-kinase inhibitor, in patients with advanced solid tumors. Clin Cancer Res *18*, 4173-4182.
Hong, S.H., Nah, H.Y., Lee, J.Y., Gye, M.C., Kim, C.H., and Kim, M.K. (2004). Analysis of estrogen-regulated genes in mouse uterus using cDNA microarray and laser capture microdissection. J Endocrinol *181*, 157-167.
Horwitz, K.B., Costlow, M.E., and McGuire, W.L. (1975). MCF-7; a human breast cancer cell line with estrogen, androgen, progesterone, and glucocorticoid receptors. Steroids *26*, 785-795.
Horwitz, K.B., Koseki, Y., and McGuire, W.L. (1978). Estrogen control of progesterone receptor in human breast cancer: role of estradiol and antiestrogen. Endocrinology *103*, 1742-1751.
Howell, A., Robertson, J.F., Quaresma Albano, J., Aschermannova, A., Mauriac, L., Kleeberg, U.R., Vergote, I., Erikstein, B., Webster, A., and Morris, C. (2002). Fulvestrant, formerly ICI 182,780, is as effective as anastrozole in postmenopausal women with advanced breast cancer progressing after prior endocrine treatment. J Clin Oncol *20*, 3396-3403.
Hsieh, H.T., Wang, C.H., Wu, M.L., Yang, F.M., Tai, Y.C., and Hu, M.C. (2009). PIASy inhibits LRH-1-dependent CYP11A1 expression by competing for SRC-1 binding. Biochem J *419*, 201-209.
Hu, X., and Lazar, M.A. (1999). The CoRNR motif controls the recruitment of corepressors by nuclear hormone receptors. Nature *402*, 93-96.
Huang, H.J., Norris, J.D., and McDonnell, D.P. (2002). Identification of a negative regulatory surface within estrogen receptor alpha provides evidence in support of a

role for corepressors in regulating cellular responses to agonists and antagonists. Mol Endocrinol *16*, 1778-1792.
Hudelist, G., Czerwenka, K., Kubista, E., Marton, E., Pischinger, K., and Singer, C.F. (2003). Expression of sex steroid receptors and their co-factors in normal and malignant breast tissue: AIB1 is a carcinoma-specific co-activator. Breast Cancer Res Treat *78*, 193-204.
Hui, D.Y., and Howles, P.N. (2002). Carboxyl ester lipase: structure-function relationship and physiological role in lipoprotein metabolism and atherosclerosis. J Lipid Res *43*, 2017-2030.
Huober, J., Fasching, P.A., Barsoum, M., Petruzelka, L., Wallwiener, D., Thomssen, C., Reimer, T., Paepke, S., Azim, H.A., Ragosch, V.*, et al.* (2012). Higher efficacy of letrozole in combination with trastuzumab compared to letrozole monotherapy as first-line treatment in patients with HER2-positive, hormone-receptor-positive metastatic breast cancer - results of the eLEcTRA trial. Breast *21*, 27-33.
Hur, J., Chesnes, J., Coser, K.R., Lee, R.S., Geck, P., Isselbacher, K.J., and Shioda, T. (2004). The Bik BH3-only protein is induced in estrogen-starved and antiestrogen-exposed breast cancer cells and provokes apoptosis. Proc Natl Acad Sci U S A *101*, 2351-2356.
Husain, A.N., Colby, T.V., Ordonez, N.G., Krausz, T., Borczuk, A., Cagle, P.T., Chirieac, L.R., Churg, A., Galateau-Salle, F., Gibbs, A.R.*, et al.* (2009). Guidelines for pathologic diagnosis of malignant mesothelioma: a consensus statement from the International Mesothelioma Interest Group. Arch Pathol Lab Med *133*, 1317-1331.
Hutcheson, I.R., Knowlden, J.M., Madden, T.A., Barrow, D., Gee, J.M., Wakeling, A.E., and Nicholson, R.I. (2003). Oestrogen receptor-mediated modulation of the EGFR/MAPK pathway in tamoxifen-resistant MCF-7 cells. Breast Cancer Res Treat *81*, 81-93.
Huynh, K.D., and Bardwell, V.J. (1998). The BCL-6 POZ domain and other POZ domains interact with the co-repressors N-CoR and SMRT. Oncogene *17*, 2473-2484.
Inokuchi, A., Hinoshita, E., Iwamoto, Y., Kohno, K., Kuwano, M., and Uchiumi, T. (2001). Enhanced expression of the human multidrug resistance protein 3 by bile salt in human enterocytes. A transcriptional control of a plausible bile acid transporter. J Biol Chem *276*, 46822-46829.
Irwin, J.J., and Shoichet, B.K. (2005). ZINC--a free database of commercially available compounds for virtual screening. J Chem Inf Model *45*, 177-182.
J. Ingle, M.D., J. Cuzick, C. Davies (2008). Aromatase Inhibitors versus Tamoxifen as adjuvant therapy for post menopausal women with estrogen receptor positive breast cancer - a meta-analysis of randomised trials of monotherapy and switching strategies. Oral presentation at 31st San Antonio Breast Cancer Symposium, San Antonio, Texas, USA
Jackson, T.A., Richer, J.K., Bain, D.L., Takimoto, G.S., Tung, L., and Horwitz, K.B. (1997). The partial agonist activity of antagonist-occupied steroid receptors is controlled by a novel hinge domain-binding coactivator L7/SPA and the corepressors N-CoR or SMRT. Mol Endocrinol *11*, 693-705.
Jemal, A., Bray, F., Center, M.M., Ferlay, J., Ward, E., and Forman, D. (2011). Global cancer statistics. CA Cancer J Clin *61*, 69-90.

Jepsen, K., Hermanson, O., Onami, T.M., Gleiberman, A.S., Lunyak, V., McEvilly, R.J., Kurokawa, R., Kumar, V., Liu, F., Seto, E.*, et al.* (2000). Combinatorial roles of the nuclear receptor corepressor in transcription and development. Cell *102*, 753-763.
Jiang, S.Y., and Jordan, V.C. (1992). Growth regulation of estrogen receptor-negative breast cancer cells transfected with complementary DNAs for estrogen receptor. J Natl Cancer Inst *84*, 580-591.
Jimenez, B., Volpert, O.V., Crawford, S.E., Febbraio, M., Silverstein, R.L., and Bouck, N. (2000). Signals leading to apoptosis-dependent inhibition of neovascularization by thrombospondin-1. Nat Med *6*, 41-48.
Johansson, A., Curran, J.E., Johnson, M.P., Freed, K.A., Fenstad, M.H., Bjorge, L., Eide, I.P., Carless, M.A., Rainwater, D.L., Goring, H.H.*, et al.* (2011). Identification of ACOX2 as a shared genetic risk factor for preeclampsia and cardiovascular disease. Eur J Hum Genet *19*, 796-800.
Johansson, L., Bavner, A., Thomsen, J.S., Farnegardh, M., Gustafsson, J.A., and Treuter, E. (2000). The orphan nuclear receptor SHP utilizes conserved LXXLL-related motifs for interactions with ligand-activated estrogen receptors. Mol Cell Biol *20*, 1124-1133.
Johansson, L., Thomsen, J.S., Damdimopoulos, A.E., Spyrou, G., Gustafsson, J.A., and Treuter, E. (1999). The orphan nuclear receptor SHP inhibits agonist-dependent transcriptional activity of estrogen receptors ERalpha and ERbeta. J Biol Chem *274*, 345-353.
Johnson, A.B., and O'Malley, B.W. (2012). Steroid receptor coactivators 1, 2, and 3: critical regulators of nuclear receptor activity and steroid receptor modulator (SRM)-based cancer therapy. Mol Cell Endocrinol *348*, 430-439.
Johnston, S., Pippen, J., Jr., Pivot, X., Lichinitser, M., Sadeghi, S., Dieras, V., Gomez, H.L., Romieu, G., Manikhas, A., Kennedy, M.J.*, et al.* (2009). Lapatinib combined with letrozole versus letrozole and placebo as first-line therapy for postmenopausal hormone receptor-positive metastatic breast cancer. J Clin Oncol *27*, 5538-5546.
Johnston, S.R., and Dowsett, M. (2003). Aromatase inhibitors for breast cancer: lessons from the laboratory. Nat Rev Cancer *3*, 821-831.
Johnston, S.R., Lu, B., Dowsett, M., Liang, X., Kaufmann, M., Scott, G.K., Osborne, C.K., and Benz, C.C. (1997). Comparison of estrogen receptor DNA binding in untreated and acquired antiestrogen-resistant human breast tumors. Cancer Res *57*, 3723-3727.
Johnston, S.R., Saccani-Jotti, G., Smith, I.E., Salter, J., Newby, J., Coppen, M., Ebbs, S.R., and Dowsett, M. (1995). Changes in estrogen receptor, progesterone receptor, and pS2 expression in tamoxifen-resistant human breast cancer. Cancer Res *55*, 3331-3338.
Jordan, V.C. (2003a). Antiestrogens and selective estrogen receptor modulators as multifunctional medicines. 1. Receptor interactions. J Med Chem *46*, 883-908.
Jordan, V.C. (2003b). Antiestrogens and selective estrogen receptor modulators as multifunctional medicines. 2. Clinical considerations and new agents. J Med Chem *46*, 1081-1111.
Ju, B.G., Lunyak, V.V., Perissi, V., Garcia-Bassets, I., Rose, D.W., Glass, C.K., and Rosenfeld, M.G. (2006). A topoisomerase IIbeta-mediated dsDNA break required for regulated transcription. Science *312*, 1798-1802.

Kahn, S.E., Haffner, S.M., Heise, M.A., Herman, W.H., Holman, R.R., Jones, N.P., Kravitz, B.G., Lachin, J.M., O'Neill, M.C., Zinman, B.*, et al.* (2006). Glycemic durability of rosiglitazone, metformin, or glyburide monotherapy. N Engl J Med *355*, 2427-2443.
Kaneko, E., Matsuda, M., Yamada, Y., Tachibana, Y., Shimomura, I., and Makishima, M. (2003). Induction of intestinal ATP-binding cassette transporters by a phytosterol-derived liver X receptor agonist. J Biol Chem *278*, 36091-36098.
Kao, Y.R., Shih, J.Y., Wen, W.C., Ko, Y.P., Chen, B.M., Chan, Y.L., Chu, Y.W., Yang, P.C., Wu, C.W., and Roffler, S.R. (2003). Tumor-associated antigen L6 and the invasion of human lung cancer cells. Clin Cancer Res *9*, 2807-2816.
Kasof, G.M., Lu, J.J., Liu, D., Speer, B., Mongan, K.N., Gomes, B.C., and Lorenzi, M.V. (2001). Tumor necrosis factor-alpha induces the expression of DR6, a member of the TNF receptor family, through activation of NF-kappaB. Oncogene *20*, 7965-7975.
Katz, A., Udata, C., Ott, E., Hickey, L., Burczynski, M.E., Burghart, P., Vesterqvist, O., and Meng, X. (2009). Safety, pharmacokinetics, and pharmacodynamics of single doses of LXR-623, a novel liver X-receptor agonist, in healthy participants. J Clin Pharmacol *49*, 643-649.
Kaufman, B., Mackey, J.R., Clemens, M.R., Bapsy, P.P., Vaid, A., Wardley, A., Tjulandin, S., Jahn, M., Lehle, M., Feyereislova, A.*, et al.* (2009). Trastuzumab plus anastrozole versus anastrozole alone for the treatment of postmenopausal women with human epidermal growth factor receptor 2-positive, hormone receptor-positive metastatic breast cancer: results from the randomized phase III TAnDEM study. J Clin Oncol *27*, 5529-5537.
Kim, M.S., Shigenaga, J., Moser, A., Feingold, K., and Grunfeld, C. (2003). Repression of farnesoid X receptor during the acute phase response. J Biol Chem *278*, 8988-8995.
Kirkegaard, T., McGlynn, L.M., Campbell, F.M., Muller, S., Tovey, S.M., Dunne, B., Nielsen, K.V., Cooke, T.G., and Bartlett, J.M. (2007). Amplified in breast cancer 1 in human epidermal growth factor receptor - positive tumors of tamoxifen-treated breast cancer patients. Clin Cancer Res *13*, 1405-1411.
Kirkegaard, T., Witton, C.J., McGlynn, L.M., Tovey, S.M., Dunne, B., Lyon, A., and Bartlett, J.M. (2005). AKT activation predicts outcome in breast cancer patients treated with tamoxifen. J Pathol *207*, 139-146.
Kishimoto, H., Wang, Z., Bhat-Nakshatri, P., Chang, D., Clarke, R., and Nakshatri, H. (2005). The p160 family coactivators regulate breast cancer cell proliferation and invasion through autocrine/paracrine activity of SDF-1alpha/CXCL12. Carcinogenesis *26*, 1706-1715.
Klein-Hitpass, L., Tsai, S.Y., Greene, G.L., Clark, J.H., Tsai, M.J., and O'Malley, B.W. (1989). Specific binding of estrogen receptor to the estrogen response element. Mol Cell Biol *9*, 43-49.
Klima, M., Brouckova, A., Koc, M., and Andera, L. (2011). T-cell activation triggers death receptor-6 expression in a NF-kappaB and NF-AT dependent manner. Mol Immunol *48*, 1439-1447.
Knower, K.C., Chand, A.L., Eriksson, N., Takagi, K., Miki, Y., Sasano, H., Visvader, J.E., Lindeman, G.J., Funder, J.W., Fuller, P.J.*, et al.* (2013). Distinct nuclear receptor expression in stroma adjacent to breast tumors. Breast Cancer Res Treat *142*, 211-223.

Knowlden, J.M., Hutcheson, I.R., Jones, H.E., Madden, T., Gee, J.M., Harper, M.E., Barrow, D., Wakeling, A.E., and Nicholson, R.I. (2003). Elevated levels of epidermal growth factor receptor/c-erbB2 heterodimers mediate an autocrine growth regulatory pathway in tamoxifen-resistant MCF-7 cells. Endocrinology *144*, 1032-1044.
Koch, M., Hussein, F., Woeste, A., Grundker, C., Frontzek, K., Emons, G., and Hawighorst, T. (2011). CD36-mediated activation of endothelial cell apoptosis by an N-terminal recombinant fragment of thrombospondin-2 inhibits breast cancer growth and metastasis in vivo. Breast Cancer Res Treat *128*, 337-346.
Koduri, S., Fuqua, S.A., and Poola, I. (2000). Alterations in the estrogen receptor alpha mRNA in the breast tumors of African American women. J Cancer Res Clin Oncol *126*, 291-297.
Korsmeyer, S.J., Shutter, J.R., Veis, D.J., Merry, D.E., and Oltvai, Z.N. (1993). Bcl-2/Bax: a rheostat that regulates an anti-oxidant pathway and cell death. Semin Cancer Biol *4*, 327-332.
Krylova, I.N., Sablin, E.P., Moore, J., Xu, R.X., Waitt, G.M., MacKay, J.A., Juzumiene, D., Bynum, J.M., Madauss, K., Montana, V.*, et al.* (2005). Structural analyses reveal phosphatidyl inositols as ligands for the NR5 orphan receptors SF-1 and LRH-1. Cell *120*, 343-355.
Lacassagne, A. (1936). Hormonal pathogenesis of adenocarcinoma of the breast. The American Journal of Cancer *XXVII*, 217-228.
LaFrate, A.L., Carlson, K.E., and Katzenellenbogen, J.A. (2009). Steroidal bivalent ligands for the estrogen receptor: design, synthesis, characterization and binding affinities. Bioorg Med Chem *17*, 3528-3535.
LaFrate, A.L., Gunther, J.R., Carlson, K.E., and Katzenellenbogen, J.A. (2008). Synthesis and biological evaluation of guanylhydrazone coactivator binding inhibitors for the estrogen receptor. Bioorg Med Chem *16*, 10075-10084.
Lai, C.F., Flach, K.D., Alexi, X., Fox, S.P., Ottaviani, S., Thiruchelvam, P.T., Kyle, F.J., Thomas, R.S., Launchbury, R., Hua, H.*, et al.* (2013). Co-regulated gene expression by oestrogen receptor alpha and liver receptor homolog-1 is a feature of the oestrogen response in breast cancer cells. Nucleic Acids Res *41*, 10228-10240.
Laudet, V. (1997). Evolution of the nuclear receptor superfamily: early diversification from an ancestral orphan receptor. J Mol Endocrinol *19*, 207-226.
Lavinsky, R.M., Jepsen, K., Heinzel, T., Torchia, J., Mullen, T.M., Schiff, R., Del-Rio, A.L., Ricote, M., Ngo, S., Gemsch, J.*, et al.* (1998). Diverse signaling pathways modulate nuclear receptor recruitment of N-CoR and SMRT complexes. Proc Natl Acad Sci U S A *95*, 2920-2925.
Lazarus, K.A., Wijayakumara, D., Chand, A.L., Simpson, E.R., and Clyne, C.D. (2012). Therapeutic potential of Liver Receptor Homolog-1 modulators. J Steroid Biochem Mol Biol *130*, 138-146.
Lazennec, G., and Katzenellenbogen, B.S. (1999). Expression of human estrogen receptor using an efficient adenoviral gene delivery system is able to restore hormone-dependent features to estrogen receptor-negative breast carcinoma cells. Mol Cell Endocrinol *149*, 93-105.
Leduc, A.M., Trent, J.O., Wittliff, J.L., Bramlett, K.S., Briggs, S.L., Chirgadze, N.Y., Wang, Y., Burris, T.P., and Spatola, A.F. (2003). Helix-stabilized cyclic peptides as selective

inhibitors of steroid receptor-coactivator interactions. Proc Natl Acad Sci U S A *100*, 11273-11278.
Lee, A.J., Cai, M.X., Thomas, P.E., Conney, A.H., and Zhu, B.T. (2003). Characterization of the oxidative metabolites of 17beta-estradiol and estrone formed by 15 selectively expressed human cytochrome p450 isoforms. Endocrinology *144*, 3382-3398.
Lee, J.M., Lee, Y.K., Mamrosh, J.L., Busby, S.A., Griffin, P.R., Pathak, M.C., Ortlund, E.A., and Moore, D.D. (2011). A nuclear-receptor-dependent phosphatidylcholine pathway with antidiabetic effects. Nature *474*, 506-510.
Lee, Y.K., Choi, Y.H., Chua, S., Park, Y.J., and Moore, D.D. (2006). Phosphorylation of the hinge domain of the nuclear hormone receptor LRH-1 stimulates transactivation. J Biol Chem *281*, 7850-7855.
Lee, Y.K., and Moore, D.D. (2002). Dual mechanisms for repression of the monomeric orphan receptor liver receptor homologous protein-1 by the orphan small heterodimer partner. J Biol Chem *277*, 2463-2467.
Lee, Y.K., Schmidt, D.R., Cummins, C.L., Choi, M., Peng, L., Zhang, Y., Goodwin, B., Hammer, R.E., Mangelsdorf, D.J., and Kliewer, S.A. (2008). Liver receptor homolog-1 regulates bile acid homeostasis but is not essential for feedback regulation of bile acid synthesis. Mol Endocrinol *22*, 1345-1356.
Leibowitz, B., and Yu, J. (2010). Mitochondrial signaling in cell death via the Bcl-2 family. Cancer Biol Ther *9*, 417-422.
Lekishvili, T., Fromm, E., Mujoomdar, M., and Berditchevski, F. (2008). The tumour-associated antigen L6 (L6-Ag) is recruited to the tetraspanin-enriched microdomains: implication for tumour cell motility. J Cell Sci *121*, 685-694.
Leong, G.M., Moverare, S., Brce, J., Doyle, N., Sjogren, K., Dahlman-Wright, K., Gustafsson, J.A., Ho, K.K., Ohlsson, C., and Leung, K.C. (2004). Estrogen up-regulates hepatic expression of suppressors of cytokine signaling-2 and -3 in vivo and in vitro. Endocrinology *145*, 5525-5531.
Leung, K.C., Doyle, N., Ballesteros, M., Sjogren, K., Watts, C.K., Low, T.H., Leong, G.M., Ross, R.J., and Ho, K.K. (2003). Estrogen inhibits GH signaling by suppressing GH-induced JAK2 phosphorylation, an effect mediated by SOCS-2. Proc Natl Acad Sci U S A *100*, 1016-1021.
Lewis, J.P. (2007). An interpretation of the EBCTCG data. Oncologist *12*, 505-509.
Li, M., Xie, Y.H., Kong, Y.Y., Wu, X., Zhu, L., and Wang, Y. (1998). Cloning and characterization of a novel human hepatocyte transcription factor, hB1F, which binds and activates enhancer II of hepatitis B virus. J Biol Chem *273*, 29022-29031.
Li, S., Shen, D., Shao, J., Crowder, R., Liu, W., Prat, A., He, X., Liu, S., Hoog, J., Lu, C., *et al.* (2013). Endocrine-therapy-resistant ESR1 variants revealed by genomic characterization of breast-cancer-derived xenografts. Cell Rep *4*, 1116-1130.
Li, Y., Choi, M., Suino, K., Kovach, A., Daugherty, J., Kliewer, S.A., and Xu, H.E. (2005). Structural and biochemical basis for selective repression of the orphan nuclear receptor liver receptor homolog 1 by small heterodimer partner. Proc Natl Acad Sci U S A *102*, 9505-9510.
Li, Y., Lambert, M.H., and Xu, H.E. (2003). Activation of nuclear receptors: a perspective from structural genomics. Structure *11*, 741-746.

Lin, B.C., Suzawa, M., Blind, R.D., Tobias, S.C., Bulun, S.E., Scanlan, T.S., and Ingraham, H.A. (2009). Stimulating the GPR30 estrogen receptor with a novel tamoxifen analogue activates SF-1 and promotes endometrial cell proliferation. Cancer Res *69*, 5415-5423.
Lin, C.I., Merley, A., Sciuto, T.E., Li, D., Dvorak, A.M., Melero-Martin, J.M., Dvorak, H.F., and Jaminet, S.C. (2014). TM4SF1: a new vascular therapeutic target in cancer. Angiogenesis.
Lipinski, C.A., Lombardo, F., Dominy, B.W., and Feeney, P.J. (2001). Experimental and computational approaches to estimate solubility and permeability in drug discovery and development settings. Adv Drug Deliv Rev *46*, 3-26.
List, H.J., Reiter, R., Singh, B., Wellstein, A., and Riegel, A.T. (2001). Expression of the nuclear coactivator AIB1 in normal and malignant breast tissue. Breast Cancer Res Treat *68*, 21-28.
Lonard, D.M., Lanz, R.B., and O'Malley, B.W. (2007). Nuclear receptor coregulators and human disease. Endocr Rev *28*, 575-587.
Lu, T.T., Makishima, M., Repa, J.J., Schoonjans, K., Kerr, T.A., Auwerx, J., and Mangelsdorf, D.J. (2000). Molecular basis for feedback regulation of bile acid synthesis by nuclear receptors. Mol Cell *6*, 507-515.
Lunglmayr, G. (1989). Casodex (ICI 176,334), a new, non-steroidal anti-androgen. Early clinical results. Horm Res *32 Suppl 1*, 77-81.
Luo, Y., Liang, C.P., and Tall, A.R. (2001). The orphan nuclear receptor LRH-1 potentiates the sterol-mediated induction of the human CETP gene by liver X receptor. J Biol Chem *276*, 24767-24773.
Lykkesfeldt, A.E., Madsen, M.W., and Briand, P. (1994). Altered expression of estrogen-regulated genes in a tamoxifen-resistant and ICI 164,384 and ICI 182,780 sensitive human breast cancer cell line, MCF-7/TAMR-1. Cancer Res *54*, 1587-1595.
Maceyka, M., Harikumar, K.B., Milstien, S., and Spiegel, S. (2012). Sphingosine-1-phosphate signaling and its role in disease. Trends Cell Biol *22*, 50-60.
MacGregor, J.I., and Jordan, V.C. (1998). Basic guide to the mechanisms of antiestrogen action. Pharmacol Rev *50*, 151-196.
Madauss, K.P., Grygielko, E.T., Deng, S.J., Sulpizio, A.C., Stanley, T.B., Wu, C., Short, S.A., Thompson, S.K., Stewart, E.L., Laping, N.J.*, et al.* (2007). A structural and in vitro characterization of asoprisnil: a selective progesterone receptor modulator. Mol Endocrinol *21*, 1066-1081.
Madoux, F., Li, X., Chase, P., Zastrow, G., Cameron, M.D., Conkright, J.J., Griffin, P.R., Thacher, S., and Hodder, P. (2008). Potent, selective and cell penetrant inhibitors of SF-1 by functional ultra-high-throughput screening. Mol Pharmacol *73*, 1776-1784.
Mahfoudi, A., Roulet, E., Dauvois, S., Parker, M.G., and Wahli, W. (1995). Specific mutations in the estrogen receptor change the properties of antiestrogens to full agonists. Proc Natl Acad Sci U S A *92*, 4206-4210.
Maira, S.M., Pecchi, S., Huang, A., Burger, M., Knapp, M., Sterker, D., Schnell, C., Guthy, D., Nagel, T., Wiesmann, M.*, et al.* (2012). Identification and characterization of NVP-BKM120, an orally available pan-class I PI3-kinase inhibitor. Mol Cancer Ther *11*, 317-328.
Markman, B., Tabernero, J., Krop, I., Shapiro, G.I., Siu, L., Chen, L.C., Mita, M., Melendez Cuero, M., Stutvoet, S., Birle, D.*, et al.* (2012). Phase I safety,

pharmacokinetic, and pharmacodynamic study of the oral phosphatidylinositol-3-kinase and mTOR inhibitor BGT226 in patients with advanced solid tumors. Ann Oncol *23*, 2399-2408.
Martin, L.A., Farmer, I., Johnston, S.R., Ali, S., Marshall, C., and Dowsett, M. (2003). Enhanced estrogen receptor (ER) alpha, ERBB2, and MAPK signal transduction pathways operate during the adaptation of MCF-7 cells to long term estrogen deprivation. J Biol Chem *278*, 30458-30468.
Martin, L.A., Pancholi, S., Chan, C.M., Farmer, I., Kimberley, C., Dowsett, M., and Johnston, S.R. (2005). The anti-oestrogen ICI 182,780, but not tamoxifen, inhibits the growth of MCF-7 breast cancer cells refractory to long-term oestrogen deprivation through down-regulation of oestrogen receptor and IGF signalling. Endocr Relat Cancer *12*, 1017-1036.
Matsukuma, K.E., Wang, L., Bennett, M.K., and Osborne, T.F. (2007). A key role for orphan nuclear receptor liver receptor homologue-1 in activation of fatty acid synthase promoter by liver X receptor. J Biol Chem *282*, 20164-20171.
McDonnell, D.P. (2004). The molecular determinants of estrogen receptor pharmacology. Maturitas *48 Suppl 1*, S7-12.
McDonnell, D.P., Chang, C.Y., and Norris, J.D. (2000). Development of peptide antagonists that target estrogen receptor-cofactor interactions. J Steroid Biochem Mol Biol *74*, 327-335.
Mellado-Gil, J.M., Cobo-Vuilleumier, N., and Gauthier, B.R. (2012). Islet beta-Cell Mass Preservation and Regeneration in Diabetes Mellitus: Four Factors with Potential Therapeutic Interest. J Transplant *2012*, 230870.
Metcalf, D., Greenhalgh, C.J., Viney, E., Willson, T.A., Starr, R., Nicola, N.A., Hilton, D.J., and Alexander, W.S. (2000). Gigantism in mice lacking suppressor of cytokine signalling-2. Nature *405*, 1069-1073.
Metivier, R., Penot, G., Hubner, M.R., Reid, G., Brand, H., Kos, M., and Gannon, F. (2003). Estrogen receptor-alpha directs ordered, cyclical, and combinatorial recruitment of cofactors on a natural target promoter. Cell *115*, 751-763.
Metivier, R., Reid, G., and Gannon, F. (2006). Transcription in four dimensions: nuclear receptor-directed initiation of gene expression. EMBO Rep *7*, 161-167.
Miki, Y., Clyne, C.D., Suzuki, T., Moriya, T., Shibuya, R., Nakamura, Y., Ishida, T., Yabuki, N., Kitada, K., Hayashi, S.*, et al.* (2006). Immunolocalization of liver receptor homologue-1 (LRH-1) in human breast carcinoma: possible regulator of insitu steroidogenesis. Cancer Lett *244*, 24-33.
Miki, Y., Suzuki, T., and Sasano, H. (2007). Controversies of aromatase localization in human breast cancer--stromal versus parenchymal cells. J Steroid Biochem Mol Biol *106*, 97-101.
Mita, M., De Bono, J., and Mita, A. (2005). A phase II and biologic correlative study investigating anastrazole in combination with gefitinib in post menopausal patients with estrogen receptor positive MBC who previously failed hormonal therapy. Breast Cancer Res Treat *94 (suppl 1) Abstract 1117*.
Moore, T.W., Mayne, C.G., and Katzenellenbogen, J.A. (2010). Minireview: Not picking pockets: nuclear receptor alternate-site modulators (NRAMs). Mol Endocrinol *24*, 683-695.

Moses, H.L., Yang, E.Y., and Pietenpol, J.A. (1990). TGF-beta stimulation and inhibition of cell proliferation: new mechanistic insights. Cell *63*, 245-247.
Moy, B., and Goss, P.E. (2006). Estrogen receptor pathway: resistance to endocrine therapy and new therapeutic approaches. Clin Cancer Res *12*, 4790-4793.
Mu, L., Katsaros, D., Wiley, A., Lu, L., de la Longrais, I.A., Smith, S., Khubchandani, S., Sochirca, O., Arisio, R., and Yu, H. (2009). Peptide concentrations and mRNA expression of IGF-I, IGF-II and IGFBP-3 in breast cancer and their associations with disease characteristics. Breast Cancer Res Treat *115*, 151-162.
Mueller, M., Cima, I., Noti, M., Fuhrer, A., Jakob, S., Dubuquoy, L., Schoonjans, K., and Brunner, T. (2006). The nuclear receptor LRH-1 critically regulates extra-adrenal glucocorticoid synthesis in the intestine. J Exp Med *203*, 2057-2062.
Musille, P.M., Pathak, M.C., Lauer, J.L., Hudson, W.H., Griffin, P.R., and Ortlund, E.A. (2012). Antidiabetic phospholipid-nuclear receptor complex reveals the mechanism for phospholipid-driven gene regulation. Nat Struct Mol Biol *19*, 532-537, S531-532.
Myers, E., Fleming, F.J., Crotty, T.B., Kelly, G., McDermott, E.W., O'Higgins N, J., Hill, A.D., and Young, L.S. (2004). Inverse relationship between ER-beta and SRC-1 predicts outcome in endocrine-resistant breast cancer. Br J Cancer *91*, 1687-1693.
Nagahashi, M., Ramachandran, S., Kim, E.Y., Allegood, J.C., Rashid, O.M., Yamada, A., Zhao, R., Milstien, S., Zhou, H., Spiegel, S.*, et al.* (2012). Sphingosine-1-phosphate produced by sphingosine kinase 1 promotes breast cancer progression by stimulating angiogenesis and lymphangiogenesis. Cancer Res *72*, 726-735.
Nagy, L., Kao, H.Y., Chakravarti, D., Lin, R.J., Hassig, C.A., Ayer, D.E., Schreiber, S.L., and Evans, R.M. (1997). Nuclear receptor repression mediated by a complex containing SMRT, mSin3A, and histone deacetylase. Cell *89*, 373-380.
Nichols, J., Zevnik, B., Anastassiadis, K., Niwa, H., Klewe-Nebenius, D., Chambers, I., Scholer, H., and Smith, A. (1998). Formation of pluripotent stem cells in the mammalian embryo depends on the POU transcription factor Oct4. Cell *95*, 379-391.
Nicholson, R.I., Hutcheson, I.R., Jones, H.E., Hiscox, S.E., Giles, M., Taylor, K.M., and Gee, J.M. (2007). Growth factor signalling in endocrine and anti-growth factor resistant breast cancer. Rev Endocr Metab Disord *8*, 241-253.
Nishigori, H., Tomura, H., Tonooka, N., Kanamori, M., Yamada, S., Sho, K., Inoue, I., Kikuchi, N., Onigata, K., Kojima, I.*, et al.* (2001). Mutations in the small heterodimer partner gene are associated with mild obesity in Japanese subjects. Proc Natl Acad Sci U S A *98*, 575-580.
Nitta, M., Ku, S., Brown, C., Okamoto, A.Y., and Shan, B. (1999). CPF: an orphan nuclear receptor that regulates liver-specific expression of the human cholesterol 7alpha-hydroxylase gene. Proc Natl Acad Sci U S A *96*, 6660-6665.
Nolte, R.T., Wisely, G.B., Westin, S., Cobb, J.E., Lambert, M.H., Kurokawa, R., Rosenfeld, M.G., Willson, T.M., Glass, C.K., and Milburn, M.V. (1998). Ligand binding and co-activator assembly of the peroxisome proliferator-activated receptor-gamma. Nature *395*, 137-143.
Noti, M., Sidler, D., and Brunner, T. (2009). Extra-adrenal glucocorticoid synthesis in the intestinal epithelium: more than a drop in the ocean? Semin Immunopathol *31*, 237-248.

Ogawa, S., Inoue, S., Watanabe, T., Orimo, A., Hosoi, T., Ouchi, Y., and Muramatsu, M. (1998). Molecular cloning and characterization of human estrogen receptor betacx: a potential inhibitor ofestrogen action in human. Nucleic Acids Res *26*, 3505-3512.
Oh, A.S., Lorant, L.A., Holloway, J.N., Miller, D.L., Kern, F.G., and El-Ashry, D. (2001). Hyperactivation of MAPK induces loss of ERalpha expression in breast cancer cells. Mol Endocrinol *15*, 1344-1359.
Oliver, W.R., Jr., Shenk, J.L., Snaith, M.R., Russell, C.S., Plunket, K.D., Bodkin, N.L., Lewis, M.C., Winegar, D.A., Sznaidman, M.L., Lambert, M.H.*, et al.* (2001). A selective peroxisome proliferator-activated receptor delta agonist promotes reverse cholesterol transport. Proc Natl Acad Sci U S A *98*, 5306-5311.
Oram, J.F., and Vaughan, A.M. (2000). ABCA1-mediated transport of cellular cholesterol and phospholipids to HDL apolipoproteins. Curr Opin Lipidol *11*, 253-260.
Ordovas, J.M. (2000). ABC1: the gene for Tangier disease and beyond. Nutr Rev *58*, 76-79.
Ortlund, E.A., Lee, Y., Solomon, I.H., Hager, J.M., Safi, R., Choi, Y., Guan, Z., Tripathy, A., Raetz, C.R., McDonnell, D.P.*, et al.* (2005). Modulation of human nuclear receptor LRH-1 activity by phospholipids and SHP. Nat Struct Mol Biol *12*, 357-363.
Osborne, C.K. (1998). Tamoxifen in the treatment of breast cancer. N Engl J Med *339*, 1609-1618.
Osborne, C.K., Bardou, V., Hopp, T.A., Chamness, G.C., Hilsenbeck, S.G., Fuqua, S.A., Wong, J., Allred, D.C., Clark, G.M., and Schiff, R. (2003). Role of the estrogen receptor coactivator AIB1 (SRC-3) and HER-2/neu in tamoxifen resistance in breast cancer. J Natl Cancer Inst *95*, 353-361.
Osborne, C.K., Neven, P., Dirix, L.Y., Mackey, J.R., Robert, J., Underhill, C., Schiff, R., Gutierrez, C., Migliaccio, I., Anagnostou, V.K.*, et al.* (2011). Gefitinib or placebo in combination with tamoxifen in patients with hormone receptor-positive metastatic breast cancer: a randomized phase II study. Clin Cancer Res *17*, 1147-1159.
Osborne, C.K., Pippen, J., Jones, S.E., Parker, L.M., Ellis, M., Come, S., Gertler, S.Z., May, J.T., Burton, G., Dimery, I.*, et al.* (2002). Double-blind, randomized trial comparing the efficacy and tolerability of fulvestrant versus anastrozole in postmenopausal women with advanced breast cancer progressing on prior endocrine therapy: results of a North American trial. J Clin Oncol *20*, 3386-3395.
Osborne, C.K., Wakeling, A., and Nicholson, R.I. (2004). Fulvestrant: an oestrogen receptor antagonist with a novel mechanism of action. Br J Cancer *90 Suppl 1*, S2-6.
Ottaviano, Y.L., Issa, J.P., Parl, F.F., Smith, H.S., Baylin, S.B., and Davidson, N.E. (1994). Methylation of the estrogen receptor gene CpG island marks loss of estrogen receptor expression in human breast cancer cells. Cancer Res *54*, 2552-2555.
Pakdel, F., Reese, J.C., and Katzenellenbogen, B.S. (1993). Identification of charged residues in an N-terminal portion of the hormone-binding domain of the human estrogen receptor important in transcriptional activity of the receptor. Mol Endocrinol *7*, 1408-1417.
Palmieri, C., Patten, D.K., Januszewski, A., Zucchini, G., and Howell, S.J. (2014). Breast cancer: current and future endocrine therapies. Mol Cell Endocrinol *382*, 695-723.
Paplomata, E., and O'Regan, R. (2014). The PI3K/AKT/mTOR pathway in breast cancer: targets, trials and biomarkers. Ther Adv Med Oncol *6*, 154-166.

Pare, J.F., Malenfant, D., Courtemanche, C., Jacob-Wagner, M., Roy, S., Allard, D., and Belanger, L. (2004). The fetoprotein transcription factor (FTF) gene is essential to embryogenesis and cholesterol homeostasis and is regulated by a DR4 element. J Biol Chem *279*, 21206-21216.
Parent, A.A., Gunther, J.R., and Katzenellenbogen, J.A. (2008). Blocking estrogen signaling after the hormone: pyrimidine-core inhibitors of estrogen receptor-coactivator binding. J Med Chem *51*, 6512-6530.
Parker, M.G. (1993). Action of "pure" antiestrogens in inhibiting estrogen receptor action. Breast Cancer Res Treat *26*, 131-137.
Parker, M.G., Arbuckle, N., Dauvois, S., Danielian, P., and White, R. (1993). Structure and function of the estrogen receptor. Ann N Y Acad Sci *684*, 119-126.
Peng, N., Kim, J.W., Rainey, W.E., Carr, B.R., and Attia, G.R. (2003). The role of the orphan nuclear receptor, liver receptor homologue-1, in the regulation of human corpus luteum 3beta-hydroxysteroid dehydrogenase type II. J Clin Endocrinol Metab *88*, 6020-6028.
Perissi, V., Jepsen, K., Glass, C.K., and Rosenfeld, M.G. (2010). Deconstructing repression: evolving models of co-repressor action. Nat Rev Genet *11*, 109-123.
Piccart M, Rugo H, Chen D, Campone M, Burris AH, Taran T, Sahmoud T, Deleu I, Hortobagyi GN, and J, B. (2013). Assessment of genetic alterations in postmenopausal women with hor-
mone receptor-positive, HER2-negative advanced breast cancer
from the BOLERO-2 trial by next-generation sequencing. Ann Oncol *24*, 25-26.
Pike, A.C., Brzozowski, A.M., Walton, J., Hubbard, R.E., Bonn, T., Gustafsson, J.A., and Carlquist, M. (2000). Structural aspects of agonism and antagonism in the oestrogen receptor. Biochem Soc Trans *28*, 396-400.
Pitson, S.M., Xia, P., Leclercq, T.M., Moretti, P.A., Zebol, J.R., Lynn, H.E., Wattenberg, B.W., and Vadas, M.A. (2005). Phosphorylation-dependent translocation of sphingosine kinase to the plasma membrane drives its oncogenic signalling. J Exp Med *201*, 49-54.
Poli, V. (1998). The role of C/EBP isoforms in the control of inflammatory and native immunity functions. J Biol Chem *273*, 29279-29282.
Polychronis, A., Sinnett, H.D., Hadjiminas, D., Singhal, H., Mansi, J.L., Shivapatham, D., Shousha, S., Jiang, J., Peston, D., Barrett, N.*, et al.* (2005). Preoperative gefitinib versus gefitinib and anastrozole in postmenopausal patients with oestrogen-receptor positive and epidermal-growth-factor-receptor-positive primary breast cancer: a double-blind placebo-controlled phase II randomised trial. Lancet Oncol *6*, 383-391.
Powell, G., Roche, H., and Roche, W.R. (2011). Expression of calretinin by breast carcinoma and the potential for misdiagnosis of mesothelioma. Histopathology *59*, 950-956.
Prout, G.R., Jr., Irwin, R.J., Jr., Kliman, B., Daly, J.J., MacLaughlin, R.A., and Griffin, P.P. (1975). Prostatic cancer and SCH-13521: II. Histological alterations and the pituitary gonadal axis. J Urol *113*, 834-840.
Qin, L., Liao, L., Redmond, A., Young, L., Yuan, Y., Chen, H., O'Malley, B.W., and Xu, J. (2008). The AIB1 oncogene promotes breast cancer metastasis by activation of

PEA3-mediated matrix metalloproteinase 2 (MMP2) and MMP9 expression. Mol Cell Biol *28*, 5937-5950.
Rajah, R., Valentinis, B., and Cohen, P. (1997). Insulin-like growth factor (IGF)-binding protein-3 induces apoptosis and mediates the effects of transforming growth factor-beta1 on programmed cell death through a p53- and IGF-independent mechanism. J Biol Chem *272*, 12181-12188.
Rashmi, R., Pillai, S.G., Vijayalingam, S., Ryerse, J., and Chinnadurai, G. (2008). BH3-only protein BIK induces caspase-independent cell death with autophagic features in Bcl-2 null cells. Oncogene *27*, 1366-1375.
Rausa, F.M., Galarneau, L., Belanger, L., and Costa, R.H. (1999). The nuclear receptor fetoprotein transcription factor is coexpressed with its target gene HNF-3beta in the developing murine liver, intestine and pancreas. Mech Dev *89*, 185-188.
Reddy, J.K., Goel, S.K., Nemali, M.R., Carrino, J.J., Laffler, T.G., Reddy, M.K., Sperbeck, S.J., Osumi, T., Hashimoto, T., Lalwani, N.D.*, et al.* (1986). Transcription regulation of peroxisomal fatty acyl-CoA oxidase and enoyl-CoA hydratase/3-hydroxyacyl-CoA dehydrogenase in rat liver by peroxisome proliferators. Proc Natl Acad Sci U S A *83*, 1747-1751.
Ree, A.H., Pacheco, M.M., Tvermyr, M., Fodstad, O., and Brentani, M.M. (2000). Expression of a novel factor, com1, in early tumor progression of breast cancer. Clin Cancer Res *6*, 1778-1783.
Reid, G., Hubner, M.R., Metivier, R., Brand, H., Denger, S., Manu, D., Beaudouin, J., Ellenberg, J., and Gannon, F. (2003). Cyclic, proteasome-mediated turnover of unliganded and liganded ERalpha on responsive promoters is an integral feature of estrogen signaling. Mol Cell *11*, 695-707.
Ren, Z., Shin, A., Cai, Q., Shu, X.O., Gao, Y.T., and Zheng, W. (2007). IGFBP3 mRNA expression in benign and malignant breast tumors. Breast Cancer Res *9*, R2.
Ring, A., and Dowsett, M. (2004). Mechanisms of tamoxifen resistance. Endocr Relat Cancer *11*, 643-658.
Robinson, D.R., Wu, Y.M., Vats, P., Su, F., Lonigro, R.J., Cao, X., Kalyana-Sundaram, S., Wang, R., Ning, Y., Hodges, L.*, et al.* (2013). Activating ESR1 mutations in hormone-resistant metastatic breast cancer. Nat Genet *45*, 1446-1451.
Rodriguez, A.L., Tamrazi, A., Collins, M.L., and Katzenellenbogen, J.A. (2004). Design, synthesis, and in vitro biological evaluation of small molecule inhibitors of estrogen receptor alpha coactivator binding. J Med Chem *47*, 600-611.
Romano, A., Adriaens, M., Kuenen, S., Delvoux, B., Dunselman, G., Evelo, C., and Groothuis, P. (2010). Identification of novel ER-alpha target genes in breast cancer cells: gene- and cell-selective co-regulator recruitment at target promoters determines the response to 17beta-estradiol and tamoxifen. Mol Cell Endocrinol *314*, 90-100.
Roth, J., Madoux, F., Hodder, P., and Roush, W.R. (2008). Synthesis of small molecule inhibitors of the orphan nuclear receptor steroidogenic factor-1 (NR5A1) based on isoquinolinone scaffolds. Bioorg Med Chem Lett *18*, 2628-2632.
Ruff, M., Gangloff, M., Wurtz, J.M., and Moras, D. (2000). Estrogen receptor transcription and transactivation: Structure-function relationship in DNA- and ligand-binding domains of estrogen receptors. Breast Cancer Res *2*, 353-359.

Sablin, E.P., Blind, R.D., Krylova, I.N., Ingraham, J.G., Cai, F., Williams, J.D., Fletterick, R.J., and Ingraham, H.A. (2009). Structure of SF-1 bound by different phospholipids: evidence for regulatory ligands. Mol Endocrinol *23*, 25-34.
Sablin, E.P., Krylova, I.N., Fletterick, R.J., and Ingraham, H.A. (2003). Structural basis for ligand-independent activation of the orphan nuclear receptor LRH-1. Mol Cell *11*, 1575-1585.
Sablin, E.P., Woods, A., Krylova, I.N., Hwang, P., Ingraham, H.A., and Fletterick, R.J. (2008). The structure of corepressor Dax-1 bound to its target nuclear receptor LRH-1. Proc Natl Acad Sci U S A *105*, 18390-18395.
Safi, R., Kovacic, A., Gaillard, S., Murata, Y., Simpson, E.R., McDonnell, D.P., and Clyne, C.D. (2005). Coactivation of liver receptor homologue-1 by peroxisome proliferator-activated receptor gamma coactivator-1alpha on aromatase promoter II and its inhibition by activated retinoid X receptor suggest a novel target for breast-specific antiestrogen therapy. Cancer Res *65*, 11762-11770.
Santen, R.J., Song, R.X., Masamura, S., Yue, W., Fan, P., Sogon, T., Hayashi, S., Nakachi, K., and Eguchi, H. (2008). Adaptation to estradiol deprivation causes up-regulation of growth factor pathways and hypersensitivity to estradiol in breast cancer cells. Adv Exp Med Biol *630*, 19-34.
Sarvari, M., Kallo, I., Hrabovszky, E., Solymosi, N., Toth, K., Liko, I., Molnar, B., Tihanyi, K., and Liposits, Z. (2010). Estradiol replacement alters expression of genes related to neurotransmission and immune surveillance in the frontal cortex of middle-aged, ovariectomized rats. Endocrinology *151*, 3847-3862.
Sarwar, N., Kim, J.S., Jiang, J., Peston, D., Sinnett, H.D., Madden, P., Gee, J.M., Nicholson, R.I., Lykkesfeldt, A.E., Shousha, S.*, et al.* (2006). Phosphorylation of ERalpha at serine 118 in primary breast cancer and in tamoxifen-resistant tumours is indicative of a complex role for ERalpha phosphorylation in breast cancer progression. Endocr Relat Cancer *13*, 851-861.
Sasieni, P.D., Shelton, J., Ormiston-Smith, N., Thomson, C.S., and Silcocks, P.B. (2011). What is the lifetime risk of developing cancer?: the effect of adjusting for multiple primaries. Br J Cancer *105*, 460-465.
Saura, C., Bendell, J., Jerusalem, G., Su, S., Ru, Q., De Buck, S., Mills, D., Ruquet, S., Bosch, A., Urruticoechea, A.*, et al.* (2014). Phase Ib study of Buparlisib plus Trastuzumab in patients with HER2-positive advanced or metastatic breast cancer that has progressed on Trastuzumab-based therapy. Clin Cancer Res *20*, 1935-1945.
Sauve, K., Lepage, J., Sanchez, M., Heveker, N., and Tremblay, A. (2009). Positive feedback activation of estrogen receptors by the CXCL12-CXCR4 pathway. Cancer Res *69*, 5793-5800.
Schiff, R., Massarweh, S.A., Shou, J., Bharwani, L., Mohsin, S.K., and Osborne, C.K. (2004). Cross-talk between estrogen receptor and growth factor pathways as a molecular target for overcoming endocrine resistance. Clin Cancer Res *10*, 331S-336S.
Schoonjans, K., Annicotte, J.S., Huby, T., Botrugno, O.A., Fayard, E., Ueda, Y., Chapman, J., and Auwerx, J. (2002). Liver receptor homolog 1 controls the expression of the scavenger receptor class B type I. EMBO Rep *3*, 1181-1187.

Schreck, R., Rieber, P., and Baeuerle, P.A. (1991). Reactive oxygen intermediates as apparently widely used messengers in the activation of the NF-kappa B transcription factor and HIV-1. EMBO J *10*, 2247-2258.
Sebastian, S., Takayama, K., Shozu, M., and Bulun, S.E. (2002). Cloning and characterization of a novel endothelial promoter of the human CYP19 (aromatase P450) gene that is up-regulated in breast cancer tissue. Mol Endocrinol *16*, 2243-2254.
Seewaldt, V.L. (2012). Cancer: Destiny from density. Nature *490*, 490-491.
Sen, B., Peng, S., Woods, D.M., Wistuba, I., Bell, D., El-Naggar, A.K., Lai, S.Y., and Johnson, F.M. (2012). STAT5A-mediated SOCS2 expression regulates Jak2 and STAT3 activity following c-Src inhibition in head and neck squamous carcinoma. Clin Cancer Res *18*, 127-139.
Seol, W., Chung, M., and Moore, D.D. (1997). Novel receptor interaction and repression domains in the orphan receptor SHP. Mol Cell Biol *17*, 7126-7131.
Shang, Y., and Brown, M. (2002). Molecular determinants for the tissue specificity of SERMs. Science *295*, 2465-2468.
Shao, D., Berrodin, T.J., Manas, E., Hauze, D., Powers, R., Bapat, A., Gonder, D., Winneker, R.C., and Frail, D.E. (2004). Identification of novel estrogen receptor alpha antagonists. J Steroid Biochem Mol Biol *88*, 351-360.
Shao, Z.M., Sheikh, M.S., Ordonez, J.V., Feng, P., Kute, T., Chen, J.C., Aisner, S., Schnaper, L., LeRoith, D., Roberts, C.T., Jr.*, et al.* (1992). IGFBP-3 gene expression and estrogen receptor status in human breast carcinoma. Cancer Res *52*, 5100-5103.
Shen, D., Nooraie, F., Elshimali, Y., Lonsberry, V., He, J., Bose, S., Chia, D., Seligson, D., Chang, H.R., and Goodglick, L. (2006). Decreased expression of annexin A1 is correlated with breast cancer development and progression as determined by a tissue microarray analysis. Hum Pathol *37*, 1583-1591.
Shen, H.M., and Tergaonkar, V. (2009). NFkappaB signaling in carcinogenesis and as a potential molecular target for cancer therapy. Apoptosis *14*, 348-363.
Shiau, A.K., Barstad, D., Loria, P.M., Cheng, L., Kushner, P.J., Agard, D.A., and Greene, G.L. (1998). The structural basis of estrogen receptor/coactivator recognition and the antagonism of this interaction by tamoxifen. Cell *95*, 927-937.
Shih, S.C., Zukauskas, A., Li, D., Liu, G., Ang, L.H., Nagy, J.A., Brown, L.F., and Dvorak, H.F. (2009). The L6 protein TM4SF1 is critical for endothelial cell function and tumor angiogenesis. Cancer Res *69*, 3272-3277.
Shin, D.J., and Osborne, T.F. (2008). Peroxisome proliferator-activated receptor-gamma coactivator-1alpha activation of CYP7A1 during food restriction and diabetes is still inhibited by small heterodimer partner. J Biol Chem *283*, 15089-15096.
Shou, J., Massarweh, S., Osborne, C.K., Wakeling, A.E., Ali, S., Weiss, H., and Schiff, R. (2004). Mechanisms of tamoxifen resistance: increased estrogen receptor-HER2/neu cross-talk in ER/HER2-positive breast cancer. J Natl Cancer Inst *96*, 926-935.
Sierens, J., Jakody, I., Poobalan, Y., Meachem, S.J., Knower, K., Young, M.J., Sirianni, R., Pezzi, V., and Clyne, C.D. (2010). Localization and regulation of aromatase liver receptor homologue-1 in the developing rat testis. Mol Cell Endocrinol *323*, 307-313.

Simpson, N.E., Lambert, W.M., Watkins, R., Giashuddin, S., Huang, S.J., Oxelmark, E., Arju, R., Hochman, T., Goldberg, J.D., Schneider, R.J.*, et al.* (2010). High levels of Hsp90 cochaperone p23 promote tumor progression and poor prognosis in breast cancer by increasing lymph node metastases and drug resistance. Cancer Res *70*, 8446-8456.
Sirianni, R., Seely, J.B., Attia, G., Stocco, D.M., Carr, B.R., Pezzi, V., and Rainey, W.E. (2002). Liver receptor homologue-1 is expressed in human steroidogenic tissues and activates transcription of genes encoding steroidogenic enzymes. J Endocrinol *174*, R13-17.
Skehan, P., Storeng, R., Scudiero, D., Monks, A., McMahon, J., Vistica, D., Warren, J.T., Bokesch, H., Kenney, S., and Boyd, M.R. (1990). New colorimetric cytotoxicity assay for anticancer-drug screening. J Natl Cancer Inst *82*, 1107-1112.
Skliris, G.P., Nugent, Z., Watson, P.H., and Murphy, L.C. (2010). Estrogen receptor alpha phosphorylated at tyrosine 537 is associated with poor clinical outcome in breast cancer patients treated with tamoxifen. Horm Cancer *1*, 215-221.
Smith, C.L., Migliaccio, I., Chaubal, V., Wu, M.F., Pace, M.C., Hartmaier, R., Jiang, S., Edwards, D.P., Gutierrez, M.C., Hilsenbeck, S.G.*, et al.* (2012). Elevated nuclear expression of the SMRT corepressor in breast cancer is associated with earlier tumor recurrence. Breast Cancer Res Treat *136*, 253-265.
Smith, C.L., Nawaz, Z., and O'Malley, B.W. (1997). Coactivator and corepressor regulation of the agonist/antagonist activity of the mixed antiestrogen, 4-hydroxytamoxifen. Mol Endocrinol *11*, 657-666.
Smith, H.O., Arias-Pulido, H., Kuo, D.Y., Howard, T., Qualls, C.R., Lee, S.J., Verschraegen, C.F., Hathaway, H.J., Joste, N.E., and Prossnitz, E.R. (2009). GPR30 predicts poor survival for ovarian cancer. Gynecol Oncol *114*, 465-471.
Smith, H.O., Leslie, K.K., Singh, M., Qualls, C.R., Revankar, C.M., Joste, N.E., and Prossnitz, E.R. (2007a). GPR30: a novel indicator of poor survival for endometrial carcinoma. Am J Obstet Gynecol *196*, 386 e381-389; discussion 386 e389-311.
Smith, I.E., Walsh, G., Skene, A., Llombart, A., Mayordomo, J.I., Detre, S., Salter, J., Clark, E., Magill, P., and Dowsett, M. (2007b). A phase II placebo-controlled trial of neoadjuvant anastrozole alone or with gefitinib in early breast cancer. J Clin Oncol *25*, 3816-3822.
Sogani, P.C., Ray, B., and Whitmore, W.F., Jr. (1975). Advanced prostatic carcinoma: flutamide therapy after conventional endocrine treatment. Urology *6*, 164-166.
Soisson, S.M., Parthasarathy, G., Adams, A.D., Sahoo, S., Sitlani, A., Sparrow, C., Cui, J., and Becker, J.W. (2008). Identification of a potent synthetic FXR agonist with an unexpected mode of binding and activation. Proc Natl Acad Sci U S A *105*, 5337-5342.
Song, R.X., Santen, R.J., Kumar, R., Adam, L., Jeng, M.H., Masamura, S., and Yue, W. (2002). Adaptive mechanisms induced by long-term estrogen deprivation in breast cancer cells. Mol Cell Endocrinol *193*, 29-42.
Souers, A.J., Leverson, J.D., Boghaert, E.R., Ackler, S.L., Catron, N.D., Chen, J., Dayton, B.D., Ding, H., Enschede, S.H., Fairbrother, W.J.*, et al.* (2013). ABT-199, a potent and selective BCL-2 inhibitor, achieves antitumor activity while sparing platelets. Nat Med *19*, 202-208.

Steffensen, K.R., Holter, E., Bavner, A., Nilsson, M., Pelto-Huikko, M., Tomarev, S., and Treuter, E. (2004). Functional conservation of interactions between a homeodomain cofactor and a mammalian FTZ-F1 homologue. EMBO Rep *5*, 613-619.
Stephens, P.J., Tarpey, P.S., Davies, H., Van Loo, P., Greenman, C., Wedge, D.C., Nik-Zainal, S., Martin, S., Varela, I., Bignell, G.R.*, et al.* (2012). The landscape of cancer genes and mutational processes in breast cancer. Nature *486*, 400-404.
Stickles, X.B., Marchion, D.C., Bicaku, E., Al Sawah, E., Abbasi, F., Xiong, Y., Bou Zgheib, N., Boac, B.M., Orr, B.C., Judson, P.L.*, et al.* (2015). BAD-mediated apoptotic pathway is associated with human cancer development. Int J Mol Med *35*, 1081-1087.
Stocco, D.M. (2001). StAR protein and the regulation of steroid hormone biosynthesis. Annu Rev Physiol *63*, 193-213.
Su, C.H., Tzeng, T.Y., Cheng, C., and Hsu, M.T. (2014). An H2A histone isotype regulates estrogen receptor target genes by mediating enhancer-promoter-3'-UTR interactions in breast cancer cells. Nucleic Acids Res *42*, 3073-3088.
Suzawa, M., and Ingraham, H.A. (2008). The herbicide atrazine activates endocrine gene networks via non-steroidal NR5A nuclear receptors in fish and mammalian cells. PLoS One *3*, e2117.
Tai, H., Kubota, N., and Kato, S. (2000). Involvement of nuclear receptor coactivator SRC-1 in estrogen-dependent cell growth of MCF-7 cells. Biochem Biophys Res Commun *267*, 311-316.
Tan, Y., Demeter, M.R., Ruan, H., and Comb, M.J. (2000). BAD Ser-155 phosphorylation regulates BAD/Bcl-XL interaction and cell survival. J Biol Chem *275*, 25865-25869.
Taouji, S., Dahan, S., Bosse, R., and Chevet, E. (2009). Current Screens Based on the AlphaScreen Technology for Deciphering Cell Signalling Pathways. Curr Genomics *10*, 93-101.
Tcherepanova, I., Puigserver, P., Norris, J.D., Spiegelman, B.M., and McDonnell, D.P. (2000). Modulation of estrogen receptor-alpha transcriptional activity by the coactivator PGC-1. J Biol Chem *275*, 16302-16308.
Teixeira, C., Reed, J.C., and Pratt, M.A. (1995). Estrogen promotes chemotherapeutic drug resistance by a mechanism involving Bcl-2 proto-oncogene expression in human breast cancer cells. Cancer Res *55*, 3902-3907.
Thiruchelvam, P.T., Lai, C.F., Hua, H., Thomas, R.S., Hurtado, A., Hudson, W., Bayly, A.R., Kyle, F.J., Periyasamy, M., Photiou, A.*, et al.* (2011). The liver receptor homolog-1 regulates estrogen receptor expression in breast cancer cells. Breast Cancer Res Treat *127*, 385-396.
Thomas, R.S., Sarwar, N., Phoenix, F., Coombes, R.C., and Ali, S. (2008). Phosphorylation at serines 104 and 106 by Erk1/2 MAPK is important for estrogen receptor-alpha activity. J Mol Endocrinol *40*, 173-184.
Tolhurst, R.S. (2006). Transduction of oestrogen receptor alpha for studies of growth and gene regulation related to human breast cancer. PhD thesis.
Tolhurst, R.S., Thomas, R.S., Kyle, F.J., Patel, H., Periyasamy, M., Photiou, A., Thiruchelvam, P.T., Lai, C.F., Al-Sabbagh, M., Fisher, R.A.*, et al.* (2010). Transient over-expression of estrogen receptor-alpha in breast cancer cells promotes cell survival and estrogen-independent growth. Breast Cancer Res Treat *128*, 357-368.

Torchia, J., Rose, D.W., Inostroza, J., Kamei, Y., Westin, S., Glass, C.K., and Rosenfeld, M.G. (1997). The transcriptional co-activator p/CIP binds CBP and mediates nuclear-receptor function. Nature *387*, 677-684.
Torres-Arzayus, M.I., Font de Mora, J., Yuan, J., Vazquez, F., Bronson, R., Rue, M., Sellers, W.R., and Brown, M. (2004). High tumor incidence and activation of the PI3K/AKT pathway in transgenic mice define AIB1 as an oncogene. Cancer Cell *6*, 263-274.
Torres-Arzayus, M.I., Zhao, J., Bronson, R., and Brown, M. (2010). Estrogen-dependent and estrogen-independent mechanisms contribute to AIB1-mediated tumor formation. Cancer Res *70*, 4102-4111.
Toy, W., Shen, Y., Won, H., Green, B., Sakr, R.A., Will, M., Li, Z., Gala, K., Fanning, S., King, T.A.*, et al.* (2013). ESR1 ligand-binding domain mutations in hormone-resistant breast cancer. Nat Genet *45*, 1439-1445.
Tran, C., Ouk, S., Clegg, N.J., Chen, Y., Watson, P.A., Arora, V., Wongvipat, J., Smith-Jones, P.M., Yoo, D., Kwon, A.*, et al.* (2009). Development of a second-generation antiandrogen for treatment of advanced prostate cancer. Science *324*, 787-790.
Tremblay, A.M., Dufour, C.R., Ghahremani, M., Reudelhuber, T.L., and Giguere, V. (2010). Physiological genomics identifies estrogen-related receptor alpha as a regulator of renal sodium and potassium homeostasis and the renin-angiotensin pathway. Mol Endocrinol *24*, 22-32.
Tsuchiya, Y., Nakajima, M., and Yokoi, T. (2005). Cytochrome P450-mediated metabolism of estrogens and its regulation in human. Cancer Lett *227*, 115-124.
Tsujimoto, Y., Cossman, J., Jaffe, E., and Croce, C.M. (1985). Involvement of the bcl-2 gene in human follicular lymphoma. Science *228*, 1440-1443.
Ueda, H., Sun, G.C., Murata, T., and Hirose, S. (1992). A novel DNA-binding motif abuts the zinc finger domain of insect nuclear hormone receptor FTZ-F1 and mouse embryonal long terminal repeat-binding protein. Mol Cell Biol *12*, 5667-5672.
Uray, I.P., Liang, Y., and Hyder, S.M. (2004). Estradiol down-regulates CD36 expression in human breast cancer cells. Cancer Lett *207*, 101-107.
Urs, A.N., Dammer, E., and Sewer, M.B. (2006). Sphingosine regulates the transcription of CYP17 by binding to steroidogenic factor-1. Endocrinology *147*, 5249-5258.
Vaillant, F., Merino, D., Lee, L., Breslin, K., Pal, B., Ritchie, M.E., Smyth, G.K., Christie, M., Phillipson, L.J., Burns, C.J.*, et al.* (2013). Targeting BCL-2 with the BH3 mimetic ABT-199 in estrogen receptor-positive breast cancer. Cancer Cell *24*, 120-129.
Vasseur, S., Hoffmeister, A., Garcia-Montero, A., Mallo, G.V., Feil, R., Kuhbandner, S., Dagorn, J.C., and Iovanna, J.L. (2002). p8-deficient fibroblasts grow more rapidly and are more resistant to adriamycin-induced apoptosis. Oncogene *21*, 1685-1694.
Vasudevan, K.M., Barbie, D.A., Davies, M.A., Rabinovsky, R., McNear, C.J., Kim, J.J., Hennessy, B.T., Tseng, H., Pochanard, P., Kim, S.Y.*, et al.* (2009). AKT-independent signaling downstream of oncogenic PIK3CA mutations in human cancer. Cancer Cell *16*, 21-32.
Vaux, D.L., Cory, S., and Adams, J.M. (1988). Bcl-2 gene promotes haemopoietic cell survival and cooperates with c-myc to immortalize pre-B cells. Nature *335*, 440-442.
Vendrell, J.A., Magnino, F., Danis, E., Duchesne, M.J., Pinloche, S., Pons, M., Birnbaum, D., Nguyen, C., Theillet, C., and Cohen, P.A. (2004). Estrogen regulation in human

breast cancer cells of new downstream gene targets involved in estrogen metabolism, cell proliferation and cell transformation. J Mol Endocrinol *32*, 397-414.
Venteclef, N., and Delerive, P. (2007). Interleukin-1 receptor antagonist induction as an additional mechanism for liver receptor homolog-1 to negatively regulate the hepatic acute phase response. J Biol Chem *282*, 4393-4399.
Venteclef, N., Jakobsson, T., Ehrlund, A., Damdimopoulos, A., Mikkonen, L., Ellis, E., Nilsson, L.M., Parini, P., Janne, O.A., Gustafsson, J.A.*, et al.* GPS2-dependent corepressor/SUMO pathways govern anti-inflammatory actions of LRH-1 and LXRbeta in the hepatic acute phase response. Genes Dev *24*, 381-395.
Venteclef, N., Jakobsson, T., Steffensen, K.R., and Treuter, E. (2011). Metabolic nuclear receptor signaling and the inflammatory acute phase response. Trends Endocrinol Metab *22*, 333-343.
Venteclef, N., Smith, J.C., Goodwin, B., and Delerive, P. (2006). Liver receptor homolog 1 is a negative regulator of the hepatic acute-phase response. Mol Cell Biol *26*, 6799-6807.
Viberti, G., Kahn, S.E., Greene, D.A., Herman, W.H., Zinman, B., Holman, R.R., Haffner, S.M., Levy, D., Lachin, J.M., Berry, R.A.*, et al.* (2002). A diabetes outcome progression trial (ADOPT): an international multicenter study of the comparative efficacy of rosiglitazone, glyburide, and metformin in recently diagnosed type 2 diabetes. Diabetes Care *25*, 1737-1743.
Vijayalingam, S., Pillai, S.G., Rashmi, R., Subramanian, T., Sagartz, J.E., and Chinnadurai, G. (2010). Overexpression of BH3-Only Protein BNIP3 Leads to Enhanced Tumor Growth. Genes Cancer *1*, 964-971.
Vincent, A.J., Ren, S., Harris, L.G., Devine, D.J., Samant, R.S., Fodstad, O., and Shevde, L.A. (2012). Cytoplasmic translocation of p21 mediates NUPR1-induced chemoresistance: NUPR1 and p21 in chemoresistance. FEBS Lett *586*, 3429-3434.
Virdee, K., Parone, P.A., and Tolkovsky, A.M. (2000). Phosphorylation of the pro-apoptotic protein BAD on serine 155, a novel site, contributes to cell survival. Curr Biol *10*, 1151-1154.
Visentin, B., Vekich, J.A., Sibbald, B.J., Cavalli, A.L., Moreno, K.M., Matteo, R.G., Garland, W.A., Lu, Y., Yu, S., Hall, H.S.*, et al.* (2006). Validation of an anti-sphingosine-1-phosphate antibody as a potential therapeutic in reducing growth, invasion, and angiogenesis in multiple tumor lineages. Cancer Cell *9*, 225-238.
Wagner, R.T., Xu, X., Yi, F., Merrill, B.J., and Cooney, A.J. (2010). Canonical Wnt/beta-catenin regulation of liver receptor homolog-1 mediates pluripotency gene expression. Stem Cells *28*, 1794-1804.
Wakeling, A.E. (1991). Regulatory mechanisms in breast cancer. Steroidal pure antiestrogens. Cancer Treat Res *53*, 239-257.
Wakeling, A.E., Dukes, M., and Bowler, J. (1991). A potent specific pure antiestrogen with clinical potential. Cancer Res *51*, 3867-3873.
Walker, S.R., Liu, S., Xiang, M., Nicolais, M., Hatzi, K., Giannopoulou, E., Elemento, O., Cerchietti, L., Melnick, A., and Frank, D.A. (2014). The transcriptional modulator BCL6 as a molecular target for breast cancer therapy. Oncogene.
Wang, Q., Young, P., and Walters, K.J. (2005a). Structure of S5a bound to monoubiquitin provides a model for polyubiquitin recognition. J Mol Biol *348*, 727-739.

Wang, S., Yuan, Y., Liao, L., Kuang, S.Q., Tien, J.C., O'Malley, B.W., and Xu, J. (2009). Disruption of the SRC-1 gene in mice suppresses breast cancer metastasis without affecting primary tumor formation. Proc Natl Acad Sci U S A *106*, 151-156.
Wang, W., Zhang, C., Marimuthu, A., Krupka, H.I., Tabrizizad, M., Shelloe, R., Mehra, U., Eng, K., Nguyen, H., Settachatgul, C.*, et al.* (2005b). The crystal structures of human steroidogenic factor-1 and liver receptor homologue-1. Proc Natl Acad Sci U S A *102*, 7505-7510.
Wang, Z., Fan, C., Zhou, H.F., Lu, J.S., Sun, M.J., Song, J.W., Le, Y., Jiang, H.D., Wang, L.H., and Jiao, B.H. (2014). S5a binds death receptor-6 to induce THP-1 monocytes differentiation via NF-kappaB pathway. J Cell Sci.
Wang, Z.N., Bassett, M., and Rainey, W.E. (2001). Liver receptor homologue-1 is expressed in the adrenal and can regulate transcription of 11 beta-hydroxylase. J Mol Endocrinol *27*, 255-258.
Watanabe, H., Takahashi, E., Kobayashi, M., Goto, M., Krust, A., Chambon, P., and Iguchi, T. (2006). The estrogen-responsive adrenomedullin and receptor-modifying protein 3 gene identified by DNA microarray analysis are directly regulated by estrogen receptor. J Mol Endocrinol *36*, 81-89.
Watson, P.J., Fairall, L., and Schwabe, J.W. (2012). Nuclear hormone receptor co-repressors: structure and function. Mol Cell Endocrinol *348*, 440-449.
Webb, P., Nguyen, P., Shinsako, J., Anderson, C., Feng, W., Nguyen, M.P., Chen, D., Huang, S.M., Subramanian, S., McKinerney, E.*, et al.* (1998). Estrogen receptor activation function 1 works by binding p160 coactivator proteins. Mol Endocrinol *12*, 1605-1618.
Whitby, R.J., Dixon, S., Maloney, P.R., Delerive, P., Goodwin, B.J., Parks, D.J., and Willson, T.M. (2006). Identification of small molecule agonists of the orphan nuclear receptors liver receptor homolog-1 and steroidogenic factor-1. J Med Chem *49*, 6652-6655.
Whitby, R.J., Stec, J., Blind, R.D., Dixon, S., Leesnitzer, L.M., Orband-Miller, L.A., Williams, S.P., Willson, T.M., Xu, R., Zuercher, W.J.*, et al.* (2011). Small molecule agonists of the orphan nuclear receptors steroidogenic factor-1 (SF-1, NR5A1) and liver receptor homologue-1 (LRH-1, NR5A2). J Med Chem *54*, 2266-2281.
Wolff, A.C., Lazar, A.A., Bondarenko, I., Garin, A.M., Brincat, S., Chow, L., Sun, Y., Neskovic-Konstantinovic, Z., Guimaraes, R.C., Fumoleau, P.*, et al.* (2013). Randomized phase III placebo-controlled trial of letrozole plus oral temsirolimus as first-line endocrine therapy in postmenopausal women with locally advanced or metastatic breast cancer. J Clin Oncol *31*, 195-202.
Wu, X., Sills, M.A., and Zhang, J.H. (2005). Further comparison of primary hit identification by different assay technologies and effects of assay measurement variability. J Biomol Screen *10*, 581-589.
Wu, Y.G., Bennett, J., Talla, D., and Stocco, C. (2011). Testosterone, not 5alpha-dihydrotestosterone, stimulates LRH-1 leading to FSH-independent expression of Cyp19 and P450scc in granulosa cells. Mol Endocrinol *25*, 656-668.
Xu, H.E., Lambert, M.H., Montana, V.G., Plunket, K.D., Moore, L.B., Collins, J.L., Oplinger, J.A., Kliewer, S.A., Gampe, R.T., Jr., McKee, D.D.*, et al.* (2001). Structural determinants of ligand binding selectivity between the peroxisome proliferator-activated receptors. Proc Natl Acad Sci U S A *98*, 13919-13924.

Xu, H.E., Stanley, T.B., Montana, V.G., Lambert, M.H., Shearer, B.G., Cobb, J.E., McKee, D.D., Galardi, C.M., Plunket, K.D., Nolte, R.T.*, et al.* (2002). Structural basis for antagonist-mediated recruitment of nuclear co-repressors by PPARalpha. Nature *415*, 813-817.
Xu, P.L., Liu, Y.Q., Shan, S.F., Kong, Y.Y., Zhou, Q., Li, M., Ding, J.P., Xie, Y.H., and Wang, Y. (2004). Molecular mechanism for the potentiation of the transcriptional activity of human liver receptor homolog 1 by steroid receptor coactivator-1. Mol Endocrinol *18*, 1887-1905.
Yan, Y., Liu, H., Wen, H., Jiang, X., Cao, X., Zhang, G., and Liu, G. (2013). The novel estrogen receptor GPER regulates the migration and invasion of ovarian cancer cells. Mol Cell Biochem *378*, 1-7.
Yang, F.M., Pan, C.T., Tsai, H.M., Chiu, T.W., Wu, M.L., and Hu, M.C. (2009). Liver receptor homolog-1 localization in the nuclear body is regulated by sumoylation and cAMP signaling in rat granulosa cells. FEBS J *276*, 425-436.
Yasuda, T., Grillot, D., Billheimer, J.T., Briand, F., Delerive, P., Huet, S., and Rader, D.J. (2010). Tissue-specific liver X receptor activation promotes macrophage reverse cholesterol transport in vivo. Arterioscler Thromb Vasc Biol *30*, 781-786.
Yazawa, T., Inaoka, Y., Okada, R., Mizutani, T., Yamazaki, Y., Usami, Y., Kuribayashi, M., Orisaka, M., Umezawa, A., and Miyamoto, K. (2010). PPAR-gamma coactivator-1alpha regulates progesterone production in ovarian granulosa cells with SF-1 and LRH-1. Mol Endocrinol *24*, 485-496.
Yeh, C.S., Wang, J.Y., Cheng, T.L., Juan, C.H., Wu, C.H., and Lin, S.R. (2006). Fatty acid metabolism pathway play an important role in carcinogenesis of human colorectal cancers by Microarray-Bioinformatics analysis. Cancer Lett *233*, 297-308.
Yu, H., Levesque, M.A., Khosravi, M.J., Papanastasiou-Diamandi, A., Clark, G.M., and Diamandis, E.P. (1996). Associations between insulin-like growth factors and their binding proteins and other prognostic indicators in breast cancer. Br J Cancer *74*, 1242-1247.
Yue, W., Wang, J.P., Conaway, M.R., Li, Y., and Santen, R.J. (2003). Adaptive hypersensitivity following long-term estrogen deprivation: involvement of multiple signal pathways. J Steroid Biochem Mol Biol *86*, 265-274.
Zajchowski, D.A., Sager, R., and Webster, L. (1993). Estrogen inhibits the growth of estrogen receptor-negative, but not estrogen receptor-positive, human mammary epithelial cells expressing a recombinant estrogen receptor. Cancer Res *53*, 5004-5011.
Zeng, L., Li, T., Xu, D.C., Liu, J., Mao, G., Cui, M.Z., Fu, X., and Xu, X. (2012). Death receptor 6 induces apoptosis not through type I or type II pathways, but via a unique mitochondria-dependent pathway by interacting with Bax protein. J Biol Chem *287*, 29125-29133.
Zha, J., Harada, H., Yang, E., Jockel, J., and Korsmeyer, S.J. (1996). Serine phosphorylation of death agonist BAD in response to survival factor results in binding to 14-3-3 not BCL-X(L). Cell *87*, 619-628.
Zhang, C.K., Lin, W., Cai, Y.N., Xu, P.L., Dong, H., Li, M., Kong, Y.Y., Fu, G., Xie, Y.H., Huang, G.M.*, et al.* (2001). Characterization of the genomic structure and tissue-specific promoter of the human nuclear receptor NR5A2 (hB1F) gene. Gene *273*, 239-249.

Zhang, H., Thomsen, J.S., Johansson, L., Gustafsson, J.A., and Treuter, E. (2000). DAX-1 functions as an LXXLL-containing corepressor for activated estrogen receptors. J Biol Chem *275*, 39855-39859.
Zhang, J.H., Chung, T.D., and Oldenburg, K.R. (1999). A Simple Statistical Parameter for Use in Evaluation and Validation of High Throughput Screening Assays. J Biomol Screen *4*, 67-73.
Zhang, Z., Huang, L., Zhao, W., and Rigas, B. (2010). Annexin 1 induced by anti-inflammatory drugs binds to NF-kappaB and inhibits its activation: anticancer effects in vitro and in vivo. Cancer Res *70*, 2379-2388.
Zhao, C., Yasui, K., Lee, C.J., Kurioka, H., Hosokawa, Y., Oka, T., and Inazawa, J. (2003). Elevated expression levels of NCOA3, TOP1, and TFAP2C in breast tumors as predictors of poor prognosis. Cancer *98*, 18-23.
Zhao, H., Rybak, P., Dobrucki, J., Traganos, F., and Darzynkiewicz, Z. (2012). Relationship of DNA damage signaling to DNA replication following treatment with DNA topoisomerase inhibitors camptothecin/topotecan, mitoxantrone, or etoposide. Cytometry A *81*, 45-51.
Zhao, Y., Nichols, J.E., Valdez, R., Mendelson, C.R., and Simpson, E.R. (1996). Tumor necrosis factor-alpha stimulates aromatase gene expression in human adipose stromal cells through use of an activating protein-1 binding site upstream of promoter 1.4. Mol Endocrinol *10*, 1350-1357.
Zhou, H.B., Collins, M.L., Gunther, J.R., Comninos, J.S., and Katzenellenbogen, J.A. (2007). Bicyclo[2.2.2]octanes: close structural mimics of the nuclear receptor-binding motif of steroid receptor coactivators. Bioorg Med Chem Lett *17*, 4118-4122.
Zhou, J., Suzuki, T., Kovacic, A., Saito, R., Miki, Y., Ishida, T., Moriya, T., Simpson, E.R., Sasano, H., and Clyne, C.D. (2005). Interactions between prostaglandin E(2), liver receptor homologue-1, and aromatase in breast cancer. Cancer Res *65*, 657-663.
Zwart, W., Theodorou, V., Kok, M., Canisius, S., Linn, S., and Carroll, J.S. (2011). Oestrogen receptor-co-factor-chromatin specificity in the transcriptional regulation of breast cancer. EMBO J *30*, 4764-4776.